APPLIED AUXETICS

Utilising Parametric Customisation to Translate Auxetic Structure Theory into Additively Manufactured Multi-Material Performative Geometries

Brittany Mark

A ninety-point thesis submitted in fulfilment of the requirements for the degree of Master of Design Innovation.

Brittany Mark

Victoria University of Wellington, School of Design Innovation
2020

Abstract

Auxetic Structures are a class of meta-materials uniquely characterised by their Negative Poisson's Ratio, thus when a lateral force is applied the structure expands longitudinally, becoming thicker and stronger, perpendicular to the strain. This counterintuitive behaviour has many enhanced behavioural properties, such as increased energy absorption, indentation resistance and fracture toughness, they also have the ability to bend in a synclastic manner, making them the ideal candidate to fit to curvature. Subsequently, this research looks to harness these exceptional mechanical properties, focusing specifically on the Auxetic response to impact forces for sports protection scenarios.

Previously manufacturing Auxetic Structures has been a challenge, as often they are constructed of single materials which compromises the auxetic performance. Recent advances in AM technology through the Stratasys J750 Printer makes multi-material fabrication of Auxetic Structures with varying density micro structures a possibility.
The multi-material printer enables outputs to be performative, with reactive physical properties. Auxetic behaviours are a result of the structures internal topology, the geometrical arrangements form the micro architecture of the structure thus dictating their dynamic responses to Impact. This study explores digital manipulation through CAD and Generative Programming of Auxetic geometries for AM.

Parametric software, Rhino and plugin Grasshopper allow for customisation of a structure's internal topology as well as morphing of the architectures to fit an assigned curvature. This digital customisation is key to the iterative development of Auxetic Structures for situational specific 4Dimensional printing; a 3Dimensional print which translates with time. 4D printing Auxetics enables the opportunity for geometries to be uniquely reactive to a force, designed for pre-determined impact scenarios.

Auxetic Structures have been clearly linked to enhanced behavioural properties in response to impact. Through systematic investigations into Auxetic theory and studies of injury data for sporting instances, as well as the analysis of existing protection solutions, design development of enhanced, impact protection application can take place. Through parametric, generative design, anatomical specific curvature can have customised, geometry assigned to the form, proposing protection componentry which demonstrates the Auxetic effect, programmed for a targeted impact context.
This study will produce multi-materiality in 4D Auxetic demonstrators, both constructed and controlled through parametric software and exploited for their structure specific behaviours, designed to complement the body through
anatomical curvature in impact scenarios.
The final speculative designs will use multi-material 4D printing to effectively takes Auxetic Structure theory and translate the mathematical models into physical objects, through parametric design to dynamically perform in an Auxetic manner.

Key words: Computational Fabrication, Auxetic Structures, Impact protection, Computational Design, Additive Manufacturing, 4D multi-material Printing

Preface

"Recent advances in material science and digital fabrication provide promising opportunities for industrial and product design, engineering, architecture, art and science. To bring these innovations to fruition, effective computational tools are needed that link creative design exploration to material realization. A versatile approach is to abstract material and fabrication constraints into suitable geometric representations which are more readily translated into numerical algorithms" (Konaković, Crane, Deng, Bouaziz, Piker & Pauly, 2016).

Acknowledgements

It is incredibly important for me to recognise the many people around me who have helped to make this possible. Thank you for celebrating the wins with me, but thank you for also recognising the sacrifices and sticking beside me through the challenges. I appreciate your commitment and kindness through it all.

There are a few people I would like to take the time to thank individually, for their significant contributions.

Tim, thank you for your unwavering support and grounding. I appreciate the immense time and effort you have invested in me.

Victoria University, Doug, Simon, Robyn, La'Chelle, Terry, Steven, Arthur and many more, thank you for all of your efforts, support and guidance, as well as your dedication to our school.

I wish to also acknowledge the MADE Stream, Product Accelerator and Callaghan Innovation for their generous contributions. Thank you Emilio for all of your technical advice.

Mum and Dad, thank you for giving me the world and for the love you share with me every day. Olivia and Claudia for your compassion, understanding and fun. Nolan and Marlo too.

To Grace, Emma, Paige, Monica and Sami, thank you for being everything and more. All of my other close friends, you know who you are, thank you for all of your love and support, I will forever appreciate you all.

Teresa, for doing so much more than your job asked of you, thank you for your guidance, care and graceful patience. Mr Enoka, thank you for believing in me from the very beginning, and thankyou for encouraging me to believe in myself.

The class of 2020, I appreciate your company and encouragement through the endless hours.

And finally, I extend my gratitude to the countless others, for the fun, support and kindness. My heart is filled with love.

Contents

Introduction

Chapter 1
Background Research

1.1 Natural Materials 06
1.1.1Biomimicry

1.2 Synthetic Materials 08
1.2.1 High Performing Synthetic Materials
1.2.2 Metamaterials

1.3 Auxetic Materials 09
1.3.1 Historical Overview
1.3.2 The Unit
1.3.3 Auxetic Behaviour in Natural Materials
1.3.4 Auxetic Structure Matrix

1.4 Scientific Understanding 12
1.4.1 Mechanical Definitions and Notations

Chapter 2
Literature Review

2.1 Auxetic Classification 20
2.1.1 Description Framework
2.1.2 Re-entrant Structures
2.1.3 Chiral Structures
2.1.4 Rotating Units

2.2 Parametric Modelling 37
2.2.1 Advanced Design Techniques
2.2.2 Software: Rhino and Grasshopper
2.2.3 Generative Design and Algorithmic Parameters

2.3 Additive Manufacturing 40
2.3.1 Multi-material Additive Manufacturing
2.3.2 Stratasys J750 Printer
2.3.3 Multi-material Metamaterials
2.3.4 Multi-material Design Parameters
2.3.5 Concept and Design of Multi-material Auxetics
2.3.6 4D Printing
2.3.7 Multi-material Manufacturing for Impact Protection

2.4 Sport and Impact 46
2.4.1 Sport Classification
2.4.2 Sport

2.5 Injury and Protection 47
2.5.1 ACC Injury Breakdown
2.5.2 Impact
2.5.3 Anatomical Effects
2.5.4 Common Injury Scenarios
2.5.5 Non Auxetic Protection
2.5.6 Case Studies

2.6 Auxetic Contextualisation 54
2.6.1 Auxetic Structures and Impact
2.6.2 Auxetic Structures for Sports Protection
2.6.3 High Performing Auxetic Protection
2.6.4 Speculative Auxetic Sport Applications
2.6.5 Design Intervention

Chapter 3
Methodological Frameworks

3.1 Domain 60

3.2 Research Question and Hypothesis 61
3.2.1 Research Question
3.2.2 Hypothesis
3.2.3 Philosophical Viewpoint

3.3 Design Criteria 62
3.3.1 Aims and Objectives

3.4 Methods and Methodologies 63
3.4.1 Methods
3.4.2 Research Frameworks
3.4.3 Aims and Objectives
3.4.4 Workflow Frameworks

3.5 Evaluation 76
3.5.1 Mechanical Testing
3.5.2 Evaluative Methods
3.5.3 Pugh Matrix

3.6 Outputs and Outcomes 79

Primary Research

Part One: Exploration for Mechanical Experimentation

Chapter 4
Mechanical Experimentation

4.1 Methodological Analysis 84
4.1.1 Experimental Design Criteria
4.1.2 Software Selection
4.1.3 J750 Additive Manufacturing Process
4.1.4 Evaluation

4.2 Auxetic Structure Survey 90

4.3 Experimental Procedures 92
4.3.1 Preliminaries

4.4 Experimentation 1 95
4.5 Experimentation 5 110
4.6 Experimentation 3 129
4.7 Experimentation 4 186
4.8 Experimentation 5 198

Part Two: Exploration for Digital Applications

Chapter 5
Digital Exploration

5.1 Methodological Analysis 209
5.1.1 Explorative Design Criteria
5.1.2 Software Selection

5.2 Auxetic Structure Survey 212

5.3 Exploratory Procedures 214
5.3.1 Preliminaries

5.4 Exploration 1 216
5.5 Exploration 5 218
5.6 Exploration 3 220
5.7 Exploration 4 222
5.8 Exploration 5 224

Chapter 6
Design Studies

6.1 Preliminaries 228

6.2 ACC Analysis 229

6.3 Overview 234

6.4 Head Injuries in Impact Sports 236
6.4.1 The Head and Force
6.4.2 Scenarios
6.4.3 Existing Solution Analysis
6.4.4 The Auxetic Intervention
6.4.5 Design 1
6.4.6 Design 2

6.5 Knee Injuries in Impact Sports 255
6.5.1 The Knees and Force
6.5.2 Scenarios
6.5.3 Existing Solution Analysis
6.5.4 The Auxetic Intervention
6.5.5 Design 1
6.5.6 Design 2

6.6 Spinal Injuries in Impact Sports 268
6.6.1 The Spine and Force
6.6.2 Scenarios
6.6.3 Existing Solution Analysis
6.6.4 The Auxetic Intervention
6.6.5 Design 1
6.6.6 Design 2

Chapter 7
Application

7.1 Scenario 284
7.2 Anatomical Customisation 286
7.3 Digital 287
7.4 Physical 291
7.5 The Digital and Physical Connection 294
7.6 Final Design Outputs 296
7.7 Expert Opinion 299

Chapter 8
Discussion and Conclusion

8.1 Discussion 301

8.2 Conclusion 309

Reference List

Introduction

Metamaterials are a class of synthetic materials, uniquely characterised for their unusual behavioural properties not often found in natural materials. One specific group is Auxetic Structures, which more recently gained widespread attention from Scientists, Engineers and Designers for their promising behavioural responses in impact scenarios, particularly, when compared to their conventional material counterparts. When struck with an external force the structures expand perpendicular to the strain exhibiting improved indentation resistance, high energy absorption properties and high fracture toughness through a range of controllable mechanical properties.

This research will involve the process of systematically digesting theory to identify key properties and their subsequent behavioural responses, through the discipline of design a translation workflow will evolve to eventually enable contextualisation of Auxetic Structures.

The research will bridge the gap between highly academic theory and tangible fabrication, necessary for contextualisation, bringing Auxetic geometries one step closer to widespread implementation.

One application area with increasingly promising reports of value, is that of impact protection. Auxetic structures are being shown to have significantly enhanced outcomes as protection in sporting scenarios.

Building upon this mounting evidence through injury data analysis and anatomical explorations, Computer Aided Design (CAD) software and Additive Manufacturing (AM) enable the assignment of tailored Auxetic geometries to target high risk sporting scenarios.

This process will require the negotiation of both digital and physical design tools.

Tong (2018) report multi-material printing techniques to be well suited to the complex geometric architectures of Auxetic Structures, with the ability to offer enhanced fabrication, controllable through increasingly sophisticated parametric software.

This in essence, is the beginnings of this researches' pursuits.

2

Motivations

In the summer of 2018 I was awarded a Summer Research Scholarship in collaboration with Callaghan Innovation, as a part of their Advanced Materials team. It was here I developed an interest in Auxetic Structures and the opportunities they possess in a range of contexts, for their excellent mechanical properties. Combined with my passion for Snow Skiing and the outdoors, this thesis follows the research involved with connecting the two fields, through the discipline of Design.

Figure 1 Victoria University, School of Design Innovation.

1 BACKGROUND RESEARCH

1.1	Natural Materials	06
1.2	Synthetic Materials	08
1.3	Auxetic Materials	09
1.4	Scientific Understanding	12

The background research is an investigation into materials, design, tools, manufacturing, impact and sport.

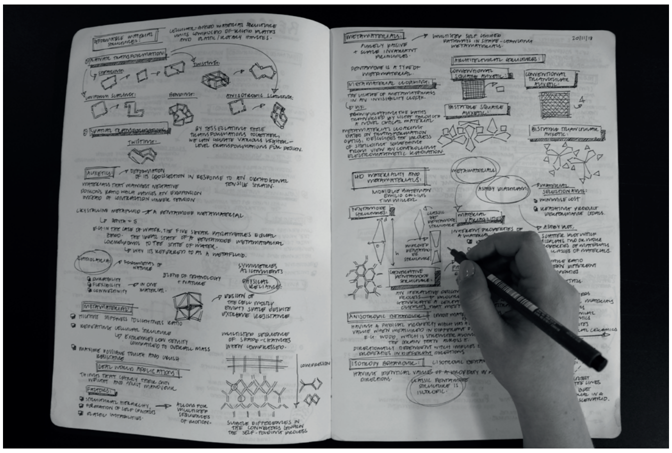

Figure 1.01 Researching.

Every tangible artefact has a material. The origins of these materials differ widely, informing fabrication as well as behavioural properties. Many natural materials continue to act as precedents to synthetically designed materials.

[1.1] Natural Materials

In nature, there exists countless examples of excellent materials, perfectly suited to their function and environment through the process of evolution. These precedents have and will continue to inform many design innovations in a range of disciplines as inspiration for novel materials, tools, systems and processes. Natural cellular materials are of particular interest, figure 1.02 below demonstrates various qualities of significant functional and behavioural advantage, including dynamic strain isolation and energy absorption.

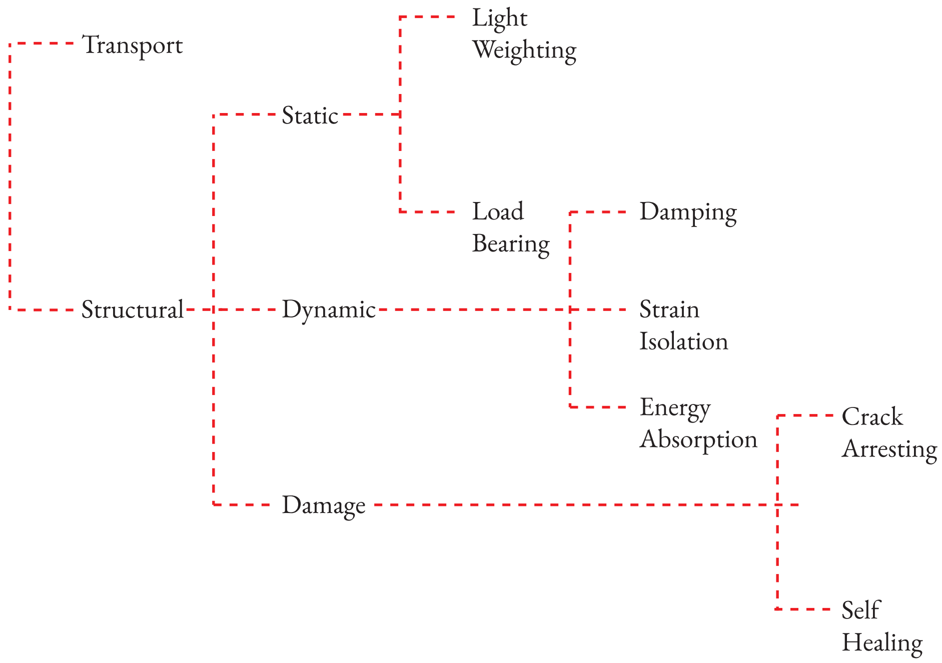

Figure 1.02 Functions of Cellular Structures in Nature, Author, 2020. Modifed from (McNulty et al., 2017).

[1.1.1] Biomimicry

Biomimicry is described as the science of imitating nature. Researchers observe and study nature to understand the principles which enable superior performance of natural materials and processes in bespoke contexts, to extract this information and allow it to inform synthetic materials innovation. Figure 1.03 below is a selection of natural precedents which exhibit qualities and behaviours similar to those developed to exist in synthetic materials.

[a] [b] [c] [d]

Figure 1.03 Natural Precedents, (a) Mussel Mollusk Shell with multimateriality, (b) Abalone Shell of Self Assembly, (c) Cats eye and (d) Tree Fern, Natural Chirality.

[1.2] Synthetic Materials

[1.2.1] High Performing Synthetic Materials

Unlike naturally occurring materials, synthetic materials refer to those artificially derived. Artificial cellular materials can be categorised into 2D and 3D designed structures. Through a precedent matrix, (see appendix) a range of natural and synthetic materials were studied for their structural and cellular properties, with particular focus on materials with geometrical architectures and subsequently exceptional properties.

One such focus group is that of Metamaterials.

[1.2.2] Metamaterials

Metamaterials are synthetic materials, engineered with tailored units to

enable them to exhibit properties, not commonly found in nature.

Their designed micro-architectures allow them to exhibit counterintuitive or unexpected, yet highly desirable properties at the macro-scale. By intentionally designing the micro units of the materials, exceptional behaviours will emerge (Chen & Fu, 2017).

[1.3] Auxetic Materials

[1.3.1] Historical Overview

In 1800 French mathematician and physician Siméon-Denis recorded the formula that defined the negative ratio of transverse to axial strain, it later became known as Poisson's Ratio (Mirante, 2016).

However, the first recorded example of Negative Poisson's ratio in a material was found by R. Love in 1944 in single crystalline Iron Pyrite (Saxena et al., 2016). Unaware of his discovery, it was dismissed at the time as twining defects in the crystals.

The earliest published example of a material with negative Poisson's ratio was Kolpakov in 1985 (Cho et al., 2019). Lakes in 1987 was the first to purposefully investigate material properties for desired outcomes. In a work titled: Foam Structure with a Negative Poisson's Ratio (Lakes, 1987), he described the discovery of Negative Poisson's Ratio in 3D, Isotropic, Polyurethane foam, through manufacturing conventional open cell foam into isotropic 'Auxetic' foam (Li et al., 2017).

Materials with this unique behaviour were described as Auxetic by K. E. Evans, derived from the Greek word αὐξητικός ,(Auxetikos) which by definition means 'that which tends to increase' (Javadi et al., 2011). The term was then first used in 1991, by Evans, in a scientific article titled 'Molecular Network Design' (Wu et al., 2019).

[1.3.2] The Unit

"[Auxetic Structures]...rely on specific spatial arrangements rather than material composition" (Saxena et al., 2016).

Auxetic Structures are differentiated from other Metamaterial groups for their distinctive Negative Poisson's ratio, that is, any material with a Poisson's ratio below 0 can be categorized as Auxetic. Poisson's Ratio measures the increased change in size of a material. "It is the ratio of transverse contraction strain to longitudinal extension strain in the direction of stretching force"

The degree of auxeticity of a structure, like its Metamaterial counterparts, is largely influenced by the internal topology of the geometrical lattice. Auxetic Structures are made up from an arrangement of units, which are constructed of nodes and struts (Barner, 2015).

The negative Poisson's Ratio of the structures is engaged through the deformation mechanism, which describes the dynamic movement of the unit geometries.

Therefore, the unit, is the most crucial aspect of the Auxetic structures.

There are many adjustable characteristics of a unit, illustrated in figure 1.04 below, including shape, size, orientation and arrangement. All impact the overall Auxetic Structures' attributes.

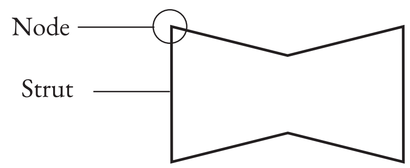

Figure 1.04 An Auxetic unit.

[1.3.3] Auxetic Behaviour in Natural Materials

There are very few examples of Auxetic behaviour in nature, however, a select few are known to scientists, they include human tendons, cancellous bone, cow teat skin, cat skin and Pomelo rind, (both seen in figure 1.05) cytoskeleton membranes in red blood cells, a small selection of minerals, pyrolytic graphite, polymorphic silicones (Cho et al., 2019) and several zeolites (Kolken & Zadpoor, 2017).

On the threshold between negative and positive Poisson's Ratio is cork, measuring 0.

[a]

[b]

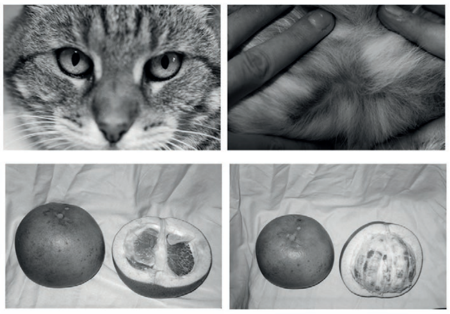

Figure 1.05 (a) Cat skin and (b) Pomelo rind are known to be naturally existing Auxetic materials, published with permission (Arie, 2018).

[1.3.4] Auxetic Structure Matrix

Exploration of natural Auxetic Structures then extended to the majority of synthetic geometries.

An Auxetic matrix was constructed to survey structures for a selection of critically influential properties, the full version of this can be found in the appendix.

Nevertheless, this extensive survey identified geometries with substantial theory to base explorations upon and those which require further mathematical development and therefore, will not be included in this design research. Structures investigated have further been refined to only include those described as open cell, geometrical configurations.

During this process of identification and elimination, key properties and subsequent behaviours were identified and are described in the preliminaries, prior to the Auxetic unit survey following below.

[1.4] Scientific Understanding

The behaviours of the unit components are described as the deformation mechanism, it is this mechanism which enables the wide range of mechanical characteristics, which in turn explain the counterintuitive behaviours of Auxetic Structures. Below is an exploration of those formulas critical to ensuring a material is Auxetic in nature, as well as those with the capacity to be manipulated through a range of values, crucial for the primary research studies.

[1.4.1] Mechanical Defintions and Notations

Geometrical Characteristics
Scale
Orientation
Curvature
Internal Topology

Mechanical Properties
Poissons Ratio (v)
Tensile and Compressive Loading
Energy
Indentation Resistance
Stiffness

(Cho et al., 2019)
(Kolken & Zadpoor, 2017)

Geometrical Characteristics

Scale

Auxetic Structures exist from the molecular to the macro and mesoscopic level. Structure's with geometries designed at the nano/micro scale exhibit enhanced properties at the meso and macro scale (Kolken & Zadpoor, 2017).

Auxetic behaviour has been explained by the same deformation mechanisms across the range of scales, shown in figure 1.06.

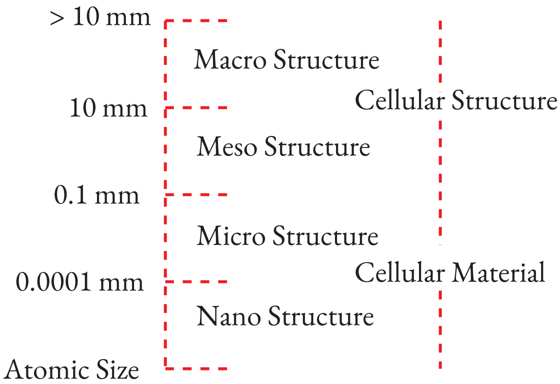

Figure 1.06 Scale.

Orientation

3 D X,Y,Z seen in the figure below.

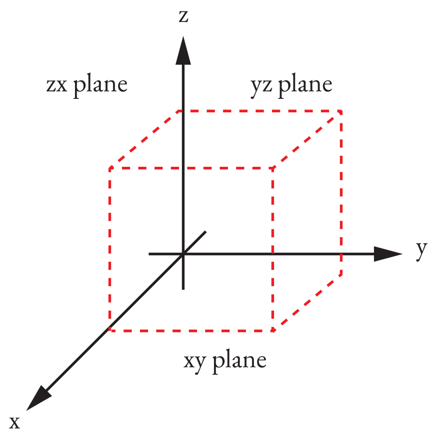

Figure 1.07 Orientation,.

Curvature

A structure's curvature can be described in terms of form and degree to which it forms a dome like structure. Synclastic structures are characterised by a doubly curved surface (Saxena, Calius, & Das, 2016), creating a dome form, whereas conventional materials typically form a saddle shaped surface, as seen in the figure below.

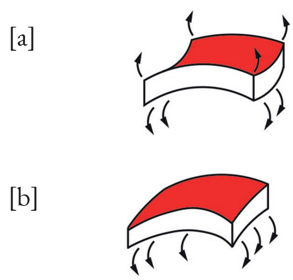

Figure 1.08 (a) Anticlastic curvature, (b) Synclastic curvature.

Internal Topology

An anisotropic material has a directional order, the voids are arranged differently depending on which direction you view them from. In contrast, Isotropic materials have disordered voids, which look the same, no matter your viewpoint (Benyus, 1997).

[a]

[b]

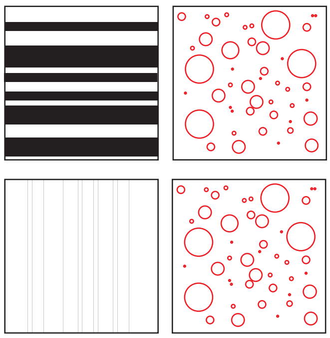

Figure 1.09 (a) Anisotropic, (b) Isotropic.

Poisson's Ratio

Most natural and conventional materials have positive Poisson's ratio, shown in figure 1.10 (a), however, Auxetic Structures possess negative Poisson's ratio (b).

Negative Poisson's ratio is characterised by lateral shrinkage against axial compression and/or axial expansion against axial compression (Cho et al., 2019).

[a]

[b]

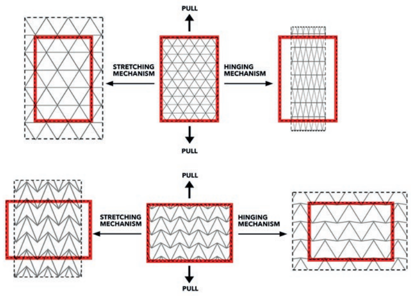

Figure 1.10 Poisson's ratio, (a) conventional material, (b) Auxetic material.

Mechanical Porperties

Tensile and Compressive Loading

Compressive strength is the materials ability to resist forces in compression (Naboni, 2015) and tensile strength is the ability to resist forces in tension. Tensile deformation is positive and compressive deformation negative, illustrated in figure 1.11 (Mirante, 2015).

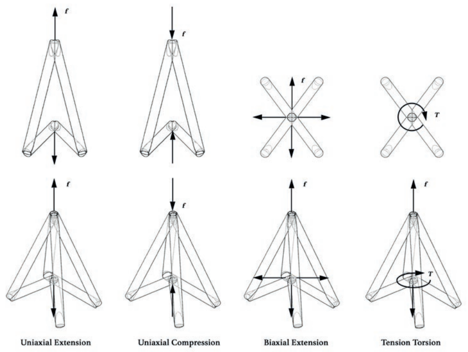

Figure 1.11 Loading.

Energy

Energy Absorption and dissipation describes the materials capacity to manage energy received from another body (Ago, 2019).

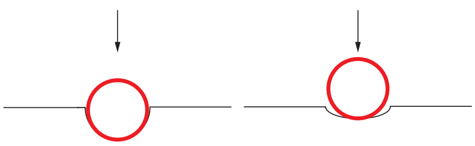

Figure 1.12 Energy Absorption.

Indentation Resistance

Indentation resistance is the materials capacity to shift mass under the point of compression (Naboni, 2015). Therefore, when an object impacts a conventional surface, the material directly below the impact flows away in the lateral direction, which leads to a reduction in the density and subsequent reduction in the indentation resistance of the material. However, in the case of Auxetic Structures, material flows into the area of impact, the result, lateral contraction and longitudinal compression. Therefore, Auxetics densify under the impact in both the longitudinal and transverse directions, leading to increased indentation resistance (Mir et al., 2014).

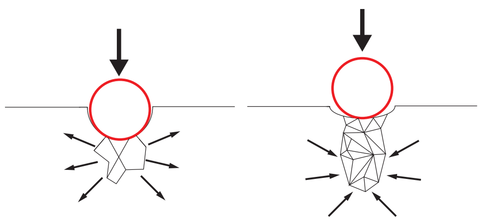

Figure 1.13 Indentation Resistance.

The described mechanical notations and principles above were collated to be those that are most critical to understand going forward, they will prove to be vital throughout the digital and physical experimentation as materiality is extensively explored in both realms.

2 LITERATURE REVIEW

2.1	Auxetic Classification	20
2.2	Parametric Modelling	27
2.3	Additive Manufacturing	40
2.4	Sport and Impact	46
2.5	Injury and Protection	47
2.6	Auxetic Contextualisation	54

There are a vast number of variations of Auxetic Structures. The list is continually being expanded through mathematical exploration and more recently, Machine Learning integration. Below are the findings of the most important structures to this research, described and visually depicted to act as the foundations for the translation workflow which the primary research studies will follow.

Figure 2.01 Research.

[2.1] Auxetic Classification

[2.1.1] Description Framework

A systematic presentation on Auxetic structures through theoretical models.

The most well reported classes of Auxetic Structures include; Re-entrant, Chiral and Rotating Rigid Units. The specific geometries described below have satisfactory literature to formulate an understanding of the properties required to construct the unit geometry, as well as those with evidence of having behavioural outcomes. For structures lacking substantial theoretical grounding or with behavioural properties not suited to this research of impact applications, it has been excluded from further exploration. Other structures which do not fall in the three main classes including fibril/nodule, Miura-folded, buckling-induced, helical auxetic yarn and crumpled structures will not be included (Cho et al., 2019).

The description framework will serve as a means to describe geometrical and mechanical properties through literature analysis and visual depiction. This research is primarily investigating the structures for design purposes, therefore, only elements integral to the digital translation of structure theory into a digital model, through design will be described.
Descriptions will be based upon a single unit.

Visual Properties
Base shape
Base points
Direction of plane

Mechanical Properties
Deformation Mechanism
Enabling geometry
Properties

[2.1.2] Re-entrant Structures

Re-entrant structures are the first class of materials exhibiting negative Poisson’s ratio.

Re-entrant refers to geometry directed inward or having a negative angle (Hu et al., 2015).

When a tensile load is applied to a re-entrant structure the struts are translated about the node, which move outwards from their resting position. This lateral deformation of the node is transferred to the neighbouring units through the neutral connecting struts and their nodes, consequently, pushing the neighbouring units to endure vertical expansion (Cho et al., 2019).

All Re-entrant structures initially investigated are listed in the figure below, the full matrix is referenced in the appendix.

Structures listed were initially surveyed, those not listed were not investigated. Those marked with an X in the figure below were analysed but later dismissed, the remaining listed and visually depicted will be used in the primary research phase.

Hexagonal Honeycomb	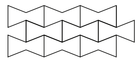
First Order Hierarchy	X
Second Order Hierarchy	X
Double Arrow Head	
Lozenge Grid	X
Square Grid	X
Honeycomb I Shaped Slit Pattern	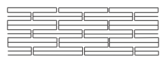
3D Sinusoidal	X
Star 3	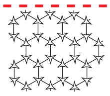
Star 4	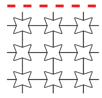
Star 6	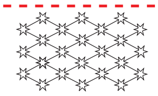
3D Honeycomb	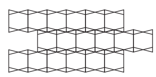
3D Triangular Arrow	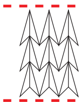

Figure 2.02 Re-entrant Structures.

Hexagonal Honeycomb

This Re-entrant structure has struts directed inwards from the four nodes, concave angles connect the two vertical struts with the re-entrant ones (Kolken & Zadpoor, 2017).

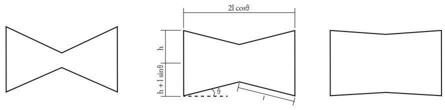

Figure 2.03 Hexagonal Honeycomb.

During deformation the re-entrant struts realign becoming less diagonal, resulting in widening of the unit laterally through the translated expansion, thereby creating the Auxetic effect (Mirante, 2015).

The stiffness of the Re-entrant honeycomb decreases when the angle is increased, increasing the overall auxeticity (Kolken & Zadpoor, 2017). The nonlinear Shear modulus of Re-entrant Hexagonal Honeycombs were found by Tong (2018) to increase with the re- entrant angle and decrease with the increase of the cell, strut length ratio. The structures are known to show in-plane isotropy and are highly anisotropic.

The Re-entrant Double Arrowhead was discovered computationally, through numerical topology optimisation method. It is a triangular truss structure with two re-entrant angles creating a concave north side (Cho et al., 2019).

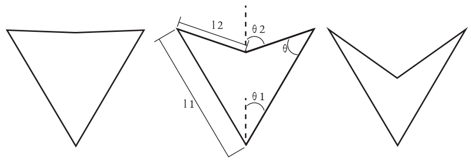

Figure 2.04 Double Arrowhead unit.

When a tensile load is applied to the structure it is transferred from the two neutral struts connected to the re-entrant vertices to unfold the re-entrant sides (Cho et al., 2019). The Auxetic behaviour depends upon the length of the struts and angle between them. Compression on the arrow head will initiate the collapse of the triangle units and lateral expansion.

The structure was reported by Kolken & Zadpoor (2017) to have a negative Poisson's ratio of 0.92 for small strains.

2D Stars

The Hexagonal Honeycomb structure described above has rotational order n=2.
Re-entrant Stars are an extension of this. These truss structures are named after the number of tips on the star. Struts connect the re-entrant vertices.

Star shaped units have rotational symmetry of orders n= 3, 4, and 6.

Star 3

Rotational symmetry of order three, Star 3 has six struts connected at three outer nodes by re-entrant angles. The three struts directed outwards from three inner nodes connect a unit to the neighbouring units.

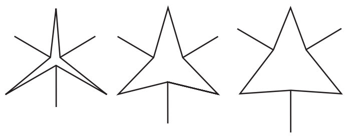

Figure 2.05 Star 3.

When stretched the star shaped cells open up, resulting in demonstration of the Auxetic effect (Saxena et al., 2016). When compared to Star structures of order four and six, order three displays the weakest Auxetic effect (Mirante, 2015). It is important to note that the stiffness of the hinges affects the overall Poisson's ratio.

When a tensile load is applied through the neutral struts in a direction, the vertices, regardless of connection point are unfolded to the same degree (Cho et al., 2019). The structure also has isotropy in three directions.

Star 4

Eight struts directed inwards to form re-entrant angles meet at four outer nodes. Two horizontal and two vertical struts point outwards, connecting the unit with its neighbours.

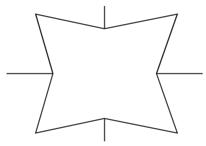

Figure 2.06 Star4.

Through opening of the star, Auxetic behaviour depends upon the hinging of the adjacent connections. Star 4 showed greater Auxetic potential, when compared to rotational order three (Saxena et al., 2016).

When a tensile load is applied through the neutral struts, the vertices, regardless of the connection points are unfolded to the same degree (Cho et al., 2019).

Star 6

Four re-entrant struts are connected by, six point stars, at the four diamond shaped nodes. A vertical strut connects the north and south nodes.

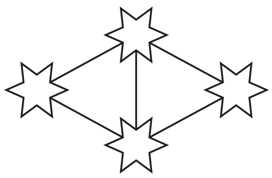

Figure 2.07 Star6.

Auxetic behaviour from opening of the stars depends on the hinging of the adjacent connections. When a tensile load is applied through the neutral struts in a specific direction, the vertices, regardless of connection point are unfolded to the same degree (Cho et al., 2019).

According to Kolken & Zadpoor (2017) the Star 6 structure has been reported to be most Auxetic of the stars, due to its anisotropic topology. Opening of the stars under uniaxial loading drives the Auxetic effect, whereas the stiffness is governed by the applied force constraints (Grima et al. 2005); (Tong, 2018).

Re-entrant

Three Dimensional Patterns

AM techniques have, recently, enabled the fabrication of 3D Metamaterials with complex micro-architectures. This has in turn, encouraged the development of 2D geometries into 3D structures.

Three Dimensional Honeycomb

The unit cell is a 3D extension of the typical 2D re-entrant cell.

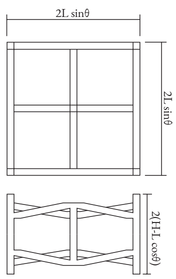

Figure 2.08 3D Honeycomb.

This 3D re-entrant structure laterally deforms due to the re-entrant sides unloading in response to the tensile strain (Cho et al., 2019).

The cross-sectional shape of the struts is square. The design parameters for a unit are: H: the length of the vertical struts, L: the length of the re-entrant struts, h: the re-entrant angle and t: the thickness of the struts cross section. Yang et al. (2015) confirm that the 3D Honeycomb, which is particularly well suited to AM for its repeatability exhibits orthotropy, with negative Poisson's ratio in all three directions.

Three Dimensional Triangular Arrow

The 3D re-entrant pyramid structure is a 3D development of the 2D Triangular Arrow (Cho et al., 2019). Lim (2015) transformed into a 3D anisotropic unit by intersecting two triangular arrowheads.

This pyramid-shaped unit has four base points, which meet at a midcentral point, through 3D re-entrant angles.

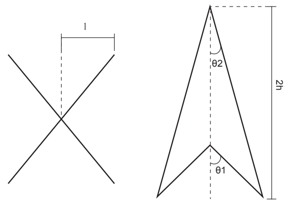

Figure 2.09 3D Arrowhead.

Kolken & Zadpoor (2017) reported that change in length ratios of the units and their subtending angles has the ability to significantly impact the Poisson's ratio.

Three Dimensional Star4

The 3D Star4 is constructed of two, 2D Star 4 units, offset 90 degrees apart about the centre.

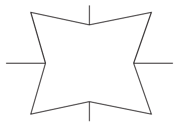

Figure 2.10 3D Star4.

Decreasing the angle between the struts, decreases the space in the interior of the structure. When no space exists, the re-entrant angle is eliminated and the structure is no longer Auxetic (Carneiro et al., 2016). When the struts are thin, significant deformation occurs, even in instances of small loads. The structure lacks rigidity and behaves more like a spring (Carneiro et al., 2016). (Carneiro et al., 2016) also observed an increasing strut width led to a general increase in the Poisson's ratio of the structure, recognising that strut length is a significantly influential parameter, determining the Poisson's ratio of the structure. The resting angle was also found to influence the Poisson's ratio of the structure, when it decreased the value of the structure's, Poisson's ratio decreased.

Re-entrant

Upon surveying a range of re-entrant structures, several general conclusions were discovered, The Shear Modulus as well as, the Poisson's ratio were found to increase with the re-entrant angle, the thickness of the struts directly affects the rigidity and thus the structures overall stiffness (Kolken & Zadpoor, 2017). Re-entrant structures are typically Anisotropic, with freedom to have a large negative value. The Young's Modulus of re-entrant structures was found to decrease as the strut thickness decreases, and the re-entrant angle increases (Kolken & Zadpoor, 2017). They are capable of simultaneously exhibiting a negative Poisson's ratio and a high stiffness (Kolken & Zadpoor, 2017).

Auxetic re-entrant structures identified from the above survey as being promising candidates for digital and experimental exploration, include Hexagonal Honeycomb, Double Arrow Head, Star3, Star4 and Star6, 3D Honeycomb, 3D Triangular Arrow, and 3D Star 4.

[2.1.3] Chiral Structures

Chiral Structures are the second class of geometries exhibiting negative Poisson's ratio.

Many Chiral structures exist in nature including plants and animals, such as helical goat horns, right and left-handed sea shells, DNA, flower petals and stems, twisted leaves, as well as chiral cellulose (Wu et al., 2019).

Figure 2.11 Chirality in seashells.

Chiral Auxetics can be classified into Chiral, Anti-Chiral and Meta-Chiral categories.

Periodic Chiral and Anti-Chiral structures are defined by the constraints of rotational symmetry. N, the order of rotational symmetry describes the number of struts attached to each node. Whilst this constraint stands, there are a limited number of structures which can be achieved, they include Tri-Chiral, Anti-Tri-Chiral, Tetra-Chiral, Anti-Tetra-Chiral and Hexa-Chiral. Once this rule is removed Meta-Chiral structures can also be achieved (Kolken & Zadpoor, 2017).

A typical chiral unit is made up of a central cylinder surrounded by tangentially attached struts, the unit cannot be mirrored onto itself to create the structure. The chiral structures can either be left or right handed to create Anti-Chiral or chiral structures (Kolken & Zadpoor, 2017). Chiral structures are designed with circular, polygonal, elliptical, sphere or cubic architectures, made up by struts connecting neighbouring nodes in 2D or 3D forms.

Anti-Chiral structures exhibit reflective symmetry as their nodes are attached on the same side of the connecting struts. The unit bodies will rotate under mechanical loading, causing the struts to flex, which results in folding or unfolding of the struts under tensile or copressive loads (Kolken & Zadpoor, 2017).

Chiral

Structures listed were initially surveyed, those not listed were not investigated. Those marked with an X in the figure below were analysed but later dismissed, the remaining listed and visually depicted will be used in the primary research phase.

Periodic Structures include: Tri-Chiral, Anti-Tri-Chiral, Tetra-Chiral, Anti-Tetra-Chiral and Hexa-Chiral (Cho et al., 2019).

Chiral Structures

Hexa-Chiral	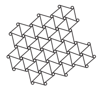
Hierarchy Metacmaterial with Fractal cuts	X
Tetra-Chiral	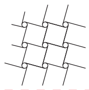
Tri-Chiral	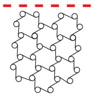
Chiral Circular	X
Rota-Chiral	X
Hexatruss	X
Anti-Tetra-Chiral	
Anti-Tri-Chiral	
Compression Twist Chiral	
Meta-Tetra-Chiral	X
3D Cellular with Planar Tetra-Chiral	

Figure 2.12. Chiral Structures.

Chiral

Hexa-Chiral

The Hexa-Chiral is arranged about a unit circle and is determined by hexagonal tessellations where each node is tangentially attached to six struts (Cho et al., 2019).

Tensile strain in one direction leads to expansion in that same direction through clockwise rotation of the nodes around the central circle, allowing the structure to expand, enabling in plane, isotropic, Auxetic behaviour (Lim, 2015). Additionally, the nodes give the structure an enhanced out of plane buckling and compressive strength, (Kolken & Zadpoor, 2017).

It was reported the structure exhibits a Poisson's ratio of negative one for in plane deformation, which is sustained under significant strain, when compared to other Auxetic Structures. Auxetic lattices can be competitive where Shear is involved, particularly for Hexa-Chiral and Anti-Tetra-Chiral lattices (Saxena et al., 2016).

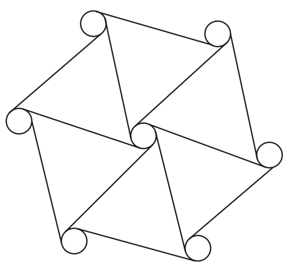

Figure 2.13 Hexa-Chiral.

Chiral

3D Metachiral

The Chiral structures described above exhibit rotational symmetry of order n, where n is the number of struts attached to each node, once this constraint is relaxed the following Meta Chiral and Meta-Anti-Chiral structures can exist amongst many others (Hu et al., 2019).

Below, many of the 3D Chiral structures are inspired by periodic 2D structures and likewise can similarly be divided into 3D Chiral and 3D Anti-Chiral-Meta geometries.

3D Compression Twist

A unit cell has four rotational struts off a central circle, rotating around the three principal axes, to form an enclosed cube. It is non-centrosymmetric, as it does not super impose on its mirror image (Frenzel et al., 2017).

(Frenzel et al., 2017) in the figure below, explored the compression twist and its multi-axial expansion, a precedent for the mechanical explorations of this research.

Figure 2.14 Compression Twist.

3D Planar Anti-Tetra-Chiral

The 3D Cellular Metamaterial with Planar Anti-Tetra-Chiral topology is constructed of a Chiral top ring. The top ring is Chiral (clockwise) and the bottom is Anti-Chiral (Anti clockwise) connected by four diagonally rotating struts.

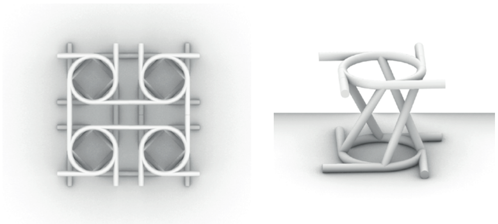

Figure 2.15 Planar Anti-Tetra-Chiral.

These structures exhibit on-axis Auxetic behaviour, where the extent of Auxeticity is dependent on the strut length, scale of the node and the angles between the struts and nodes (Hu et al., 2015).

(Ebrahimi et al., 2018) in the figure above, parametrically model this geometry and used AM to fabricate it in a single material, to demonstrate negative Poisson's ratio under non-linear strain.

Chiral

Chiral and Anti-Chiral 3D metastructures exist with circular, polygonal, elliptical, sphere and cubic node and strut units, which connect to neighbouring nodes to form 2D or 3D geometries.

The deformation mechanisms of chiral structures are enabled through node rotation and strut bending under externally applied loads. (Wu et al., 2018). However, Chiral structures have limited structural variation and therefore, pose fewer design opportunities when compared to their Rotating Unit and re-entrant counterparts.

Attard et al. proposed a particular instance where Chiral Auxetic Structures could be used to morph to synclastic dome surfaces, through relatively simple deformations (Wu et al., 2019). (Wu
et al., 2019) also note that 2D and 3D Chiral structures present many multifunctional uses, including Auxetic Stents and flexible robotics among others, (Wu et al., 2019) as a result of their unique compression-twist effects. This desired deformation has more recently been enabled through AM, for sportswear and blast impact devices (Wu et al., 2019).

[2.1.4] Rotating Rigid Units

Survey of Rotating Rigid and Semi Rigid Structures including Rotating Squares, Rotating Bisquares, Rotating Triangles, Star Perforations, 3D Rotating Units.

The last studied class of Auxetic structures is the Rotating Units mechanisms. Rotating squares, rectangles, rhombi, triangles, parallelograms and tetrahedral geometries have all been reported.

Rotating Rigid Unit mechanisms are arranged in their initial position slightly tilted in the clockwise or counter clockwise directions, which is opposite to the tilting direction of the nearby units (Cho et al., 2019). When a load is applied the Rotating units will rotate at the nodes (Kolken & Zadpoor, 2017).

Local rotation causes the Auxetic effect in which the hinges connected to the left and right units move outward and expand in all directions, continuing until the polygons are aligned with the tensile load, and the Negative Poissons ratio is at its maximum.

Semi Rigid Models

Semi Rigid models are also studied in addition to Rigid Rotating models.

When the Rotating Squares are considered to be semirigid, the Poissons ratio are dependent on the relative rigidity of the units with respect to the rigidity of the hinges, as well as the direction of loading (Hu et al., 2019).

Structures listed were initially surveyed, those not listed were not investigated. Those marked with an X in the figure below were intially analysed but later dismissed, the remaining listed and visually depicted will be used in the primary research phase.

Rotating Units	
Rotating Squares	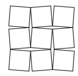
Rotating Bi-Squares	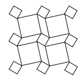
Rotating Rectangles	X
Rotating Trans-Rectangles	X
Rotating Bi-Rectangles	X
Rotating Rhombi	X
Rotating Triangles	X
Rotating Isosceles Triangles	X
Rotating Bi -Triangles	X
Rotating Hexa-Triangular	X
Rotating Tetrahedral	X
Hierarchical Rotating	X
3D Rotating Squares	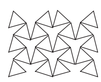
Regular Square Prism	X
Regular Triangular Prism	X

Figure 2.16 Rotating Units.

Rotating Units

Rotating Squares

Rotating Rigid Squares are repeated units of Rigid Squares with hinges at the converging nodes. The squares are tilted slightly in, in their resting positions, revealing rhombic voids.

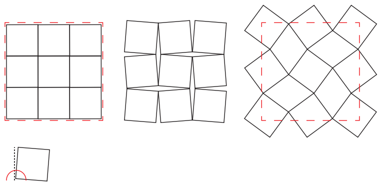

Figure 2.17 Rotating Units.

The initial tilt of each unit initiates rotation in respect to the tensile load and subsequent lateral deformation. A tensile force is a torque applied to a unit, the units rotate in the clockwise or counter clockwise directions, or more simply, the opposite direction to the neighbouring units.

Grima et al. (2010), experimented with planar Rotating Rigid units in both tension and compression, the structures were found to exhibit a wide range of Poissons Ratios. As the material in between the perforations increases, the conformations lose their resemblance and become less Auxetic. In contrast, the system will become more Auxetic once the length of these perforations is increased. Slann et al. (2015) described higher in plane stiffness, explained by the generation of thin, high aspect ratio intercellular regions, which reduce the stiffness and increase the Auxeticity.

It is interesting to note that the Rotating Squares when semirigid have an effect on the Poissons ratio of the structure. This knowledge is critical to the investigations in this research as it validates the concept that the hinge connection plays a prominent role in a structures behaviour. It encourages exploration of multi-material printing using varied densities to allow a range of densities amongst the structure to attempt to enhance the Auxetic effect.

Rotating Bi-Squares

Rotating square structure of different sized squares, the squares have two different length values, one for each square. The Poisson's ratio is strain dependent in all directions of loading, consequently, the structures are isotropic (Hu et al., 2015).

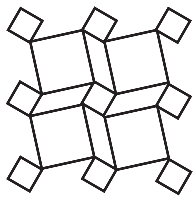

Figure 2.18 Rotating Bi-Squares.

Rotating Triangles

A system of hinged equilateral rigid triangles.

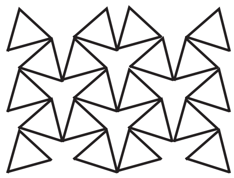

Figure 2.19 Rotating Triangles.

The Poisson's ratio keeps a constant value of negative one regardless of the size of the triangles, the angles between the triangles and the direction of loading. The structure is isotropic, with scale reported to not affect its Auxeticity (Hu et al., 2015).

The stiffness of the hinge was found to hinder the Rotating Triangle's mechanism (Kolken & Zadpoor, 2017) which poses an opportunity for multi-material manufacturing investigations, where a more elastic hinge could enable greater translation.

3D Rotating Units

Kolken & Zadpoor (2017) note that 3D Rotating Rigid Structures are by far the least studied of all Auxetics. Various geometries do exist, where structures are constructed with cuboids. The possible values for n are three, four and six for structures constructed with regular, triangular prisms, square prisms and hexagonal prisms (Kim et al., 2017).

Many rotating units were found to be planar and lack dimensionality, those that were dimensional were often newly discovered and lacked theoretical details.

Rotating Unit structures deform through rotation of the geometry. It has been reported that the degree of rigidity of the joints in the Rotating Units Structures can negatively influence the Auxetic effect, when not managed.

The Rotating Rigid Squares, Type II Rectangles, Equilateral Triangles, Type b Rhombi and Type II b Parallelograms show in-plane isotropy with Poisson's ratios close to negative one. Whereas the Poisson's ratio of the other systems are highly dependent on the direction of loading, and often, the aspect ratio of its units are influential (Kolken & Zadpoor, 2017).

Structural componentry can be customised through geometry, dimension, and composition to achieve different mechanical properties in varied directions (Saxena et al., 2016).

[2.2] Parametric Modelling

A parameter is a factor which defines or determines another operations measure. In parametric CAD software, the term parameter usually signifies a variable term in an equation, which determines other measures, characterised by having a range of possible values.

"Generative design based on parametric models uses algorithmic patterns that rely on geometric relations" (Cucakovic et al., 2016).

[2.2.1] Advanced Design Techniques

Many parameters interconnected in a system can produce a range of outcomes when assigned different values, the system is capable of producing many alternative outputs. When these parameters are customised at different ratios to one another, the system can produce generative results.

Generative design utilises advanced design techniques through parametric control to create highly complex, often difficult to envision results, which are refined to fit within the bounds of which the parameters are based upon.

(Cho et al., 2019) further extend their analysis to describe the dynamic relationship between digital and physical. Where geometry and property characteristics can be manipulated throughout the design process, with the parametric design system, illustrating the interdependency of mediums within the workflow.

Carlos (2012) contextualise the design techniques specifically to Auxetic Structures, describing their design opportunities as two distinct categories; the modelling of the behaviours and the experimental characterisation of the structures. "From these results, the relationship between some geometric parameters and material properties could be found" (Cho et al., 2019).

For example, they describe how the parametric Poisson's ratio directly comments on the maximum area change measure for 2D structures and the volume for 3D structures. (Wu et al., 2019), also recognise the interaction between the various steps in Auxetic Structure investigation which make up the system of realisation, also adding comparisons between physical experimentation and finite element analysis can further inform our understanding of relationships between Poisson's ratio, modulus, porosity and geometry.

Although, digital property testing isn't within the scope of this research, it is interesting to note here and in numerous other examples beyond here, that Auxetic Structures have been found to perform very similarly when computationally simulated as they do in physical experimentation, making the need for both methods of testing in this research unnecessary.

Rather, what is included, and validated by (Wu et al., 2019) is physical experimentation analysis, to inform digital development. A key step in revealing deformation mechanisms and their relationship to digital design parameters, to be managed with software.

Through the analysis of literature, it has become clear that this process of translation involving parametric software is often tailored for the study, (Wu et al., 2019) refer to the relationship as 'Proposed theory and experimentation verification', described by (Konaković-Luković et al., 2018) as engineering, or designing including CAD, shape modelling and mesh geometry models. Studied properties may refer to physical sciences and engineering, whilst analytical formulas may include, theory of computation, geometry and discrete structure or computing methodologies. The close relatability of the two described workflows, demonstrates the necessary steps taken by researchers in the design process to understand, evaluate, design and manufacture Auxetic Structures.

[2.2.2] Software: Rhino and Grasshopper

Rhino is a CAD programme operated by manually selecting operations from a library of available actions. It's plugin, Grasshopper is a visual programming environment, which allows users to design by dragging and dropping predetermined functions to connect them, in what becomes a built script. Grasshopper creates generative designs (Janssen et al. 2011).

The visual data flow of Grasshopper programming creates a larger network, which controls the design artefact in real-time. By altering parameters one can control properties such as shape and size to generate complex geometrical structures and patterns (Oxman & Gu, 2014).

An example of this complexity is Konaković-Luković et al. (2018), development of a biomedical neck brace through tailored Auxetic geometries. The work looks to address the need for varied density of patterning, greater density in higher need areas, and more sparse geometry in less sensitive areas of wearable protection.
Of course, force is not uniformly applied, and therefore, optimisation allows for greater density in some areas and material economy in others, resulting in an irregular cellular structure, which is a fractal hybrid of re-entrant and Rotating Unit Cells.

Figure 2.20 Tailored Auxetic Biomedical Neck brace, (Konaković- Luković et al., 2018).

The design or purposefully placed irregularity of geometries based upon physiological needs, is a conscious consideration required when designing for wearable protection. When a balance is struck, a design harmony is felt, where the art of movement, as well as anatomical needs, are considered equally as structural restraints, a precarious design task. Cho et al. (2019) report in agreement, that gradient structures provide the opportunity for enhanced bending, without sacrificing stiffness, reduced mass and improved comfort, fit and durability for potential snow and racket sport applications.

Also, important to note is the opportunities multi-material printing enables for Parametric development of Auxetic Structures, (Naboni, 2015) demonstrate the computational labour required of the designer to imitate varied density materials with a single material. However, through the capabilities of multi-material printing, a range of material densities on a singular print bed can be achieved, the digitalisation labour is significantly reduced.

[2.2.3] Generative Design and Algorithmic Parameters

Parametric modelling offers clear advantages for the realisation of Auxetic Structures, Carlos (2012), recognise geometries have been well summarised in previous works, but what is repeatedly reoccurring, are details regarding relevant properties and behaviours in a heavily theoretical realm. The theory is desperately in need of a design intervention, entailing the capabilities to translate Auxetics into 3D working models, whilst mitigating unpredictable obstacles which occur naturally in any process of discovery, but ultimately enable the progression of the field.

An interdisciplinary approach, where knowledge exchange between the various disciplines concerned with Auxetic Structures will strengthen the understanding of the materials and enable avenues for the fabrication of structures tailored for specific applications, (Buckmann, 2012).

[2.3] Additive Manufacturing

Upon settling with a generative definition and the combination of parameters, CAD models can be exported to the AM software for manufacture.

The term AM includes all methods which build an object by adding material to a 3D form, layer upon layer. AM techniques have shown unparalleled advantages to traditional manufacturing processes, as they enable rapid prototyping of complex topologies, relatively cheaply and at large scale, built with a range of mechanical properties (Li et al., 2018).

[2.3.1] Multi-material Additive Manufacturing

The multi-material AM process is similar to that of typical AM, both involve importing a CAD model into a pre-processing software, as mentioned above, here lies the key difference. During multi-material manufacturing, print choices such as material assignment, (which entails a range of Digital Material options), speed and resolution are set, the printer and bed is prepared and the file is sent for manufacturing (Barner, 2015).

[2.3.2] Stratasys J750 Printer

The Stratasys J750 is a multi-material printer, available at VUW School of Design Innovation and therefore, the printer at the focus of this research. It is made up of 6 printing nozzles, seen in the figure below, each extrude a different material. Models can be printed using any of these materials on the same print job, as well as a combination of materials during extrusion enables an even greater range of material options, referred to as Digital Materials (Wang et al., 2015).

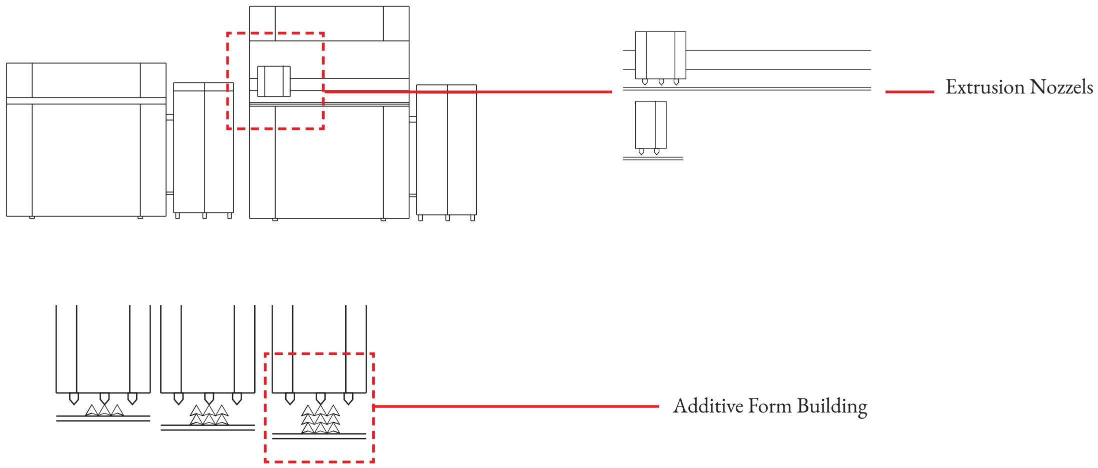

Figure 2.21 Stratasys J750 printer.

[2.3.3] Multi-material Metamaterials

Prior to multi-material printing, it had been difficult to print high fidelity, performative models with intricate architectures. Having the capacity to tune more than one material quality of an Auxetic geometry, simultaneously poses opportunity for a range of design applications, where different density and elasticity in the lattice enhances performance, particularly valuable in impact protection (Chen & Zheng, 2018). These Multi-material Auxetics enable mechanical Auxetics, which has encouraged mounting attention.

[2.3.4] Multi-material Design Parameters

Tuning Auxetic geometry for multi-material cellular structures has many advantages. (Saxena et al. 2016) reported the Poisson's ratio of a multi-material cell is higher than that of a cell manufactured with a single material. The Poisson's ratio of the multi-material re-entrant cell is influenced mainly by geometrical parameters, it is reactive to small strains, which increases its suitability to applications which require intricate responses, such as wearable impact protection devices, which critically situates this research.

Auxetics are no longer limited to theoretical concept, but rather can be now realised in practice (Stratasys, 2016).

The J750 at VUW has primary materials Vero and Agilius. The printer receives the assigned materials as: Agilius30Clear, VeroBlackPlus, VeroCyan-V, VeroMagenta-V, VeroPureWhite, VeroYellow-V. With support material SUP706 and Agilius Shore hardness ranging from 30-95. Resulting combinations of mixing these base materials is illustrated below, understanding these twin material qualities will be fundamental to performative mechanical Auxetics.

Amongst Digital Material assignment are other programmable parameters including hinge angle, strut length and diameter.

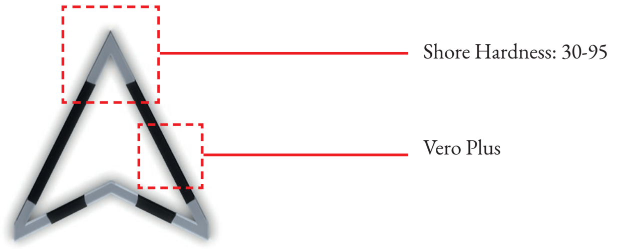

Figure 2.22 Digital Materials.

[2.3.5] Concept and Design of Multi-material Auxetics

Harnessing these Digital Material combinations enables enhanced performance of the geometries when intentionally assigned. There are numerous reports to support the augmentation of the Auxetic effect through multi-material structures, predominantly, where the hinge or vertex is rubber like in its elasticity qualities and the struts are more rigid and robust.

Saxena et al (2016) describe how a softer material assigned to a re-entrant corner will reduce the stiffness at the vertices in a manufactured structure, allowing the struts to articulate with greater ease and subsequently, augmenting the Auxetic effect. The soft material hinge facilitates movement during loading of the Auxetic, as well as allowing tuning of the stiffness of the units overall, this technique has evolved in order to "maximise the Auxetic response" (Saxena et al. 2016). They also reported the multi-material re-entrant cell as having exhibited high strain sensitivity, meaning they are responsive to relatively low strains, an ideal candidate for apparel devices.

In the figure below (Miller & Wilson, 2015), using the Stratasys Connex and materials Vero White and Tango Plus, demonstrated what was one of the very first examples illustrating the benefits of multi-material assignment in Auxetic geometries. Wang et al (2015) further added evidence using the Stratasys Connex350

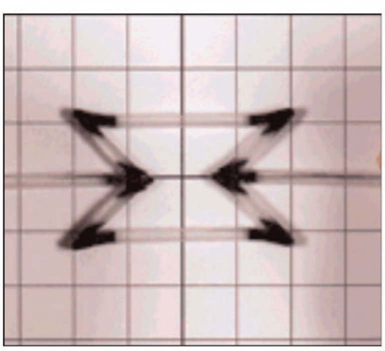

Figure 2.23 Multi-material Auxetic unit, (Miller & Wilson, 2015.

3D printer, demonstrating material selection as a critical parameter in tuning the Auxetic effect. The design articulation involved is complex, however, through assigning flexible material at the vertices of a structure and rigid material at the struts of the geometries, movement is maximised and hence the beginnings of a new dimension in the design space for Auxetic Mechanical Metamaterials.

Bezazi & Scarpa, 2007) experimented further with Auxetic tuning through design development of the vertices, by curving the structures pointed hinges to be more rounded, it removed the stress singularities the structure became exposed to, whilst also investigating the effect internal angles have on the Poisson's ratio.

Another consideration involved with tuning Yang et al. (2015) report, is the implications of altering the thickness of the structures, the increased width of the struts changes their effective length. The tilted geometry of the structure makes it difficult to estimate the effects of the length reduction, further complicated by fillets at the vertices of the structures (Yang et al., 2015).

Multi-materiality of the structure's enables easier translation about the vertices and subsequent rotation of the struts, increasing structural flexibility, an advantage in wearable applications (Stavric & Wiltsche, 2019). Ultimately, greatest control over cell deformation is desired, to enable mechanical tuning of a structure without changing its geometry.

[2.3.6] 4D Printing

4D printing refers to 3D prints which translate through time. Multi-materiality encourages maximised articulation of movement and enhanced 4D nature.

[2.3.7] Multi-material Manufacturing for Impact Protection

The design of impact protection is particularly well suited to multi-material Auxetics for their range of stiffness values, as well as good strain sensitivity. The negative Poisson's ratio can be manipulated by altering the geometrical parameters. The unit cells' stiffness can be altered by controlling the materials density through the hinge and strut. The soft rubber like material will impart good strain sensitivity for protection against low velocity impacts (Bickel et al., 2010). The dual material designs could enable a range of strength and crushing strains in sports helmets, reports Saxena et al., (2016), also noting the ability to tailor the stiffness of the materials cells is highly desired.

Novel Auxetic Structures using AM techniques make ideal candidates for sports protection equipment design writes (Shepherd et al., 2017). (Lu et al. 2016) highlighted Auxetic potential for body protection applications in sport, including helmets, gloves and shoulder pads.

Recent advances in AM techniques are enabling fabrication of materials with complex micro-architectures (Kolken & Zadpoor, 2017), those such as Auxetic Structures, through exploiting manufacturing techniques novel functionalities emerge (Tong, 2018).

Multi-material combinations and assignment have the capacity to start new paradigms
in the design of mechanical metamaterials, enriching the possibilities for design and manufacturing of active, adaptable, and programmable geometries (Zadpoor, 2016).

The translation process from Auxetic theory to digital means and subsequently manufacturing, leads to some fundamental questions around the Auxetic effect. Theoretical models are derived and recorded as rigid line drawings, continuous experimentation with multi-material printing will enable more substantial experimentation with tuning variables to form robust understandings to best inform sports protection applications (Wang et al., 2015).

[2.4] Sport and Impact

[2.4.1] Sport Classification

Sport, in some capacity is part of every person's life. Whether simply as a means of commuting or for recreation, to being competitive, any sport comes with some risk of injury.

Accident Compensation Corporation (ACC), in New Zealand, records injuries amongst a range of other measures to form detailed data around sport and injury and aid recovery.

However, better than recovery is management to avoid injury and one of the most effective ways to achieve this is through wearable protection. Of course, sports protection does already exist, however, it often lacks tailored properties for impact, does not fit the body in a customised manner, or is misplaced.

Auxetic componentry could be different. It doesn't seek to replace existing protection, rather aid further injury prevention or target vulnerable areas in new ways.

The ACC data includes all reported accidents causing harm through the years 2015- 2019.

Auxetic Structures are well suited to impact for their superior capacity to absorb and dissipate energy received from another body (Naboni, 2015) as well as excellent resilience under dynamic impact loading (Cho et al., 2019), making them very well suited for the opportunities to minimise injury in sport.

[2.4.2] Sport

Sports can be categorised into primary groups, including physical, mind, motorised, coordination, and animal supported.

This research will focus on those that are most heavily affected by impact, in order to maximise Auxetic Potential. Therefore, only physical based, coordination, motorised and animal supported will continue to be included.

[2.5] Injury and Protection

[2.5.1] ACC Injury Breakdown

However, when injuries do occur, they are often complex and the result of a range of contributing factors. ACC have further categorised incidents causing injury into categories including, collision/ knocked over by an object, lifting/carrying/strain, loss of balance, person, animal supressed values, twisting movement (ACC, 2019). By analysing the scenarios in greater detail, it is easier to understand anatomical effects of impact.

[2.5.2] Impact

Impact in sport can stem from a range of origins, the most common injury scenarios involve Mechanical, Gravitational and Kinetic energy through human to human or human to object collision, as well as human striking environment.

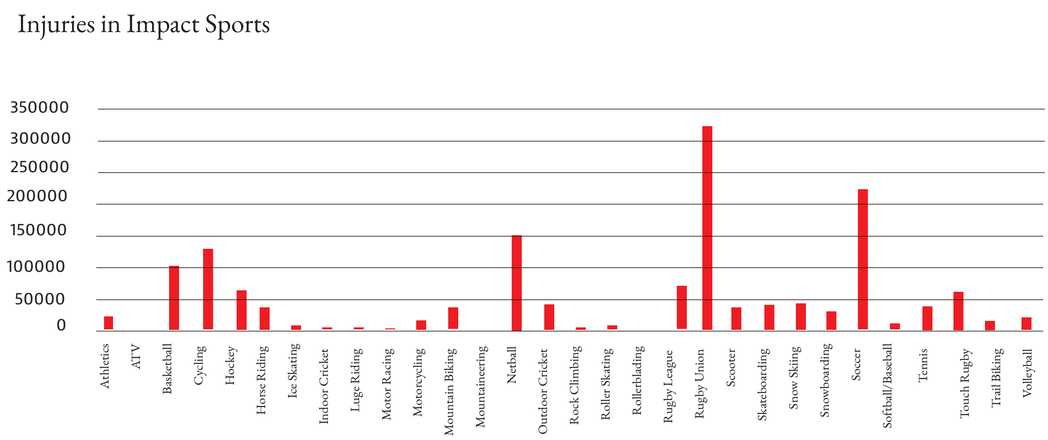

Figure 2.24 Injuries in impact Sports, published with permission from ACC NZ.

Anatomical Regions

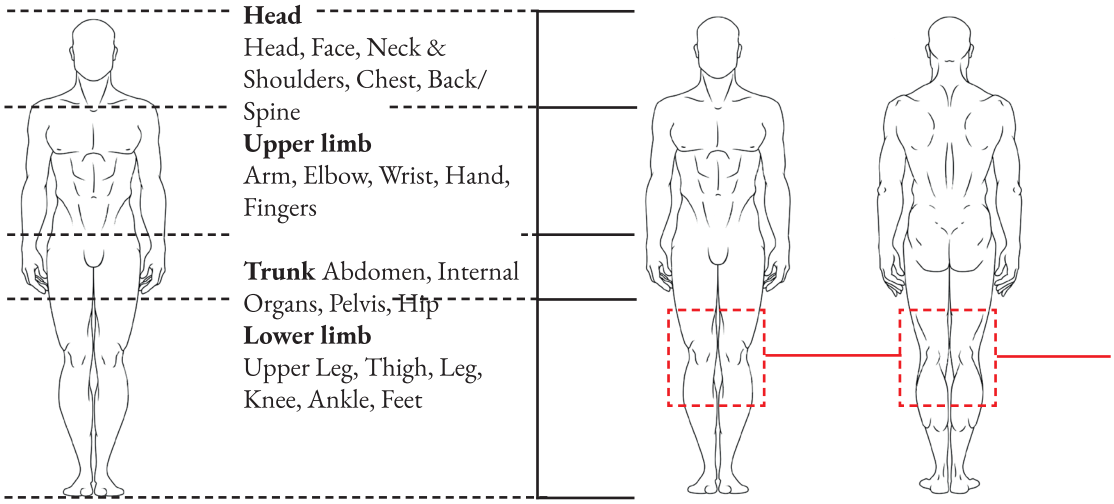

Figure. 2.25 Impact and injury.

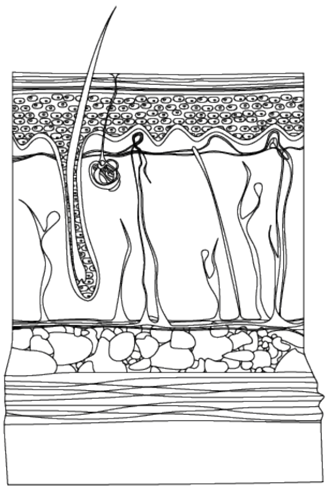

Depth of Injury	Injuries
Skin Epidermis and Dermis	**Surface Wounds**
Fat (Nerve and Vein) Nervous System	**Soft Tissue/Nerve Injury**
Muscle Muscular System	**Muscle Injuries**
Bone Skeletal System	**Breaks/Fractures**
	Brain Injuries

[2.5.3] Anatomical Effects

Injuries can be anywhere on the body. The site is critically important to understanding the intensity of the injury, as well as its lasting affects. Body Sites where data injury is recorded include:

Abdomen/ Pelvis
Ankle
Back/Spine
Chest
Ear
Elbow
Face
Finger, Thumb
Foot
Hand/ Wrist
Head (Except Face) Hip/ Upper Leg/ Thigh
Internal Organ
Knee
Lower Leg
Multiple Locations
Neck/ Back of Head Vertebrae
Nose
Shoulder (Including Clavicle/ Blade)
Toe
Upper and Lower Arm

(ACC, 2019).

The human body areas are all apart of larger operating systems, only those known to suffer from impact injuries will be included in this research, they are, Circulatory, Respiratory, Nervous, Skeletal and Muscular.

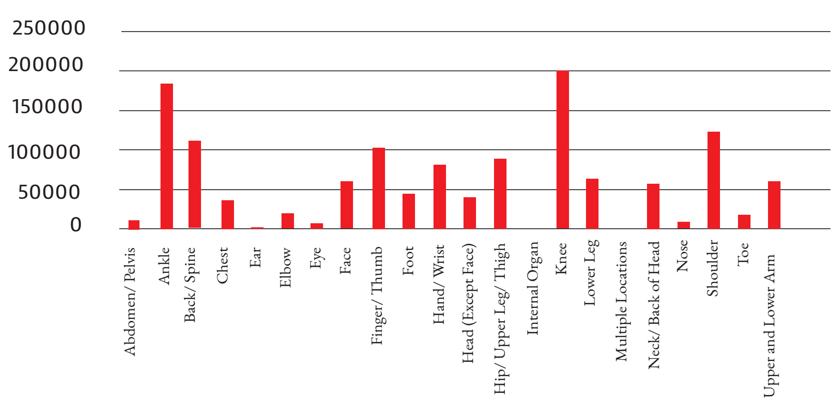

Figure 2.26 Injuries sites in Impact Sports, published with permission from ACC NZ.

[2.5.4] Common Injury Scenarios

Integral to understanding anatomy and the implications of sports related impacts causing injury in the human body, is understanding the scenarios which allow these injuries to come about. Although there are endless ways in which one could incur an injury, there are certainly some sporting instances responsible for far more injuries that others.

Further analysis of situation specific details or injuries and impact will be explored further in Part Two of the Primary Research, during contextualisation, however, a collection of notable starting points are described below.

Brain injuries induced by biomechanical forces lead to structural damage, rapid onset of short lived impairment, but they can also cause long term functional disturbance with cognitive effects (Malcolm, 2019). The most common diagnosis of impact to the head is concussion or traumatic brain injury.

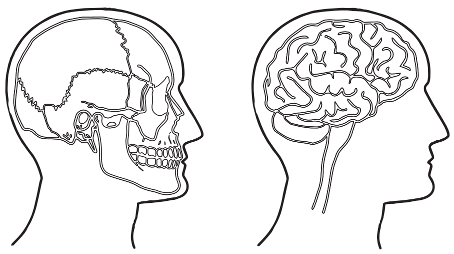

Figure. 2.27 (a) Human skull and (b) Brain.

Soft Tissue Knee Injury

The knee joint is the connection point where the tibia and femur meet at the patella. The meniscus or cartilage provides both impact support and lubricant to the joint. The ligaments control motion and prevent against unnatural movement.

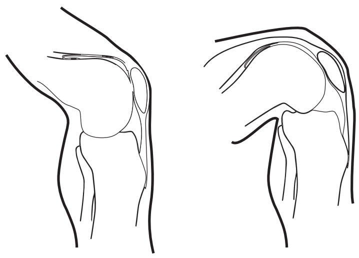

Figure. 2.28 (a) Human knee flexed and (b) extended.

Often ACL injuries occur when a person suddenly twists without having the necessary strength to counteract this motion, as a result the knee is at risk of slipping out and tearing the ACL. In other circumstances, an impact to the inside of the knee compounds stress on the outside of the knee, overwhelming magnitude can cause the ACL to tear. Similarly, the meniscus can be torn as a result of sudden, violent movement.

[2.5.5] Non Auxetic Protection

Protection includes any measure taken to guard against damage caused by external forces.
In a sports context, its primary purpose is to maximise the safety of an athlete.

Protection can be either Personal Protection Equipment (PPE) or an addition to the environment, such as a crash mat or barrier. This research focuses on the enhancement of protective equipment through Auxetic componentry in order to provide support to the nervous, muscular and skeletal systems. Through limiting peak accelerations and subsequent transferal of force, increasing
contact time, distributing load and performing energy attenuation through dissipating and absorbing energy, Auxetic Structures provide many opportunities to increase athlete safety when faced with impact.

One particularly notable area of innovation is improving helmet design. In terms of protection against concussion, biotechnical innovation is focused on the enhancement of preventative equipment, as well as diagnostic tools (Malcolm, 2019). Although helmets in high impact, gravity sports are desperately essential, everyday activities such as commuter cycling is increasingly, bringing growing concern for current helmets, their responsibility and current certifications for primarily protecting against linear accelerations.

Rotational acceleration has been identified as the principal cause of head injury. The MIPS Brain Protection System, however, is a multi-directional Impact Protection System, fitted between the comfort padding and EPS foam, allowing the head to move inside the helmet.
By reducing damaging rotational motion being transferred to the brain, through redirection of energies, strain on brain tissue, leading to serious damage is limited. The MIPS technology serves as a component, contributing to improved helmet protection, illustrating that protection can be as effective when it is combined with already existing technology, validating this researches' pursuit to offer Auxetic componentry to compliment already existing protection and provide better safety for athletes.

Bateman (2018) designed a speculative helmet using Pentamode strucutres, another class of Metamaterials, harnessing the excellent qualities of the synthetic structure for enhanced protection.

Figure 2.29 Pentamode protection, (Bateman, 2018).

[2.5.6] Case Studies

Pacific Helmets

Pacific Helmets are a world class PPE company, specialising in head protection for motorised sports, as well as first responders.

They offer a range of models targeting different impact natures with customisable features.
The figure illustrates a part of the extensive case study undertaken to understand user needs and market demand of protection equipment for high performing athletes, as well as requirements for responder professionals.

One notable design is the F15 Structural Firefighting Helmet Jet Style. The Pacific F15 combines a Kevlar and Fiberglass composite shell with a flexible polymer chassis to ensure its lightweight and durable nature. The helmet protects the human from external impact as well as foreign penetration, chemicals and flames. With an optimised centre of gravity, it also includes the dual pivot face shield through a dual pivot system. It involves 8 structural and aesthetic customisable options, illustrating the value in assembly of componentry for customisation.

OBO

OBO specialise in American Field Hockey, providing the highest quality protection from head to toe. One design is their Carbon Helmet, constructed from Carbon fibre it is both strong and lightweight,
allowing maximum movement and protection.
A flexible resin formula, combined with closed cell polyethylene makes it comfortable whilst durable, highlighting the need to strike the perfect balance between comfort and protection.

The OBO ROBO Body Amour range is constructed from individual pieces of foam, allowing for free movement, ensuring agility, whilst remaining highly protective. The components can move independently, to ensure live positioning. The high-density foam covers the vital organs while the chest and heart are further protected with a comfortable and breathable inner pad. The protection is customisable through adjustable back straps, which sculpt to the body, highlighting conformability as highly valued in protection.

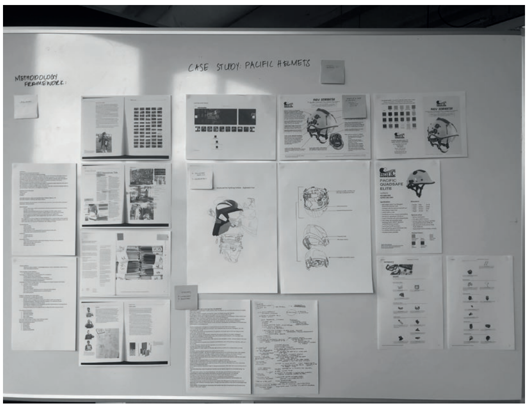

Figure 2.30 & 2.31 Case Study Research.

[2.6] Auxetic Contextualisation

Many high performing sports protection devices will serve as exceptional precedents for Auxetic impact contextualisation, the background research above has clearly demonstrated the high incident rates
of injuries in sports, particularly in those where protection already exists or is typically worn, this validates the need for an Auxetic intervention in the form of componentry, to further enhance the reduction of long-term suffering as a result of sport injuries. Few studies have made it to realistic application of Auxetic geometries, nor digitally or physically, however, the beginnings are well on their way.

High Indentation Resistance, but low Young's Modulus, could be harnessed to optimise material performance. Assuming a constant Young's Modulus, as Poisson's ratio increases towards −1, the geometry is expected to exhibit higher resistance to Shear, whilst retaining high Indentation Resistance.

[2.6.1] Auxetic Structures and Impact

Auxetic Structures provide protection against impact by absorbing and dissipating energy to reduce peak forces, pressures and impulses. Additionally, they also have increased Shear Modulus, Indentation Resistance and decreased Bulk Modulus, made possible through lateral expansion due to axial tensile loading. The negative Poisson's ratio enables them to adopt a dome shape, referred to as synclastic curvature. The ability to control individual units and increase cell density through an Auxetic dome leads to greater strut deformation and subsequent higher energy absorption. In contrast, a lowered cell density in an Auxetic lattice leads to lower stiffness, higher bending and increased rotation of the struts, ultimately, increasing the negative Poisson's ratio. Auxetics show enhanced porosity variation when stretched or compressed, which often leads to enhanced energy absorption during impact.

Negative Poisson's ratio has also been measured for Auxetics subject to high-speed compression, they have been shown to be superior when compared to a semi rigid typical shell, at limiting forces from concentrated impact loads (Allen et al., 2017). Additionally, the ability to change the Shear modulus of a material through tuning of the Poisson's ratio can lead to reduced rotational acceleration.

[2.6.2] Auxetic Structures for Sports Protection

Auxetic Structures have potential for various sporting and impact scenarios, where their unique architectures can be exploited for the superior mechanical responses they produce. A range of safety devices could benefit from the described behavioural qualities, such as pads, gloves, helmets and mats, all enhancing energy absorption, whilst remaining relatively lightweight.

Further developments to Auxetic protection could include gradient sheets with a range of Poisson's ratios, designed to be tailored to smart garments for sporting situations, such as Auxetic Rugby tops, Snow Sport helmets,
Tennis rackets and Hockey stick handles. All of which could benefit from increased rigidity and lower mass. The multi-axial expansion materials with dome curvature have also been proposed for implementation into footwear and helmet pad products to deform with the movements of the athlete (Duncan et al., 2018).

Ultimately, there is substantial evidence to support the pursuit of contextualising Auxetic Structures for sports protection, aiming to limit harmful impact forces (Duncan et al., 2016).

[2.6.3] High Performing Auxetic Protection

The Nike Free RN Fly knit Auxetic Patent running shoe expands with a runner's foot, reducing uncomfortable pressure points. The Flyknit exhibits an architectured, closed cell foam outer sole, of Auxetic rotating triangles, designed to biaxially expand as the runner moves about, increasing energy absorption and comfort (Duncan, 2018).

When the material is under tension, it expands in both directions, the geometrical configuration has hinged polygons which rotate with respect to one another when the sole is under lateral or longitudinal tension, increasing the lateral and longitudinal dimensionality (Cross et al., 2016).

"Auxetic's versatility in reacting to the shape of impacting bodies is three fold; higher density, more lateral deformation and more compressed material" (Duncan, 2018).

[redacted]

Figure 2.32. Auxetic Sports Protection, (Franz, 2018).

[2.6.4] Speculative Auxetic Sports Applications

Auxetic Structures have been suggested for a range of sports protection applications. Continuous developing manufacturing techniques are bringing speculative protection concepts closer to realisation.

A key characteristic of Auxetic Structures is their ability to flexibly withstand both compressive and tensile loads, resisting penetrating objects, whilst remaining compliant over large areas ultimately, dissipating more energy than their conventional counterparts. As they become more Auxetic, the Shear modulus increases during indentation, providing a larger compressed area, with more material involved, increasing energy absorption.

Figure 2.33 Background research.

[2.6.5] Design Intervention

Existing Auxetic topologies are based on the use of a single material for fabrication. Exploration into multi-material Auxetics could in the future enable new Auxetic mechanisms. However, this research is the beginnings of exploration into the opportunities for Auxetic Structures constructed with multi-materials, driven by the discipline of design.

Contextualisation of Auxetic Structures in this research, is a specific response to the proven need for improved protection for athletes in high impact sports. It doesn't wish to replace current impact protection, but rather investigate means in which the structures can be used to add additional support to pre-existing protection, by harnessing highly desired Auxetic properties and implementing them into speculative sporting componentry. (Kolken & Zadpoor, 2017).

Saxena et al. (2016) detail exactly how Auxetic Structures make ideal candidates for sports protective devices. The Chiral Arrowhead showed promising performance for helmet protection, their particularly low stiffness explained by freedom gained through rotation of the cylinders. The Anti-Tetra-Chiral shows great potential for its highly negative Poisson's ratio and anisotropic nature. The Tri-Chiral structures can be considered the least Auxetic, in-plane isotropy can be achieved with Hexa-Chiral unit cells. (Kolken & Zadpoor, 2017) suggest that re-entrant structures outperform Chiral and Rotating Rigid Models in terms of their Poisson's ratios and subsequent stiffness. Anisotropic re-entrant structures appear to offer a balance between structural rigidity and negative Poisson's ratio. In contrast, Rotating Rigid Structures offer a relatively high Young's Modulus, as a result of the bulk material, which decreases the negative Poisson's ratio.

The specifics of geometry characteristics understood through the background research will inform the beginnings of the Primary Research.

3 METHODOLOGICAL FRAMEWORKS

3.1	Research Domain	60
3.2	Research Question and Hypothesis	61
3.3	Design Criteria	62
3.4	Methods and Methodologies	63
3.5	Evaluation	76
3.6	Outputs and Outcomes	79

The following methodologies present frameworks of theoretical processes to ensure a systematic inquiry, to create explicit knowledge. The chapters structure is shaped by (Rodriguez Ramirez, 2017), A Postgraduate Thesis Model.

Figure 3.01 Domain analysis: Situating the research.

[3.1] Domain

This research seeks to use the discipline of design to contextualise Auxetic Structures for speculative sports scenarios. Through the translation of theory into digital models, which are parametrically controlled, it will enable both customisation and digital fabrication, of Auxetic Structures. Both necessary mediums to design within, in order to achieve contextualisation.

The background research above, identified the most viable Auxetic Structures for exploration, additionally, it recognised the opportunities for building upon future research. The methodologies described below are the necessary processes required to bring these discoveries to life.

[3.2] Research Question and Hypothesis

[3.2.1] Research Question

The problem-solving research question below will guide exploration in the research domain.

How can we optimise multi-material 4D printing to dictate dynamic performance in Biaxial Auxetic Structures, for enhanced human protection in safety applications?

[3.2.2] Hypothesis

Parametric customisation of geometry in Auxetic Structures will allow for predictable, resultant behaviours. Additionally, multi-material printing can enable the manufacture of ergonomically designed forms for body and sport specific, injury protection.

[3.2.3] Philosophical Standpoint

This is a primarily science-based research approach. The ontology involves engaging with proven Auxetic Structure principle mechanics. The epistemology reflects the mathematics of the mechanics, which the structures are built upon. The methodologies all take primarily mathematical laws into consideration when designing. The products are speculative designs with calculated material behaviours, designed to optimise geometrical characteristics.

[3.3] Design Criteria

The design criteria will be used to assess designs created throughout the research portfolio. Outputs will be systematically assessed for fulfilling the criteria, describing how the designs explicitly contribute to the research field.

The initial criteria is motivational based and demonstrates the designer's interest from a personal perspective. For example; designs should, be reflective of a passion to contribute to human protection and minimising injury in sports, by targeting high impact protection, utilise Auxetic Structure theory to enable improved material behaviours, explore multi-material printing advantages, controlled through emerging parametric and generative software.

Furthermore, the motivational criteria is built upon to reflect the academic intentions of the research.

Design Criteria
Based on findings from the literature review, designs should

[1] Exhibit multidirectional Auxetic behaviour through biaxial geometries

[2] Should be parametrically controlled through Grasshopper and Rhino to enable manipulation of characteristics and resultant behaviours

[3] Be printed using the J750 to utilise multi-material AM and promote dynamic movement

[4] Tangibly translate Auxetic theory into applicable contexts through parametric modelling

[5] Be focused on minimising human injury in sport by targeting componentry for protection in high impact sports.

[3.4] Methods and Methodologies

A combination of Divergent and Convergent thinking, (Laurel, 2003) will make up the design actions working to fulfil the described design criteria. Divergent design discovery will be carried out through surveying of the metamaterial classes, observing existing studies and identifying opportunities for parametric modelling and AM. Convergent thinking approach will be implemented when designing structure geometries and mechanical movements, so as to stay within the bounds of Auxetic behaviour.

[3.4.1] Methods

Researching, exploring, experimenting and testing will follow systematic forms of research. Each methodology is guided by methods used to fulfil the design criteria, as well as the research aims and objectives. The methods are achieved through design and are described in the methodology tables below.

[3.4.2] Research Frameworks

The theoretical frameworks used in this research are a constructed combination of methodologies, used to both guide analytical explorations through the aims and objectives and to fulfil the design criteria. The design process illustrated below is a mixed methods approach, combining both Quantitative and Qualitative research approaches (Creswell and Creswell, 2018).

Research for Design (Milton & Rogers, 2013)

The background research was conducted through Research for Design. Systematic data collection and analysis of both a quantitative and qualitative nature both informed preliminary understandings, as well as refined the design domain and situated the research amongst a greater context and a Design Science paradigm. Research for Design is at essence, research to enable design, it enables a framework for meaningful information and data to be collected and collated in order to inform the design process.

Scientific Design

Scientific design is the design practice based upon scientific knowledge. It is the systematic use of scientific and technological knowledge through the design process and discipline of design to enable the creation of artefacts.

Design science is a rational approach to design, utilising scientific knowledge from fields such as material science and engineering. The design science relationship is one reliant on the other to enable expression, (Cross, 2001), design "makes science visible" (Willem, 1990).

Research through Design

Research through design, is an applied research approach of action through practice, involving both qualitative and quantitative research methods. Through systematic, experimental discovery, research through practical discovery produces design artefacts.

Research through design involves three phases, research, design and publication. The discoveries of the design experimentation and design research process are not limited to the context in which the knowledge is applied to in the application phase. Rather, the discoveries are of value in a range of contexts, this is a key difference to note between research and product development.

The figure below is a modified iterative process cycle, it describes the design actions of looking, learning, prototyping, testing, evaluating and communicating as described by (Milton & Rogers, 2013) and will be implemented for each Auxetic Structure survey explored.

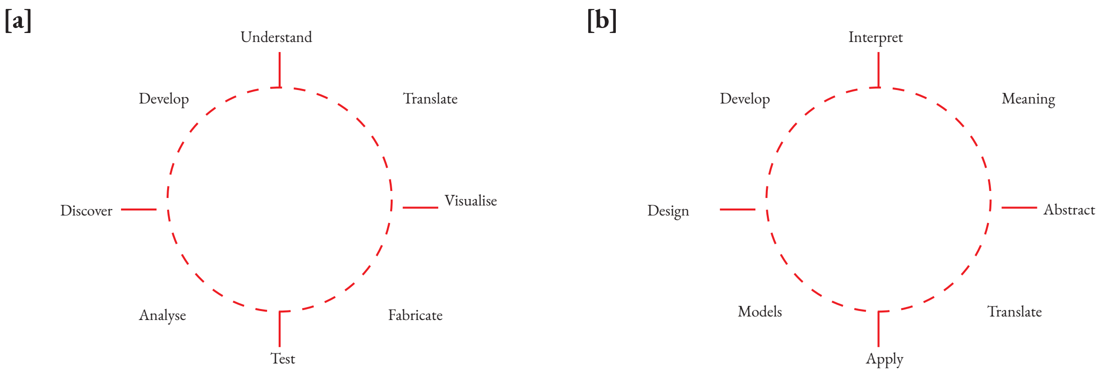

Figure 3.02 Simplified Research through Design, Design Process. (a) Part One of the Primary Research, (b) PartTwo.

[3.4.3] Aims and Objectives

Methodology: Research For Design

Chapter		**Background Research**
Aims	**Aim One: Research** Through secondary metamaterial-based research resources, explore how biaxial Auxetic Structures behave differently to typical Auxetic Structures in various application scenarios.	
Objectives		**Objective 1a.** Gain a physics-based understanding of metamaterial science through exploratory secondary research (Martin & Hannington, 2012), to establish structure characteristics as well as properties of multiaxial Auxetics.
Design Criteria		**Criteria 1**
Methods		**Secondary Research** (Martin & Hannington, 2012)

	Literature Review	**Methodological Frameworks**
Objective 1b. Systematically analyse and evaluate previous projects in the field of Auxetics through exploratory Precedent Based Analysis (Eilouti, 2019) with a refined focus for Case Study topics (Yin, 2017) and compare the existing precedents in a Pugh Matrix.	**Objective 1c.** Through exploratory secondary research understand domain connections, to develop a refined metamaterial understanding through the use of the Literature Review (Martin & Hannington, 2012).	**Objective 1d.** Formulate design points through Criteria Based Design (Martin & Hannington, 2012) to establish critical Auxetic characteristics, integral axial movements and environment constraints, as well as application directions.
		Criteria 2
Precedent Based Design (Eilouti, 2019) Utilising industry products and innovation to inform research explorations. Design precedents include any prior design solutions that are of interest to new design solutions and using them to inform this research. **Case Study** (Yin, 2017) Collecting case study evidence through documentation, archival records, and observations, amongst other sources.	**Literature Review** (Martin & Hannington, 2012).	**Criteria Based Design** (Rodriguez Ramirez, 2017).

Aims and Objectives

Methodology: Research Through Design & Scientific Design

Chapter	**Primary Research**	
Aims	**Aim Two: Design** Design and build parametric biaxial Auxetic models using Rhino and plugin Grasshopper, to exploit control and produce digitally generated structures and AM prototypes which can be used for application testing.	
Objectives		**Objective 2a.** With a divergent thinking (Laurel, 2001) perspective use generative and evaluative Iterative Prototyping (Martin & Hannington, 2012) to parametrically design and develop a range of biaxial geometries through Grasshopper.
Design Criteria	**Criteria 2**	**Criteria 3**
Methods		**Iterative Prototyping** (Laurel, 2003). Based upon a process of design prototyping, testing, analysing and refining the work in progress. An ongoing dialogue between the designer and the designs (Laurel, 2003).

Additive Manufacturing and Evaluation	Design Studies	Application
Objective 2b. AM of various structure prototypes for testing using evaluative experiment method (Martin & Hannington, 2012) to determine material integrity and resulting impact effects under various applied forces.	**Objective 2c.** Test against the design criteria from objective 1d to ensure the structures are Auxetic in nature and axially consistent as prototypes. Use Evaluative Matrices to visually represent the results of structures in relation to one another.	**Objective 2d.** Utilise generative research method, Concept Mapping, (Martin & Hannington, 2012) to refine the design domain in which the applications will be most effective.
		Criteria 4
Material Testing Experiments (Milton & Rogers, 2017). Technical evaluations undertaken through the use of test rigs, aimed to apply mechanical strains. Evaluate prototypes to validate design decisions, (Milton & Rogers, 2013).	**Evaluative Matrix** (Milton & Rogers, 2017). Experiments measure the effect that an action has on a situation, by demonstrating a relationship. Material testing experiments (Milton & Rogers, 2013).	**Concept Mapping** (Martin & Hannington, 2012). Mapping materials by characteristics and behavioural properties, as well as high risk injuries, anatomy effected, most common sports and connecting domains in a meaningful way, (Martin & Hannington, 2012).

Aims and Objectives

Methodology: Research Through Design & Scientific Design

Chapter	**Primary Research**	
Aims	**Aim Three: Evaluation** Evaluate most promising and developed 4D multi-material, biaxial Auxetic geometric structural and refined application opportunities for a proposed design output.	
Objectives		**Objective 3a** For initial evaluation allow industry partner specialists at Pacific Helmets to detect baseline issues in the analytical workings.
Design Criteria		**Criteria 5**
Methods		

Application

Discussion

Objective 3b
Refine any structural development through established CAD parametric controls, ensuring biaxial, Auxetic, dynamic behaviours are being optimised by multi-material printing in the applied context.

Objective 3c
Final high fidelity biaxial Auxetic Structure proof of concept prototypes: exhibiting 4D printed multi-material capabilities with most successful contextualisation, situationally specific and structurally robust parameters.

Objective 3d
Systematically reflect upon design criteria requirements, analysing and evaluating the performance of the 4D multi-material, High Fidelity Biaxial Auxetic Structure prototypes, from both a theoretical structural point, as well as a manufacturing perspective.

Evaluative Matrix
(Milton & Rogers, 2017).

[3.4.4] Workflow Frameworks

The following process is a combination of several methodological frameworks. Integrated and modified to carve a bespoke, systematic journey for this research, through models of similar studies combined. This process is based upon rich feedback - loops, across interdisciplinary fields which facilitate synergistic perspectives. Parametric modelling through Rhinoceros and plugin Grasshopper allow for a wide range of design customisation, where conventional programs had rigid constraints. Where traditional methods of CAD modelling meant the creations were static upon realisation. Here, design principles are translated into parametric models with characteristic features. Multi-material 3D printing is used to fabricate rapid prototypes. The samples are then mechanically tested, with their performance characteristics evaluated.

Although, the discovery and development of Auxetic Structures stems from precedents found in nature, this research will focus on the stages of the workflow involved with the digital design, fabrication and application of Auxetic Structures.

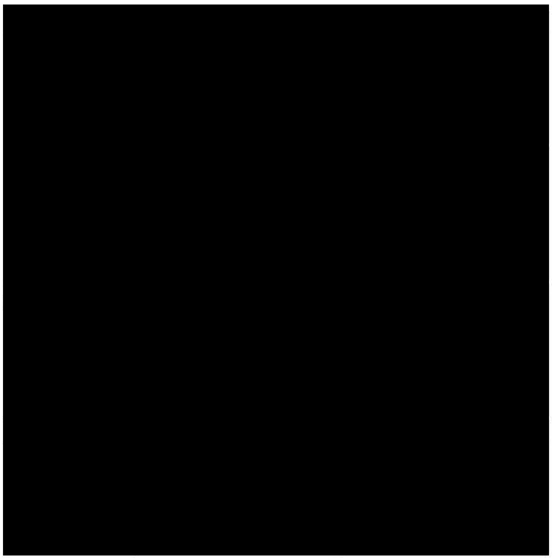

Figure 3.03 Incorporation of biomimicry thinking into the selection of cellular material designs, along with an example for the use of honeycomb designs in mechanical structures. Phylogenetic tree from OneZoom.org, reprinted with permission (Bhate, 2019).

The figure demonstrates a basic, precedent workflow, beginning with scoping, to obtain specific details, and functional requirements are defined. Discovering, involves abstracting parameters which lead to design principles. Creating, where design principles are developed. to translate the abstracted science into useful means for the engineering designer. Finally, evaluating, the design is compared against other models through numerical and experimental techniques, which work to validate the hypothesised designs.

The methodology described by (Bhate, 2019) is a synthetic specific translation of the process of digital materials design and manufacturing. It simply highlights the capabilities or opportunities in the various stages of the framework, as well as the challenges which can be expected.

This workflow model highlights the importance in considering and selecting geometries for their unique qualities, a key question asked, "what is the optimum unit cell to select relative to performance requirements, manufacturability and other constraints" (Bhate, 2016). This research focuses on the translation of Auxetic Structures from theory to fabrication through multi-material printing. Therefore, the optimisation phase will not be explored, instead emphasis will be on the preparation of files for fabrication on the J750 printer.

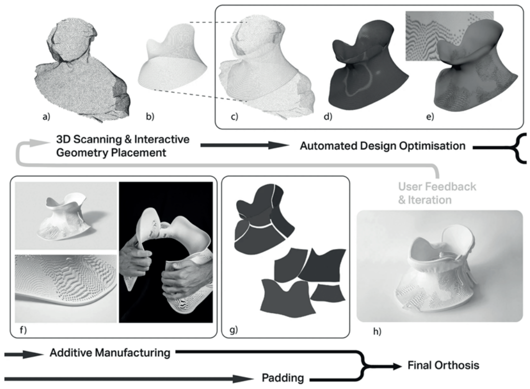

Figure 3.04 Schematic representation of design workflow and fabrication process of custom orthosis. Reprinted with permission, converted to grayscale. Creative Commons Attribution 4.0 International License, http://creativecommons.org/licenses/by/4.0/. (Hale, et al., 2020).

Workflow Framework

Design Process	**Inspiration**	**Background Research**	**Abstract knowledge**
Design Phase	Natural Precedents 	Theory 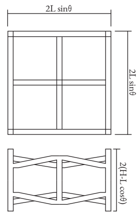	Theoretical Modelling 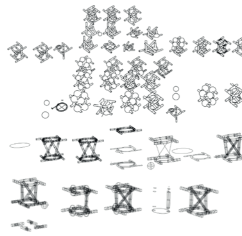
CAD Software		Rhino	
Methodology	Research for Design		Research through Design
Aims & Objectives	**Aim One: Research**	Objective 1a Objective 1c	Objective 1b
Methods		Secondary Research Literature Review	Precedent Based Design Case Study

Part1: Mechanical Experimentation

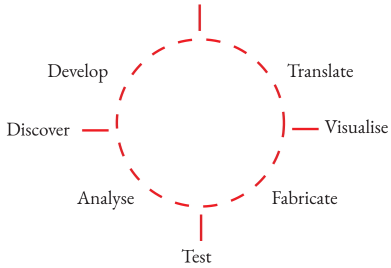

Design Process	**Design Development**			**Evaluation**
Design Phase	Prototyping 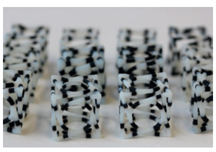	Additive Manufacturing 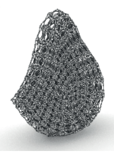	Fabrication and Post-processing 	Experimental Tes 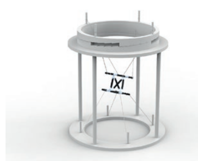
CAD Software		GrabCAD		
Methodology	Research through Design	Scientific Design		
Aims & Objectives		Objective 2b		Objective 2c
Methods	Material Testing Experiments			Evaluative Matrix

Primary Research	Conceptualisation	
Design Principles	Mechanical Design	Parametric Modelling
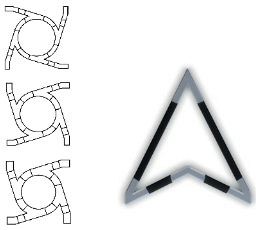		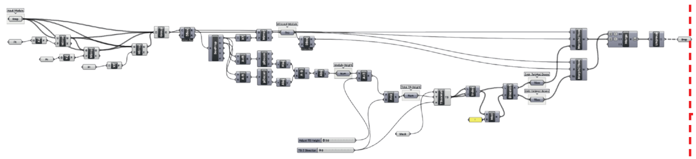
		Grasshopper Grasshopper Plugins

	Scientific Design		
Objective 1d	**Aim Two: Design**	Objective 2a	
Criteria Based Design		Iterative Prototyping	

Iterative Prototyping

Part2: Digital Exploration

Interpret

Develop

Meaning

Design

Abstract

Models

Translate

Apply

Integration	Contextualisation	Application	Development	Design Evaluation
		Applied knowledge	Refined Exploration	Communicating
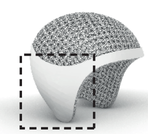		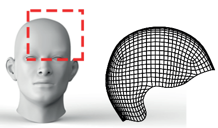		
		Blender	Grasshopper Plugins	Keyshot

	Objective 2d	**Aim Three: Evaluation**	Objective 3a Objective 3b	Objective 3c Objective 3d	
	Concept Mapping		Evaluative Matrix		

[3.5] Evaluation

[3.5.1] Mechanical Testing

The mechanical testing analysis will be circumstantial and described more in the primary research experiments overview. However, some aspects of the evaluation will be universal. Photo documentation through image comparisons and overlaid analysis illustrations, will be practiced in order to compare behavioural outcomes of experiments.

Capturing the mechanical responses of 3D printed materials; Vero and Agilius will be crucial, (Li et al., 2018) report uniaxial compression tests on materials, VeroWhite and TangoPlus performed based on ASTM D695 standard. The evaluations in this research are not ready for industry standard evaluation yet, as the study remains a speculative exploration to develop a workflow, to, in the future make Auxetic Structures accessible for product application.

However, (Li et al., 2018) do also describe the ease of measuring the Poisson's ratio through digital image correlation by recording low speed stretching or compression, through tracking the position of markers on a sample with a video camera. Laser based measurements are good for relatively small displacements and the image-based ones work well for larger displacements. However, the initial evaluation will be in response to the steps required to tangibly realise performative, multi-material geometries.

[3.5.2] Evaluative Methods

Radar Plot

The Radar Plot will be used to evaluate the structures based upon points defined by the design criteria. It includes a general evaluation of theoretical, digital, physical and mechanical relevance.

Experimental Radar Plots will be used throughout the primary research, with experimentation-based criteria to evaluate and guide the discovery.

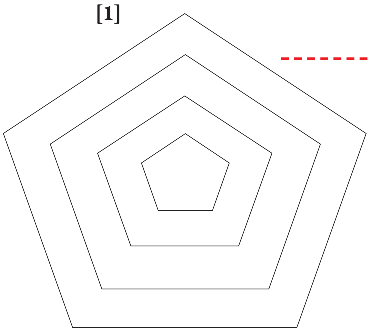

Figure 3.06 Research Radar Plot.

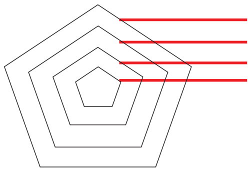

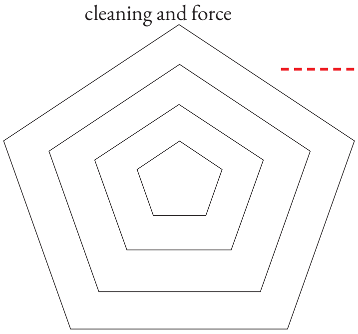

Figure 3.07 Experimental Radar Plot.

[3.5.3] Application

Design criteria developed to be application based and industry specific.

[1] Exhibit multidirectional Auxetic behaviour through biaxial geometries

[2] Should be parametrically controlled through Grasshopper and Rhino to enable manipulation of characteristics and resultant behaviours

[3] Be printed using the J750 to utilise multi-material AM and promote dynamic movement

[4] Tangibly translate Auxetic theory into applicable contexts through parametric modelling

[5] Be focused on minimising human injury in sport by targeting componentry for protection in high impact sports.

[3.6] Outputs and Outcomes

The outputs of the research will describe the final expressions, in the form of digital and physical models, the outcomes are a collated summary of findings. Outputs and outcomes are categorised by methodology.

Research for Design will produce a Literature Review and subsequently, a set of Design Criteria, as a result the outcome will be parametric Auxetic knowledge gained through generative CAD modelling and multi-material printing.

Research through Design will create high fidelity prototypes and industry based speculative applications which will demonstrate beneficial componentry for human protection in high impact sports.

Additionally, through Scientific Design, combined with Research through Design a translation workflow and design system for theory to application will emerge. Demonstrating a process of translation from Auxetic theory to tangible experimentation, through AM process enabled through CAD software.

PRIMARY RESEARCH

Part 1 Exploration for Mechanical Experimentation

Part 2 Exploration for Digital Applications

The primary research is divided into two parts, the first is the physical experimentation and mechanical testing of the fabricated structures, the second is the digital exploration of contextualising Auxetic Structures, through their application into scenarios which exploit the enhanced properties of the geometrical materials.

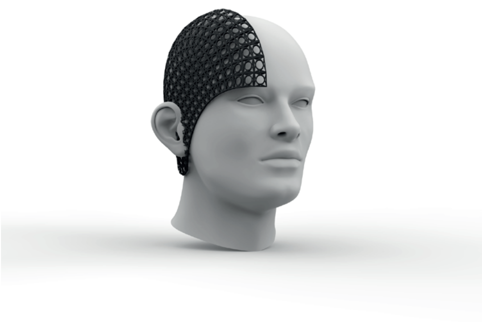

Figure 3.08 Connecting the digital and physical through deisgn.

The following studies through experimentation and development take the next steps towards widespread implementation of Auxetic Structures in designed products.

4 MECHANICAL EXPERIMENTATION

4.1	Methodological Analysis	84
4.2	Auxetic Structure Theory	90
4.3	Experimental Procedures	92
4.4	Experimentation 1	95
4.5	Experimentation 2	110
4.6	Experimentation 3	129
4.7	Experimentation 4	186
4.8	Experimentation 5	198

Part 1

Physical, mechanical experimentation to develop knowledge of materiality of multi-material Auxetic Structures

Figure 4.01 Meta-Chiral Compression Twistt.

[4.1] Methodological Analysis

The methodologies are used to ensure the research is carried out in a meaningful and analytical manner.

The Primary research will be practiced with Research through Design, as well as Scientific Design, as the established workflow is refined and executed.

[4.1.1] Experimental Design Criteria

The overall design criteria for the research is further broken down to evaluate the experiments in Part 1 of the Primary Research. This experimental criteria is formed to access the mechanical responses of the experiments and achieve mechanical development specific goals.

Designs should

[1] Tangibly translate Auxetic theory into parametrically modelled geometry sub entities

[2] Exhibit multidirectional mechanical articulation through controlled hinge variables

[3] Demonstrate a thorough and well-articulated exploration of J750 multi- material printing materials, illustrating their opportunities

[4] Focus on achieving the greatest range of movement with the less amount of prolonged structural damage, through survey of the extremities

[5] Have support material which is removable without inflicting structural damage to the unit

[4.1.2] Software Selection

After some initial digital preparation of structures, a decision is made to use Rhino primarily for unit and structure modelling in the first part of the research. Grasshopper will then be used to generate the structures mapped onto the surfaces. The figure below demonstrates the complexity of making units parametric, which is counter-intuitive to the goal of ensuring units are true to Auxetic theory, and therefore possess fixed dimensions. Units will be modelled in Rhino and then assigned to the Grasshopper script for generation of the morphed lattice.

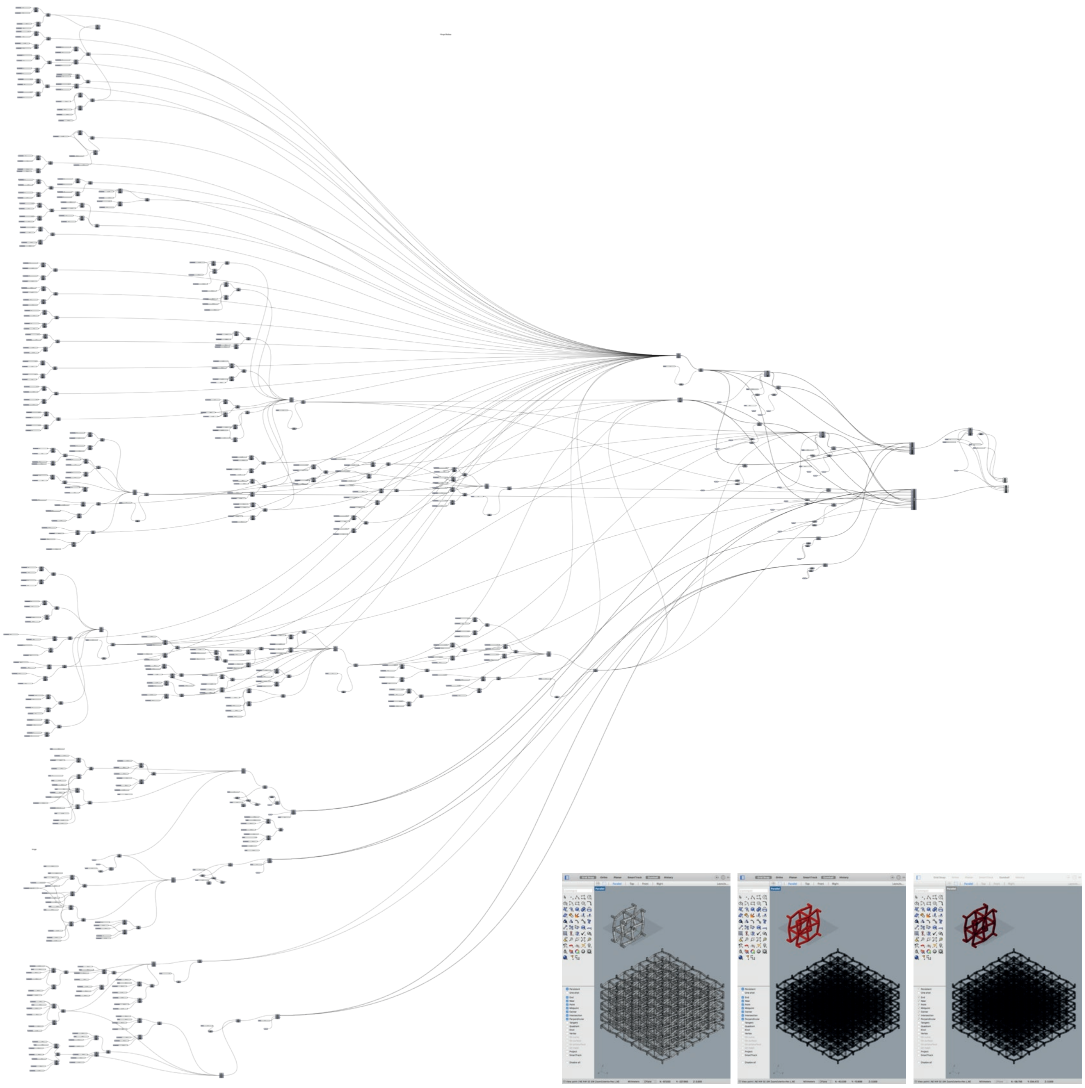

Figure 4.02 Grasshopper script of Auxetic unit.

[4.1.3] J750 Additive Manufacturing Process

Once the geometries are finished being computationally modelled in Rhino and Grasshopper, they can be exported as STL component bodies into GrabCAD, the program used to process the files for printing and assign the digital material combinations. Upon exporting the models from GrabCAD, the printer can then be calibrated and initiated. The Objzf, files with the models and material profiles can then be optimised, for economy, placement and success rate on the printer bed. All models are held in place and built inside water soluble support material. A chemical process can accelerate the removal of such support material, but regardless some manual cleaning is still necessary.

The full J750 printing process is illustrated below.

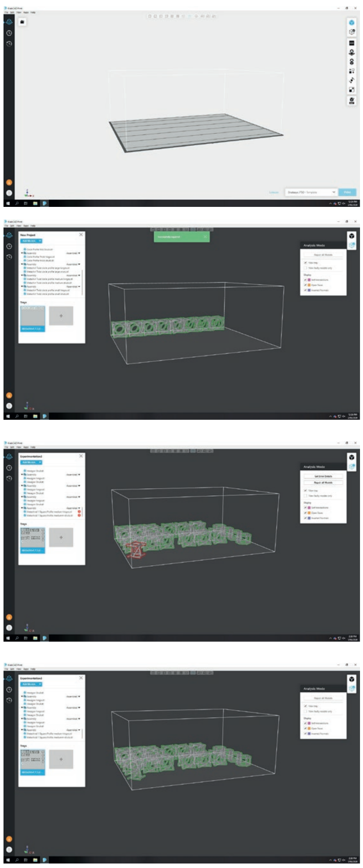

Figure 4.03 GrabCAD repairing a model.

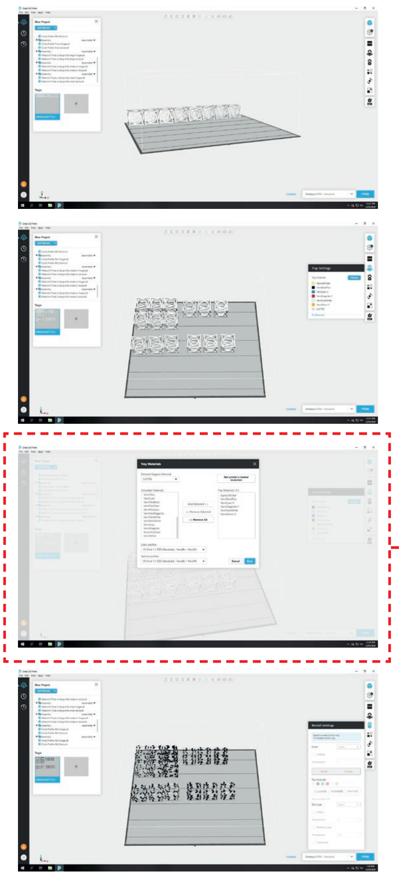

Figure 4.04 GrabCAD assigning materials.

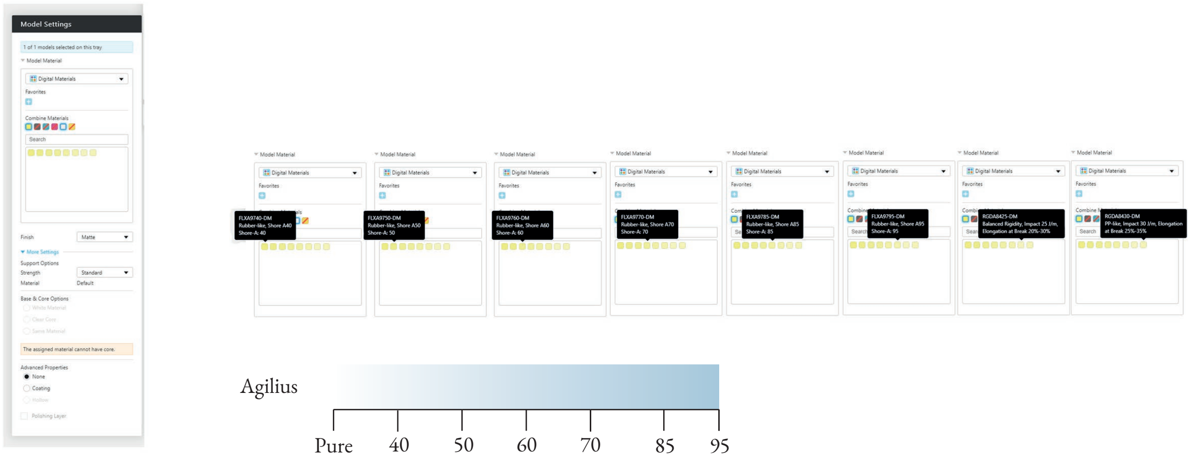

Figure 4.06 J750 Print materials, (Author, 2020).

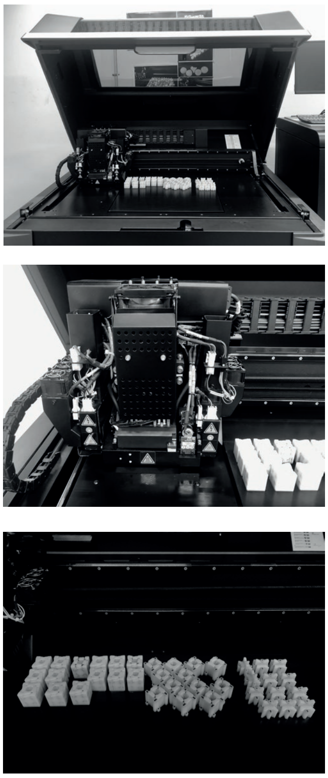

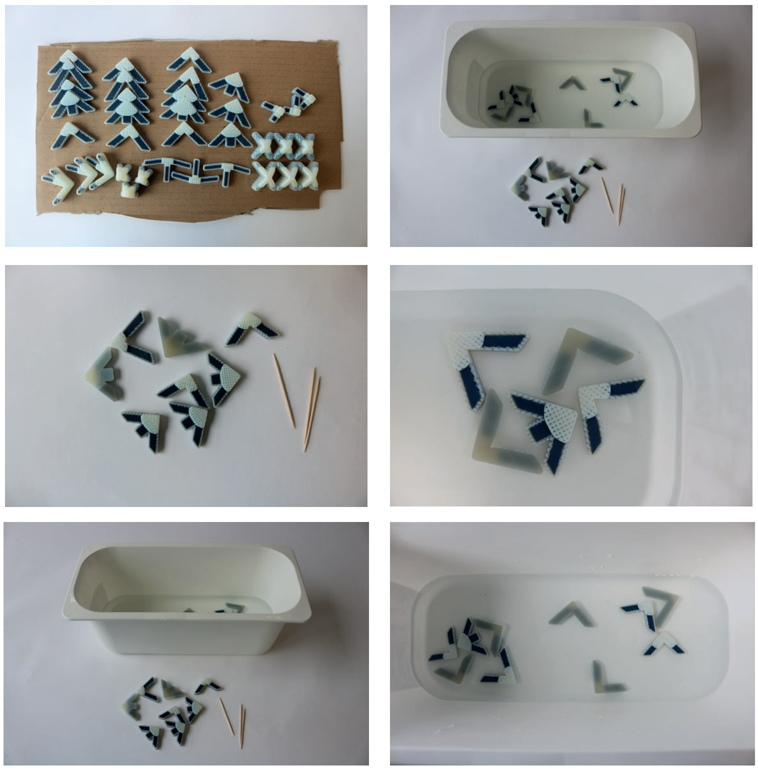

Figure 4.05 J750 Printer.

Figure 4.07 Manufactured materials, removing support process.

[4.1.4] Evaluation

The models which are studied in further detail will be evaluated against the developing criteria, which becomes more refined as the process evolves.

(Yang et al., 2015) described the caution needed when testing AM structures as they can endure aging post production. They state it is worth waiting 24 hours for the model's materials to fully cure before they are tested as the polymers are prone to changes with age. Therefore, it is important for samples in the same test series to be printed and tested in the same time frame as the experiments batch counterparts in this research.

Each experimental stage will be reflected upon with a Radar Plot described below.

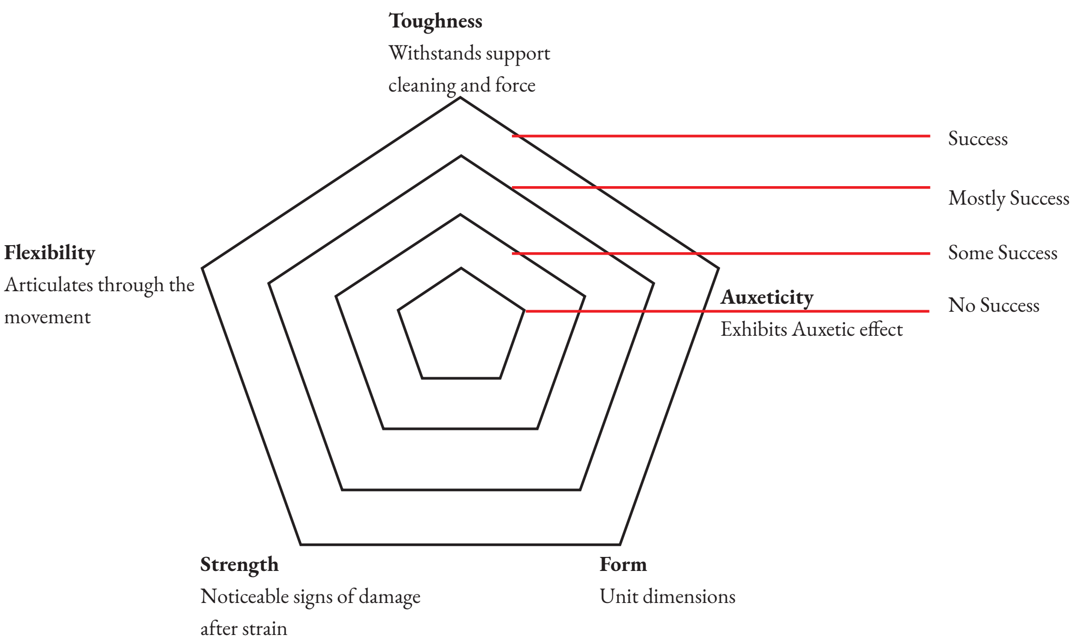

Figure 4.08 Physical experimental Radar Plot.

Figure 4.09 Physical experimentation.

[4.2] Auxetic Structure Survey

As exploration continues the list becomes refined to only include structures which consistently exhibit the Auxetic effect, have robust theory, high suitability to be parametrically modelled, are biaxial in nature to increase their suitability in application, and are geometries which have the ability to be AM.

Structures which don't fulfil these requirements will no longer be explored in this study.

Re-entrant Structures

2D Structures

Hexagonal Honeycomb
First Order Hierarchy
Second Order Hierarchy
Double Arrow Head
Square Grid
Honeycomb I Shaped Slit Pattern
Sinusoidal
Re-entrant Variant 1 and 2
Star 3: Order 3
Star 4: Order 4
Star 6: Order 6

3D Structures

3D Star 4
3D Star 6
3D Honeycomb
3D Triangular Arrow
3D Anti-Tri-Chiral Honeycomb

Rotating Units

Rotating Squares
Rotating Bi Square
Rotating Rectangles
Rotating Trans-rectangular
Rotating Bi Rectangles
Rotating Rectangles Variant 1
Rotating Rectangles Variant 2
Rotating Rectangles Type I
Rotating Rectangles Type II
Rotating Rhombi
Type a Rotating Rhombi
Type b Rotating Rhombi
Type 1a
Type 1b
Type IIa
Type IIb
Rotating Triangular
Rotating Isosceles Triangular
Rotating Bi Triangular
Rotating Hexa Triangular
Cellular plates with Rectangular Perforations
Rotating Rigid Triangles
Rotating Tetrahedral
Hierarchical Rotating Auxetics

Rotating Squares
Regular Square Prism Configuration
Regular Triangular Prism Configuration
Regular Hexagonal Prism Configuration

Chiral Structures

Hexa-Chiral
Hierarchical with Fractal Cuts
Tetra-Chiral
Tri-Chiral
Tri-Tetra
Chiral-Circular
Tri-Chiral Honeycomb
Rota-Chiral

Anti-Chiral
Anti-Tetra-Chiral
Anti-Hexa-Chiral
Anti-Tri-Chiral

Meta Chiral 1
Meta-Tetra-Chiral
Meta-Anti-Tetra-Chiral
Meta-Chiral-Compression-Twist
Tetra-Meta-Chiral
Chiral-Chiral-Anti-Chiral
Hexatruss

[4.3] Experimental Procedures

Described below are the procedures of the research for planar and dimensional Auxetics.

Structures

1 Biaxial Squares
2 Hexagonal Honeycomb
3 Star4
4 Triangular Arrow
5 Anti-Tetra-Chiral
6 Honeycomb I-shaped Slit
7 Tetra-Chiral
8 Meta-Chiral Compression Twist
9 3D Planar Anti-Tetra-Chiral

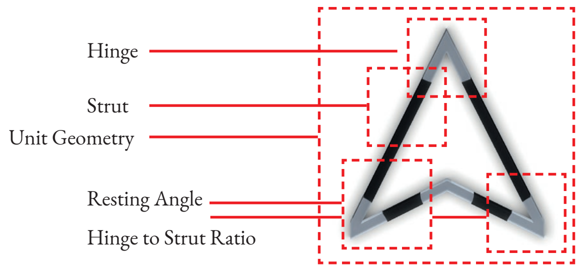

Figure 4.10 Design Parameters.

Experiments

1 POC Planar and Dimensional Auxetics
2 Auxetic Hinges
3 Auxetic Units
4 Absence of the Multi-material Hinge
5 Unit Relationships
6 To Scale Prototyping

Phases

1 Digital Translation
2 POC Manufacturing and Testing
3 Experimentation and Discovery
4 Refined Variation Exploration
5 Discoveries

Proof of Concept (POC)

Depicting Geometrical Parameters

Through analytical modelling, geometrical design parameters are identified as key factors in varying the mechanical responses of the structures. Material aware, computational design will focus on the parametric factors of the following characteristics.

Design Parameters
Material Aware Computational Design.

Digital	Physical	Mechanical Characteristics
Geometry		
Unit Geometry	Deformation Mechanism	Resting Angle
Strut + Hinge Geometry	Auxetic Effect	Geometry
Materials		
Digital Combinations	Shore Hardness	Shore Hardness
Scale		
Hinge to Strut Ratio		Hinge Scale

[4.3.1] Preliminaries

Interpreting the Key

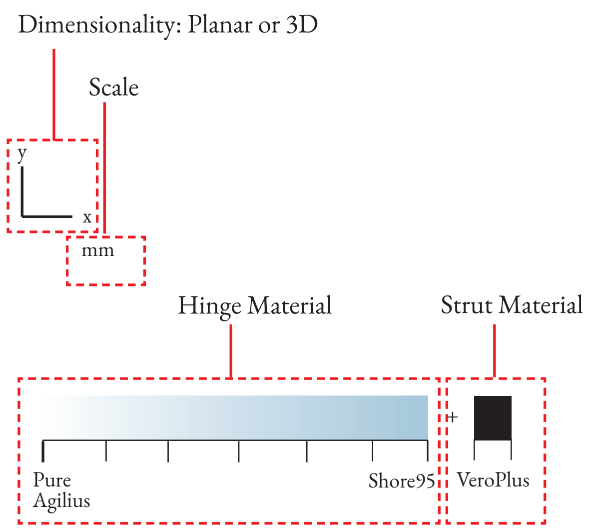

Figure 4.11 Experiment key.

FDM Auxetics

The below Fused Deposition Modelling (FDM) Auxetic Structure demonstrates the problems associated with single material manufacturing and therefore, the beginnings of multi-material Auxetics are born.

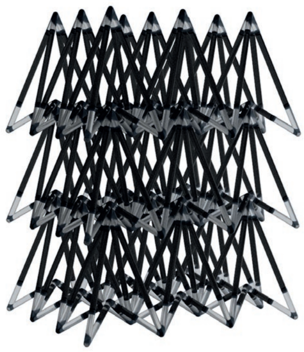

Figure 4.12 Triangular Arrow Auxetic Structure.

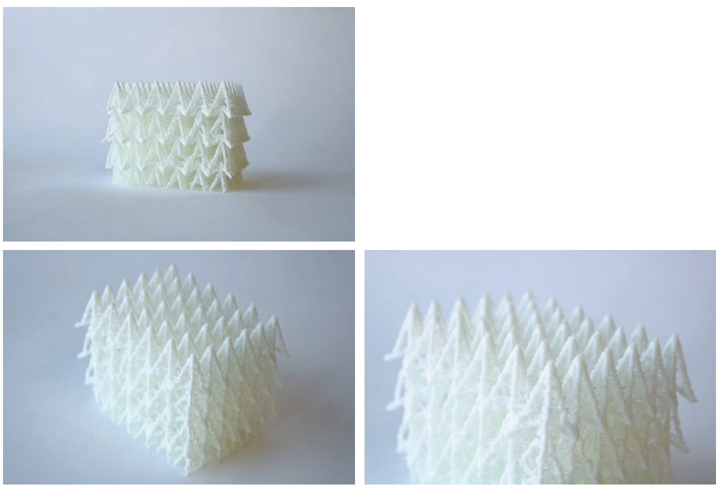

Figure 4.13 FDM Auxetic Structure.

[4.4] Experimentation 1: Planar and Dimensional Proof of Concept Auxetics

Planar

Exploration of 2D and 3D geometries to enable the analysis of Auxetic Structures with multi-materiality to define scale and material selection.

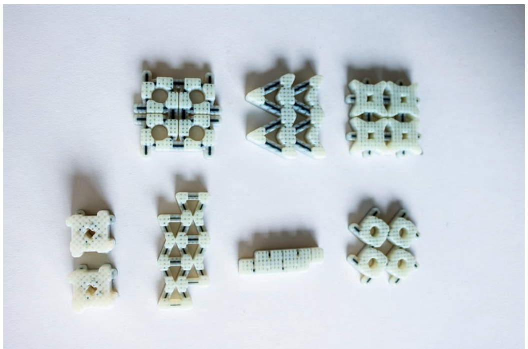

Figure 4.14 & 4.15 2D and 3D POC geometries.

Re-entrant

Biaxial Squares

Design Variable: Shore Hardness

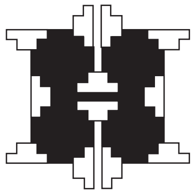

1:1

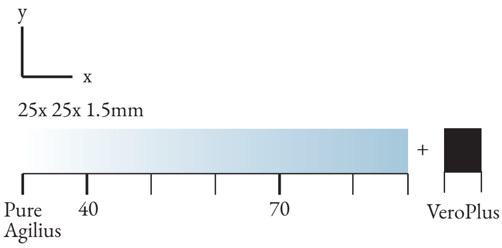

X and Y expansion of the biaxial square units, tested with shore hardnesses 30, 40 and 70.

Digital Translation

Biaxial deformaton mechanism

1:2

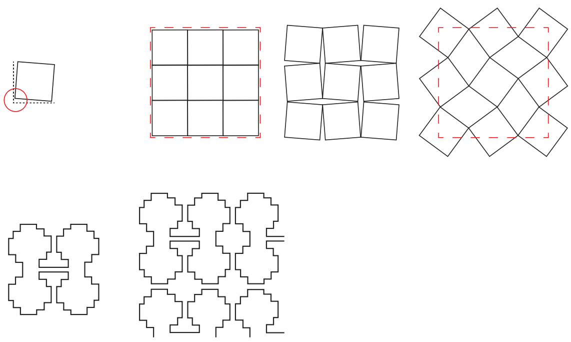

Figure 4.16 Biaxial Squares translation,.

POC Manufacturing & Testing

Permanent tearing damage

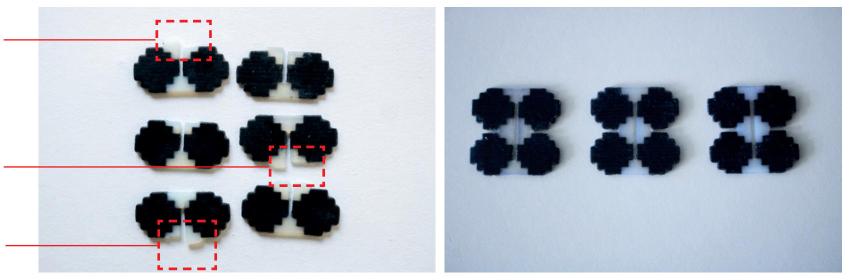

Figure 4.17 Biaxial Squares damage.

Refined Variation Exploration

Shore 30 40 70

1:4

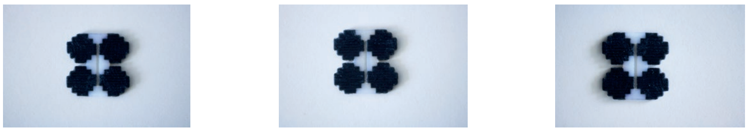

Auxetic Performance

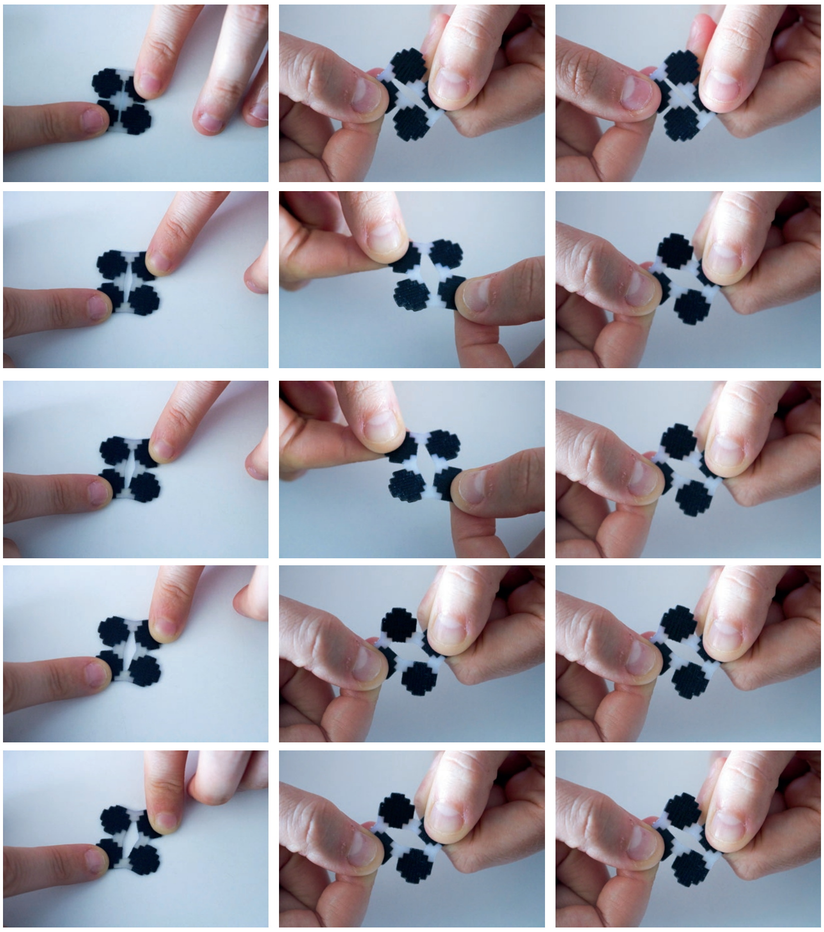

Figure 4.18 Biaxial Squares of shore hardness 30, 40 & 70.

Re-entrant deformation mechanism, observed through expansion of the square plates.

Discoveries

The Auxetic effect was observed, however, the hinge ripped: most likely caused by the extrusion height of the entire unit being too small. There was also too much elasticity in the hinge joint, leading to material stretching rather than the structure utilising the deformation mechanism.

Re-entrant

Hexagonal Honeycomb

Design Variable: Deformation Mechanism

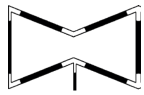

1:1

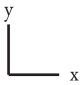

50x 20x 1mm

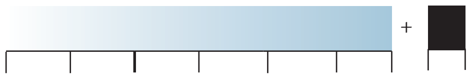

Agilius 50 VeroPlus

Digital Translation

1:1 1:2

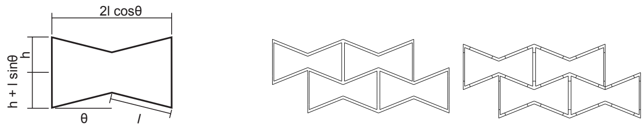

Figure 4.19 Hexagonal Honeycomb theory.

1:2

Auxetic Performance

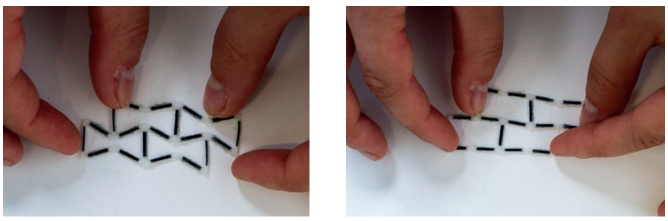

Figure 4.20 Hexagonal Honeycomb expansion.

POC Manufacturing & Testing

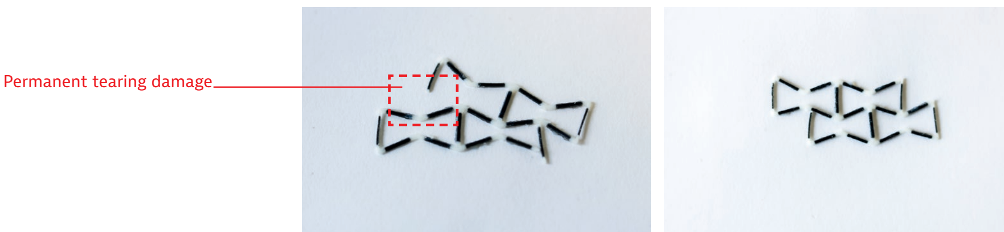

Figure 4.21 Hexagonal Honeycomb damage.

Discoveries

Extrusion height is too small, the geometry lacks structural integrity and fails to hold its form.

Re-entrant

Triangular Arrow

Design Variable: Deformation Mechanism

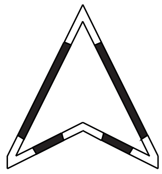

1:1

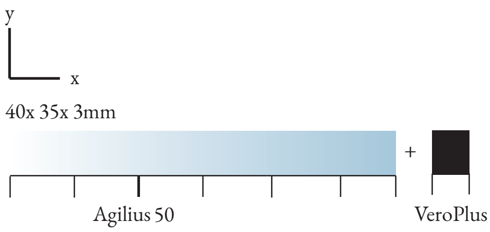

Digital Translation

1:2

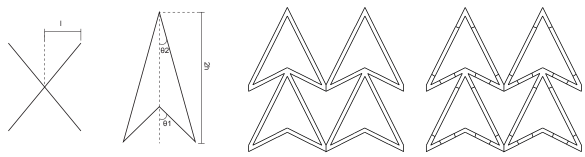

Figure. 4.22 Triangular Arrow theory.

POC Manufacturing & Testing

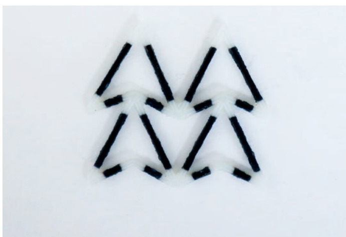

Figure 4.23 Triangular Arrow.

The triangular arrow opening when laterally stretched, causing horizontal expansion.

1:4

Auxetic Performance

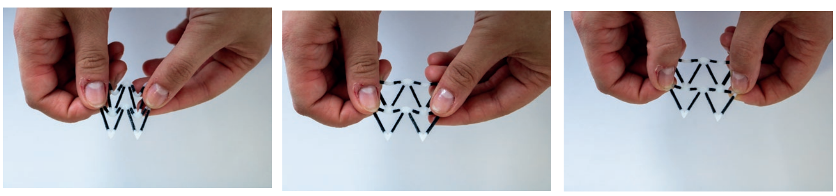

Figure 4.24 Triangular Arrow expansion.

Discoveries

This structure was more successful than previous geometries, due to having thicker struts and hinges.

Re-entrant

Star4

Design Variable: Deformation Mechanism

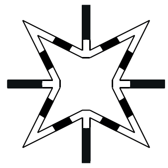

1:1

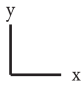

40x 35x 3mm

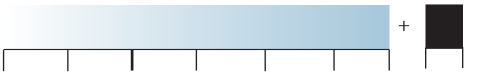

Digital Translation

1:2

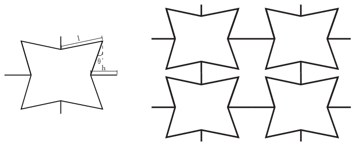

Figure 4.25 Star4 theory.

Refined Variation Exploration

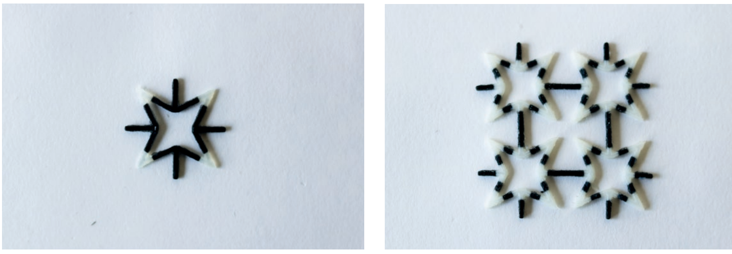

Figure 4.26 Star4.

Auxetic Performance

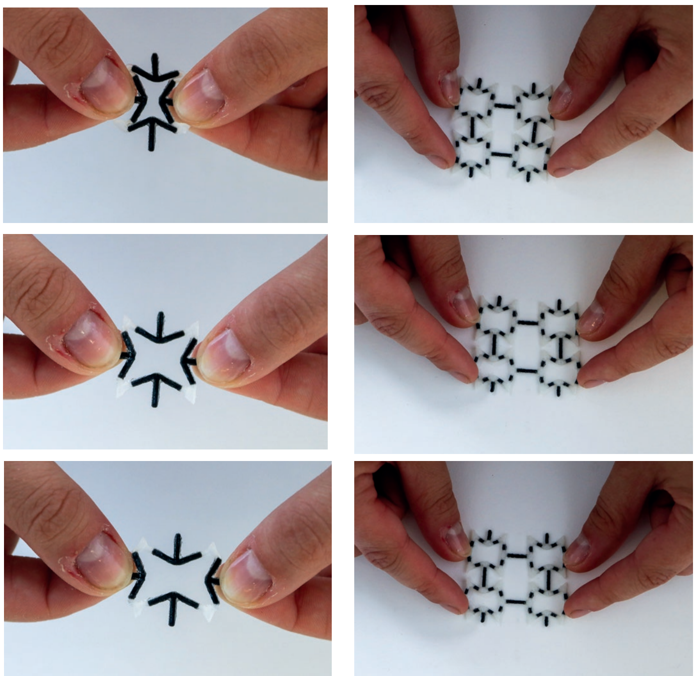

Figure 4.27 Star4 expansion.

POC Manufacturing & Testing

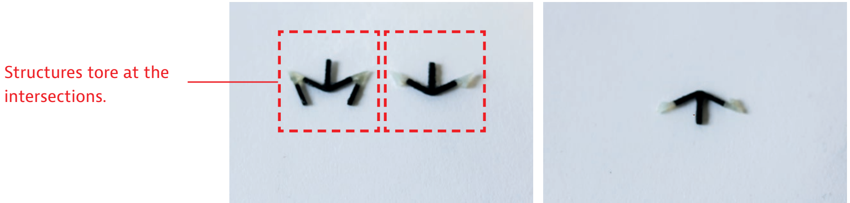

Figure 4.28 Star4 damage.

Discoveries

Planar structures translate well on flat surfaces, however, they are easily pulled out of shape when an uneven strain is applied along the x axis.

Re-entrant

Honeycomb I-shaped Slit

Design Variable: Deformation Mechanism

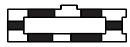

1:1

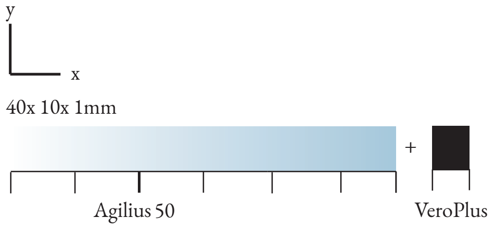

Digital Translation

1:2

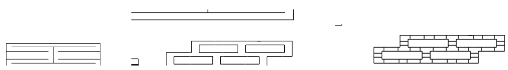

Figure 4.29 Honeycomb I-shaped Slit theory, (Author, 2020).

Auxetic Performance

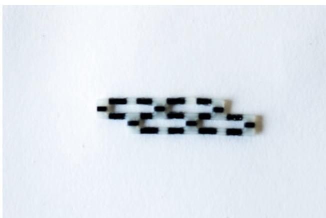

Figure 4.30 Honeycomb I-shaped Slit.

POC Manufacturing & Testing

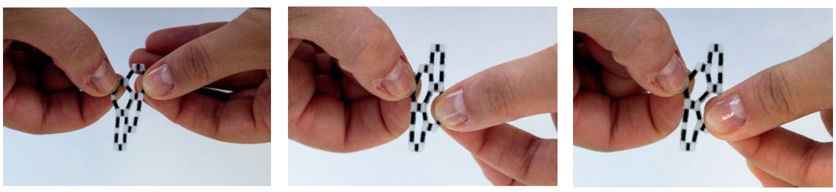

Figure 4.31 Honeycomb I-shaped Slit expansion.

Discoveries

The scale of the printed geometry is proving to be restricting some movement, ultimately causing damage at the hinge.

Chiral

Anti-Tetra-Chiral

Design Variable: Deformation Mechanism

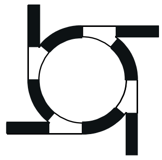

1:1

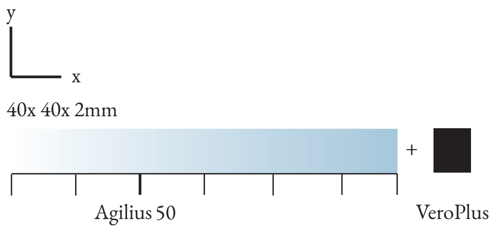

Digital Translation

1:2

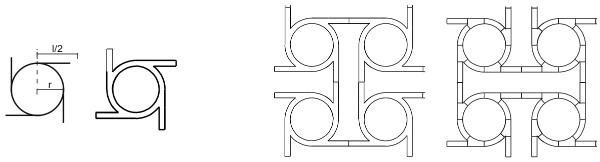

Figure 4.32 Anti-Tetra-Chiral theory.

Auxetic Performance

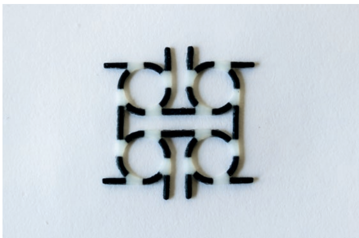

Figure 4.33 Anti-Tetra-Chiral.

POC Manufacturing & Testing

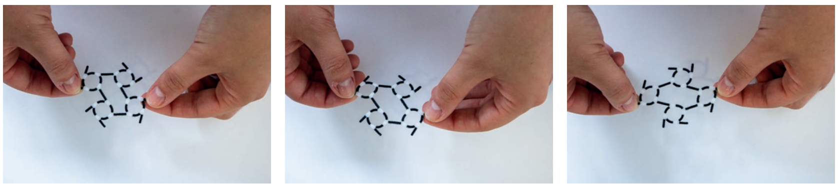

Figure 4.34 Anti-Tetra-Chiral expansion.

Discoveries

Geometry translates easily across the x axis.

Chiral

Tetra-Chiral

Design Variable: Deformation Mechanism

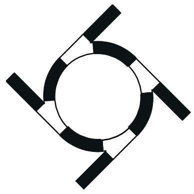

1:1

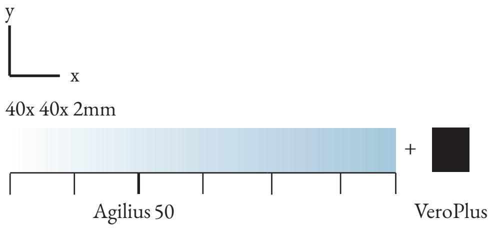

Digital Translation

1:2

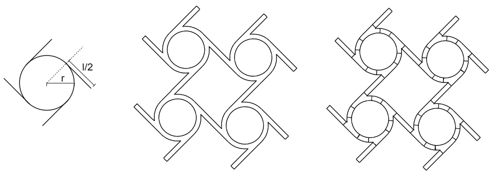

Figure 4.35 Tetra-Chiral theory translation.

POC Manufacturing & Testing

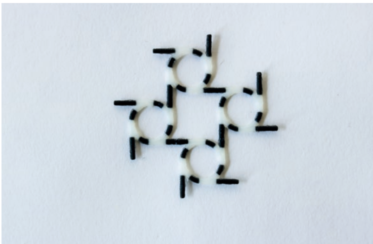

Figure 4.36 Tetra-Chiral.

Auxetic Performance

Figure 4.37 Tetra-Chiral expansion.

Discoveries

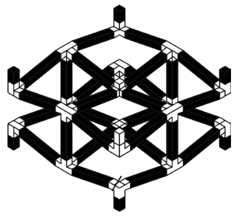

1:2

3D Re-entrant Hexagon

Design Variable: Deformation Mechanism

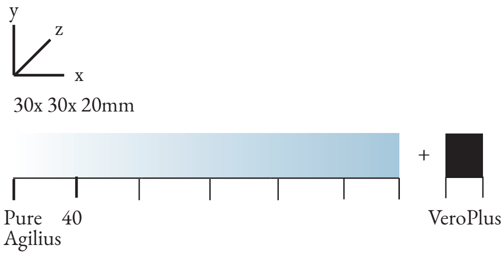

The 3D Honeycomb structure exhibits high indentation strength when subject to impact, responding with a uniaxial deformation mechanism.

Digital Translation

1:2

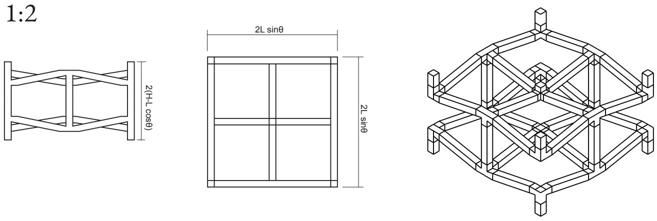

1:4

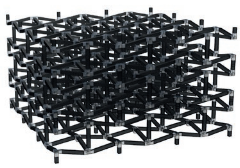

Figure 4.38 3D Hexagonal Honeycomb translation.

Shore 30

Auxetic Performance

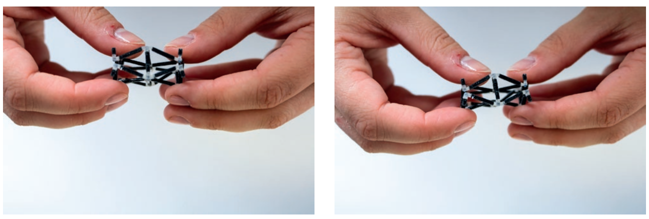

Figure 4.39 3D Hexagonal Honeycomb expansion.

POC Manufacturing
& Testing

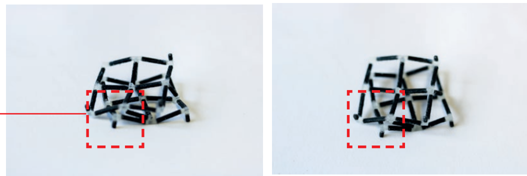

Figure 4.40 3D Hexagonal Honeycomb damage.

Shore 40

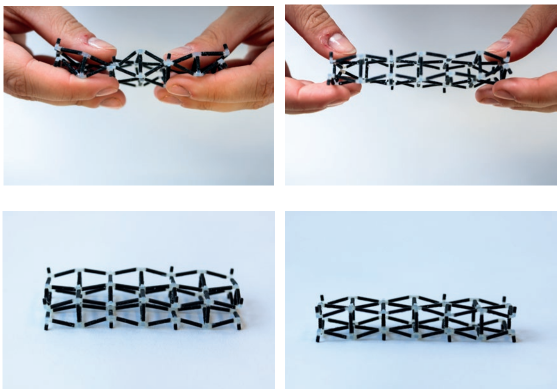

Figure4.41 3D Hexagonal Honeycomb damage.

Discoveries

The singular unit had weak agilius hinges, and broke at the connection point, although initially, the Auxetic effect was observed. Too much elasticity in the hinge joint, caused the damaged but also enabled unwanted stretching rather than utilising the deformation mechanism.

The three connected units with Shore 40 were more successful and the Auxetic effect was observed.

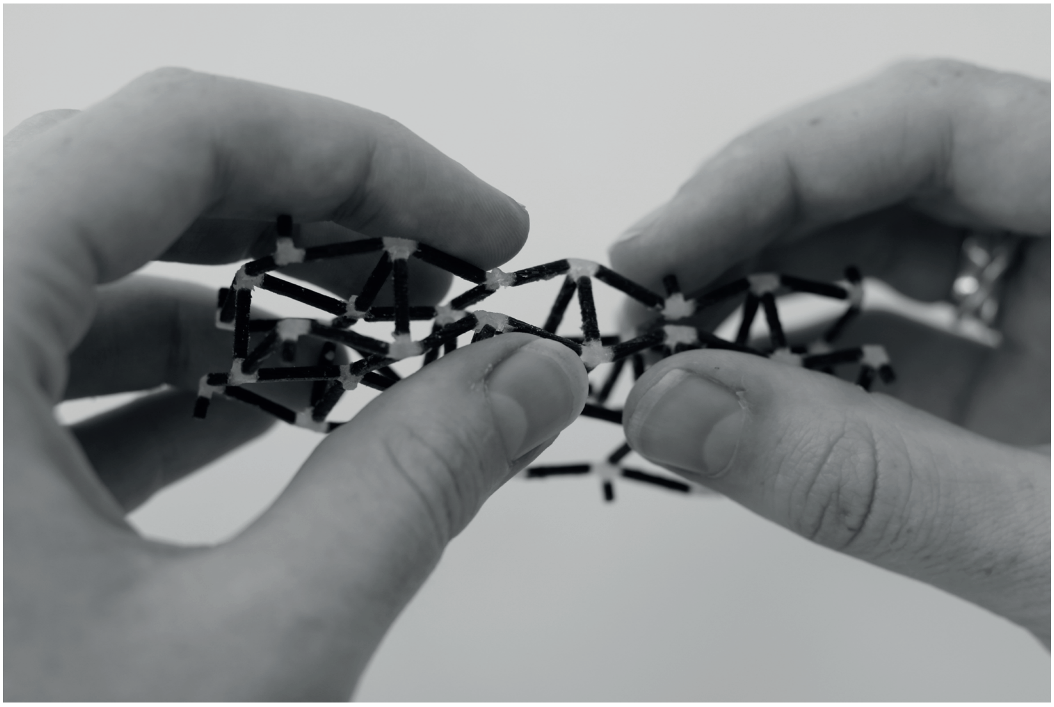

Figure 4.42 3D Hexagonal Honeycomb.

Experimentation One Reflection

After surveying the shore hardness at the three different elasticities; Shore 30, 50 and 70, Shore 30 was found to be too soft more often than not and therefore will not be tested with in future experiments. It displayed a lack of conformality to its geometry, lacked self-support of its resting form and was subject to the most damage. In contrast the Vero Black Plus struts never showed any damage after being exposed to the strain and will therefore be continued to be used as the strut material from this point forward.

Shore 40 demonstrated consistently good longevity during and after strain and therefore structures with Shore hardness within this vicinity for hinge assignment will continue to be explored.

Important to note, is that the extrusion height of the struts and subsequently the depth of the hinges that needs to be more closely monitored as some structures in experiment one were too thin in the Z direction and tore as a result.

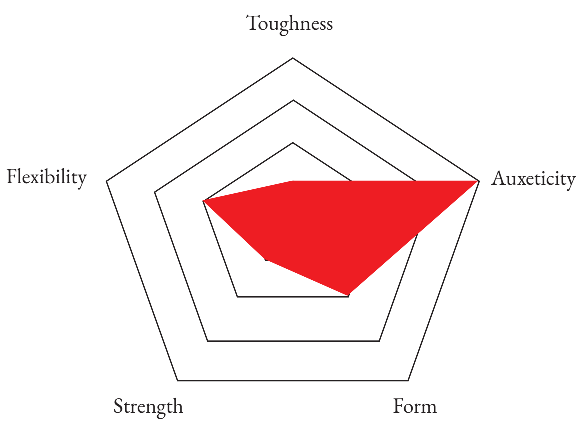

Figure 4.43 Experiment one Radar Plot.

Experimentation One Evaluative Matrix

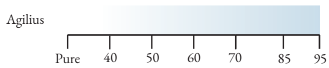

Topology	Shore Hardness	Designed Hinge (Deformation Mechanism utilised)	Auxetic Effect Observed (Resting Position 0 – 1 – 2 – 3 Utilised to Maximum)	Damage Sustained (Unit unusable again 0 – 1 – 2 – 3 No damage Observed)
1:2 **Rotating Units**				
Biaxial Squares 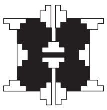	Shore 30	✓	3	1
	Shore 40	✓	3	1
	Shore 70	✓	2	1
Re-entrant				
Hexagonal Honeycomb 	Shore 50	✓	3	0
Triangular Arrow 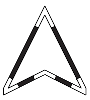	Shore 50	✓	3	3
Star4 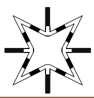	Shore 50	✓	3	3
Honeycomb I-shaped Slit 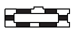	Shore 50	X	1	3
1:4 3D Re-entrant Hexagon 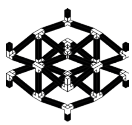	Shore 30	X	3	0
	Shore 40	✓	3	3
1:2 **Chiral Topologies**				
Anti-Tetra-Chiral 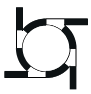	Shore 50	✓	3	3
Tetra-Chiral 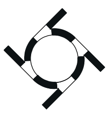	Shore 50	✓	3	3

[4.5] Experimentation 2: Auxetic Hinges

Preliminaries

Interpreting the Key

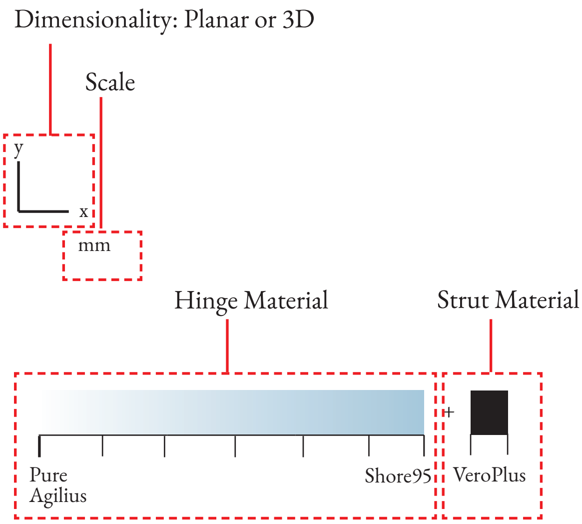

Figure 4.44. Recording observations, (Author, 2020).

Figure 4.45 Recording observations.

Experimentation two will focus on the development of hinges in the Auxetic geometries as this was the least successful component of the structures explored in Experimentation one. This experimentation begins from the work of Miller & Wilson (2015).

Initial Experimental Design Criteria

[1] The initial experimentation testing designs should:

[2] Tangibly translate Auxetic theory into parametrically modelled geometry sub entities

[3] Exhibit multidirectional mechanical articulation through controlled hinge variables, which show the connections ability to translate

[4] Optimise digital material combinations to demonstrate advantages to Multi material Auxetics

[5] Be focused on achieving the greatest range of movement with the least amount of structural damage e.g. survey the extremities and then the materials capability to perform again

[6] The tests will be evaluated against the experimental design criteria above, the individual pieces in the tests will be commented on as key observations

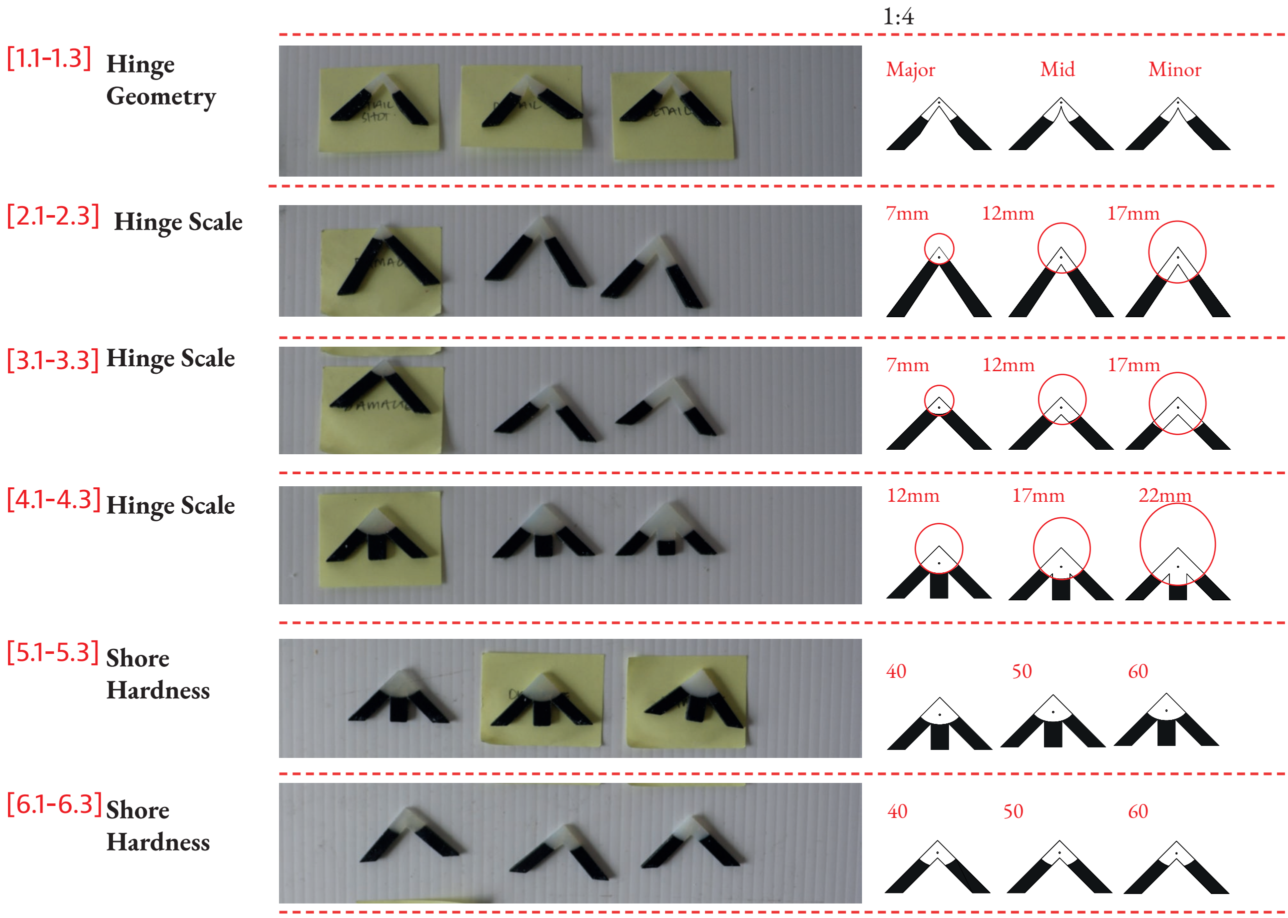

Figure 4.46 2D hinge experimentation.

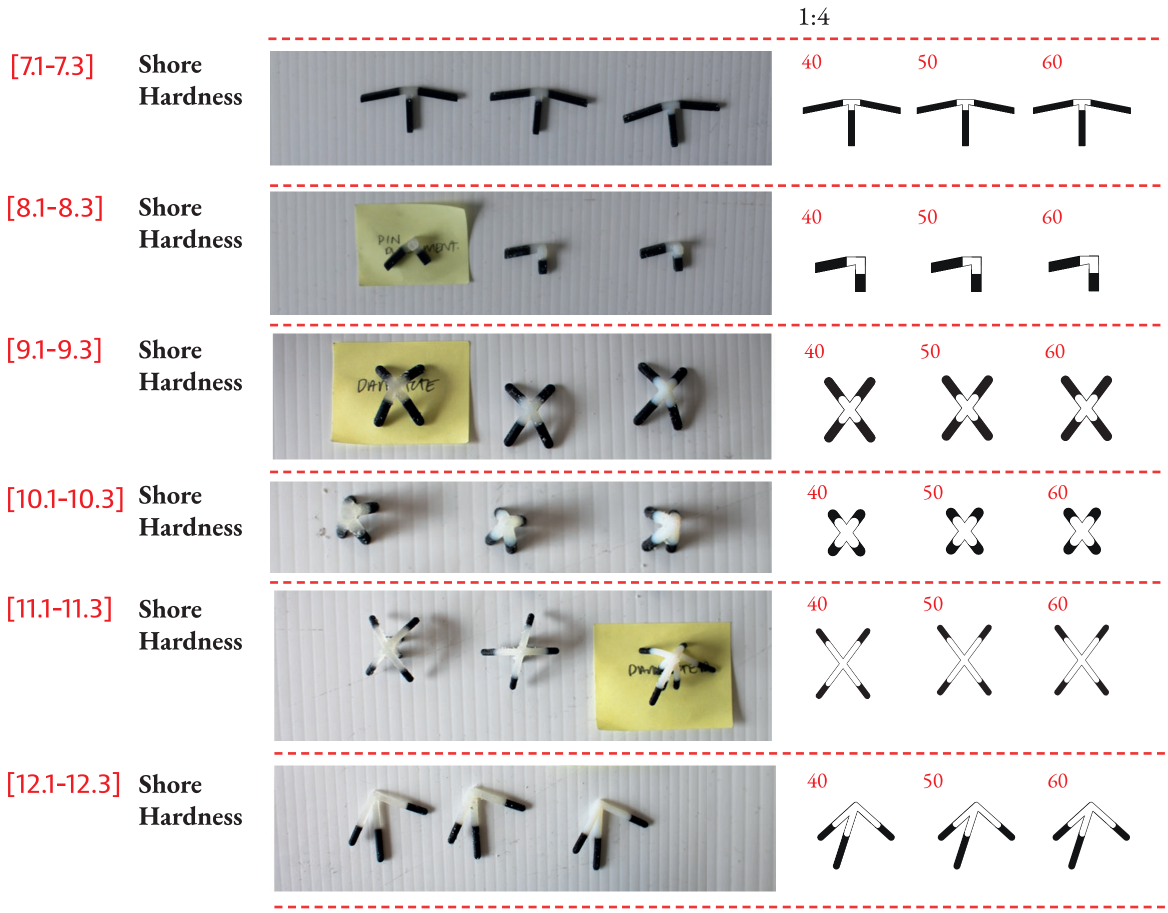

Figure 4.47 3D hinge experimentation.

Mechanical testing will consist of four tests, exposing the structures to strain, as well as involving assessment of their design and manufacture details. Testing includes the following phases with hinge geometry, hinge scale, materiality, and damage sustained amongst evaluative points.

[1] Resting Position
The relaxed (resting state) of the hinge, that is the position it was printed in must be recorded with a protractor.

[2] Minimum Angle
By using the alligator clips and aluminium rod arms, the minimum angle possible can be recorded, where zero is the smallest the hinge will be tested to.

[3] Maximum Angle
The same as the minimum angle method, however, hinges will be articulated to their widest possible opening hinge.

[4] Any Damage Sustained
Noting any damage sustained through the articulation of the hinges.

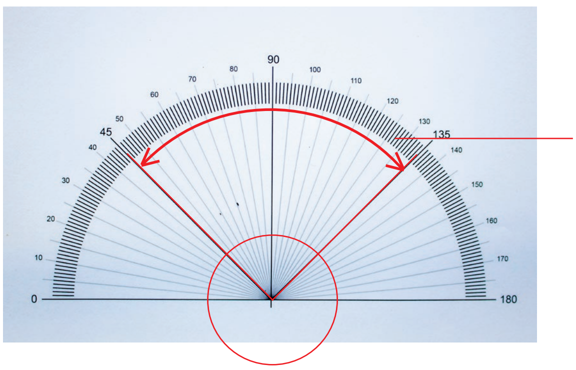

Figure 4.48 Experiment analysis.

Re-entrant

2D Triangular Arrow
2D Two Strut 90 Degree Hinge

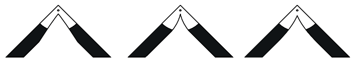

1:4

[1.1-1.3] Design Variable: Hinge Geometry

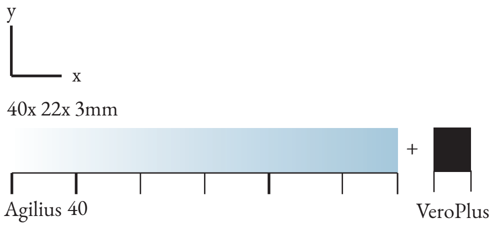

POC Manufacturing & Testing

Hinge Geometry: the geometry alterations are unnecessary at this scale

(c) lack of material lowers structural integrity

(a) Major Cut (b) Mid Cut (c) Minor Cut

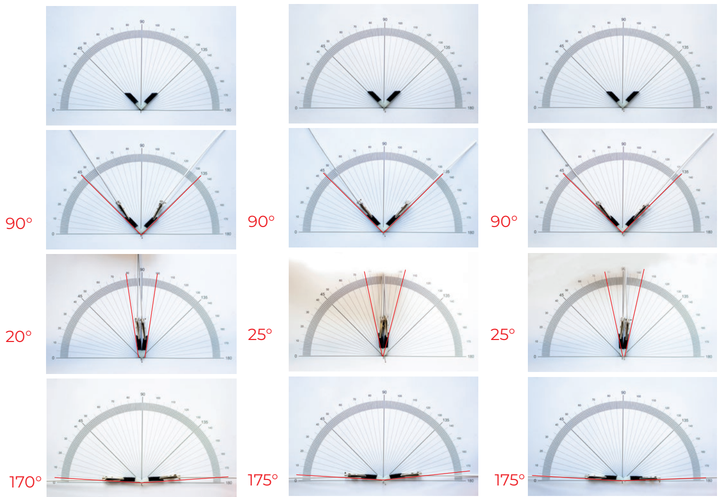

Figure 4.49 Hinge expansion.

Auxetic Performance

Maximum Angle
20-25°

Minimum Angle
170-175°

Tearing further towards the vertex than the form is designed for

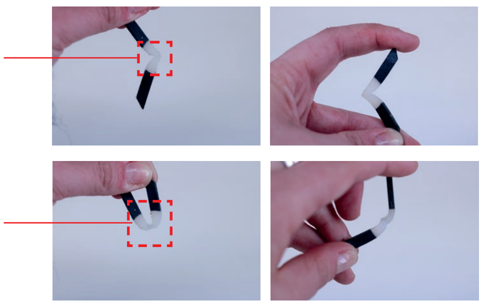

Figure 4.50 Hinge damage.

Discoveries

Geometry alterations can be deemed unnecessary, material in unadjusted hinges do not limit hinge articulation. Geometry modifications to hinges will not be pursued.

Re-entrant

[2.1-2.3]

2D Triangular Arrow
2D 2 Strut 70 Degree Hinge

Design Variable: Hinge Scale

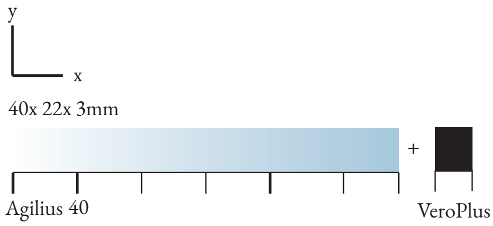

1:4

POC Manufacturing & Testing

The small hinge restricts full articulation

The larger hinges are more successful in enabling a wider range of movement

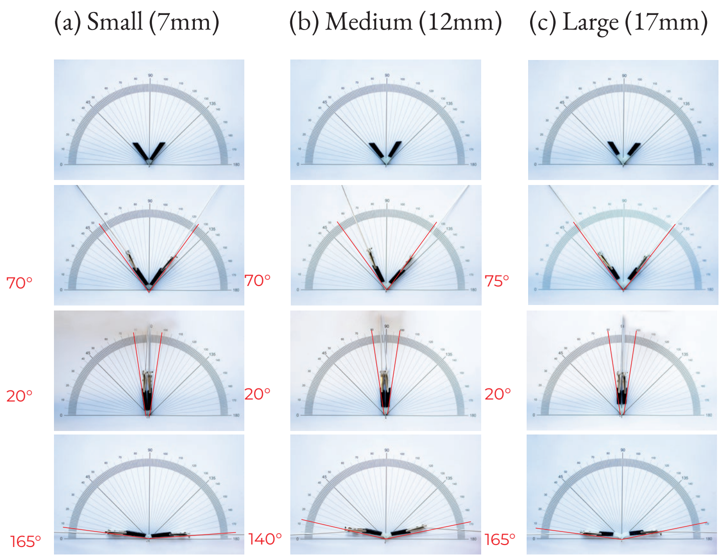

Figure 4.51 Hinge expansion.

Auxetic Performance

Maximum Angle
20°

Minimum Angle
140-165°

Permanent tearing damage

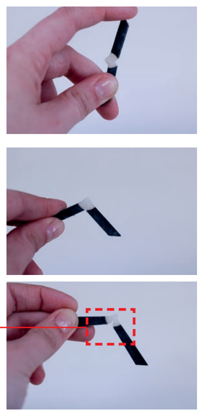

Figure 4.52 Hinge damage.

Discoveries

The small hinge, doesn’t allow full articulation, the medium is the best fit as it allows movement and doesn’t intrude too much into the structures need for robust, rigid struts.

Re-entrant [3.1-3.3]

2D Triangular Arrow
2D 2 Strut 90 Degree Hinge

Design Variable: Hinge Scale

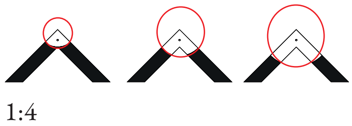

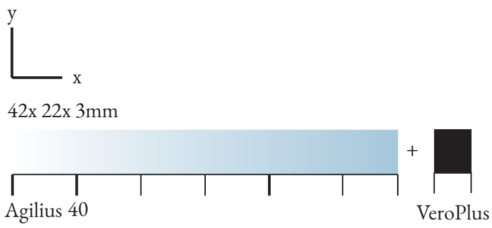

POC Manufacturing & Testing

Auxetic Performance

Maximum Angle
15°

Minimum Angle
160°

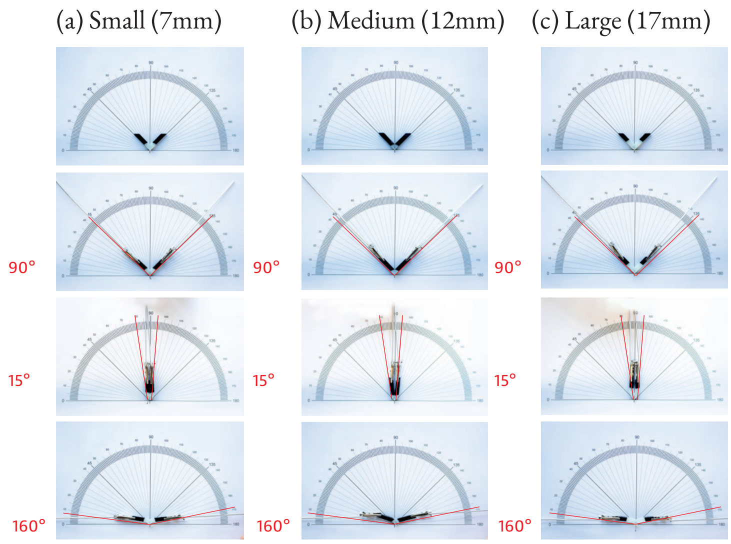

Figure 4.53 Hinge expansion.

Re-entrant
[4.1-4.3]

2D Triangular Arrow
2D 3 Strut 90 Degree Hinge

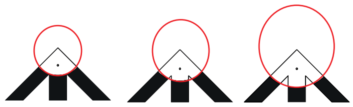

1:4

Design Variable: Hinge Scale

y
x

42x 22x 3mm

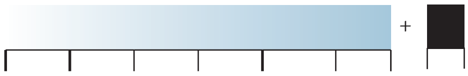

Agilius 40

VeroPlus

POC Manufacturing & Testing

(a) Small (b) Medium (c) Large

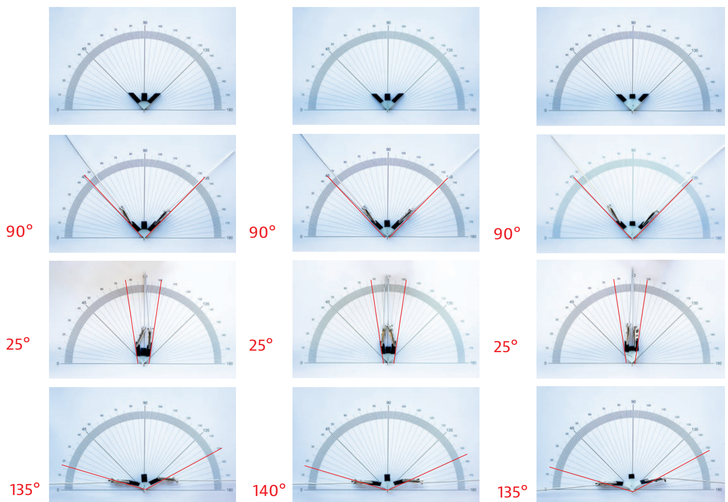

Figure 4.54 Hinge expansion,

Auxetic Performance

Maximum Angle
25°

Minimum Angle
135-140°

Hinge opening past the intersection

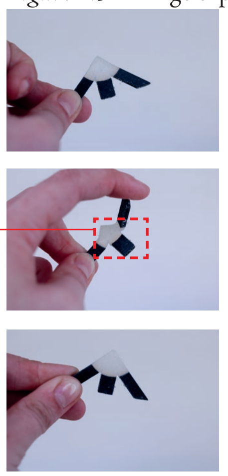

Figure 4.55 Hinge damage.

Discoveries

The largest hinge is the only one which enables movement of all three struts, the two smaller hinges do not include the vertex of all connections and therefore the hinge is locked in its printed state.

Re-entrant

[5.1-5.3]

3D Triangular Arrow
2D 3 Strut 160 Degree Hinge

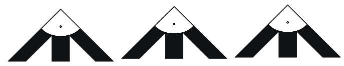

1:4

Design Variable: Shore Hardness

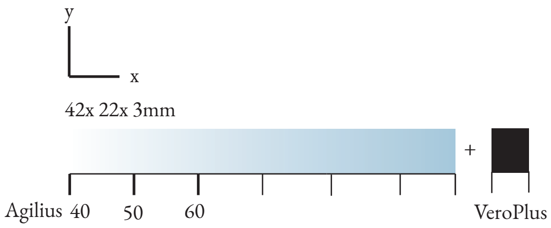

POC Manufacturing & Testing

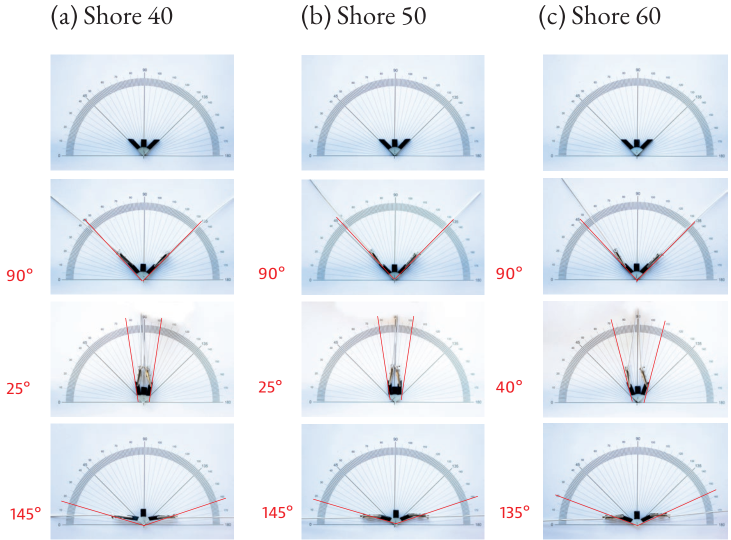

Figure 4.56 Hinge expansion.

Auxetic Performance

Maximum Angle
25-40°

Minimum Angle
135-145°

Hinge opening past the intersection, causing damage

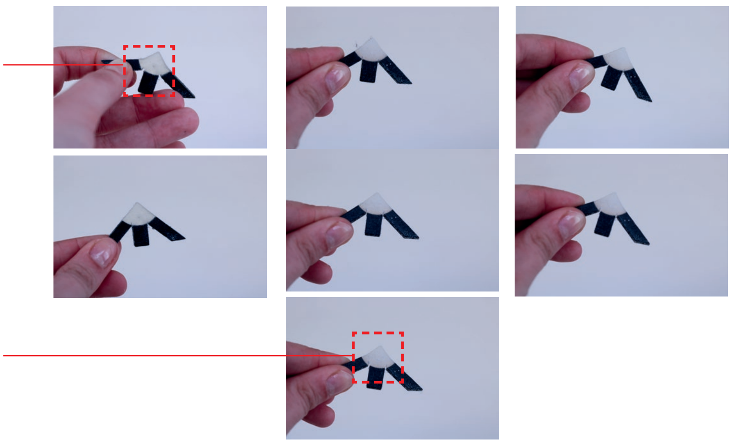

Figure 4.57 Hinge damage.

Discoveries

The mid range shore hardness is most suitable for the movement required. Harder Shore hardness limits the hinges movement and the lowest shore hardness endured some damage. Values around 40 will be further explored.

Re-entrant

2D Triangular Arrow
2D 2 Strut 90 Degree Hinge

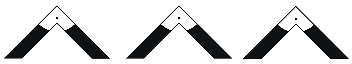

1:4

[6.1-6.3] Design Variable: Shore Hardness

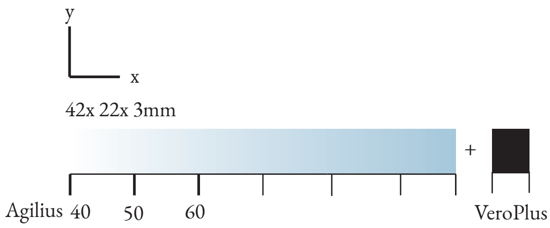

POC Manufacturing & Testing

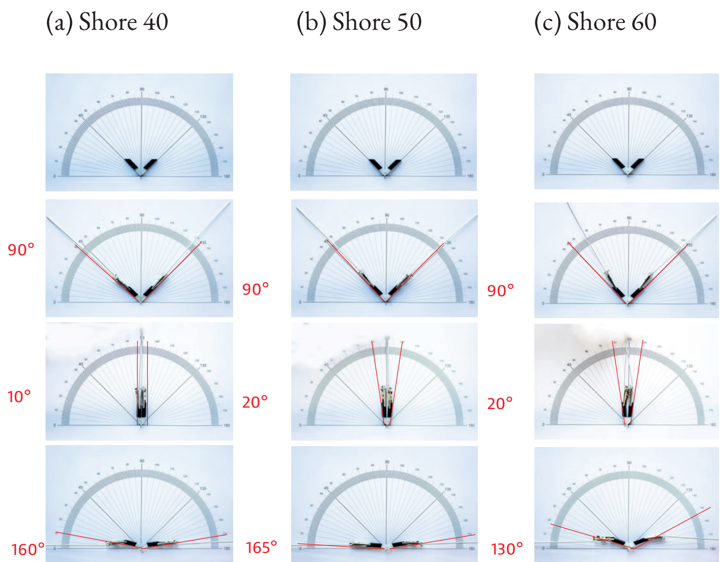

Figure 4.58. Hinge expansion, (Author, 2020).

Auxetic Performance

Maximum Angle
10-20°

Minimum Angle
130-165°

Permanent tearing damage

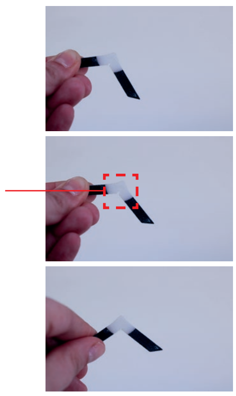

Figure 4.59 Hinge damage.

Discoveries

Shore hardness around 40 provided the best movement and material integrity, the higher range limits the hinges movement and the lowest shore hardness endured some damage. Values above 40 will be further explored.

Re-entrant

3D Hexagonal Honeycomb
2D 3 Strut Hinge

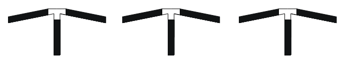

[7.1-7.3] Design Variable: Shore Hardness

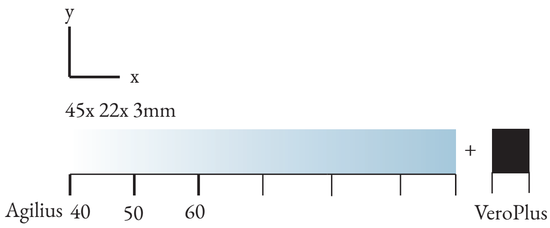

POC Manufacturing & Testing

Auxetic Performance

Maximum Angle
15°

Minimum Angle
175°

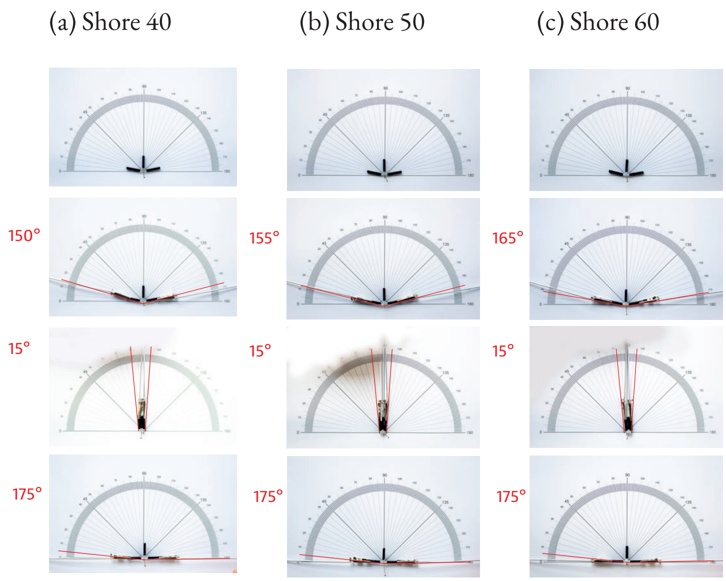

Figure 4.60 Hinge expansion.

Re-entrant

3D Hexagonal Honeycomb
3D 3 Strut Square Hinge

1:4

Design Variable: Shore Hardness

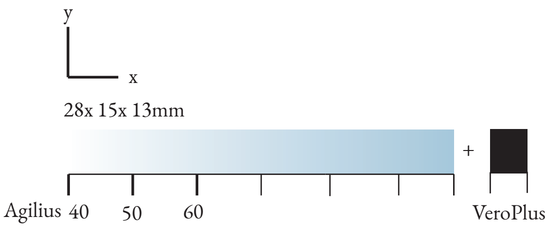

POC Manufacturing & Testing

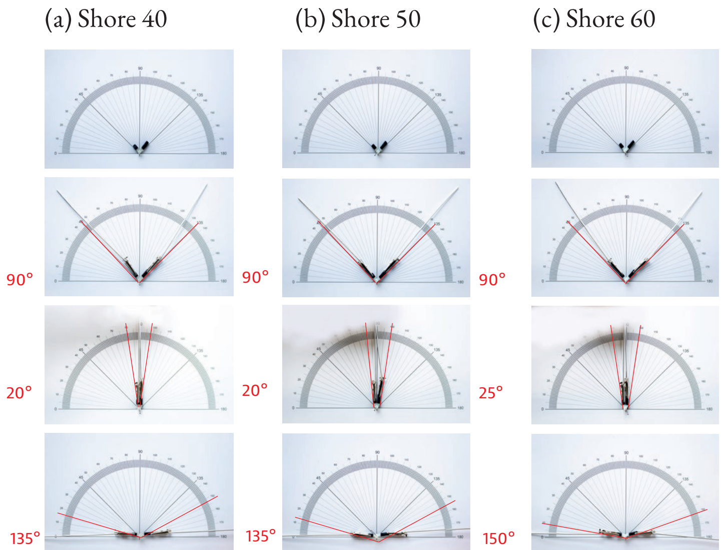

Figure 4.61. Hinge expansion.

Auxetic Performance

Maximum Angle
20-25°

Minimum Angle
135-150°

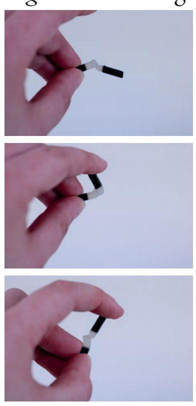

Figure 4.62 Hinge damage.

Discoveries

Shore 40 was the only hinge to show signs of permanent damage.

Re-entrant

3D Triangular Arrow
3D 4 Strut Low Hinge

[9.1-9.3] Design Variable: Shore Hardness

1:4

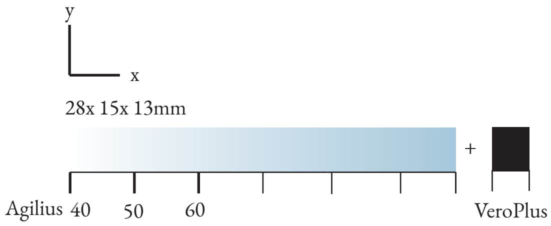

POC Manufacturing & Testing

Shore40 was too elastic and failed to hold its form, the hardest material hinge was too rigid and fixed the hinge in place

Auxetic Performance

Maximum Angle
75-90°

Minimum Angle
165-175°

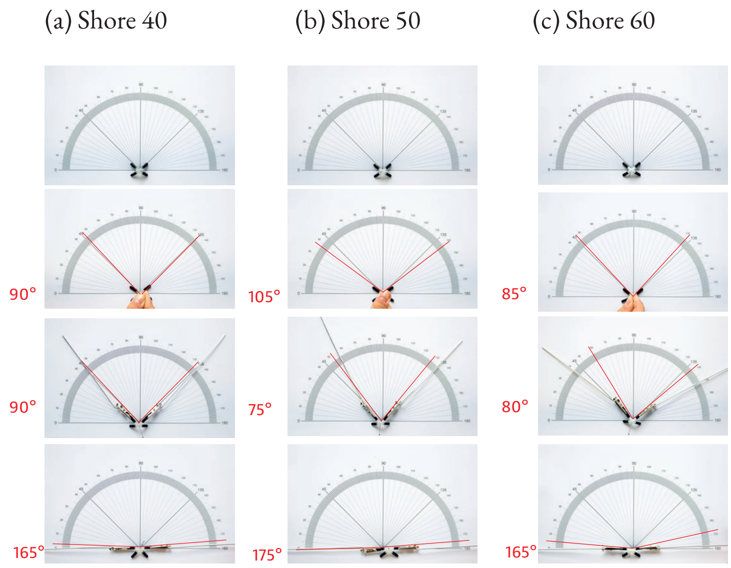

Figure 4.63 Hinge expansion.

Re-entrant

3D Hexagonal Honeycomb
3D 4 Strut High Hinge

1:4

[10.1-10.3] Design Variable: Shore Hardness

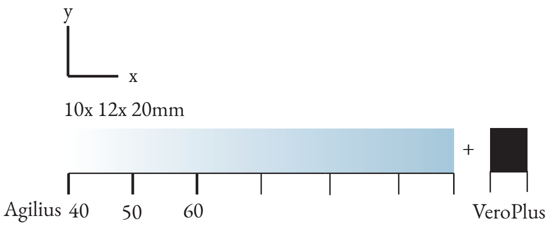

POC Manufacturing & Testing

(a) Shore 40 (b) Shore 50 (c) Shore 60

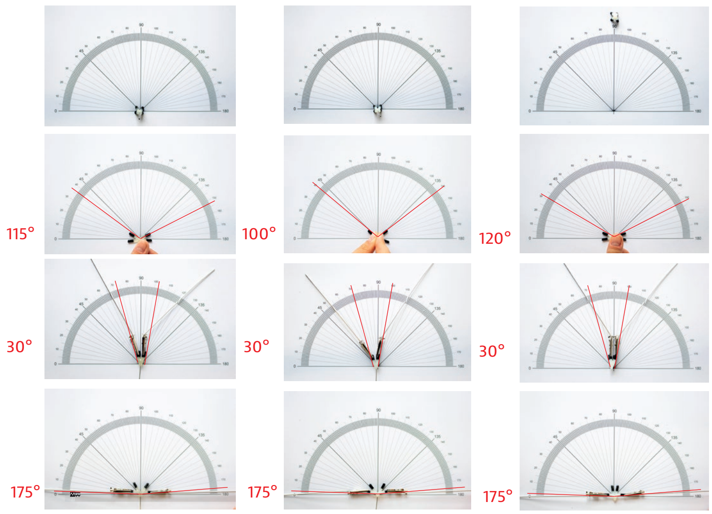

Figure 4.64 Hinge expansion.

Auxetic Performance

Maximum Angle
30°

Minimum Angle
175°

Re-entrant

3D Hexagonal Honeycomb
3D 8 Strut High Hinge

1:4

[11.1-11.3] Design Variable: Shore Hardness

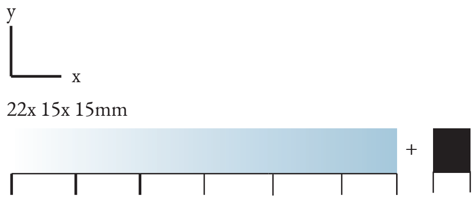

POC Manufacturing & Testing

(a) Shore 40 (b) Shore 50 (c) Shore 60

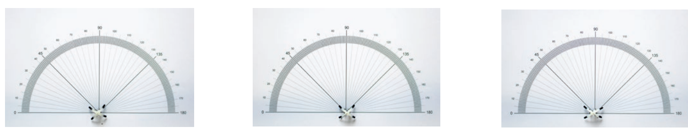

Figure 4.65. Hinge expansion.

Auxetic Performance

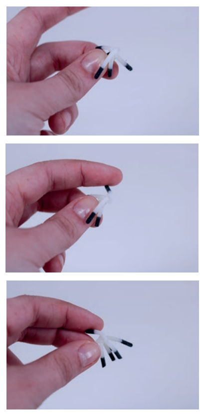

Figure 4.66 Hinge damage.

Discoveries

Shore 40 could not support its own form and therefore is too elastic for the model. Structures were too elastic to test.

Re-entrant

[12.1-12.3]

3D Hexagonal Honeycomb
3D 3 Strut Hinge

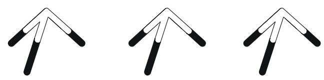

1:4

Design Variable: Shore Hardness

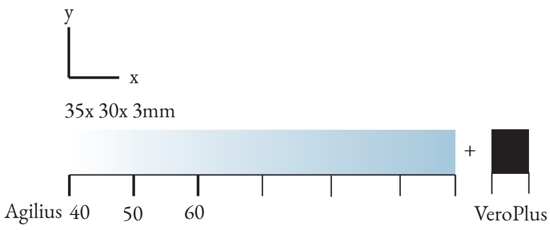

POC Manufacturing & Testing

(a) Shore 40 (b) Shore 50 (c) Shore 60

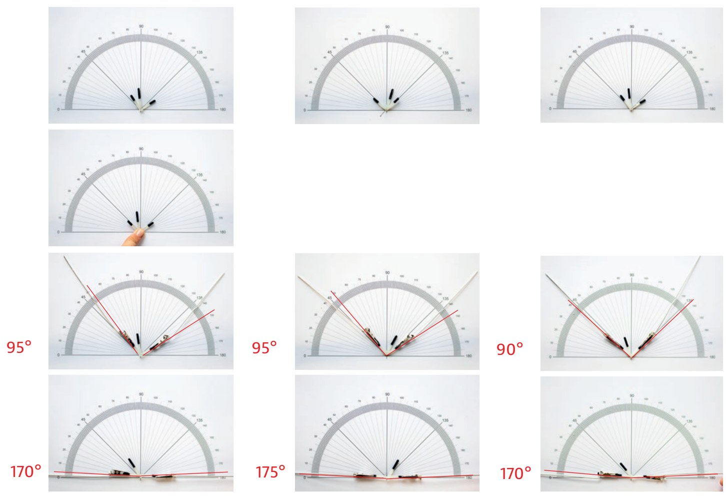

Figure 4.67 Hinge damage.

Auxetic Performance

Maximum Angle
90-95°

Minimum Angle
170-175°

Discoveries

Failed to support its form at Shore40.

Experimentation Two Reflection

Care was taken to ensure the pin always remained directly about the 0,0,0 point on the protractor measurer, as a fixed point of reference.

Hinges with harder Shore hardnesses above 40 were most successful. Those lower than 40 could not support their own weight and lacked structural integrity.

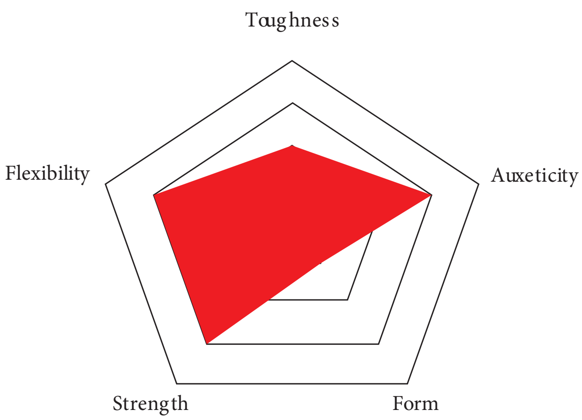

Figure 4.68 Experiment 2 Radar Plot.

Experimentation Two Evaluative Matrix

2D structures will not be accessed as they were the beginnings for establishing suitable parameters of the 3D structures which are the pursuits of this research.

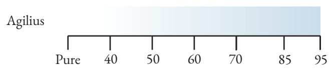

	Topology	Shore Hardness	Designed Hinge (Deformation Mechanism utilised)	Damage Sustained Unit unusable again — No damage Observed 0 1 2 3
1:4	**Re-entrant 3D Hexagonal Honeycomb**			
	2D 3 Strut Hinge 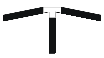	Shore 40	✓	3
		Shore 50	✓	3
		Shore 60	✓	3
	3D 3 Strut Square Hinge 	Shore 40	X	1
		Shore 50	✓	2
		Shore 60	✓	2
	3D 4 Strut Low Hinge 	Shore 40	X	3
		Shore 50	✓	3
		Shore 60	X	3
	3D 4 Strut High Hinge 	Shore 40	✓	3
		Shore 50	✓	3
		Shore 60	X	3
	3D 8 Strut High Hinge 	Shore 40	X	1
		Shore 50	X	3
		Shore 60	X	3
	3D 3 Strut Hinge 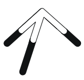	Shore 40	✓	1
		Shore 50	✓	1
		Shore 60	✓	1

[4.6] Experimentation 3: Auxetic Units

Experimentation three is focused on the development of dimensional units. The chosen structures are biaxial and harness the material properties found to be successful in the previous experiments

Digital	Physical	Mechanical Characteristics
Geometry		
Unit Geometry	Deformation Mechanism	Resting Angle
Strut + Hinge Geometry	Auxetic Effect	Geometry
Materials		
Digital Combinations	Shore Hardness	Shore Hardness
Scale		
Hinge to Strut Ratio		Hinge Scale

Experimentation Geometries

Design 1: Meta-Chiral Compression Twist
Design 2: 3D Planar Anti-Tetra-Chiral
Design 3: Star4

Structures are tested for their directional expansion qualities, through a rig designed to evenly across the eight corners, expand and rotate structures.

The figure below illustrates the rig built to test the Auxetic geometries, designed to simultaneously activate the structures 3D expansion, the geometries Chiral nature is utlised as the structure twists to expand.

Different ramps were used in the rig experiments to vary the intensity of the ramp in relation to the distance of circular rotation.

Expansion

The direction of rotation is dependent on the Auxetic cell and the pre programmed strain direction required for expansion.

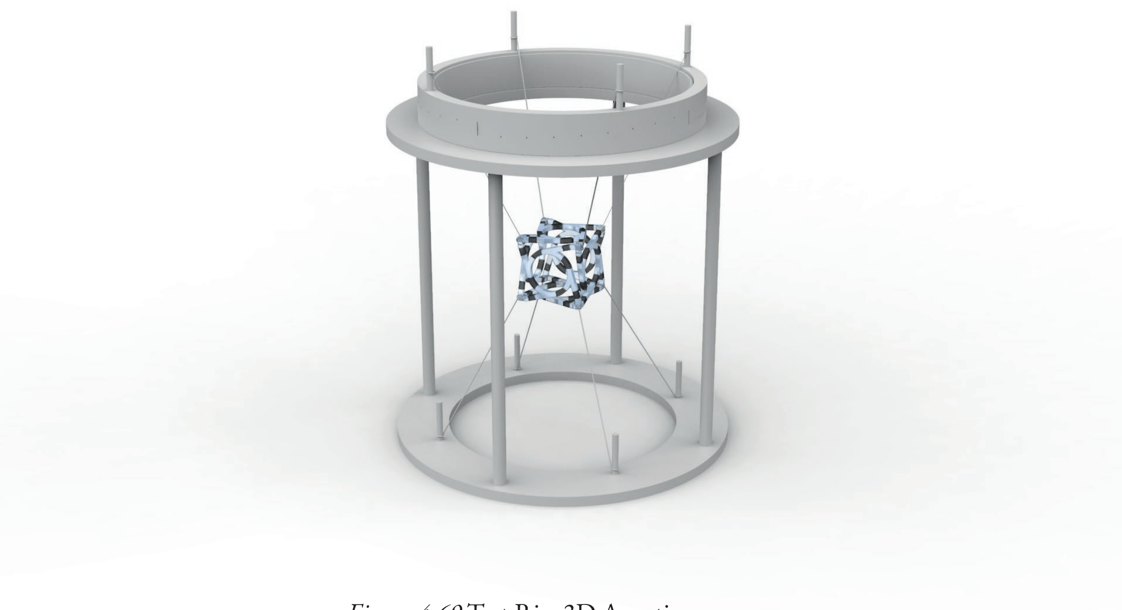

Figure 4.69 Test Rig, 3D Auxetics.

Inducing Axial Expansion through Rotation

Once manual rotation begins, the Auxetic cells will expand exhibiting the Auxetic effect.

Units are connected one at a time via eight strings, four at the top and four at the bottom. Each test can rotate up to 80 degrees, clockwise or counterclockwise.

Direction of Rotation

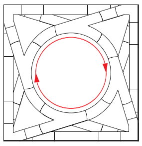

Figure 4.70. The structures must be rotated to aid the direction the struts are designed to translate through, (Author, 2020).

Expansion through rotation, exhibiting the Auxetic effect at a unit level.

[a] **[b]**

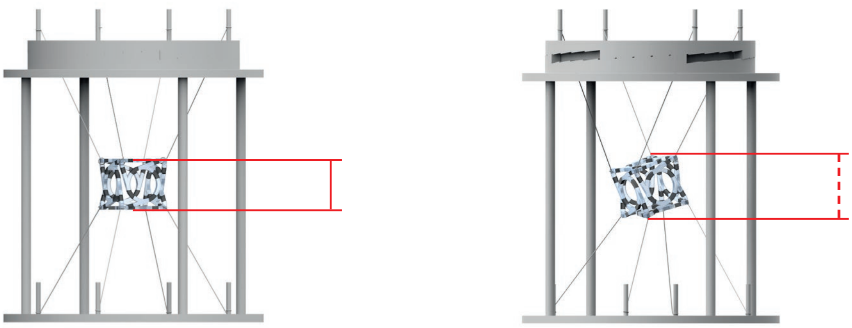

Figure. 4.71 (a) & (b) Test Rig relaxed and expanded.

Two different ramp angles were used, aswell as both directions of rotation.

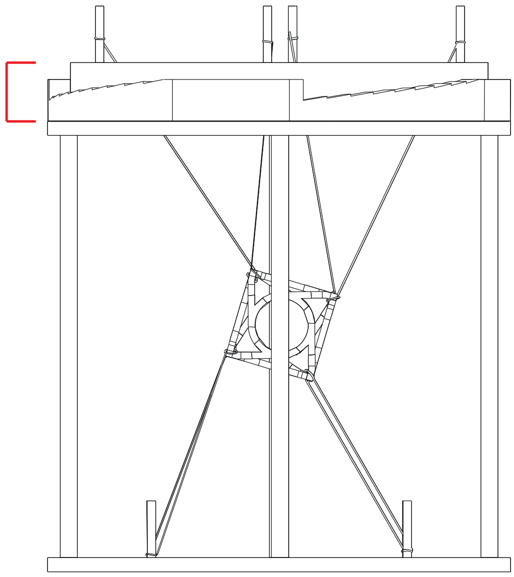

Shallow Ramp (A)
Ramp Angle 3.75 degree
Rotation 80 degrees to a height of 8mm

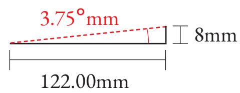

Steep Ramp (B)
Ramp Angle 5.46 degree
Rotation 48 degrees to a height of 8mm

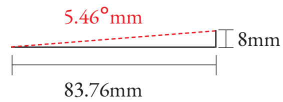

Figure 4.72 Test Rig, 3D Auxetics.

Figure 4.73 Experimentation.

Design 1: Meta-Chiral Compression Twist

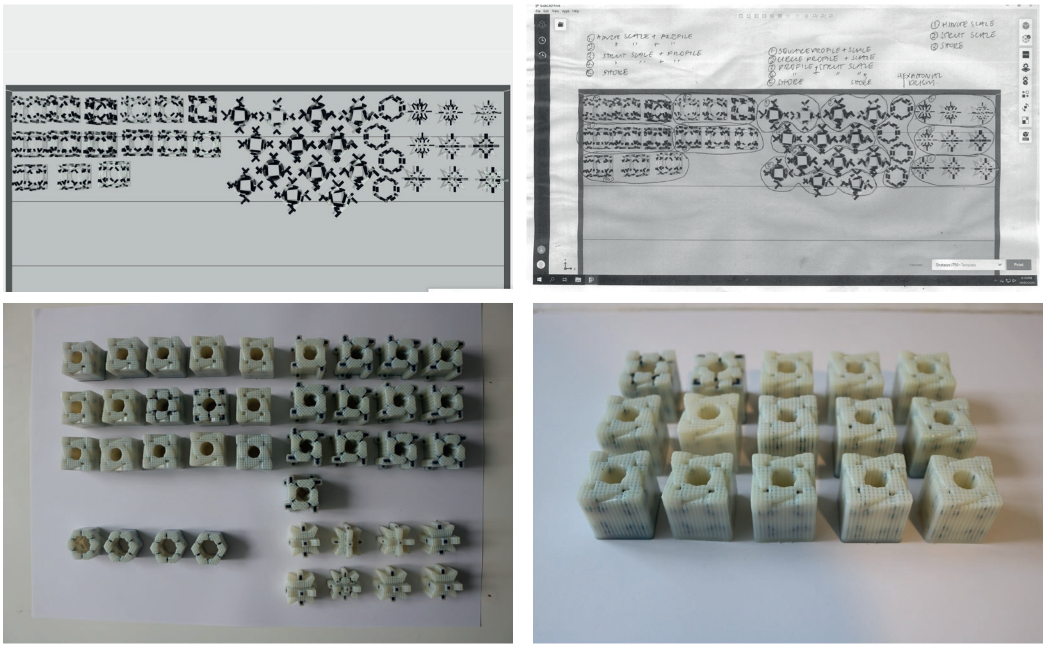

Figure 4.74 J750 Print Bed and models with support material still attached.

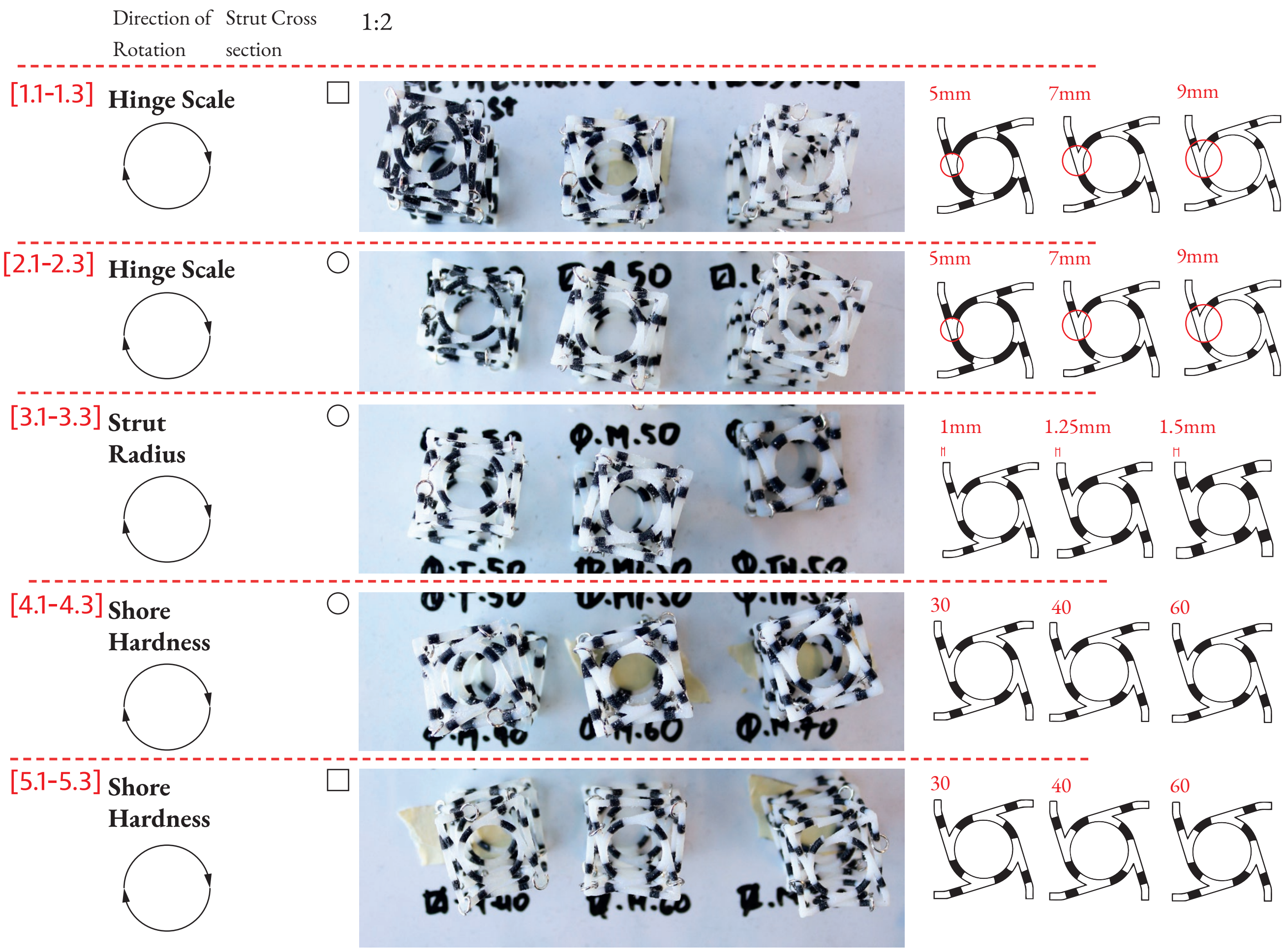

Figure 4.75 Clockwise rotation.

Chiral

Meta-Chiral Compression Twist

[1.1] Square cross section

Design Variables: Hinge Scale

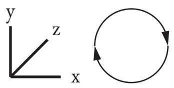

25x 25x 25mm

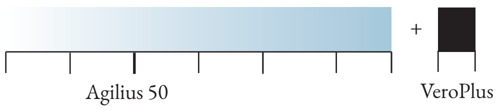

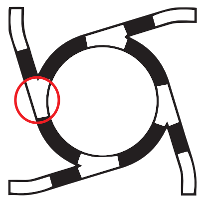

1:1

POC Manufacturing & Testing

Shallow Ramp (A)
Ramp Angle 3.75 degree
Rotation 80 degrees to a height of 8mm

Auxetic Performance

Maximum Expansion
Vertical Expansion
10mm

Rotational Expansion
20°

1:4 Small (5mm) Hinge Scale

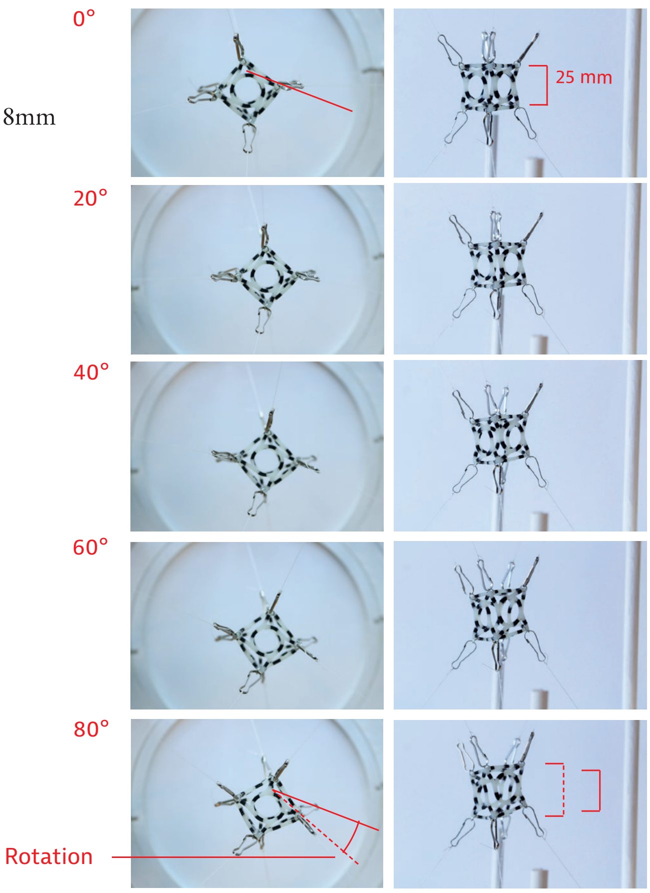

Figure 4.77 Meta-Chiral experimentation.

Discoveries

The unit has rotated little but is ununiformly skewed out of shape.

Chiral

Meta-Chiral Compression Twist

[1.1] Square cross section

Design Variables: Hinge Scale

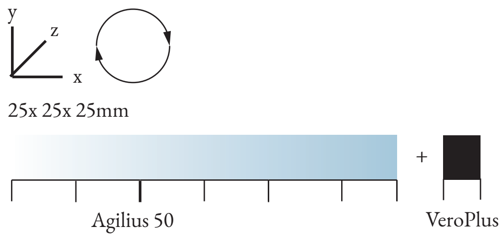

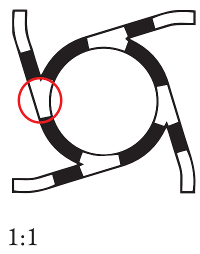

POC Manufacturing & Testing

Steep Ramp (B)
Ramp Angle 5.46 degree
Rotation 48 degrees to a height of 8mm

Auxetic Performance

Maximum Expansion
Vertical Expansion
15mm

Rotational Expansion
35°

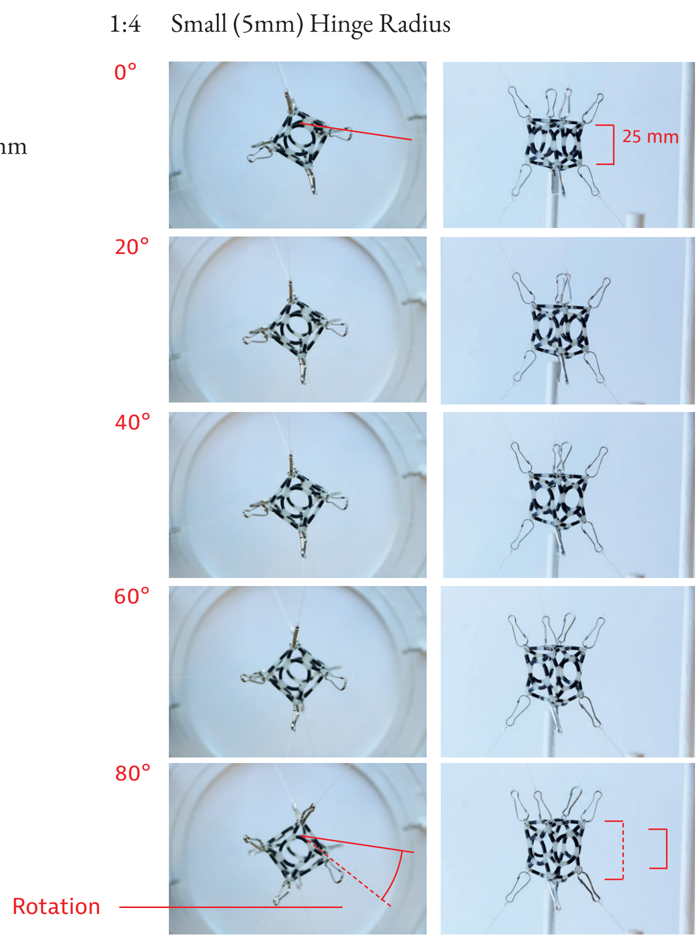

Figure 4.76 Meta-Chiral experimentation.

Discoveries

Large amount of unit stretching observed with rotation, suggesting the model is too elastic.

Chiral

Meta-Chiral Compression Twist

[1.2] Square cross section

Design Variables: Hinge Scale

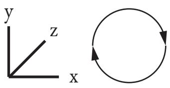

25x 25x 25mm

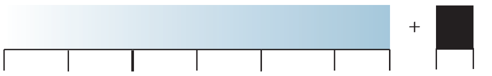

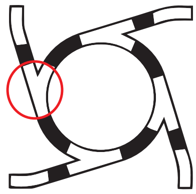

POC Manufacturing & Testing

Steep Ramp (B)
Ramp Angle 5.46 degree
Rotation 48 degrees to a height of 8mm

Auxetic Performance

Maximum Expansion
Vertical Expansion
15mm

Rotational Expansion
35°

Medium (7mm) Hinge Scale

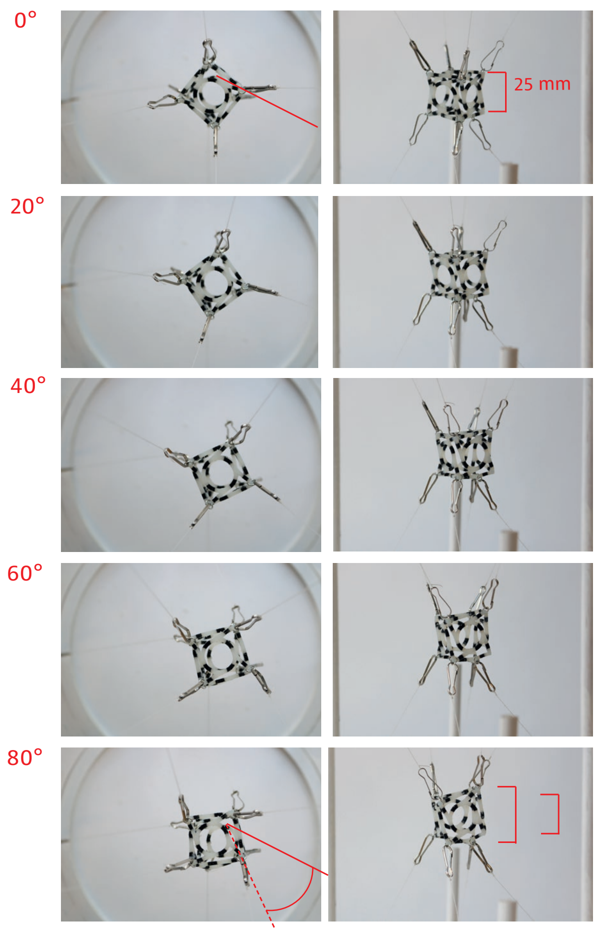

Figure 4.78. Meta-Chiral experimentation.

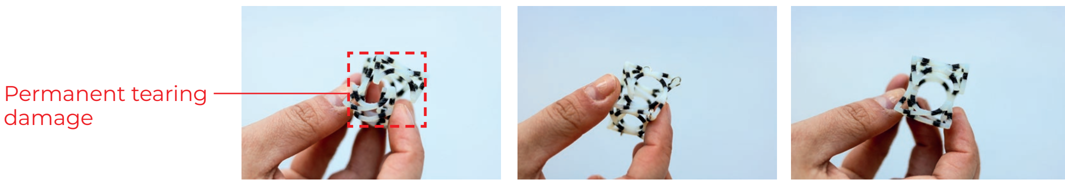

Figure 4.79 Meta-Chiral damage.

Chiral

Meta-Chiral Compression Twist

[1.3] Square cross section

Design Variables: Hinge Scale

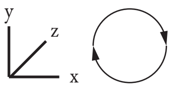

25x 25x 25mm

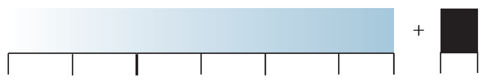

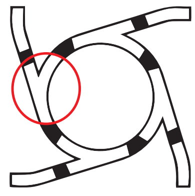

POC Manufacturing & Testing

Steep Ramp (B)
Ramp Angle 5.46 degree
Rotation 48 degrees to a height of 8mm

1:4 Large (9mm) Hinge Scale

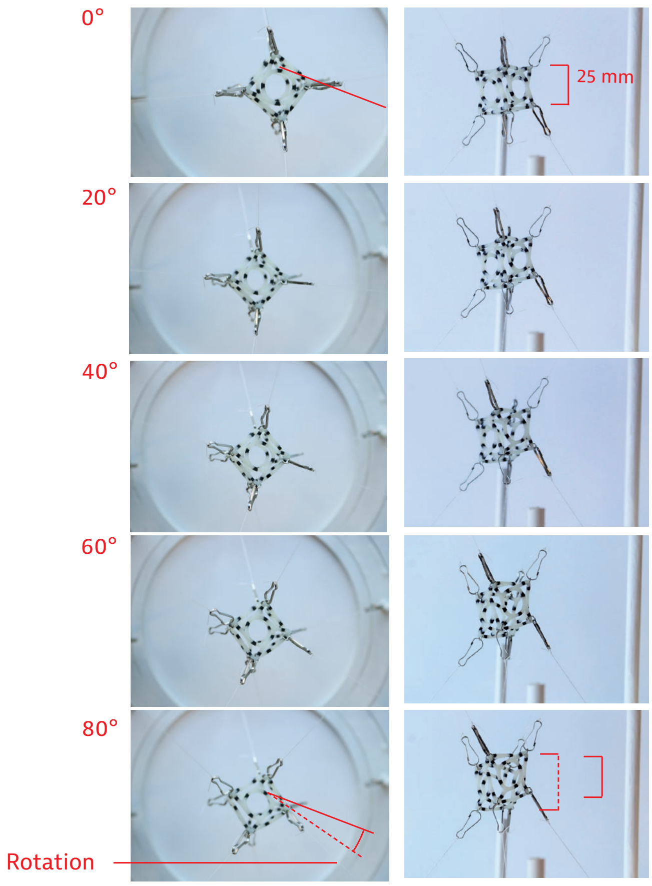

Figure 4.80 Meta-Chiral experimentation.

Auxetic Performance

Maximum Expansion
Vertical Expansion
15mm

Rotational Expansion
15°

Discoveries

The square profiles have shown to be less structurally robust than the circular strut profiles, because forces are unevenly concentrated in the square profiles and the edges experience high strain causing tearing damage

Chiral

Meta-Chiral Compression Twist

Circle cross section

[2.1] Design Variables: Hinge Scale

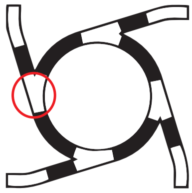

1:1

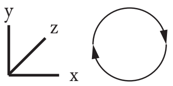

25x 25x 25mm

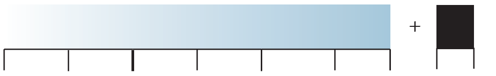

POC Manufacturing & Testing

Shallow Ramp (A)
Ramp Angle 3.75 degree
Rotation 80 degrees to a height of 8mm

Auxetic Performance

Maximum Expansion
Vertical Expansion
5mm

Rotational Expansion
40°

Small (5mm) Hinge Radius

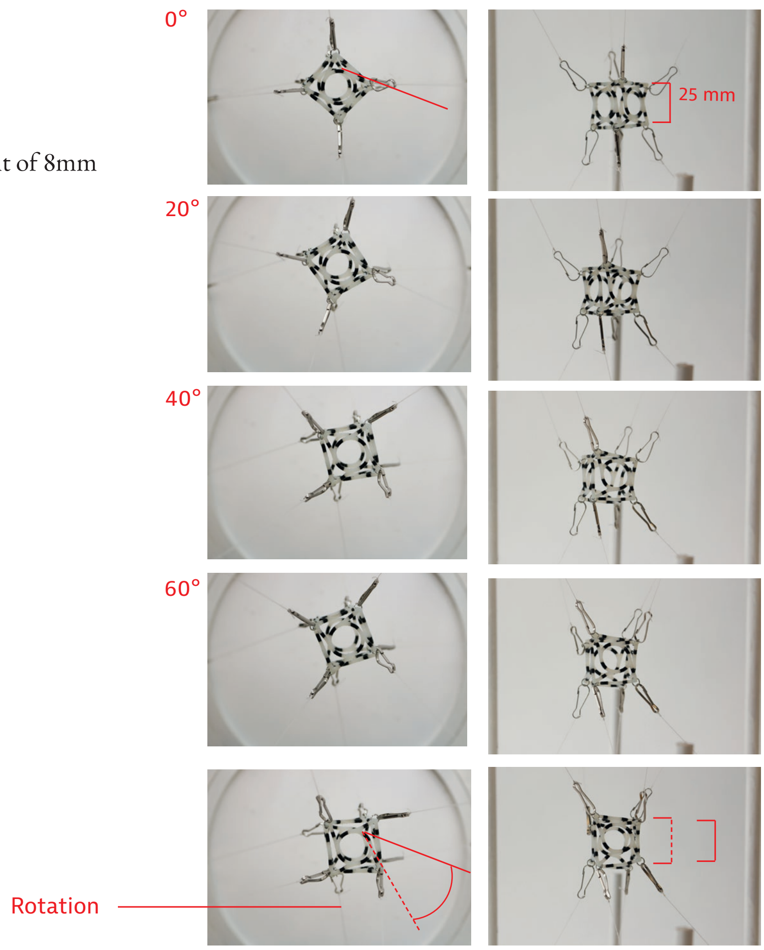

Figure 4.82 Meta-Chiral experimentation.

Discoveries

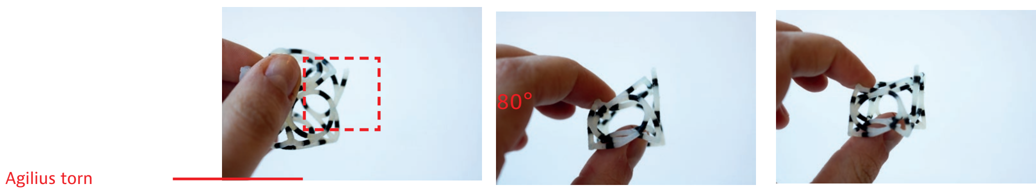

Figure 4.83 Meta-Chiral damage.

Chiral

Meta-Chiral Compression Twist

Circle cross section

[2.1] Design Variables: Hinge Scale

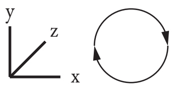

25x 25x 25mm

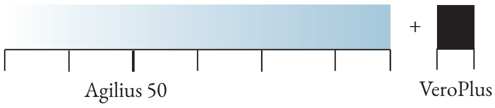

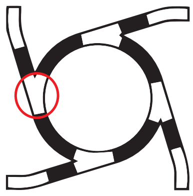

1:1

POC Manufacturing & Testing

Steep Ramp (B)
Ramp Angle 5.46 degree
Rotation 48 degrees to a height of 8mm

Auxetic Performance

Maximum Expansion
Vertical Expansion
10mm

Rotational Expansion
20°

1:4 Small (5mm) Hinge Radius

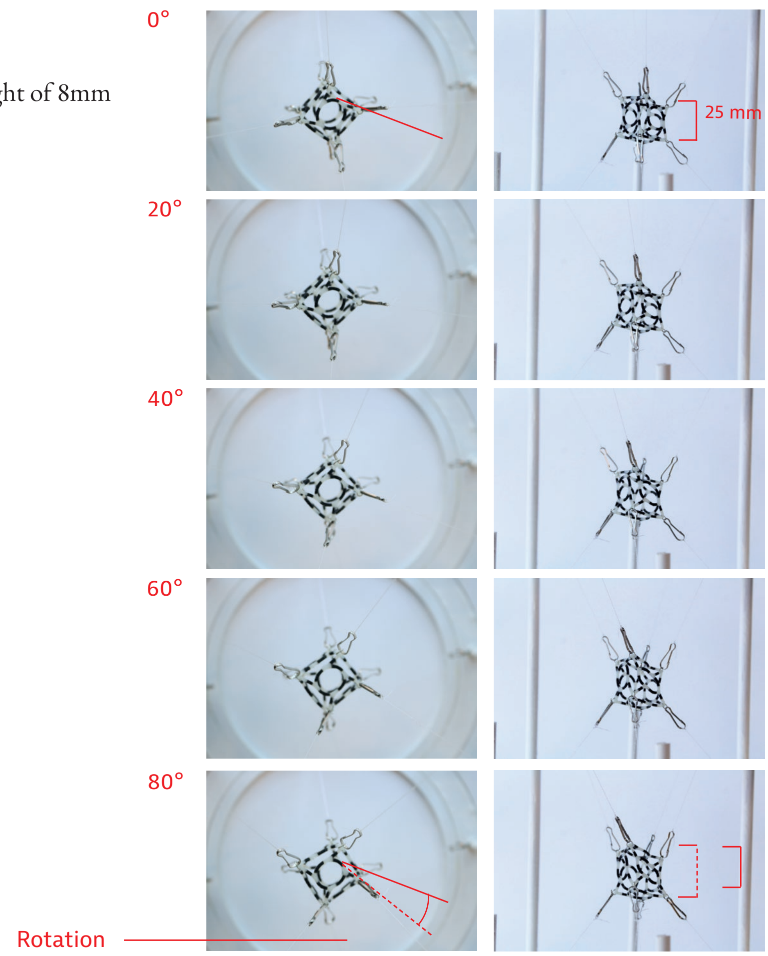

Figure 4.81 Meta-Chiral experimentation.

Discoveries

Circular profile much more resistant to damage.

Chiral

Meta-Chiral Compression Twist

Circle cross section

[2.2] Design Variable: Hinge Scale

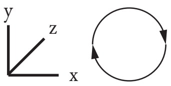

25x 25x 25mm

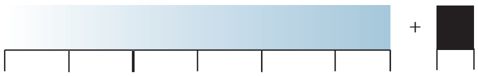

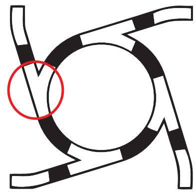

POC Manufacturing & Testing

Steep Ramp (B)
Ramp Angle 5.46 degree
Rotation 48 degrees to a height of 8mm

Auxetic Performance

Maximum Expansion
Vertical Expansion
10mm

Rotational Expansion
15°

1:4 Medium (7mm) Hinge Scale

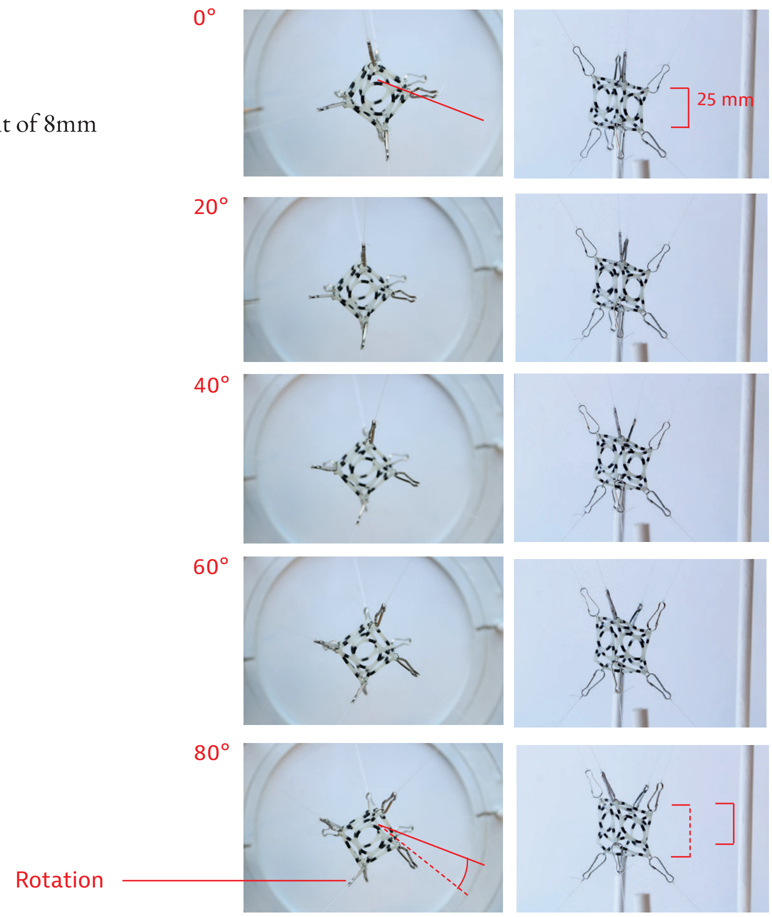

Figure 4.84 Meta-Chiral experimentation.

Chiral

Meta-Chiral Compression Twist

Circle cross section

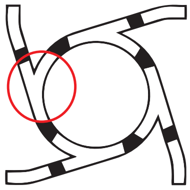

[2.3] Design Variable: Hinge Scale

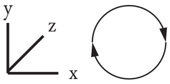

25x 25x 25mm

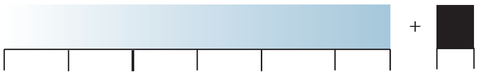

POC Manufacturing & Testing

Steep Ramp (B)
Ramp Angle 5.46 degree
Rotation 48 degrees to a height of 8mm

Auxetic Performance

Maximum Expansion
Vertical Expansion
10mm

Rotational Expansion
20°

1:4 Large (9mm) Hinge Scale

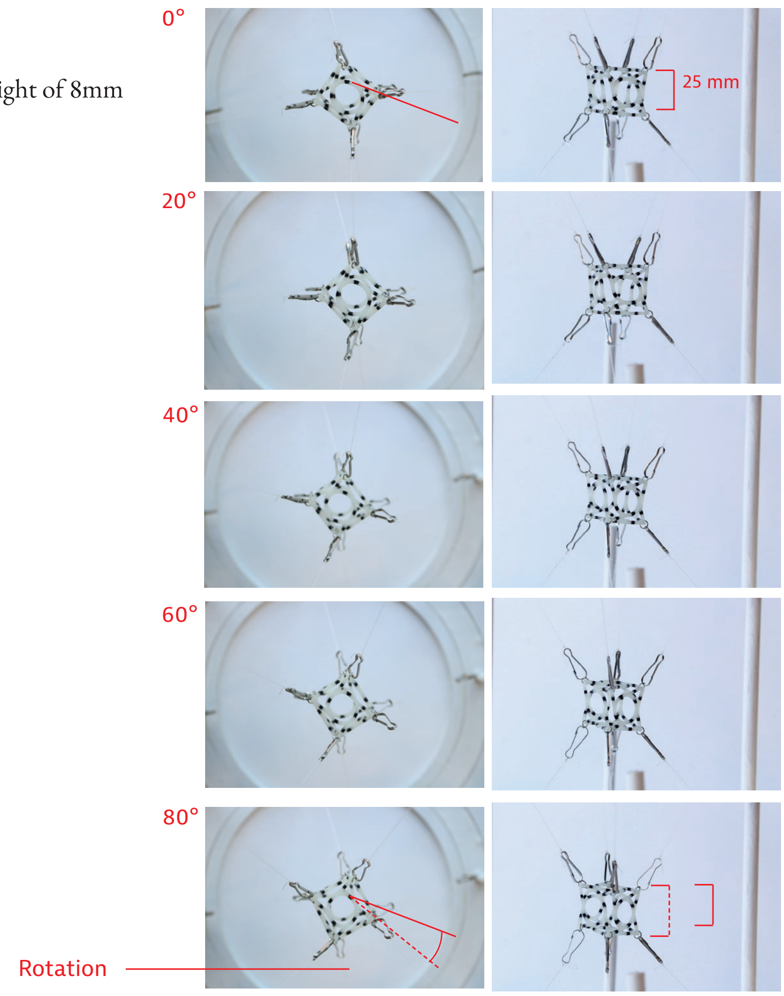

Figure 4.85 Meta-Chiral experimentation.

Chiral

Meta-Chiral Compression Twist

Circle cross section

[3.1] Design Variable: Hinge Scale

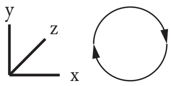

25x 25x 25mm

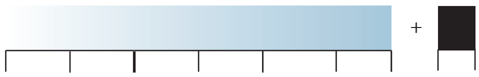

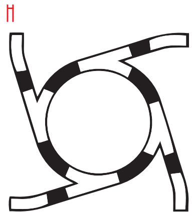

1:1

POC Manufacturing & Testing

Steep Ramp (B)
Ramp Angle 5.46 degree
Rotation 48 degrees to a height of 8mm

Auxetic Performance

Maximum Expansion
Vertical Expansion
10mm

Rotational Expansion
15°

1:4 Thin (1mm) Strut Radius

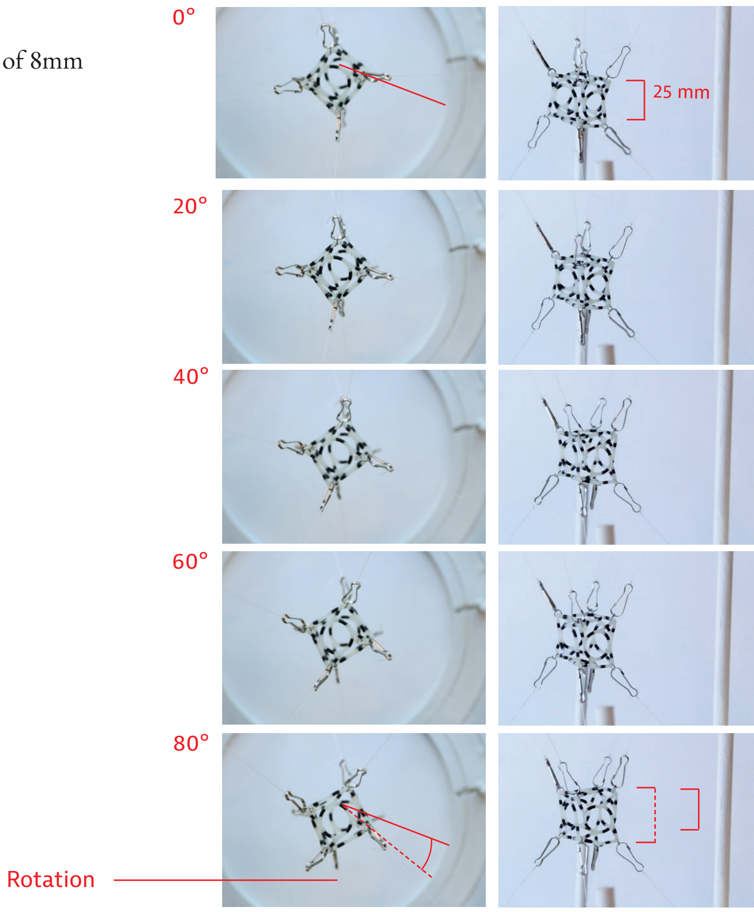

Figure 4.86 Meta-Chiral experimentation.

Chiral

Meta-Chiral Compression Twist

Circle cross section

[3.3] Design Variable: Hinge Scale

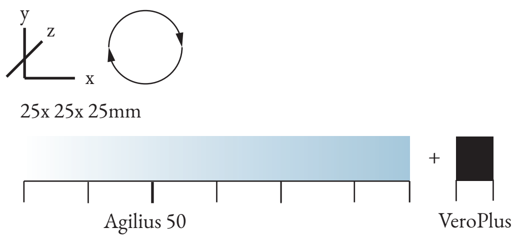

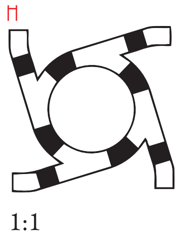

POC Manufacturing & Testing

Steep Ramp (B)
Ramp Angle 5.46 degree
Rotation 48 degrees to a height of 8mm

Auxetic Performance

Maximum Expansion
Vertical Expansion
10mm

Rotational Expansion
25°

1:4 Thick (1.5mm) Strut Radius

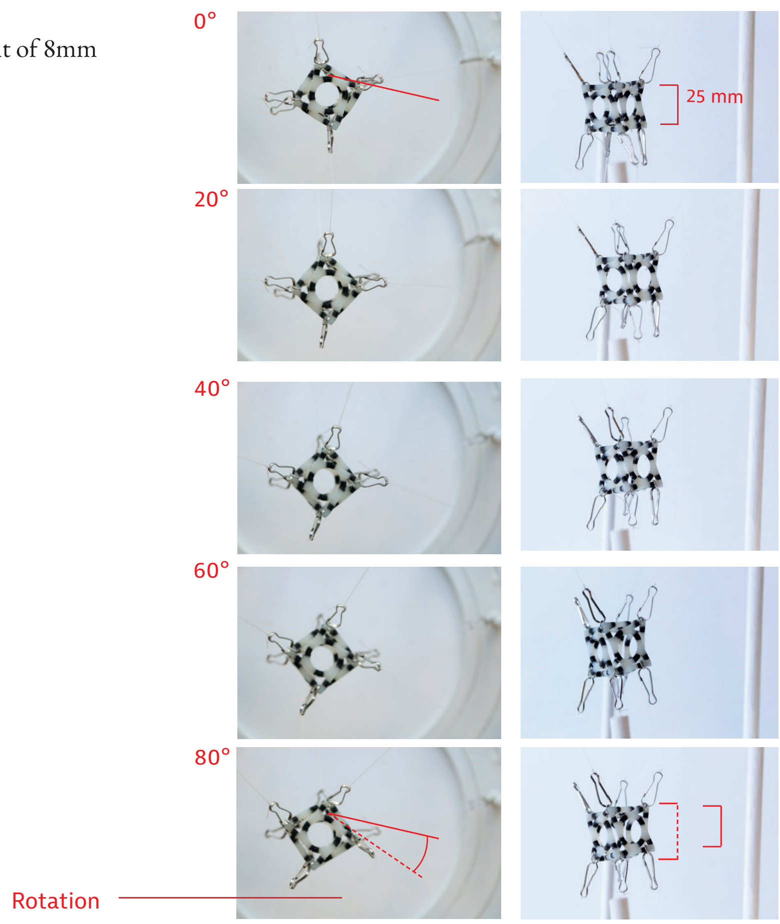

Figure 4.87 Meta-Chiral experimentation.

Chiral

Meta-Chiral Compression Twist

Circle cross section

[4.1] Design Variable: Shore Hardness

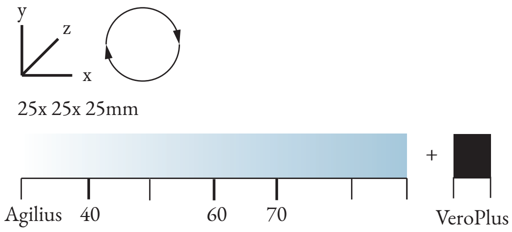

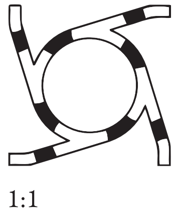

POC Manufacturing & Testing

Steep Ramp (B)
Ramp Angle 5.46 degree
Rotation 48 degrees to a height of 8mm

Auxetic Performance

Maximum Expansion
Vertical Expansion
15mm

Rotational Expansion
20°

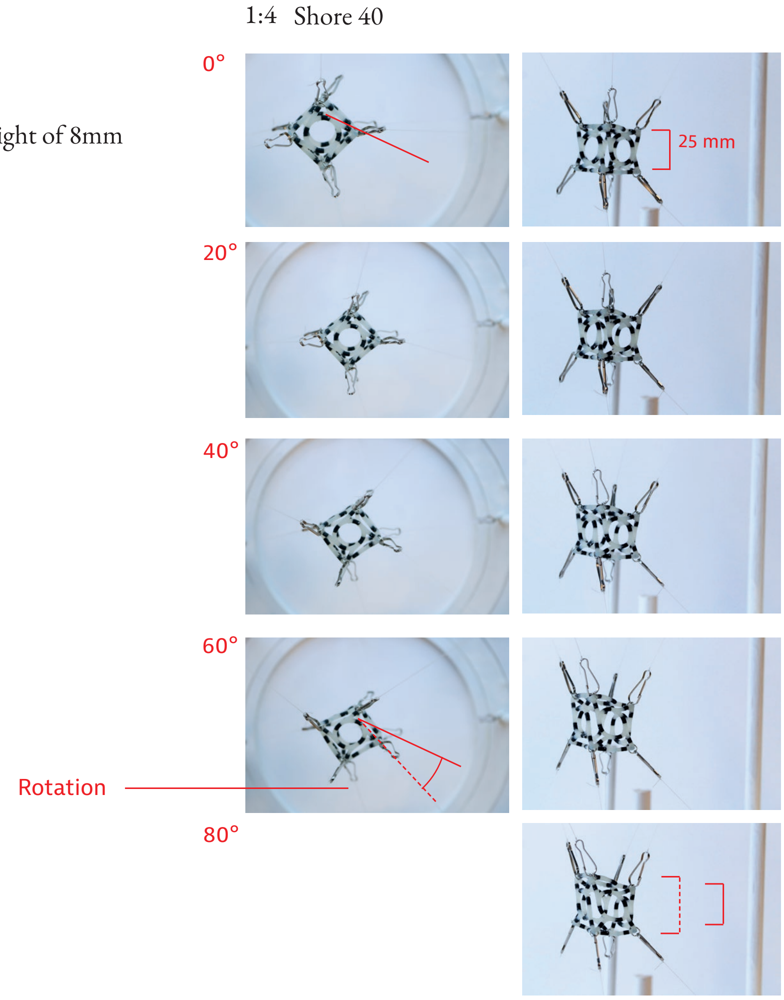

Figure 4.88 Meta-Chiral experimentation.

Chiral

Meta-Chiral Compression Twist

Circle cross section

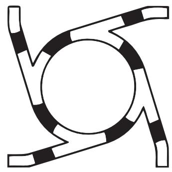

1:1

[4.2] Design Variable: Shore Hardness

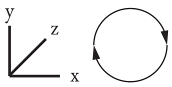

25x 25x 25mm

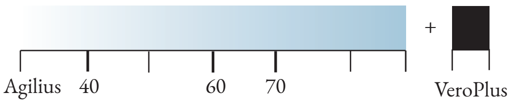

POC Manufacturing & Testing

Steep Ramp (B)
Ramp Angle 5.46 degree
Rotation 48 degrees to a height of 8mm

Auxetic Performance

Maximum Expansion
Vertical Expansion
15mm

Rotational Expansion
5°

1:4 Shore 60

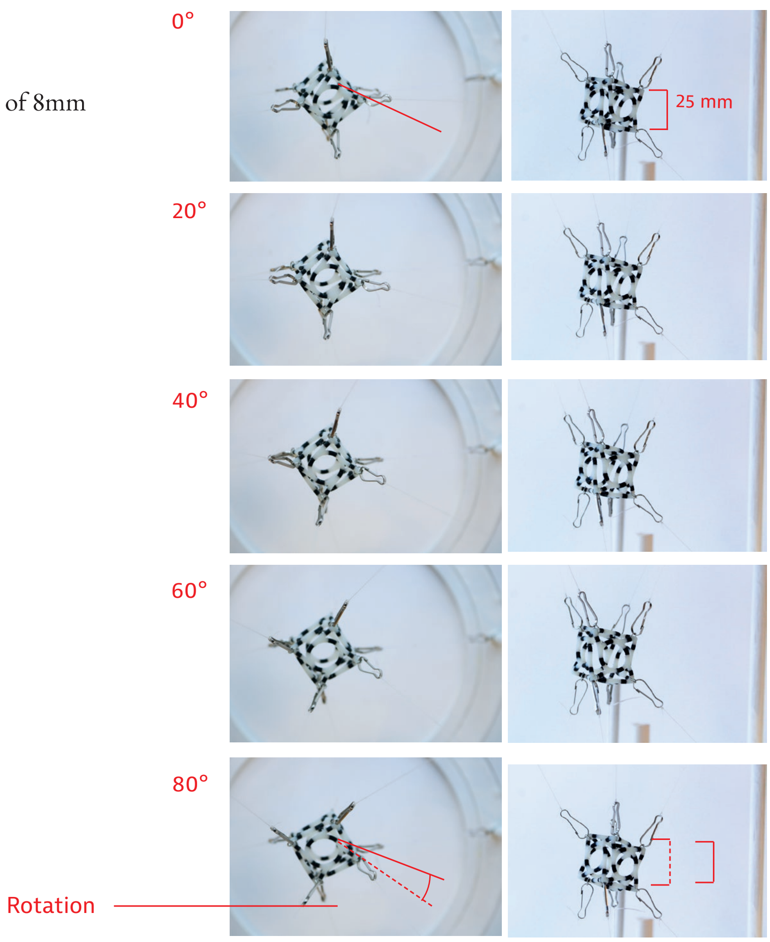

Figure 4.90 Meta-Chiral experimentation.

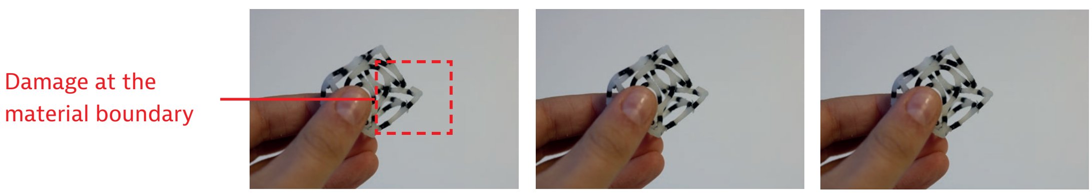

Figure 4.89 Meta-Chiral damage.

Chiral

Meta-Chiral Compression Twist

Circle cross section

[4.3] Design Variable: Shore Hardness

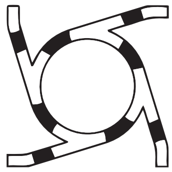
1:1

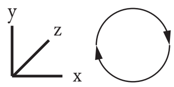

25x 25x 25mm

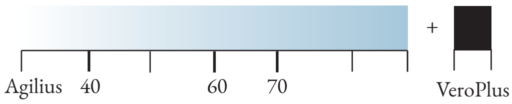

POC Manufacturing & Testing

1:4 Shore 70

Steep Ramp (B)
Ramp Angle 5.46 degree
Rotation 48 degrees to a height of 8mm

Auxetic Performance

Maximum Expansion
Vertical Expansion
10mm

Rotational Expansion
15°

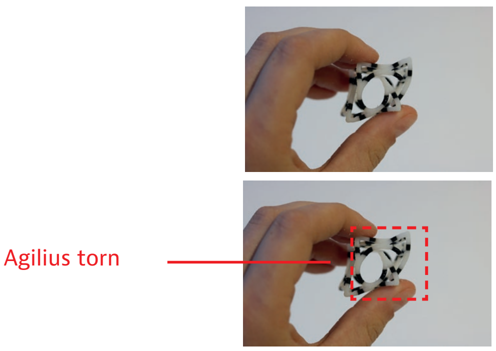

Figure 4.91. Meta-Chiral damage.

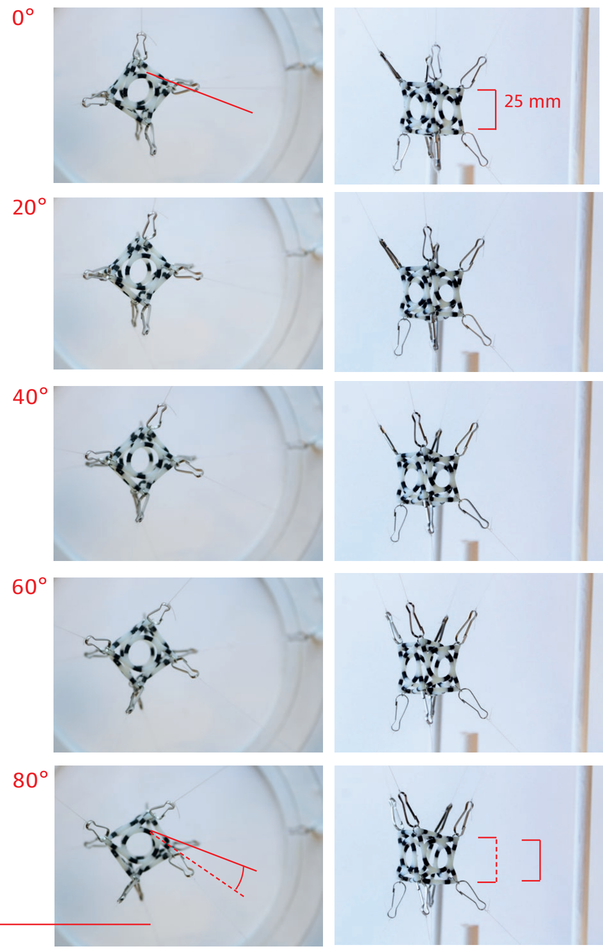

Figure 4.92 Meta-Chiral experimentation.

Chiral

Meta-Chiral Compression Twist

Square cross section

[5.1] Design Variable: Shore Hardness

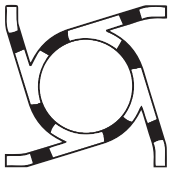

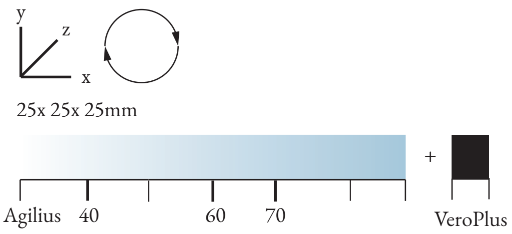

POC Manufacturing & Testing

Steep Ramp (B)
Ramp Angle 5.46 degree
Rotation 48 degrees to a height of 8mm

Auxetic Performance

Maximum Expansion
Vertical Expansion
15mm

Rotational Expansion
20°

1:4 Shore 40

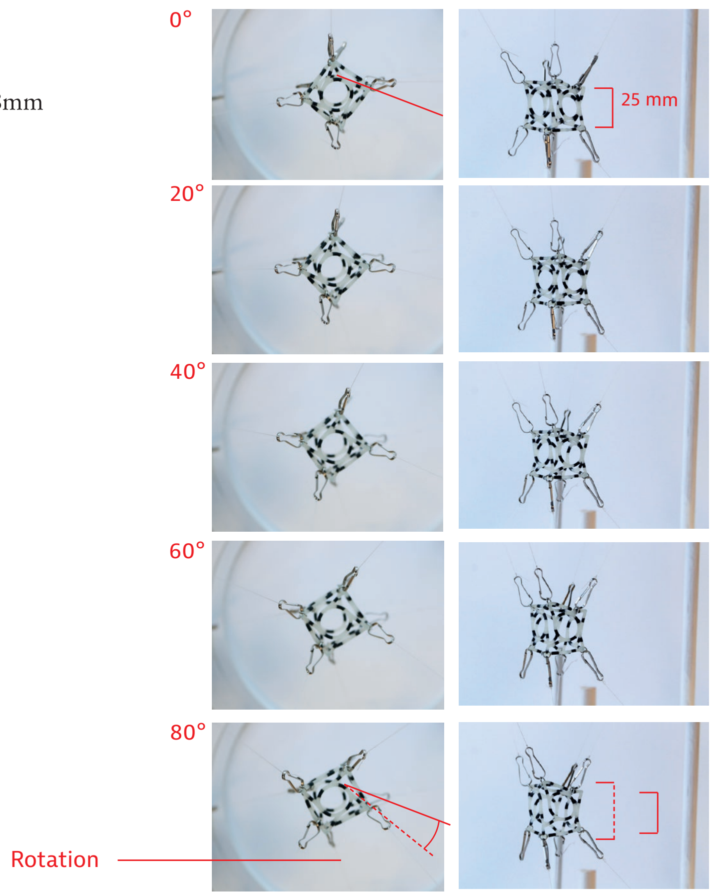

Figure 4.93 Meta-Chiral experimentation.

Discoveries

The unit is too elastic and lacks structural integrity.

Chiral

Meta-Chiral Compression Twist

[5.2] Square cross section

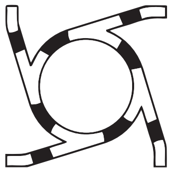

1:1

Design Variable: Shore Hardness

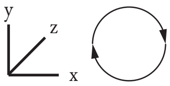

25x 25x 25mm

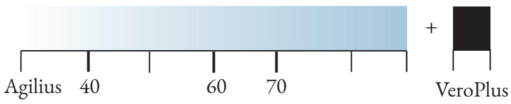

POC Manufacturing
& Testing

Steep Ramp (B)
Ramp Angle 5.46 degree
Rotation 48 degrees to a height of 8mm

Auxetic Performance

Maximum Expansion
Vertical Expansion
5mm

Rotational Expansion
15°

1:4 Shore 60

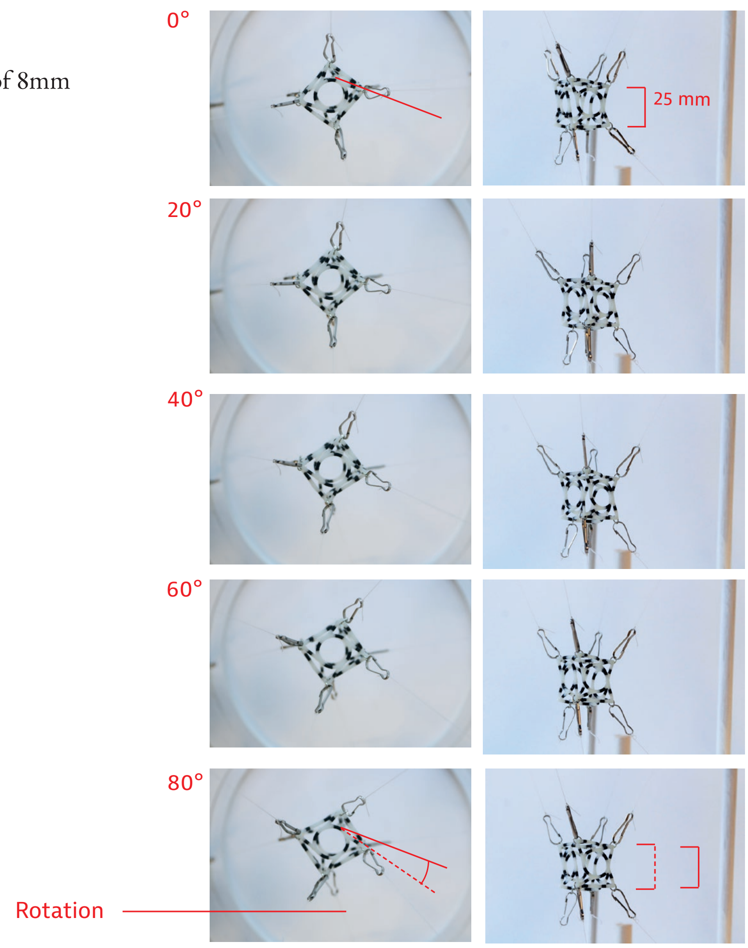

Figure 4.94 Meta-Chiral experimentation.

Chiral

Meta-Chiral Compression Twist

[5.3] Square cross section

Design Variable: Shore Hardness

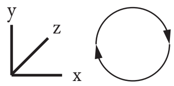

25x 25x 25mm

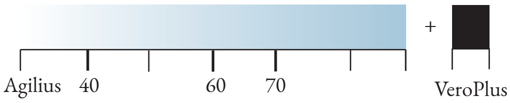

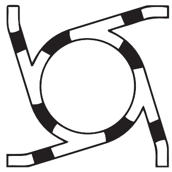

1:1

POC Manufacturing & Testing

1:4 Shore 70

Auxetic Performance

Maximum Expansion
Vertical Expansion
No measurement

Rotational Expansion
10°

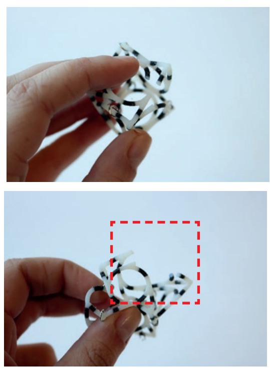

Figure 4.95. Meta-Chiral damage.

Rotation

Figure 4.96 Meta-Chiral experimentation.

Discoveries

The unit snapped during testing. Failed to collect adequate data.

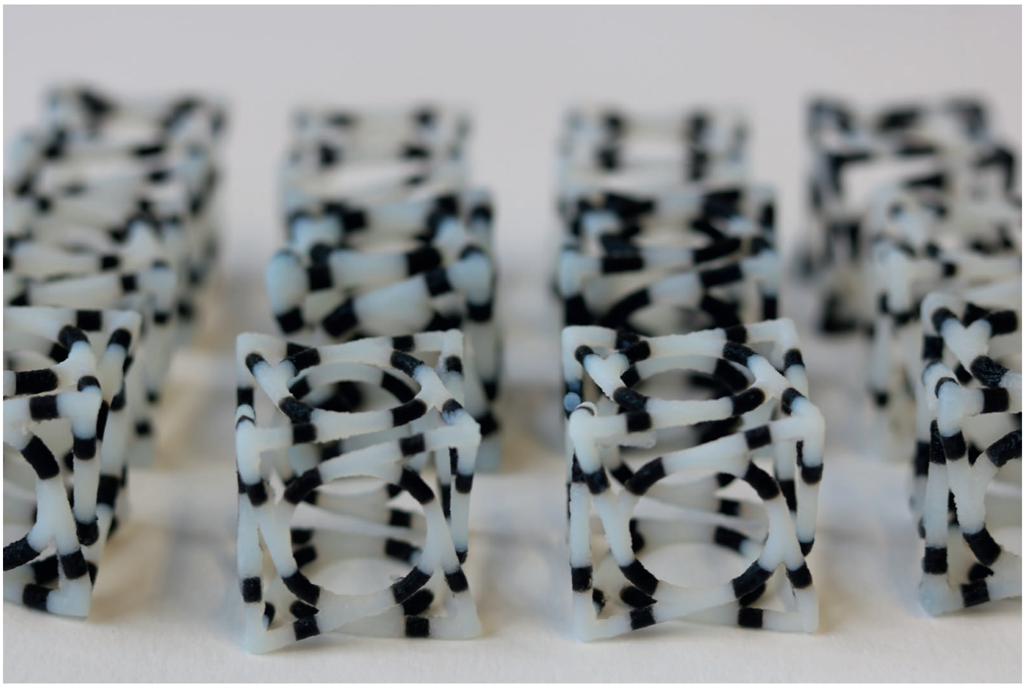

Figure 4.98 Meta-Chiral Compression Twist.

Experimentation 3 Design 1 Meta-Chiral Compression Twist Reflection

It was observed that a structure's geometry has a significant impact on its mechanical properties. Throughout the experimentation the mechanical designs of the 2D and 3D geometries were investigated and their deformation mechanisms tested through force and strain energy analysis to determine structures which are theoretically suitable for application and then additionally viable for fabrication.

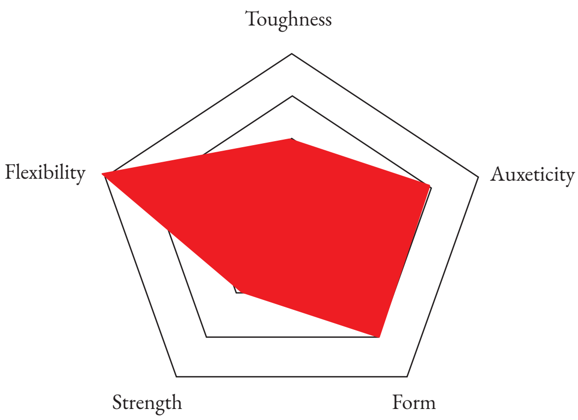

Figure 4.97 Experiment 3 Radar Plot.

Experimentation 3 Design 1 Evaluative Matrix

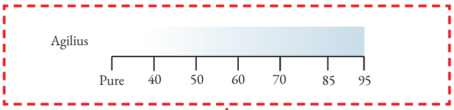

Topology		Shore Hardness	Designed Hinge (Deformation Mechanism utilised)	Auxetic Effect Observed Resting Position — Utilised to Maximum 0 1 2 3	Damage Sustained Unit unusable again — No damage Observed 0 1 2 3
1:2 **Chiral Topologies**					
	5mm	Shore 50			
	7mm				
	9mm				
	1mm				
	1.25mm				

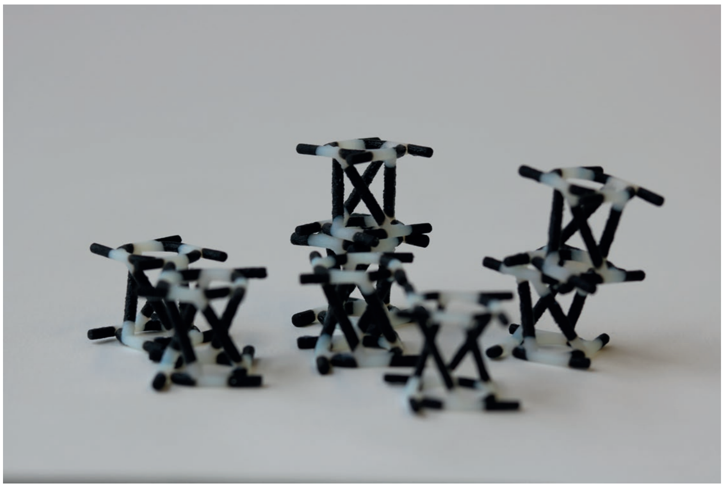

Figure 4.99 3D Planar Anti Tetra Chiral.

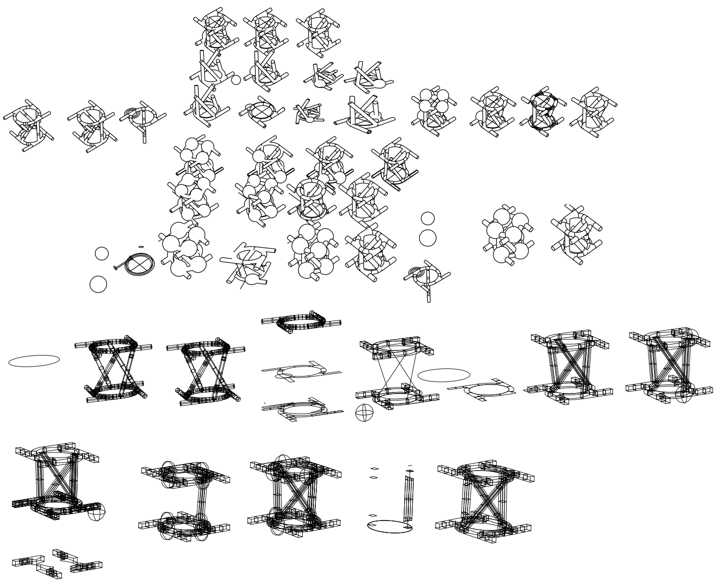

Figure 4.100 Planar Anti-tetra-chiral Digital Development.

3D Planar Anti-Tetra-Chiral has only one test as the process was made efficient through the Meta-Chiral Compression Twist exploration.

Testing variables include
Direction of rotation
Cross section form
Hinge radius scale
Shore hardness

The procedure for testing involves starting the top geometry one phase ahead of the bottom, to increase the twist and ensure the twisting struts end up straight after 45 degrees. The unit should not rotate more than full 360 phase.

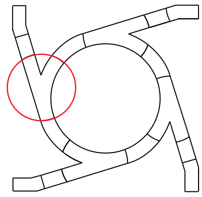

1:1

Figure 4.102 3D Planar Anti-Tetra-Chiral.

Shallow Ramp (A)
Ramp Angle 3.75 degree
Rotation 80 degrees to a height of 8mm.

Steep Ramp (B)
Ramp Angle 5.46 degree
Rotation 48 degrees to a height of 8mm.

Strain Applied
8mm vertical lift through 122mm counterclockwise rotation.

3.75° vertical slope per step, 2 steps moved (20° counterclockwise) per recorded image.

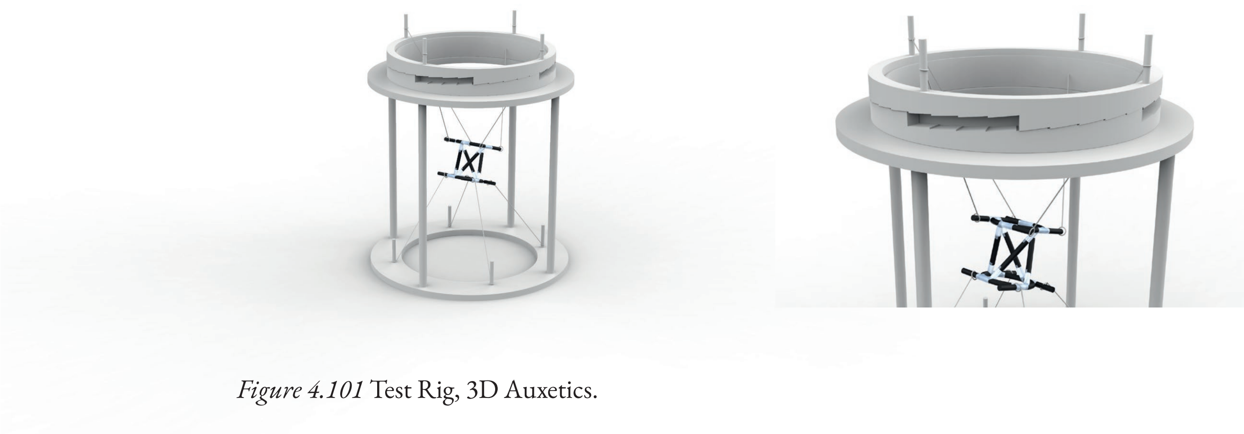

Figure 4.101 Test Rig, 3D Auxetics.

Clockwise and Counterclockwise Rotation

Red measurements are truth.
Illustrations and figures are scaled 1:2.

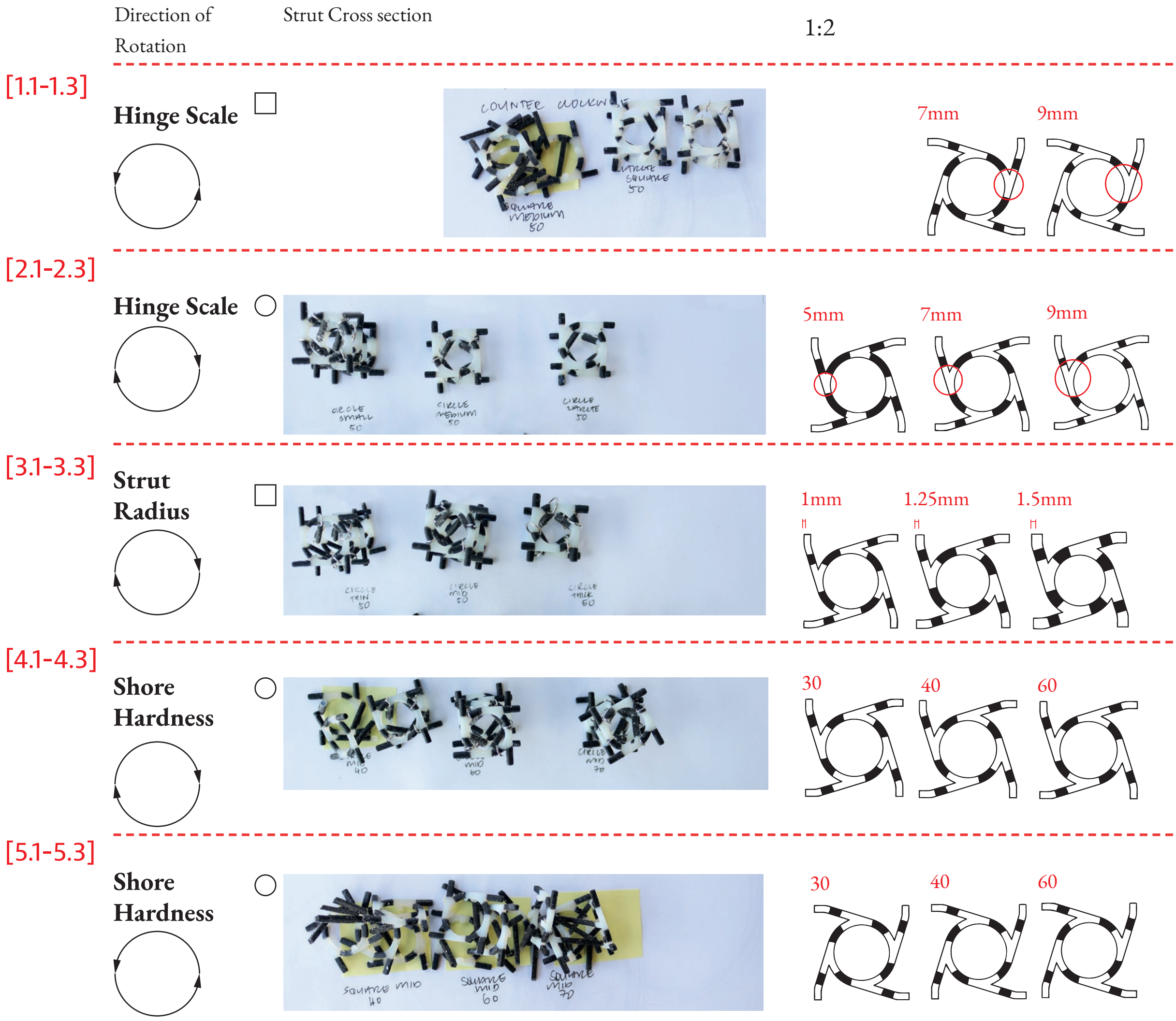

Figure 4.103 Clockwise & counterclokwise rotation.

Two different ramp angles were used, aswell as both directions of rotation.

Shallow Ramp (A)
Ramp Angle 3.75 degree
Rotation 80 degrees to a height of 8mm

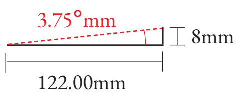

Steep Ramp (B)
Ramp Angle 5.46 degree
Rotation 48 degrees to a height of 8mm

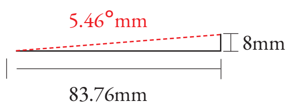

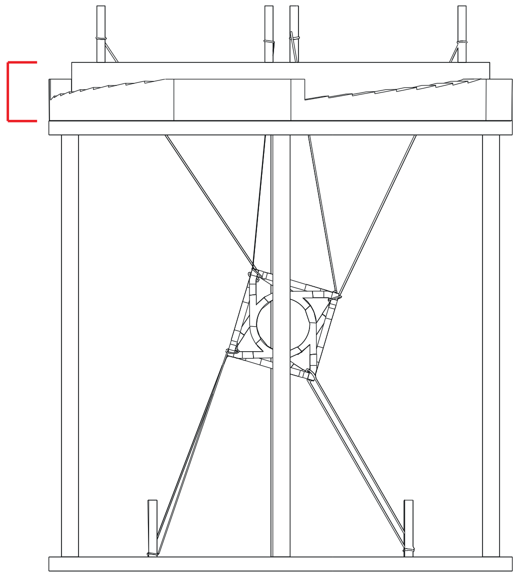

Figure 4.104 Test Rig, 3D Auxetics.

Although the bottom geometry was suspended in place, it did move some what when the top was twisted The bottom geometry has moved counterclockwise.

Maximum measurements will have the counterclockwise rotation of the bottom geometry minused from the movement of the top geometry to get the actual reading of the rotation.

Chiral

3D Planar Anti-Tetra-Chiral

Square cross sectionv

Design Variable: Hinge Scale

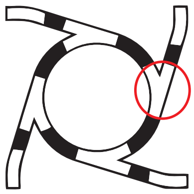

1:1

[1.2]

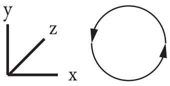

25x 25x 25mm

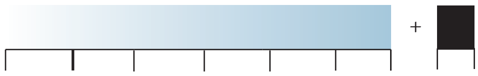

The 7mm radius is the smallest hinge size possible, as if it is reduced any further, not all of the intersection of the struts is agilius and therefore, the geometry becomes locked in its printed state.

POC Manufacturing & Testing

1:4 Medium (7mm) Hinge Scale

No model endured cleaning and rig assembly, therefore no test was carried out.

Broken apart during removal of support material

Auxetic Performance

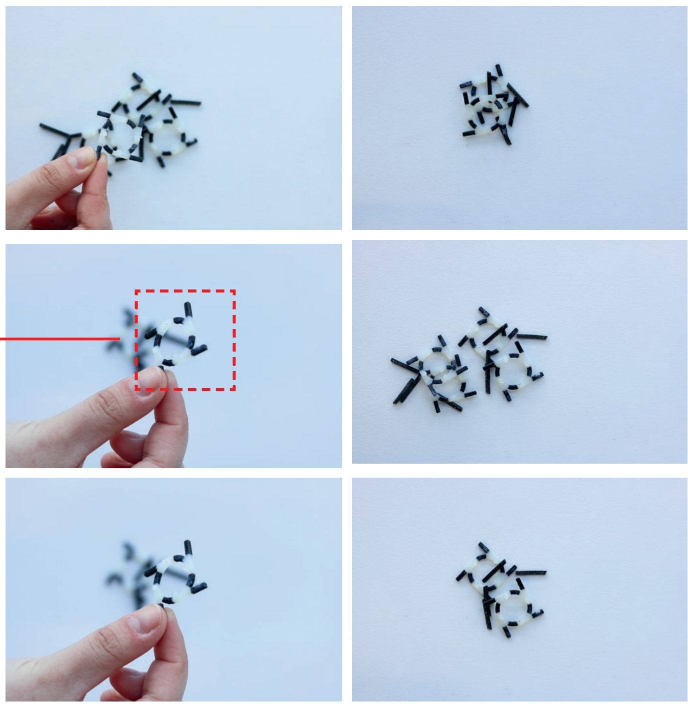

Figure 4.105 3D Anti-Tetra-Chiral experimentation.

Discoveries

Unsuccessful square cross section strut, most likely due to uneven distribution of strain along the edges of the square struts.

Chiral

3D Planar Anti-Tetra-Chiral

[1.3] Square cross section

Design Variable: Hinge Scale

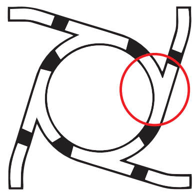

1:1

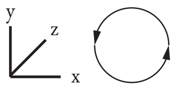

25x 25x 25mm

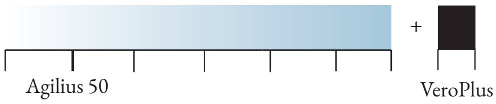

POC Manufacturing & Testing

Steep Ramp (B)
Ramp Angle 5.46 degree
Rotation 48 degrees to a height of 8mm

1:4 Large (9mm) Hinge Scale

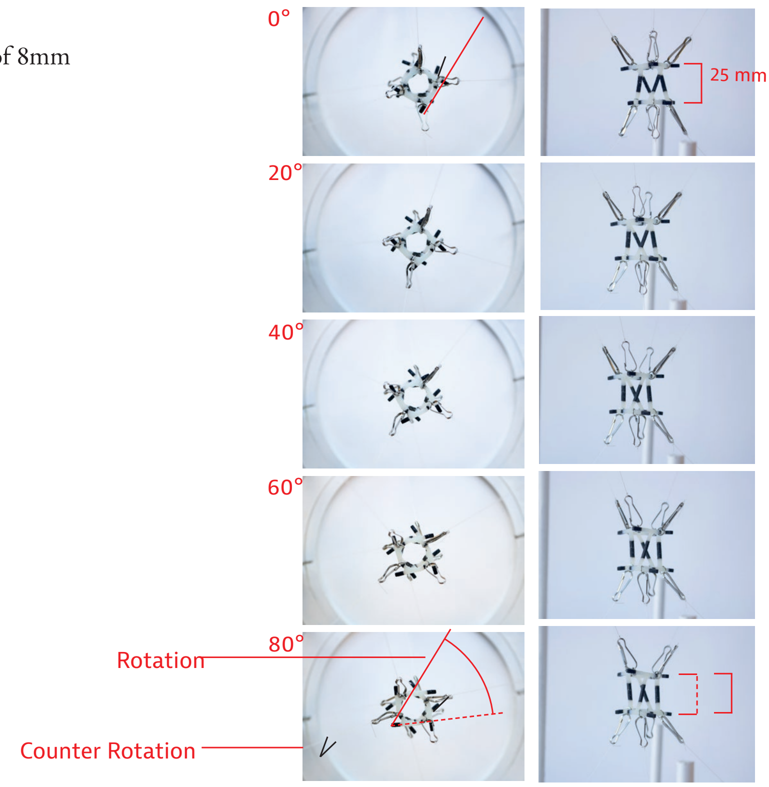

Figure 4.106 3D Anti-Tetra-Chiral experimentation.

Auxetic Performance

Maximum Expansion
Vertical Expansion
4mm

Rotational Expansion
Counter Rotation: 35°
Rotation: 70°
70-35=
30°

Discoveries

Some counter rotation experienced, but an overall rotational expansion of 30 degrees observed.

Chiral

3D Planar Anti-Tetra-Chiral

[2.1] Circle cross section
Clockwise

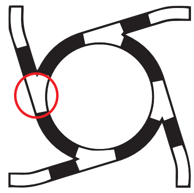

1:1

Design Variable: Hinge Scale

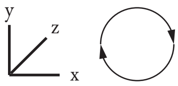

25x 25x 25mm

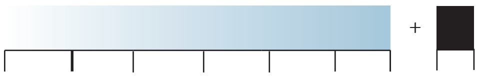

POC Manufacturing
& Testing

Steep Ramp (B)
Ramp Angle 5.46 degree
Rotation 48 degrees to a height of 8mm

1:4 Small (5mm) Hinge Scale

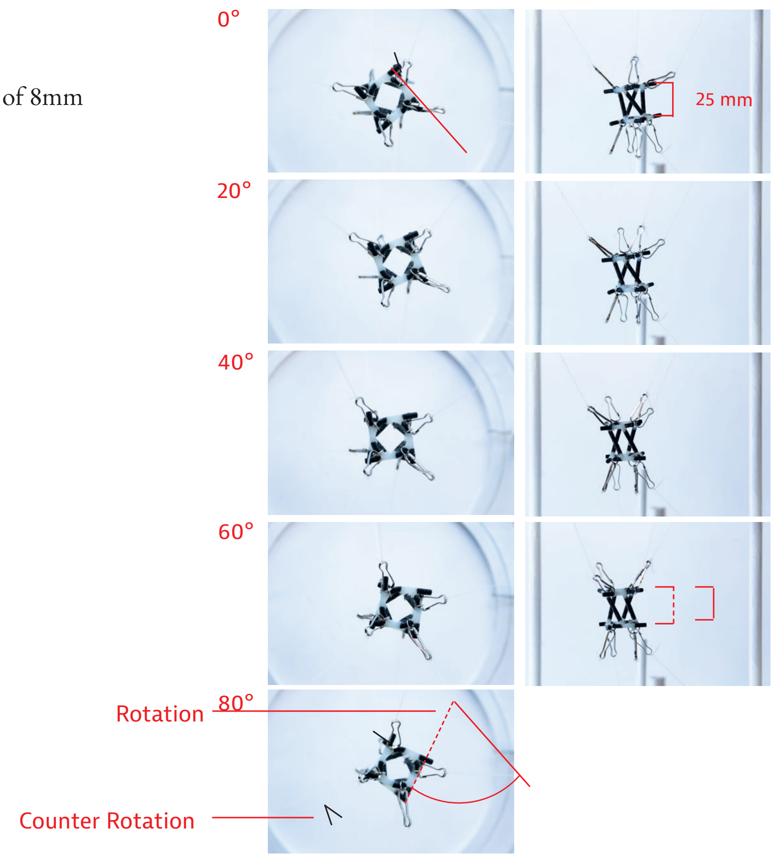

Auxetic Performance

Maximum Expansion
Vertical Expansion
3mm

Counter Rotation
35°
Rotational Expansion
70-35=
35°

Figure 4.107 3D Anti-Tetra-Chiral experimentation.

Chiral

[2.2]

3D Planar Anti-Tetra-Chiral

Circle cross section
Clockwise

Design Variable: Hinge Scale

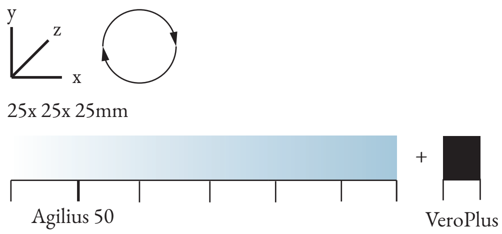

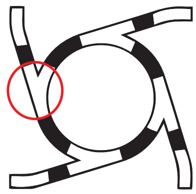

1:1

POC Manufacturing & Testing

Auxetic Performance

1:4 Medium (7mm) Hinge Scale

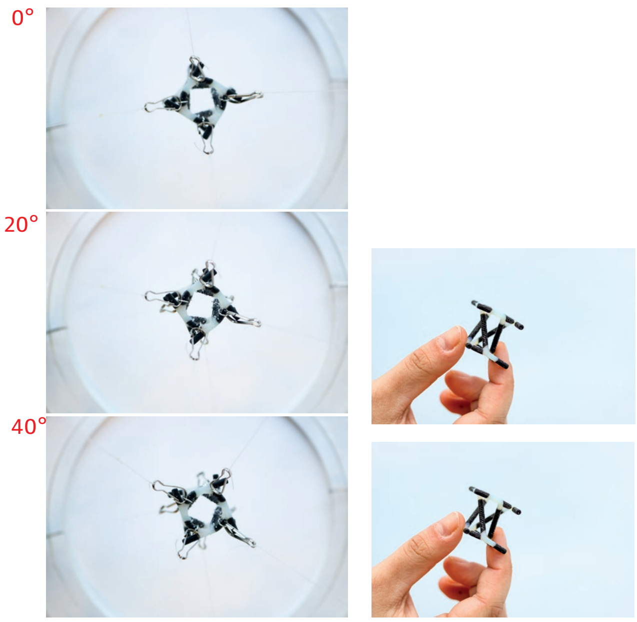

Figure 4.108 3D Anti-Tetra-Chiral experimentation.

Discoveries

Failed to collect adequate data.

Chiral

3D Planar Anti-Tetra-Chiral

[2.3]

Circle cross section
Clockwise

Design Variable: Hinge Scale

y z x

25x 25x 25mm

Agilius 50 + VeroPlus

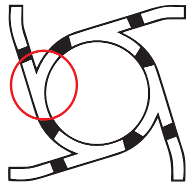

1:1

1:4 Large (9mm) Hinge Scale

POC Manufacturing & Testing

Steep Ramp (B)
Ramp Angle 5.46 degree
Rotation 48 degrees to a height of 8mm

Auxetic Performance

Maximum Expansion
Vertical Expansion
3mm

Counter Rotation
35°
Rotational Expansion
55-35=
25°

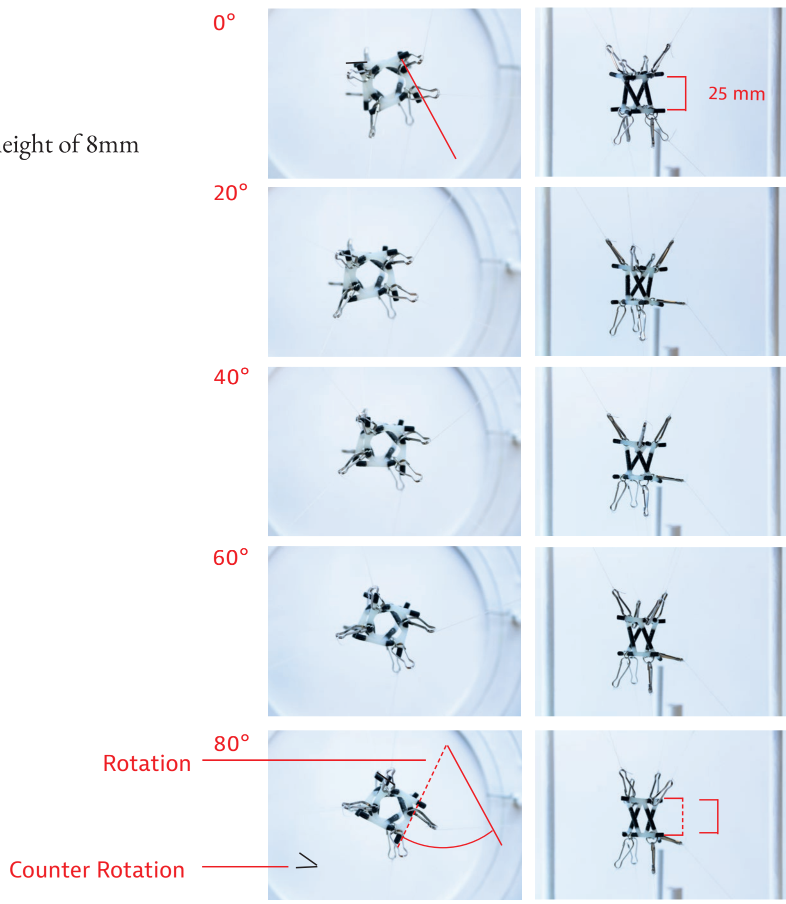

Figure 4.109 3D Anti-Tetra-Chiral experimentation.

Chiral

3D Planar Anti-Tetra-Chiral

[3.1]

Circular cross section

Design Variable: Strut Diameter

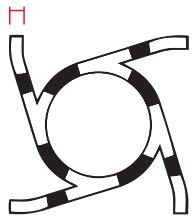

25x 25x 25mm

Agilius 50 + VeroPlus

POC Manufacturing & Testing

The thinest of the circle cross sectional struts.

Steep Ramp (B)
Ramp Angle 5.46 degree
Rotation 48 degrees to a height of 8mm

Auxetic Performance

Inaccurate reading due to elasticity of unit.

1:4 Thin (1mm radius) Strut

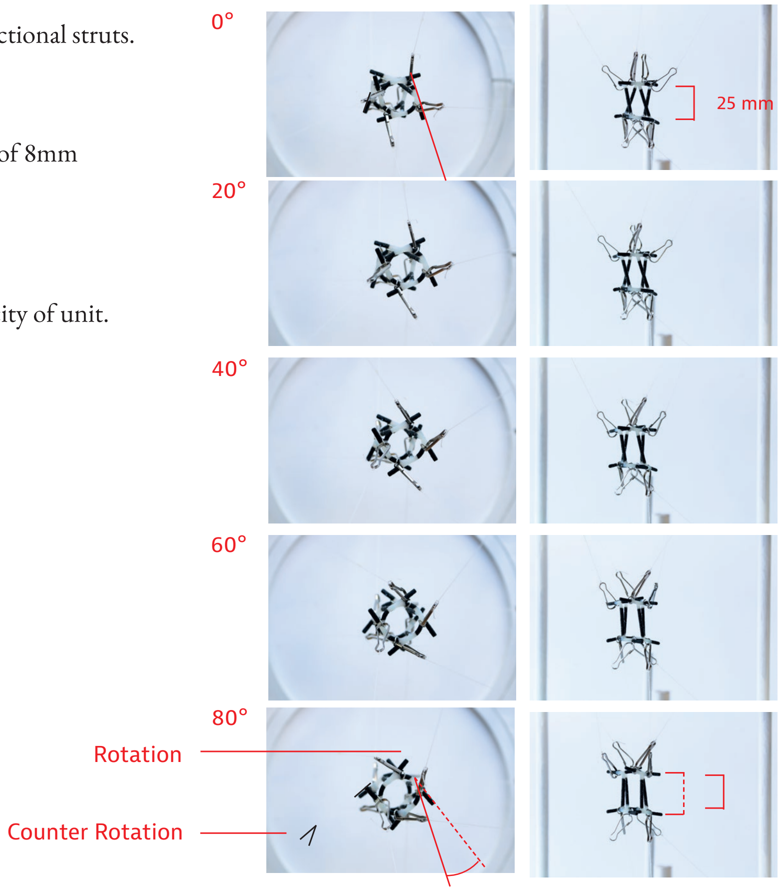

Figure 4.110 3D Anti-Tetra-Chiral experimentation.

Discoveries

The struts were too thin, the unit was already stretched unintentionally in its resting position, and became more elastic as it expanded, without utilising the deformation mechanism.

Chiral **3D Planar Anti-Tetra-Chiral**

[3.2] Circle cross section

Clockwise

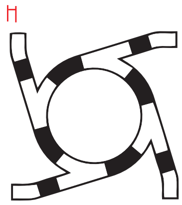

1:1

Design Variable: Strut Diameter

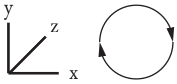

25x 25x 25mm

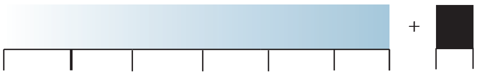

POC Manufacturing & Testing

Steep Ramp (B)
Ramp Angle 5.46 degree
Rotation 48 degrees to a height of 8mm

1:4 Mid (1.25mm) Strut Radius

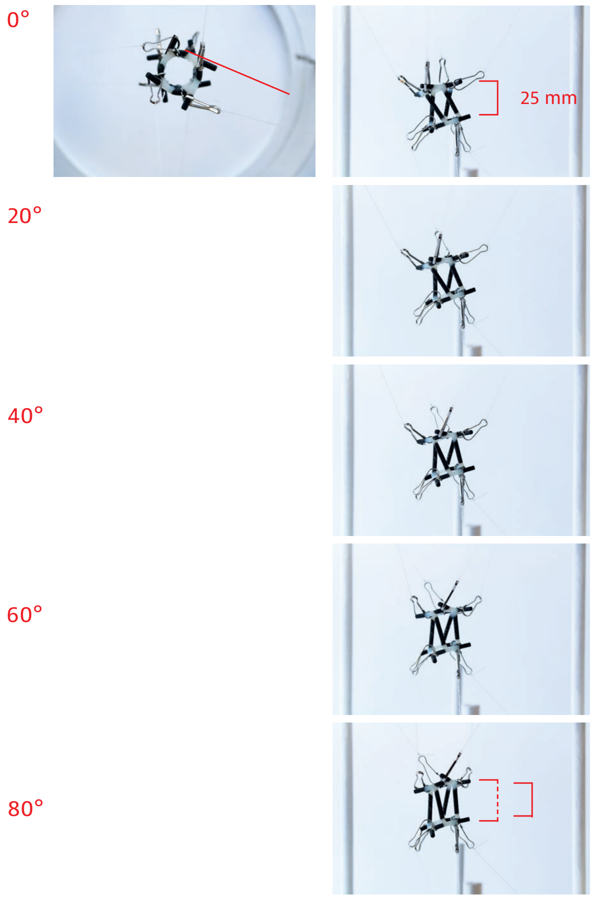

Figure 4.111 3D Anti-Tetra-Chiral experimentation.

Auxetic Performance

Maximum Expansion
Vertical Expansion
5mm

Counter Rotation
35°
Rotational Expansion
55-35=
25°

Discoveries

Structure broke during testing.

Chiral

3D Planar Anti-Tetra-Chiral

[3.3] Circle cross section

Clockwise

Design Variable: Strut Diameter

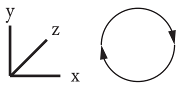

25x 25x 25mm

Agilius 50 + VeroPlus

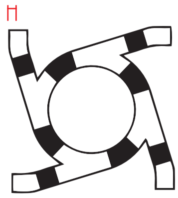

1:1

POC Manufacturing & Testing

Steep Ramp (B)
Ramp Angle 5.46 degree
Rotation 48 degrees to a height of 8mm

Auxetic Performance

Maximum Expansion
Vertical Expansion
3mm

Counter Rotation
35°
Rotational Expansion
50-25=
35°

1:4 Thick (1.5mm) Strut Radius

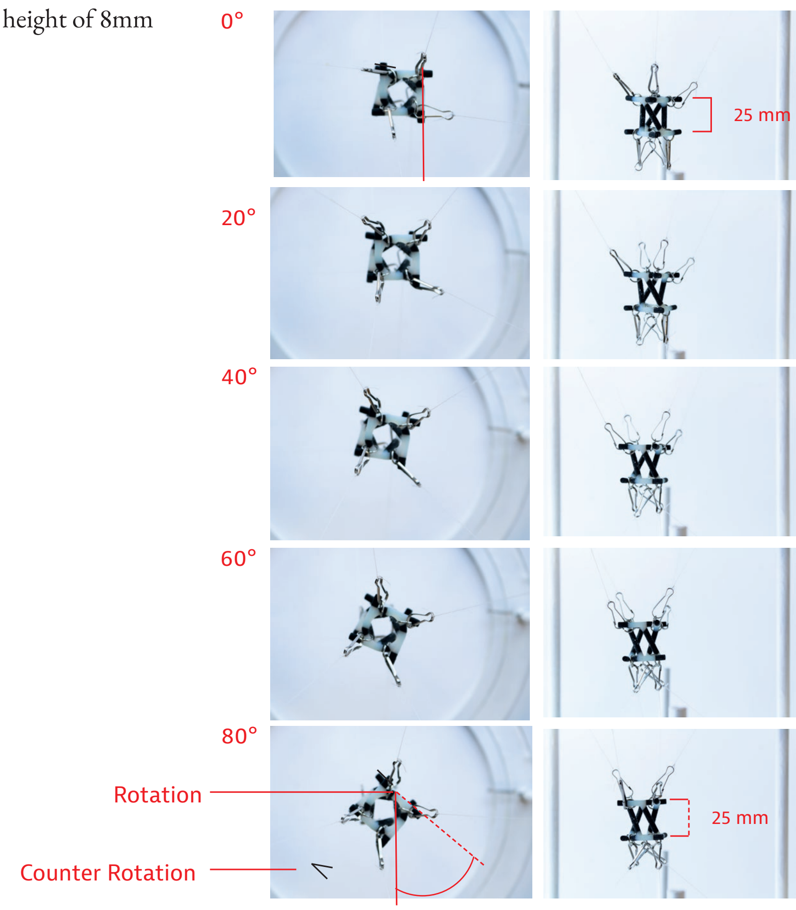

Figure 4.112 3D Anti-Tetra-Chiral experimentation.

Discoveries

Structure was most Auxetic and remained robust

Chiral

3D Planar Anti-Tetra-Chiral

[4.1] Circle cross section

Clockwise

Design Variable: Shore Hardness

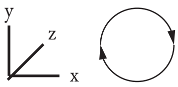

25x 25x 25mm

Agilius 40

VeroPlus

30

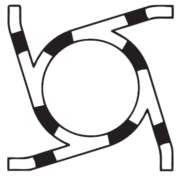

1:1

Mid Thickness Strut to test shore hardness

POC Manufacturing & Testing

Steep Ramp (B)
Ramp Angle 5.46 degree
Rotation 48 degrees to a height of 8mm

Auxetic Performance

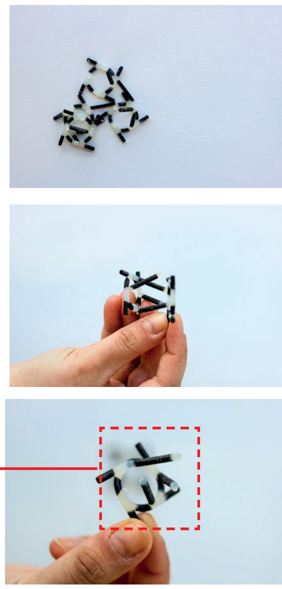

Broken apart during removal of support material

Figure 4.113 3D Anti-Tetra-Chiral damage.

1:4 Shore 30

0°

20°

40°

60°

80°

Figure 4.114 3D Anti-Tetra-Chiral experimentation.

Discoveries

One unit broke apart, one didn't.

Chiral

3D Planar Anti-Tetra-Chiral

[4.2]

Circle cross section
Clockwise

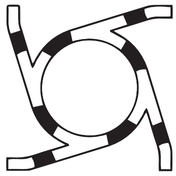

1:1

Design Variable: Shore Hardness

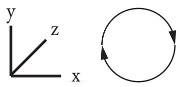

25x 25x 25mm

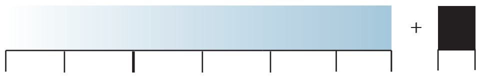

Mid Thickness Strut to test shore hardness

POC Manufacturing
& Testing

Steep Ramp (B)
Ramp Angle 5.46 degree
Rotation 48 degrees to a height of 8mm

Auxetic Performance

Maximum Expansion
Vertical Expansion
4mm

1:4 Shore 40

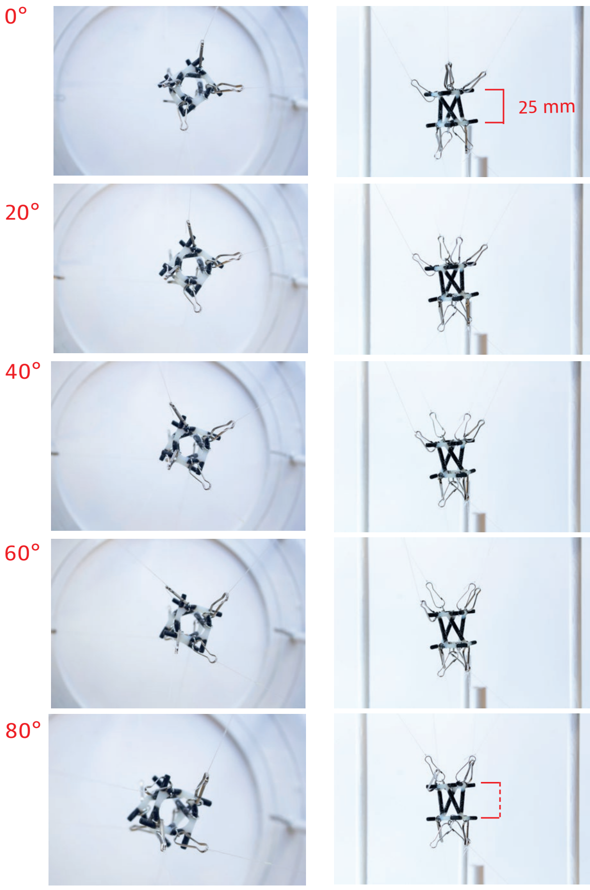

Figure 4.115 3D Anti-Tetra-Chiral experimentation.

Chiral

3D Planar Anti-Tetra-Chiral

[4.3] Circle cross section
Clockwise

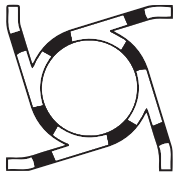

1:1

Design Variable: Shore Hardness

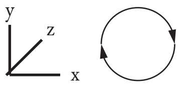

25x 25x 25mm

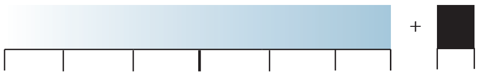

POC Manufacturing & Testing

Steep Ramp (B)
Ramp Angle 5.46 degree
Rotation 48 degrees to a height of 8mm

Auxetic Performance

Maximum Expansion
Vertical Expansion
2mm

Counter Rotation
25°
Rotational Expansion
40-25=
15°

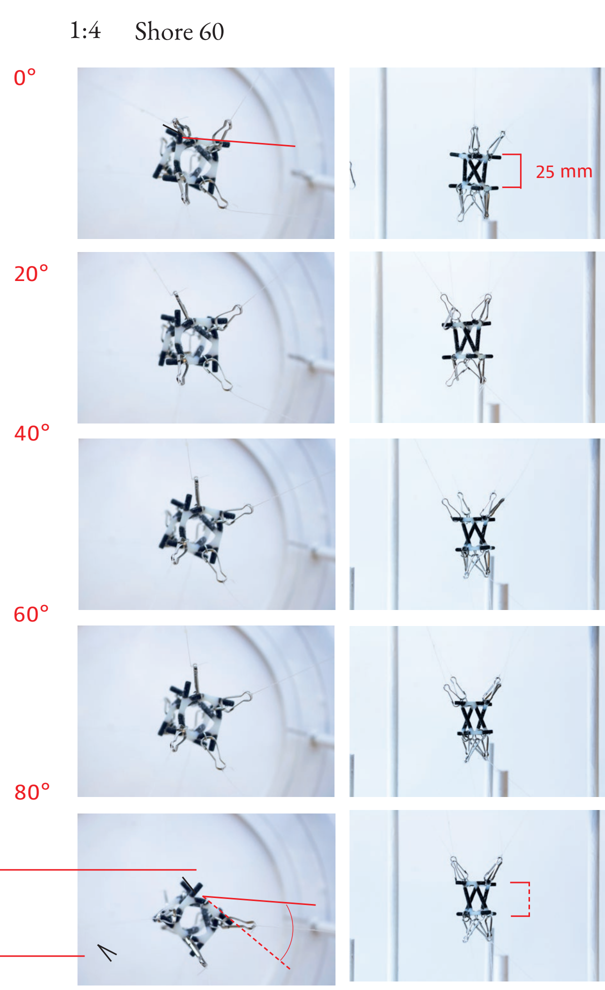

Figure 4.116 3D Anti-Tetra-Chiral experimentation.

Chiral

3D Planar Anti-Tetra-Chiral

[5.1] Square cross section

Counterclockwise

Design Variable: Shore Hardness

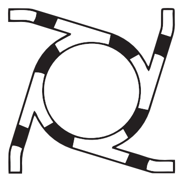

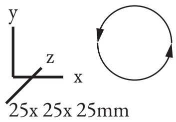

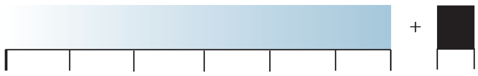

1:4 Shore 30

POC Manufacturing & Testing

Mid strut width
for shore hardness

Auxetic Performance

Broken apart at intersection of material.

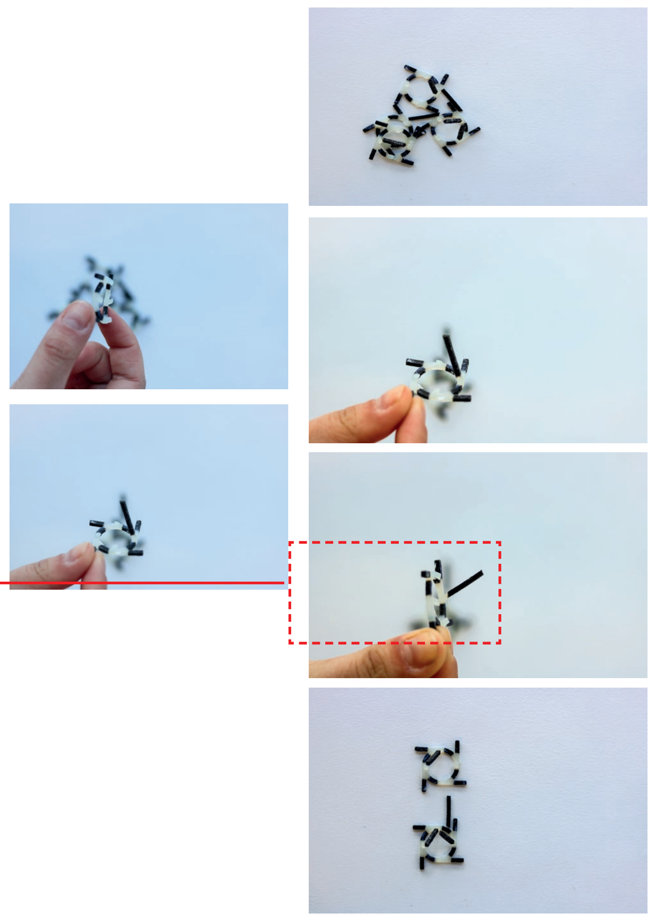

Figure 4.117 3D Anti-Tetra-Chiral damage.

Discoveries

Unsuccessful square cross section, no teseting carried out.

Chiral

3D Planar Anti-Tetra-Chiral

[5.2] Square cross section

Counterclockwise

Design Variable: Shore Hardness

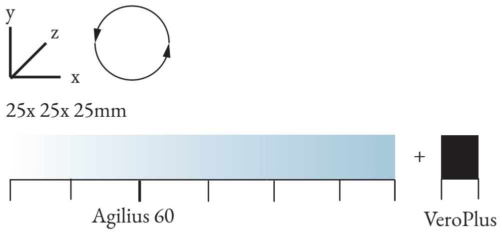

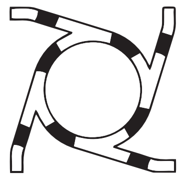

POC Manufacturing & Testing

Mid radius cross section

1:4 Shore 40

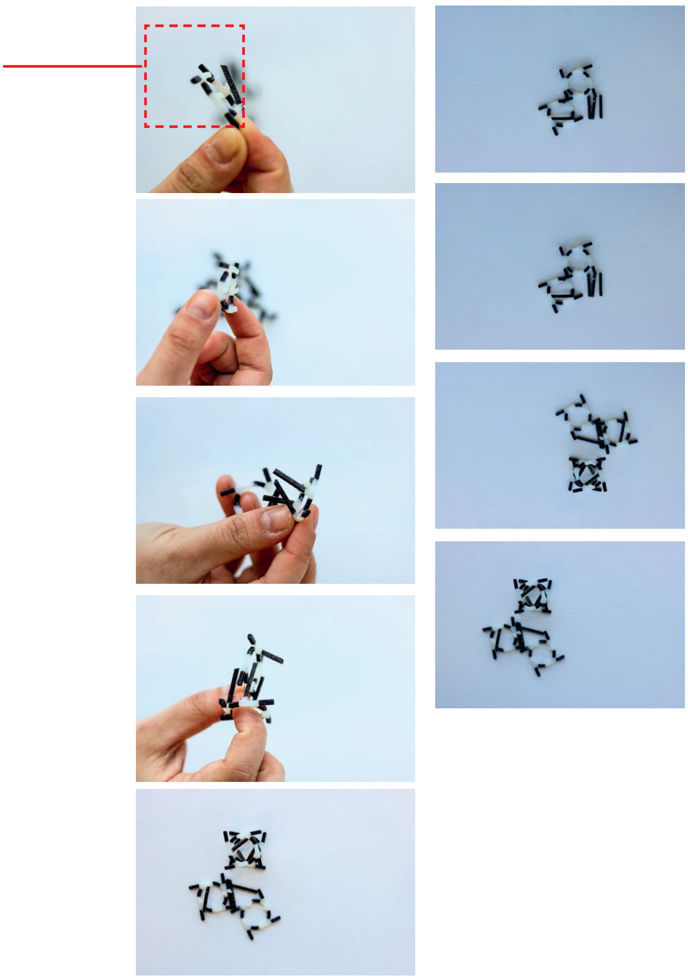

Figure 4.118 3D Anti-Tetra-Chiral damage.

Auxetic Performance

Discoveries

Unsuccessful square cross section, no testing carried out.

Chiral

3D Planar Anti-Tetra-Chiral

Square cross section

Counterclockwise

Design Variable: Shore Hardness

[5.3]

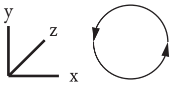

25x 25x 25mm

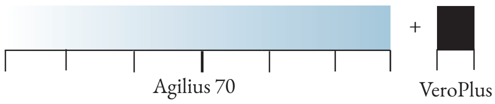

60

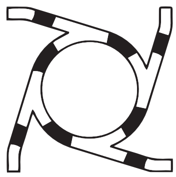

1:1

POC Manufacturing & Testing

Mid radius cross section

Auxetic Performance

1:4 Shore 60

Figure 4.119 3D Anti-Tetra-Chiral experimentation.

Discoveries

Unsuccessful square cross section, no testing carried out.

Experimentation Three: 3D Anti-Tetra-Chiral Reflection

The square cross sectional struts were particulary unsuccessful, handling strain poorly. As a result these structures were weak and too flexible, ultimately leading to the breaking apart of the majority of the square hinge structures.

Also worth noting, is the scale, in the application structures would be reduced in size to increase effectiveness.

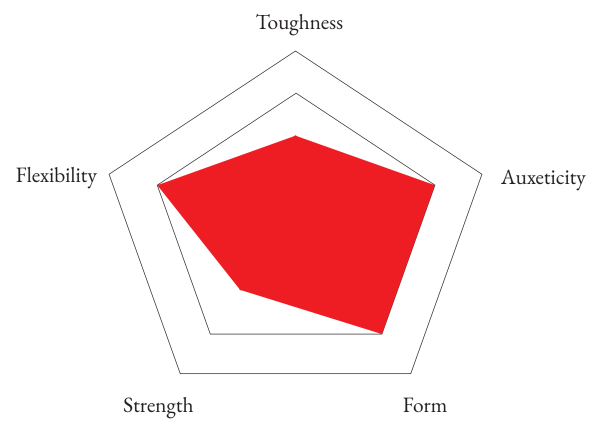

Figure 4.120 Experimentation two Design three Radar Plot.

Experimentation 3 Design 2 Evaluative Matrix

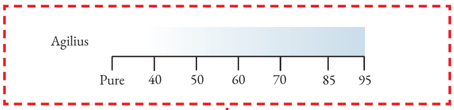

Topology	Design Parameter	Shore Hardness	Designed Hinge (Deformation Mechanism utilised)	Auxetic Effect Observed (Resting Position 0 – 1 – 2 – 3 Utilised to Maximum)	Damage Sustained (No damage Observed 0 – 1 – 2 – 3 Unit unusable again)
1:2 3D Planar Anti-Tetra-Chiral 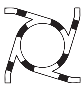					
Hinge Scale Square	7mm	Shore 50	X	0	0
	9mm	Shore 50	✓	3	3
Hinge Scale Circle	5mm	Shore 50	✓	3	3
	7mm	Shore 50	✓	2	3
	9mm	Shore 50	✓	3	3
Strut Radius Square	1.0mm	Shore 50	X	1	3
	1.25mm	Shore 50	✓	3	3
	1.5mm	Shore 50	✓	3	3
Shore Hardness Circle		Shore 30	X	0	2
		Shore 40	✓	3	3
		Shore 70	✓	3	3
Shore Hardness Square		Shore 30	X	0	0
		Shore 40	X	0	0
		Shore 70	X	0	0

Design 3: Re-entrant Star4

(Kolken & Zadpoor, 2017) recorded that the Star4 and Star6 geometries demonstrated the greatest potential for exhibiting on axis Auxetic behaviour over the Star3 structure, here the Star4 structure will be explored.

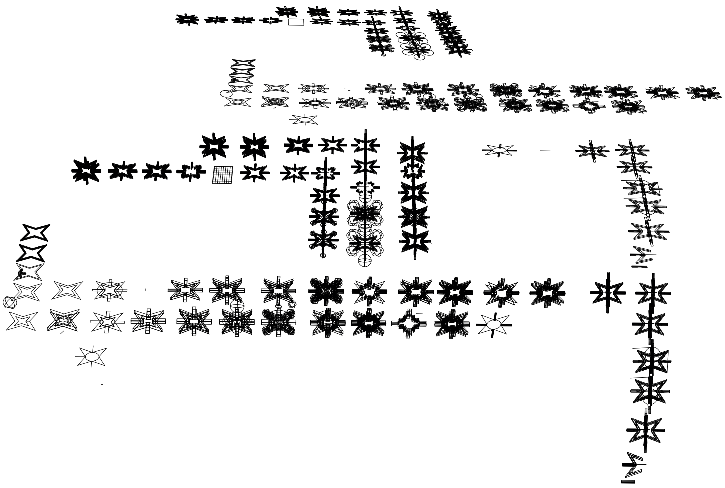

Figure 4.121 Star4 digital development.

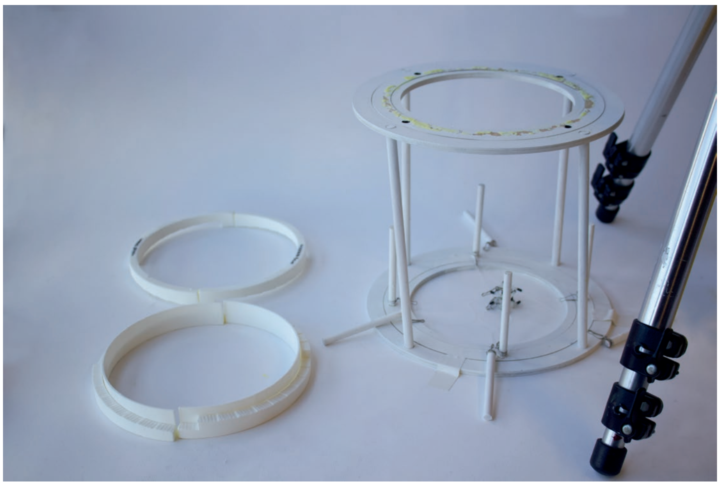

Figure 4.122 Experimentation Setup.

1:2

[1.1-1.3] **Hinge Scale**

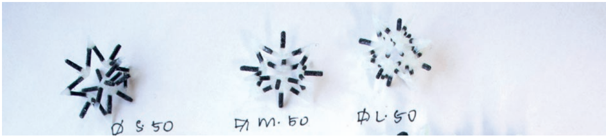

[2.1-2.3] **Strut Radius**

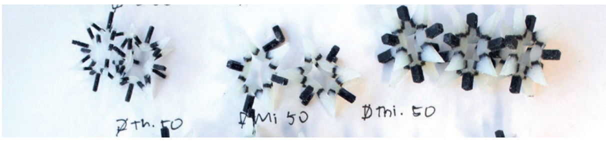

[3.1-3.3] **Shore Hardness**

[4.1-4.3] **Shore Hardness**

Figure 4.123 Star experimentation.

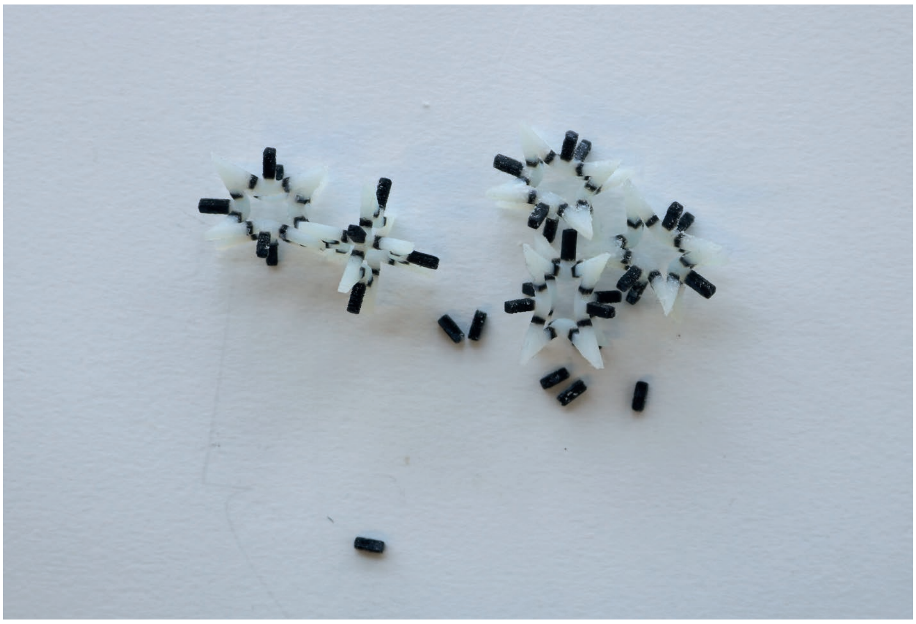

Figure 4.124 Star experimentation.

Re-entrant **Star4**

[3.1] Square cross section

1:1

Design Variable: Shore Hardness

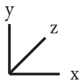

25x 25x 25mm

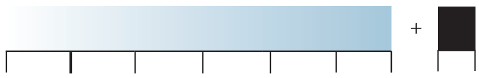

Agilius 40 VeroPlus

Shore 40

POC Manufacturing & Testing

Mid strut radius

Auxetic Performance

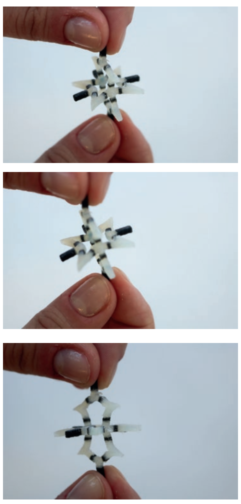

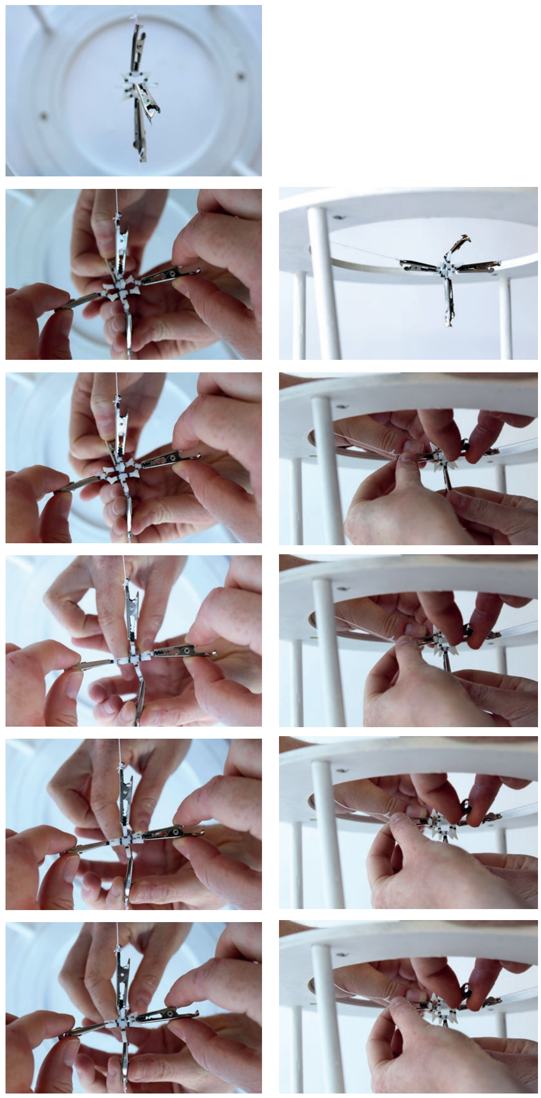

Figure 4.125 Star4 experimentation.

Re-entrant **Star4**

[3.2] Square cross section

Design Variable: Shore Hardness

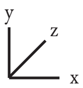

25x 25x 25mm

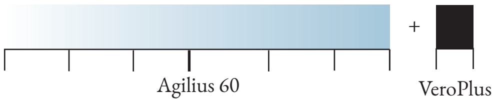

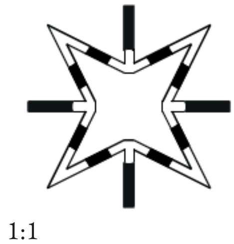

POC Manufacturing & Testing

Mid strut radius

Auxetic Performance

Shore 60

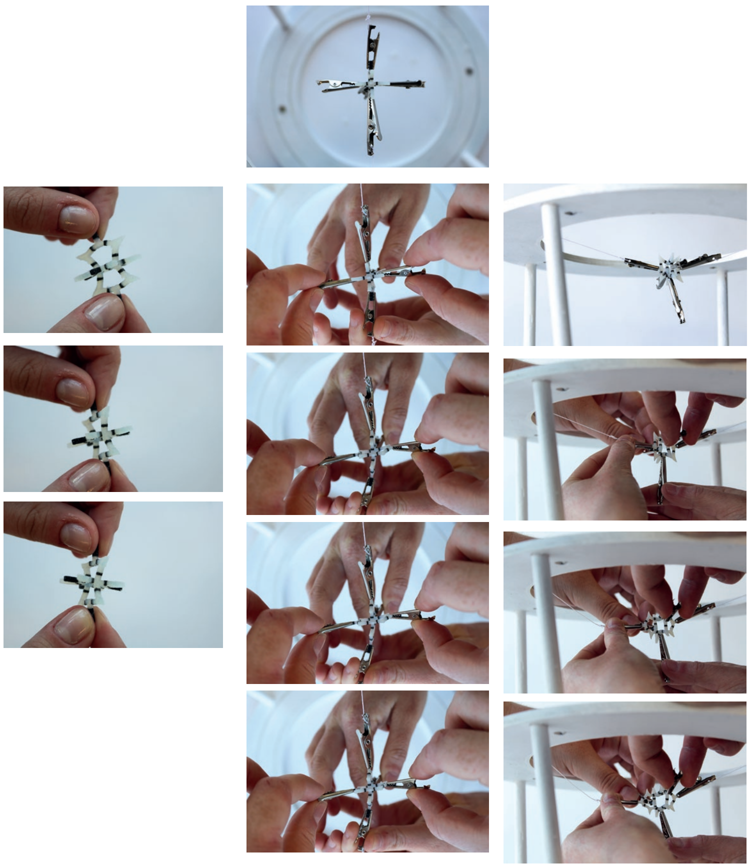

Figure 4.126 Star4 experimentation.

Re-entrant **Star4**

[3.3] Square cross section

1:1

Design Variable: Shore Hardness

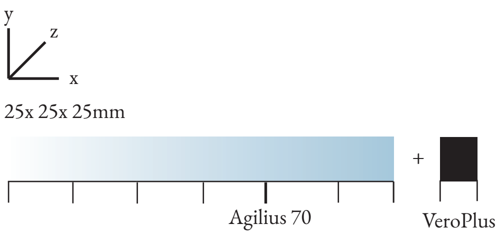

70 Mid

POC Manufacturing & Testing

Auxetic Performance

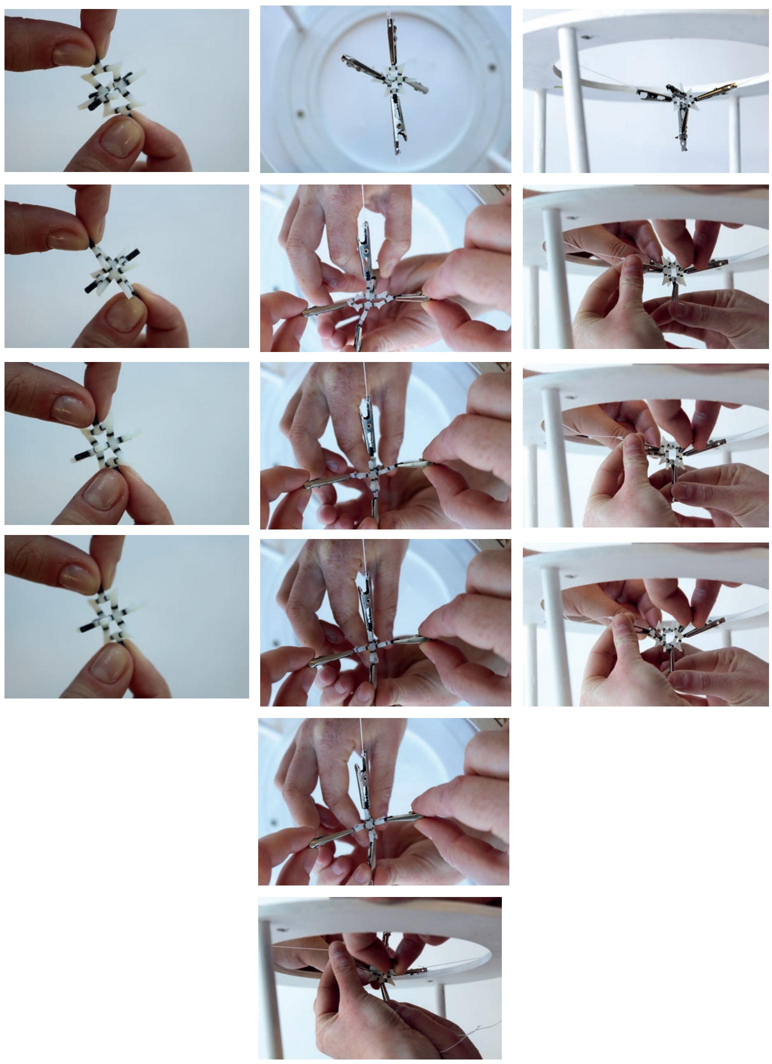

Figure 4.127 Star4 experimentation.

Star4 Damage

1:1

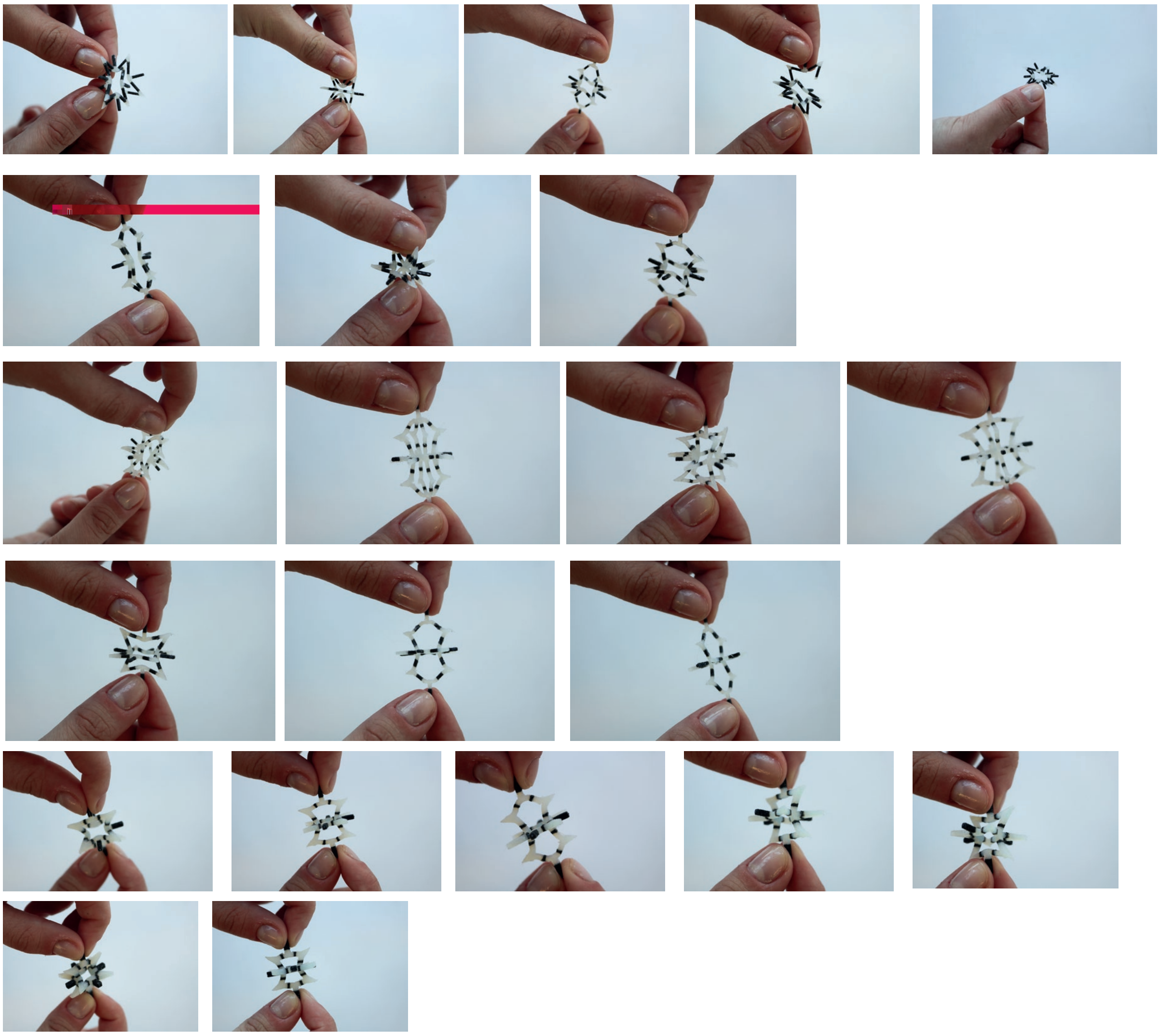

[1.1]
[1.2]
[1.3]
[2.1]
[2.2]
[2.3]

Figure 4.128 Star4 Experimentation.

Re-entrant

Star4

Square cross section

Design Variable: Shore Hardness

1:1

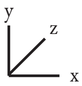

25x 25x 25mm

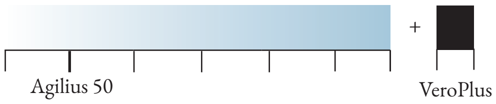

Once the process was resolved and the design error reconnected the last two Star structures were printed and experimented with. They show successful examples of hinge and shore hardness combinations.

POC Manufacturing & Testing

Large Hinge

Thick 50

Auxetic Performance

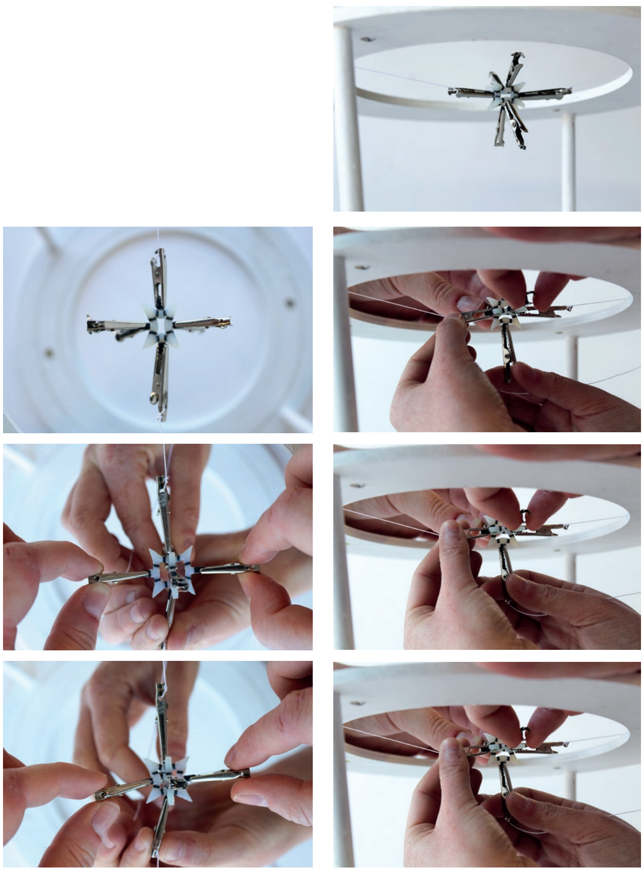

Figure 4.129 Star4 experimentation.

Re-entrant

Star4

Design Variable: Shore Hardness

Square cross section

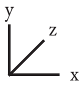

25x 25x 25mm

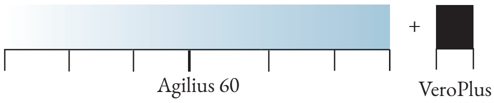

1:1

POC Manufacturing & Testing

Large Hinge

Thick 60

Auxetic Performance

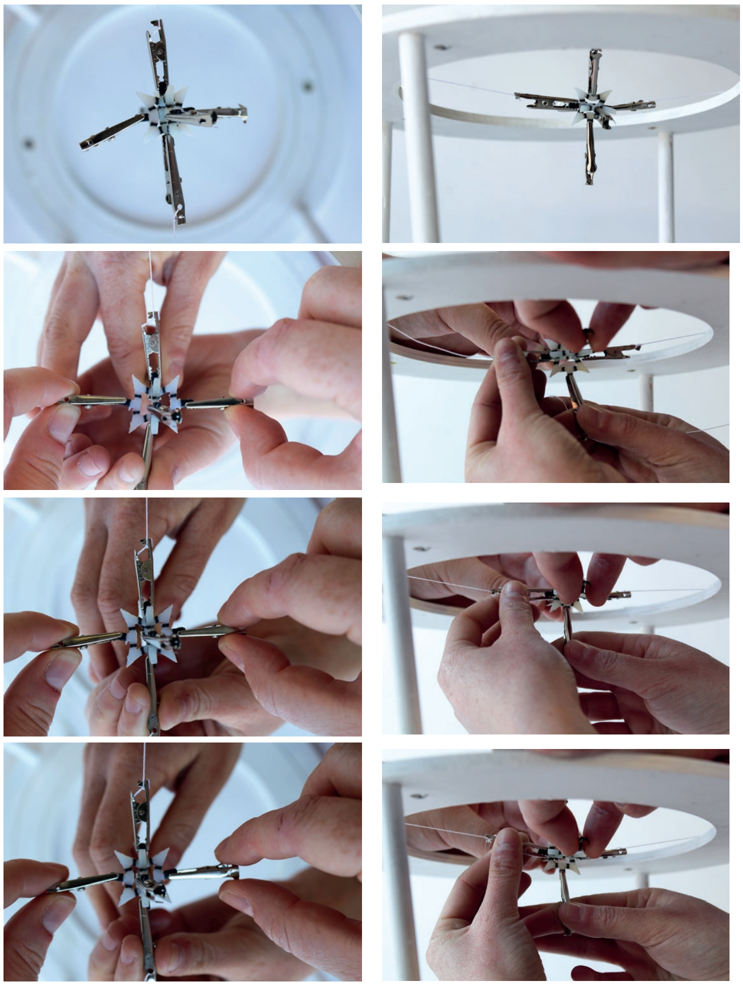

Figure 4.130 Star4 experimentation.

Experimentation 3 Deisgn 3: Star4 Reflection

The Star4 structure, although projected as being a suitable candidate based upon literature, suffered by far the most failures during the physical experimentation. Partly during the removal of support material, where the sparse nature of the unit, makes it a difficult geometry to AM, additionally, through a modelling area, many structures were not properly connected to the body and broke apart as seen in the figure below.

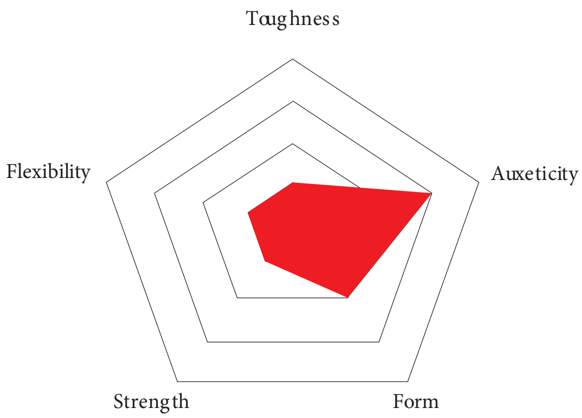

Figure 4.130 Experiment three Radar Plot.

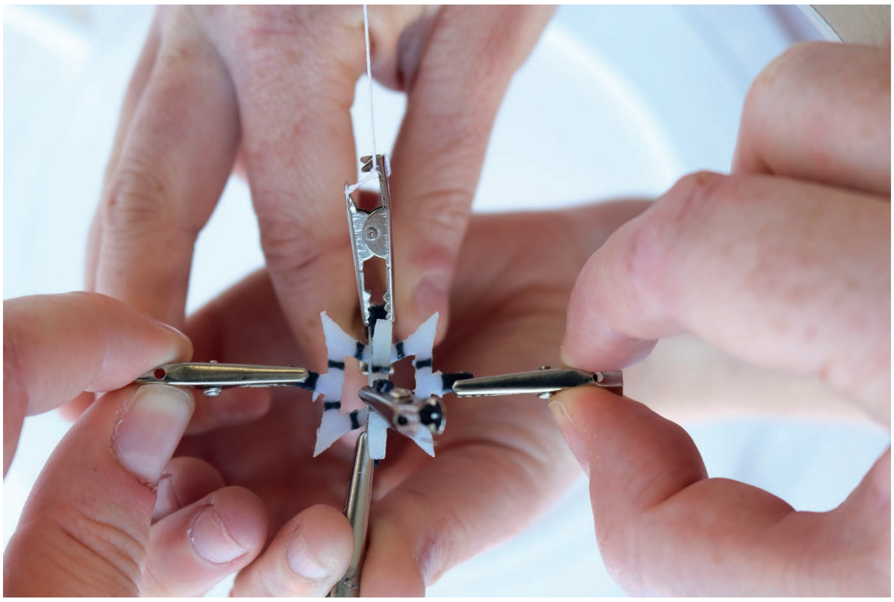

Figure 4.131 Complications with Star4 testing.

[4.7] Experimentation 4: Absence of the Multi-material Hinge

When the first half of this research was presented at the 4D Printing and Metamaterials conference held from Eindhoven, Netherlands in May 2020, several questions where raised in regard to how necessary the multi-materiality was for the Auxetic effect to be observed in AM models. In order to explore this in greater detail, the following experimentation involves the printing of structures with a singular material, as well as models with the reverse material assignment to those manufactured throughout this research.

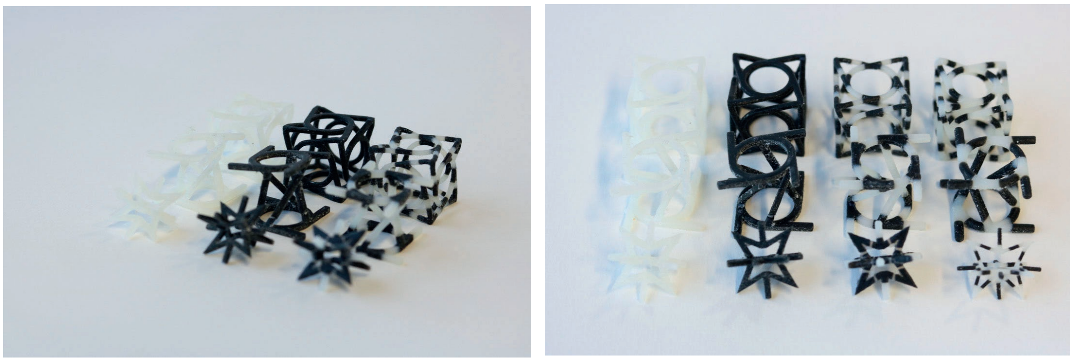

Figure 4.132 Justifying the multi-material hinge.

Design Tests

Meta-Chiral Compression Twist
Pure Agilius (Soft)
Pure Tango (Rigid)
Swapped Assignment (Soft Struts, Rigid Hinges)

3D Anti-Tetra-Chiral Reflection
Pure Agilius (Soft)
Pure Tango (Rigid)
Swapped Assignment (Soft Struts, Rigid Hinges)

Star4
Pure Agilius (Soft)
Pure Tango (Rigid)
Swapped Assignment (Soft Struts, Rigid Hinges)

Chiral

Meta-Chiral Compression Twist

Circle cross section

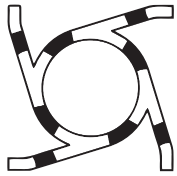

1:1

Design Variable: Shore Hardness

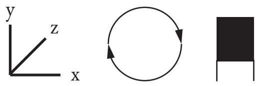

25x 25x 25mm

VeroPlus

POC Manufacturing & Testing

Single material for the unit

Snapped top vertex, from applied strain, demonstrating value in the hinge and strut various materiality assignment

Damage at the vertex boundaries

Full rigid model with no elasticity in the unit to enable movement

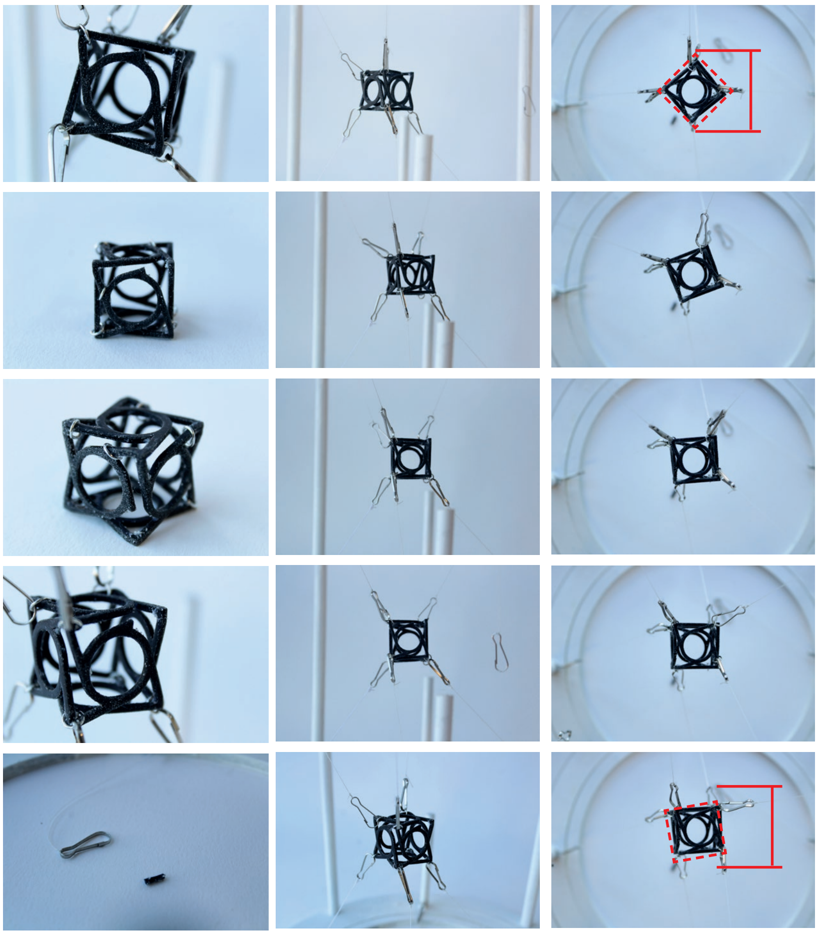

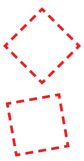

Figure *4.133* Damage to the full rigid TangoPlus unit.

Discoveries

No expansion observed.

Chiral

Meta-Chiral Compression Twist

Circle cross section

Design Variable: Shore Hardness

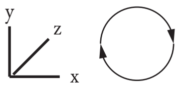

25x 25x 25mm

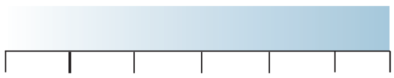

Agilius 50

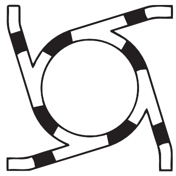

1:1

POC Manufacturing & Testing

Auxetic Performance

Single material for the unit

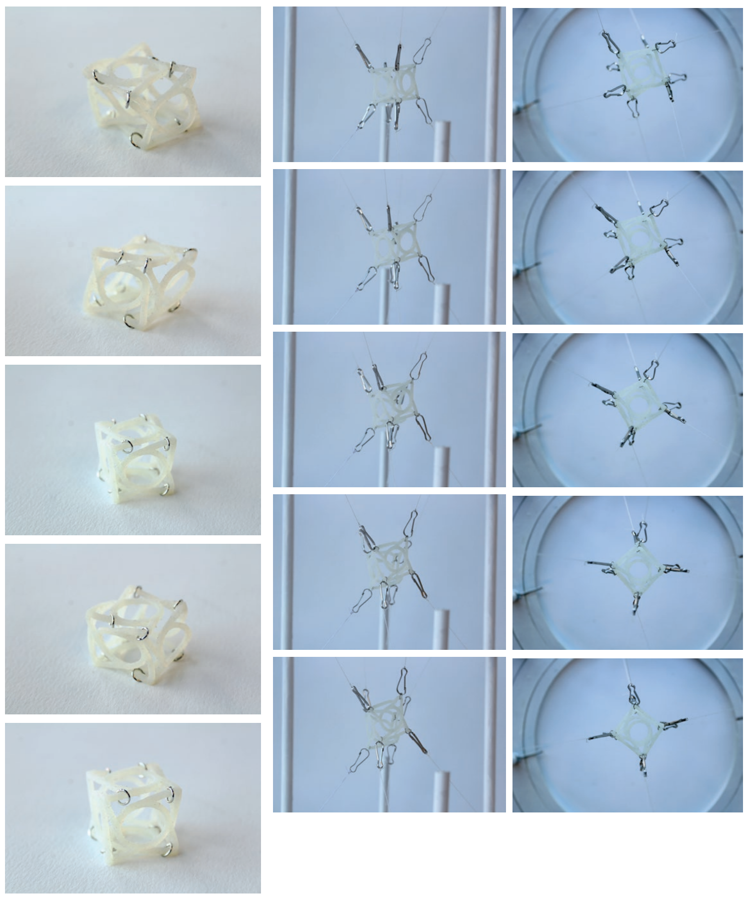

Figure *4.134* Full elastic Agilius unit.

Chiral

Meta-Chiral Compression Twist

Circle cross section

Design Variable: Shore Hardness

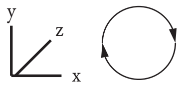

25x 25x 25mm

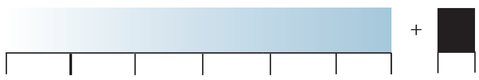

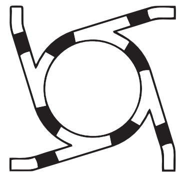

1:1

POC Manufacturing & Testing

Auxetic Performance

Opposite Hinge and Strut

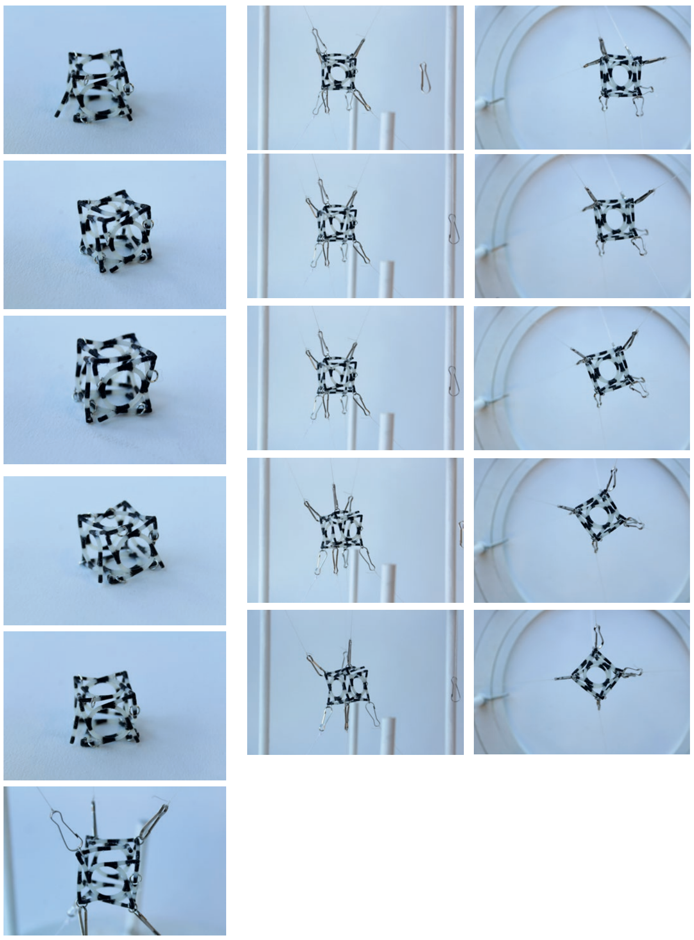

Figure *4.135* Swapped material qualities.

Chiral

3D Planar Anti-tetra-chiral

Square cross section

Design Variable: Shore Hardness

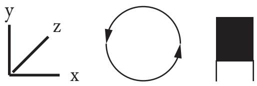

25x 25x 25mm VeroPlus

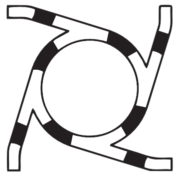

1:1

POC Manufacturing & Testing

Mid strut width for shore hardness

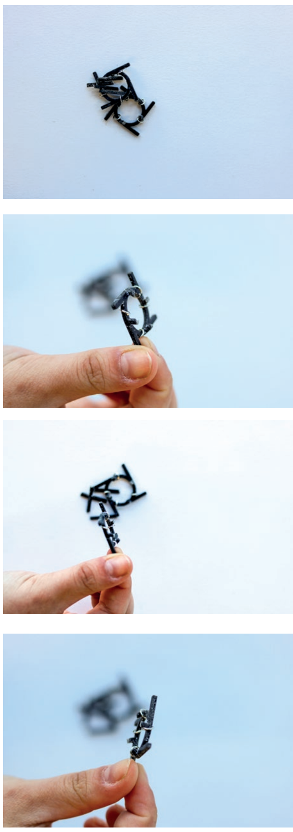

Figure *4.136* Damage.

Auxetic Performance

Discoveries

No more successful than the other square profile failures.

Chiral

3D Planar Anti-tetra-chiral

Square cross section

Design Variable: Shore Hardness

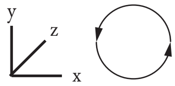

25x 25x 25mm

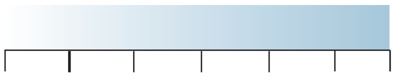

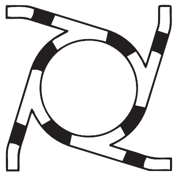

1:1

POC Manufacturing
& Testing

Auxetic Performance

Agilus 50

Figure *4.137* Damage.

Chiral

3D Planar Anti-Tetra-Chiral

Square cross section

Design Variable: Shore Hardness

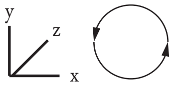

25x 25x 25mm

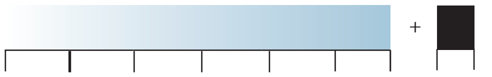

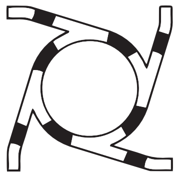

1:1

POC Manufacturing & Testing

Auxetic Performance

Opposite Hinge and Strut

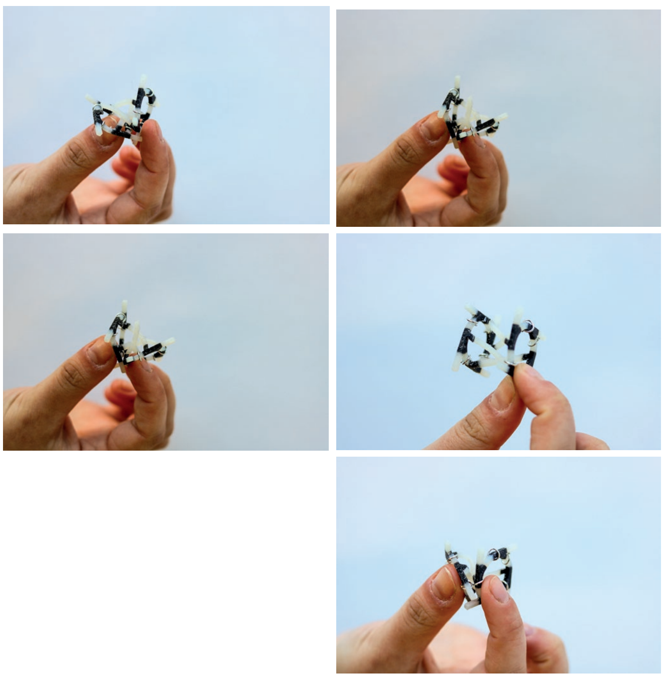

Figure *4.138* Swapped material damage.

Re-entrant

Star4

Square cross section

Design Variable: Shore Hardness

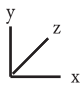

25x 25x 25mm

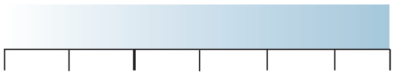

Agilius 50

1:1

POC Manufacturing & Testing

Auxetic Performance

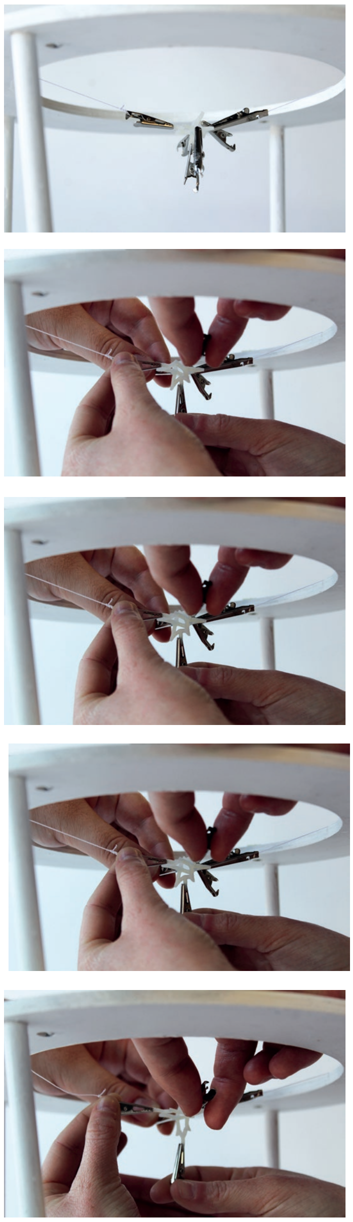


Figure *4.139* Elastic unit.

Re-entrant

Star4

Square cross section

Design Variable: Shore Hardness

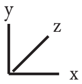

25x 25x 25mm

Agilius 50

VeroPlus

1:1

POC Manufacturing
& Testing

Auxetic Performance

Opposite Hinge and Strut

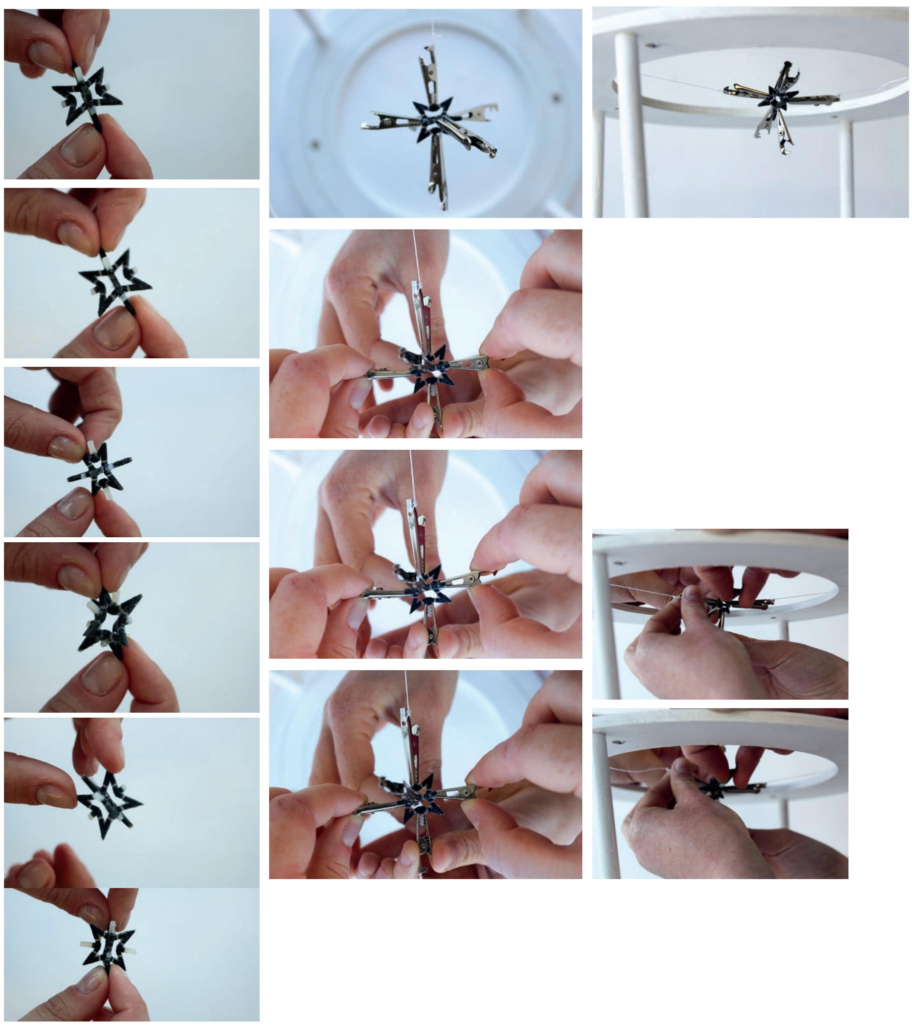

Figure *4.140* Swapped materiality unit.

Re-entrant

Star4

Square cross section

Design Variable: Shore Hardness

1:1

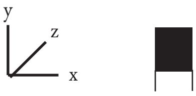

25x 25x 25mm VeroPlus

POC Manufacturing
& Testing

Tango

Auxetic Performance

Figure *4.141* Rigid unit.

Experiment 4 Reflection

It was observed that the fully agilius hinges were too elastic and failed to hold their form, whilst the fully rigid structures were 'locked' in their resting position. Models where the materials were assigned 'backwards' lacked structural integrity and stretched rather than utilising the deformation mechanism.

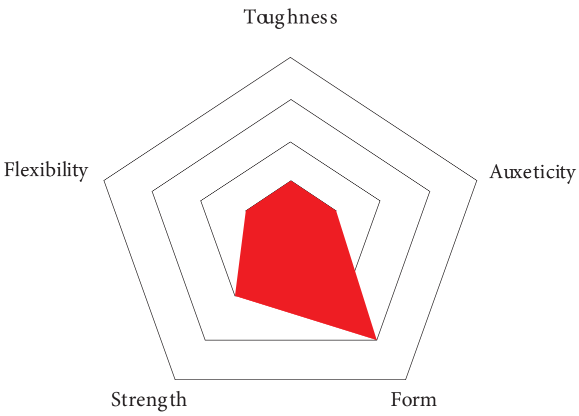

Figure. 4.142 Experiment four Radar Plot.

Experimentation 4: Evaluative Matrix

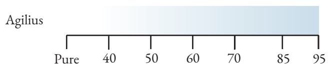

Topology	Shore Hardness	Designed Hinge (Deformation Mechanism utilised)	Auxetic Effect Observed Resting Position – Utilised to Maximum 0 1 2 3	Damage Sustained Unit unusable again – No damage Observed 0 1 2 3
1:2 **Chiral**				
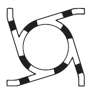	Agilius	X	0	3
	Tango	X	0	0
	Swapped	X	0	3
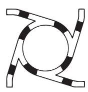	Agilius	X	0	3
	Tango	X	0	0
	Swapped	X	0	0
Re-entrant 	Agilius	X	0	3
	Tango	X	0	0
	Swapped	X	0	0

[4.8] Experiment 5: Auxetic Boundaries

The boundary refers to the intersection of two hinges.

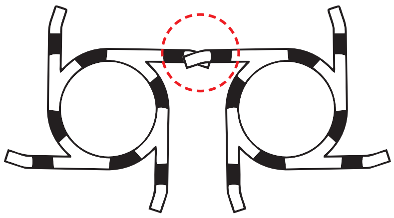

Testing boundaries and a structures unit relationship with other units in order to test its responses in a lattice form.

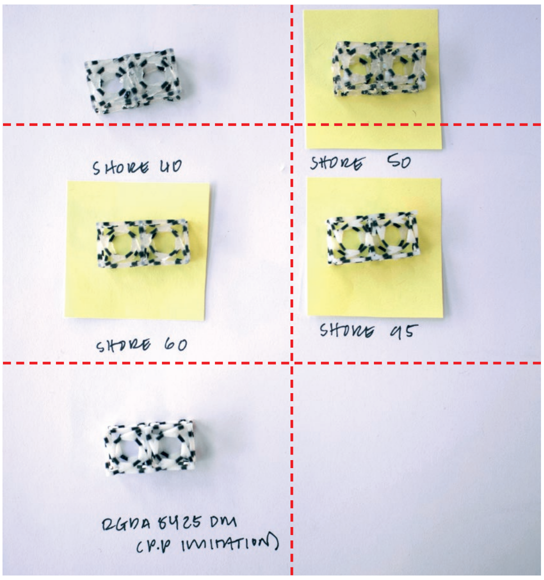

Figure 4.143 Auxetic Boundaries.

Chiral **Meta-chiral Compression Twist**

Square Cross Section

Design Variable: Shore Hardness

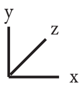

15x 25x 15mm

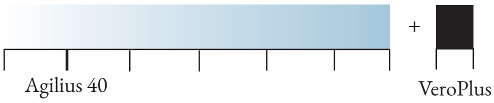

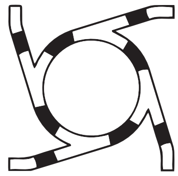

1:1

Shore40

POC Manufacturing & Testing

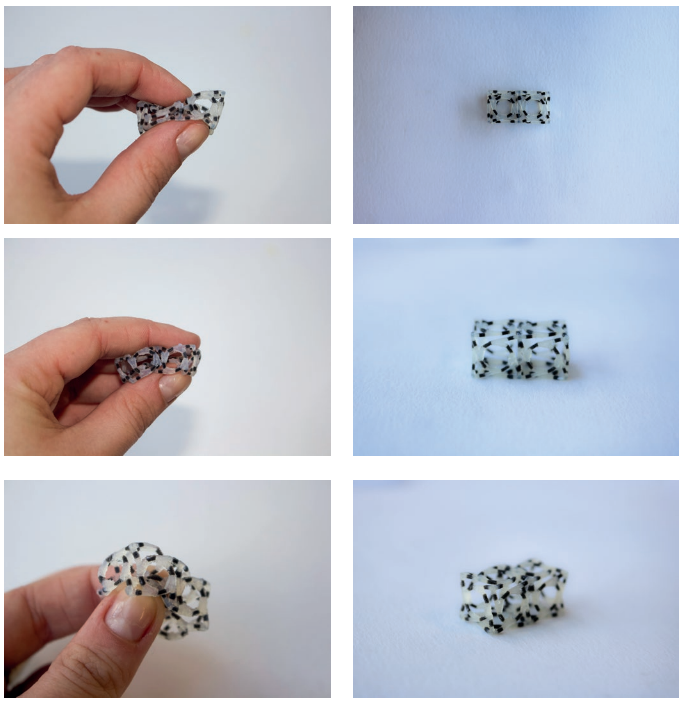

Figure 4.144 Auxetic Boundaries.

Chiral

Meta-chiral Compression Twist

Square Profile

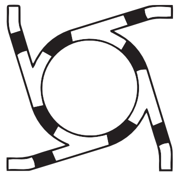

1:1

Design Variable: Shore Hardness

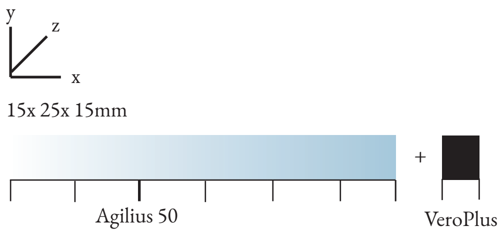

Shore50

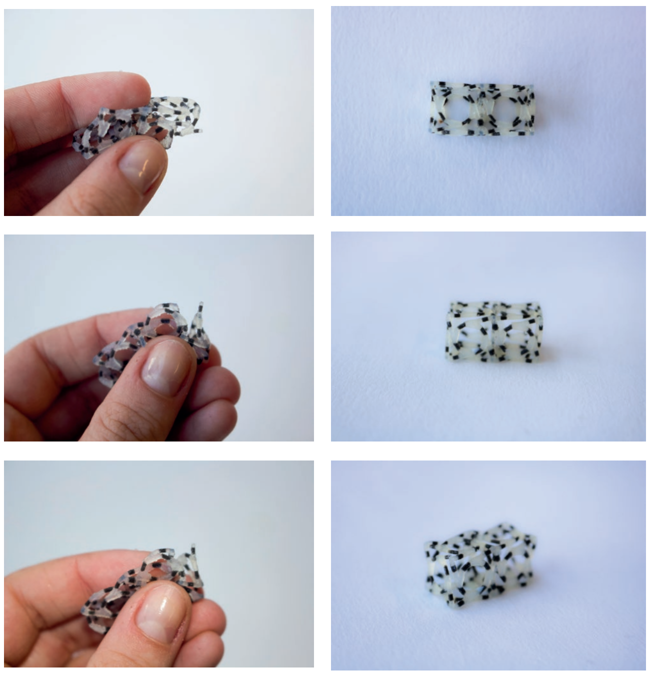

Figure 4.145 Auxetic Boundaries.

Chiral

Meta-chiral Compression Twist

Square Profile

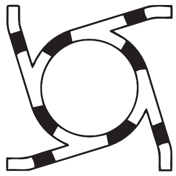

1:1

Design Variable: Shore Hardness

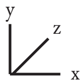

15x 25x 15mm

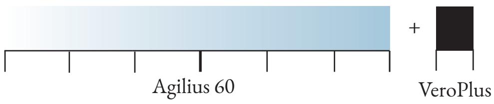

POC Manufacturing
& Testing

Shore60

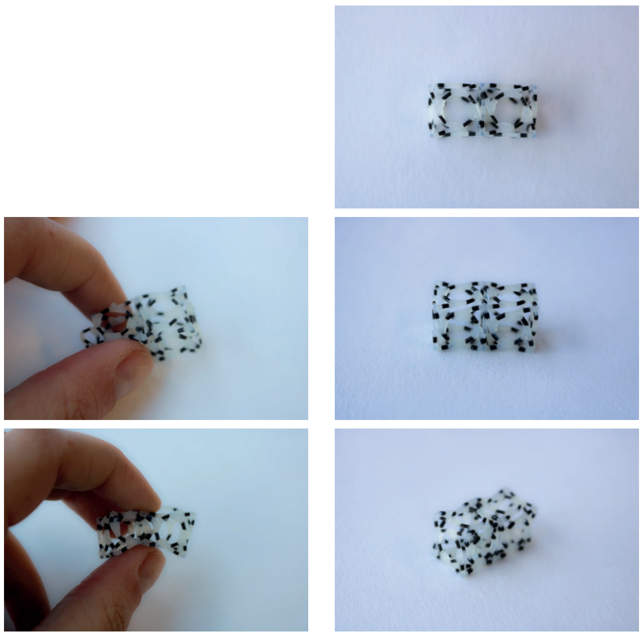

Figure 4.146 Auxetic Boundaries.

Chiral

Meta-chiral Compression Twist

Square Profile

Design Variable: Shore Hardness

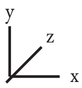

15x 25x 15mm

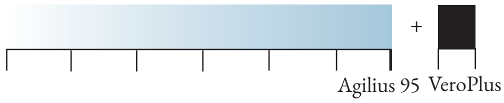

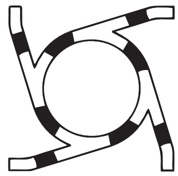

Shore95

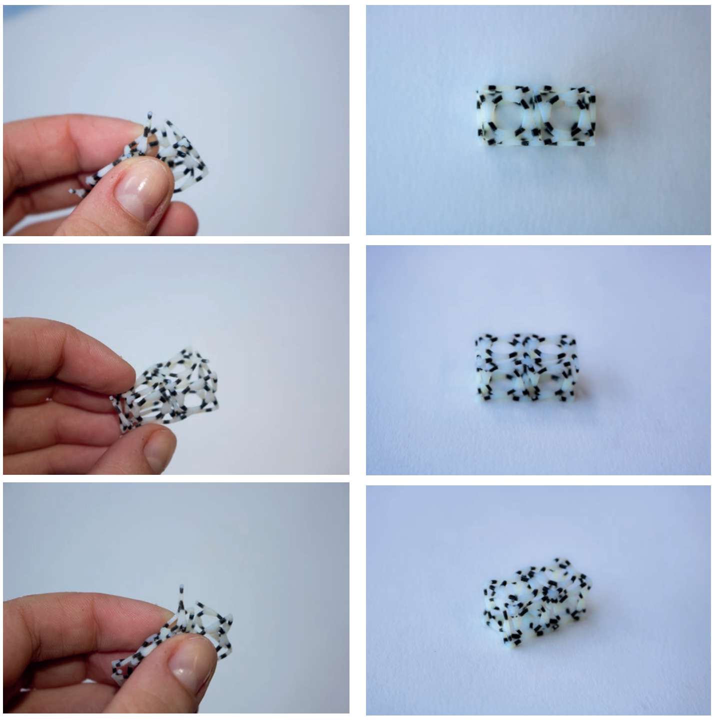

Figure 4.147 Auxetic Boundaries.

Chiral

Meta-chiral Compression Twist

Square Profile

Design Variable: Shore Hardness

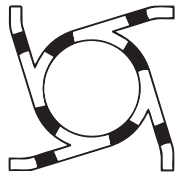

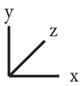

15x 25x 15mm

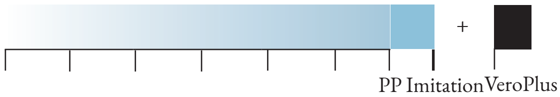

RGDA 8425 DM
PP Imitation

POC Manufacturing & Testing

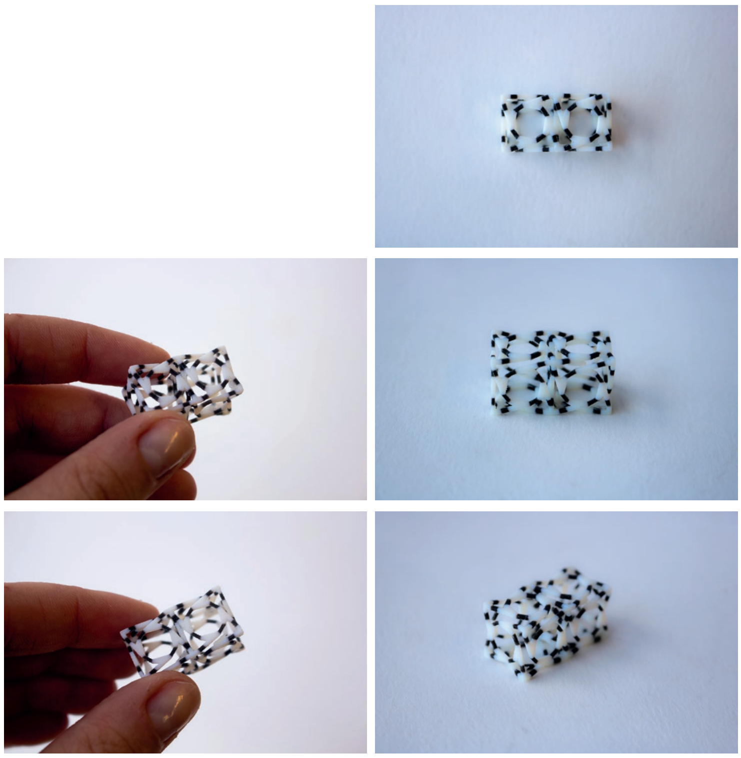

Figure 4.148 Auxetic Boundaries.

Discoveries

The least successful test, the structure was completely rigid and did not rotate, but rather broke.

Experimentation 5 Reflection

The scale of the units in experiment five is more in proportion to the scale of application structures, this enabled more accurate observations towards the contextualisation of Auxetic Structures. The structures fitted together well and behaved in an Auxetic manner whilst remaining connected.

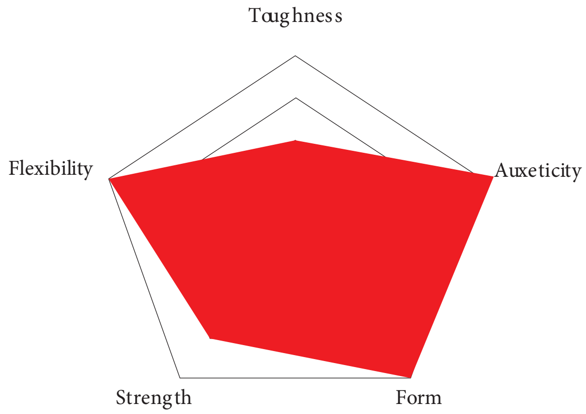

Figure 4.149 Experiment 5 Radar Plot.

Experimentation 5 Evaluative Matrix

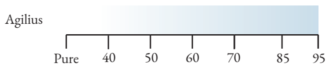

Topology	Shore Hardness	Designed Hinge (Deformation Mechanism utilised)	Auxetic Effect Observed (Resting Position 0 – 1 – 2 – 3 Utilised to Maximum)	Damage Sustained (Unit unusable again 0 – 1 – 2 – 3 No damage Observed)
	1			
1:2 **Re-entrant**				
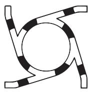	Shore 40	X	1	3
	Shore 50	X	1	0
	Shore 60	X	1	3
	Shore 95	X	1	0
	RGDA 8425 DM	X	1	0

Primary Research Part One Reflection

Digital materials refer to combinations of materials created through the mixing of material with varied density and elasticity, for example Shore hardness 40 is primarily Agilius elasticity with a small percentage of Tango plus rigidity, the ability to mix these digital material combinations proved to be critical to the success of the manufacturing of the Auxetic Structures experimented with. The process of creating successful combinations whilst managing behavioural outcomes and design parameters is a delicate negotiation, the above experimentation proved critical to understanding variables to be assigned when manufacturing Auxetic Structures on multi-material printers in the future.

It was observed that structures fabricated with Agilius Shore hardness 50, provide the most successful combination of elasticity and rigidity, the structure has the strength to retain its printed or relaxed state, as well as the capacity when impacted by an external strain to deform according to its geometry, ultimately, demonstrating the greatest translation of the Auxetic effect. Structures with Shore 30 were found to be most susceptible to damage when strain was applied. Shore hardness 70 at the hinges was found to be too rigid and showed signs of damage due to the brittle nature of the digital material.

5 DIGITAL EXPLORATION

5.1	Methodological Analysis	209
5.2	Auxetic Survey	212
5.3	Exploration Procedure	214
5.4	Exploration 1: Proof of Concept	216
5.5	Exploration 2: Surface Morph	218
5.6	Exploration 3: Synclastic Surface Morph	220
5.7	Exploration 4: Curvature Mapping	222
5.8	Experiment 5: Auxetic Curvature	224

Auxetic sports protection for high impact scenarios

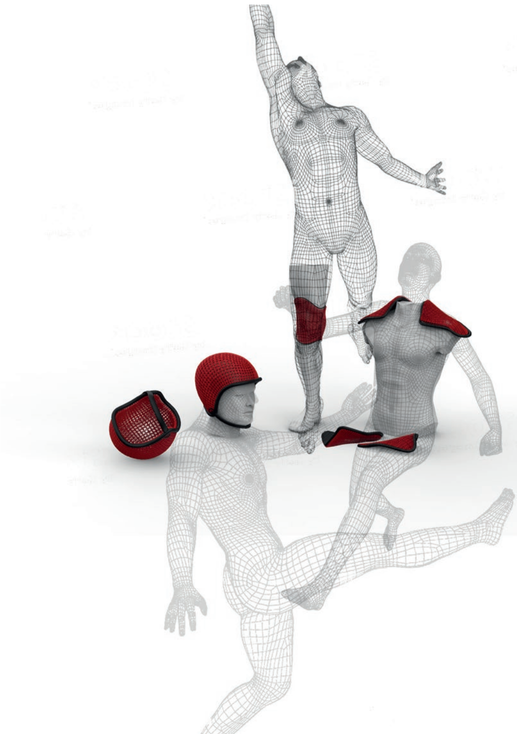

Figure 5.01 Auxetic Protection.

Part 2

Digital, computational exploration of anatomical curvature through mapping of Auxetic Structures onto synclastic curvature.

The following experimental studies take the next step towards widespread implementation of Auxetic Structures through development of geometries and curvature computationally.

[5.1] Methodological Analysis

The primary research will be practiced using Research through Design, as well as Scientific Design.

The overall design criteria for the research is further broken down to guide the exploration in part two of the primary research. This criteria is formed to access the digital explorations and guide the computational work.

Designs should

[1] Accurately represent Auxetic theory in parametrically modelled geometries and sub entities.

[2] Have structures fitted to curvature determined by anatomical site and synclastic in nature

[3] Be made up of unit geometry with accurate boundary and cell relationships through utilising quad division

[4] Be customisable to different curvature and anatomy through parametric freedom

[5.1.2] Software Selection

All structures will be mapped to the curvature through Grasshopper, quad meshes and subdivisions will be manually manipulated through Blender where necessary.

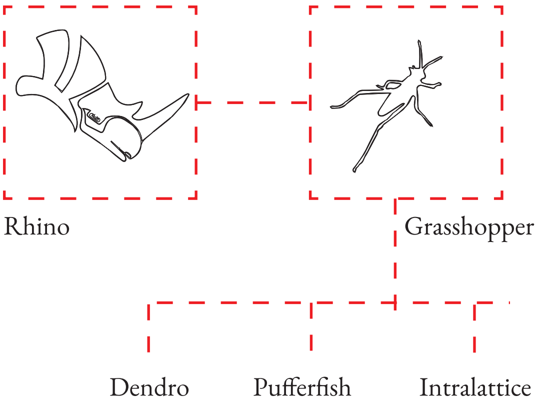

Figure 5.02 Software.

[5.1.3] Evaluation

Each digital prototype will be reflected upon with a Radar Plot as described below. The points on the plot correspond with the digital criteria set out above.

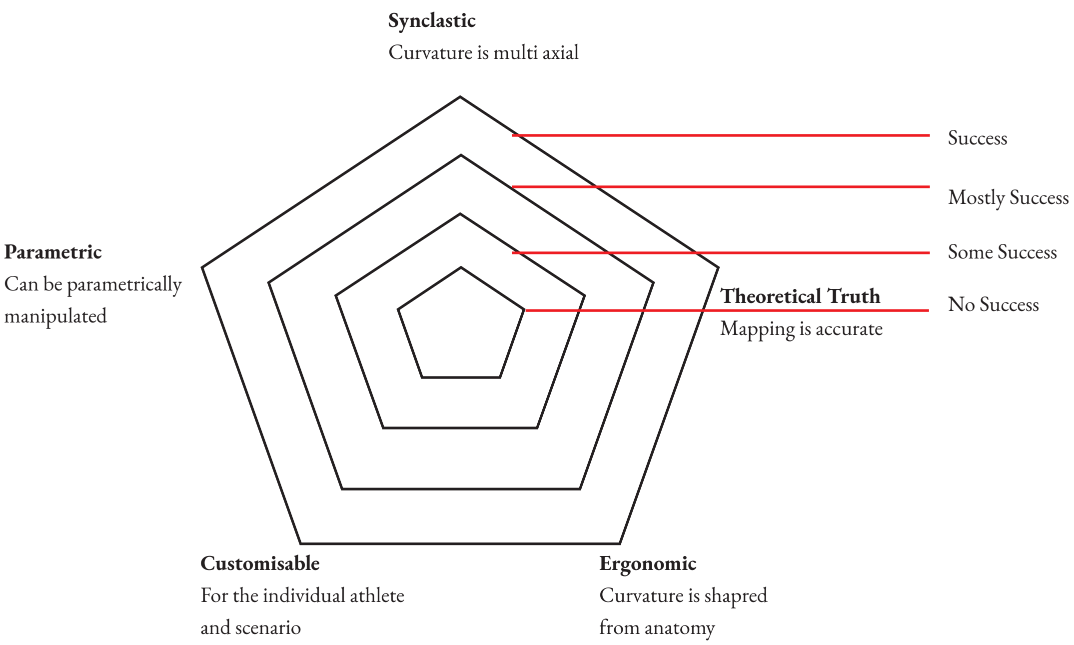

Figure 5.03 Digital Exploration Radar Plot.

[5.2] Auxetic Survey

The three Auxetic structures will be mapped to curvature for their manufacturing successes, digital ccontrollability and behavioural properties to be tailored to the specific scenarios.

To increase workflow speed, the structures have been joined to create one polysurface per unit, to decrease computing time and enable greater exploration.

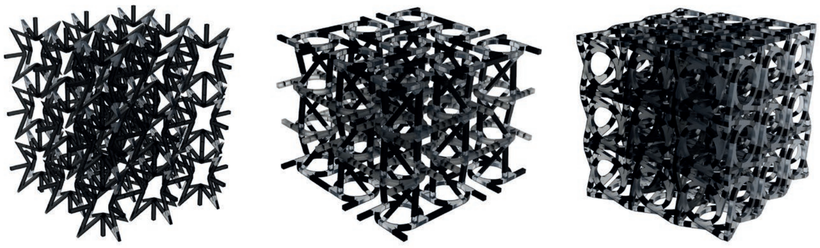

Figure 5.04 Biaxial Auxetic Structures.

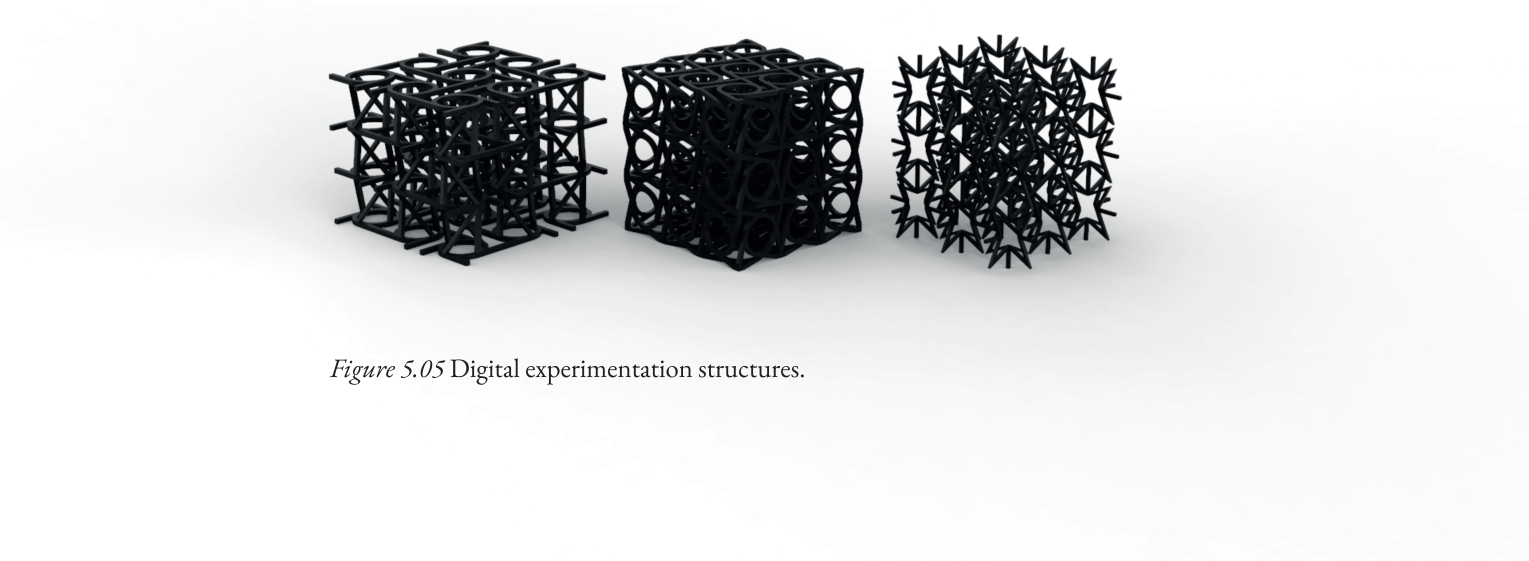

Figure 5.05 Digital experimentation structures.

[5.3] Exploration Procedures

Structures

1 Meta-Chiral Compression Twist
2 3D Anti-Tetra-Chiral
3 Star4

Experiments
1 Proof of Concept
2 Surface Morph
3 Synclastic Surface Morph
4 Curvature Mapping
5Auxetic Curvature

Phases

1 Unit Assignment and Curvature Extraction
2 Script Development
3 Structure Mapping
4 Morphing
5 Refined Variation Exploration
6 Contextualisation

Depicting Geometrical Parameters

In part two of the research the design parameters move from being unit focused to having design characteristics which are more structurally or form based.

The below structures will be used to map to the curvature.

Through analytical modelling, geometrical design parameters are identified as key factors in varying the mechanical responses of the structures. Material aware, computational design will focus on the parametric factors of the following characteristics.

Material Aware Computational Design

Physical	Digital	Computational Characteristics
Deformation Mechanism Auxetic Effect	**Geometry** Unit Geometry Strut + Hinge Geometry	Z Direction Geometry
Shore Hardness	**Materials** Digital Combinations	Componentry
	Scale Hinge to Strut Ratio	Curvature Mapping Divisions

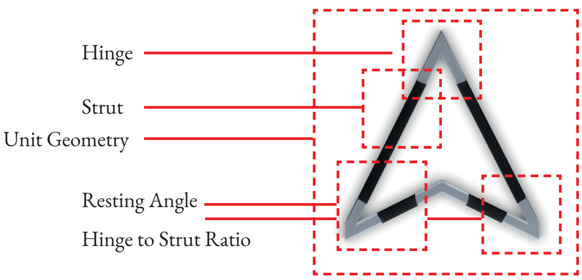

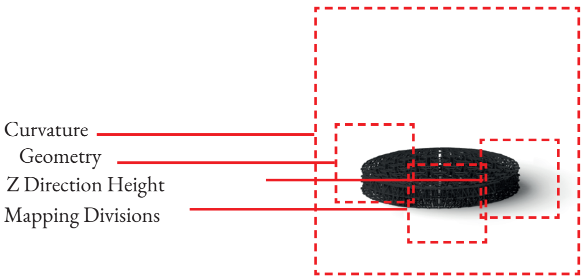

Figure 5.06 Design Parameters unit to lattice.

Re-entrant

[5.4] Exploration 1: Proof of Concept

Grasshopper

Design Variable: Curvature

Mapping Auxetic geometries to curvature.

Unit Assignment and Curvature Extraction

3D Anti-Tetra-Chiral with hinge and strut bodies connected to make one multi-unit body.

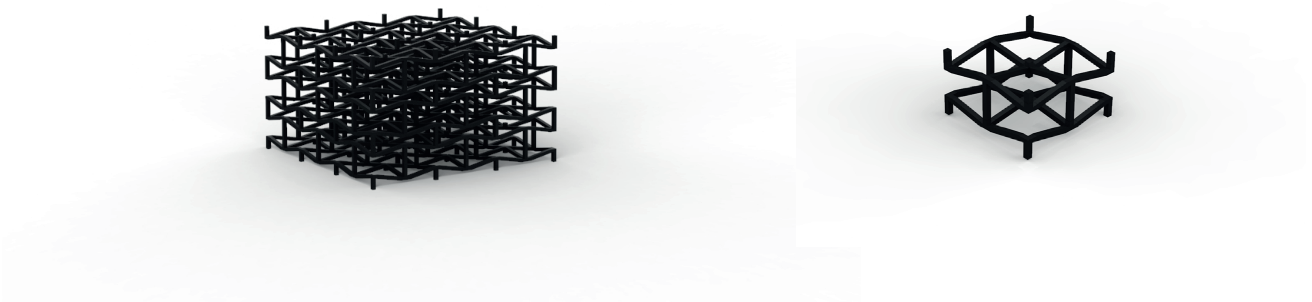

Figure 5.07 Hexagonal Honeycomb.

Script Development

The first and second script iterations use Grasshopper's surface morph to assign geometry to a surface.

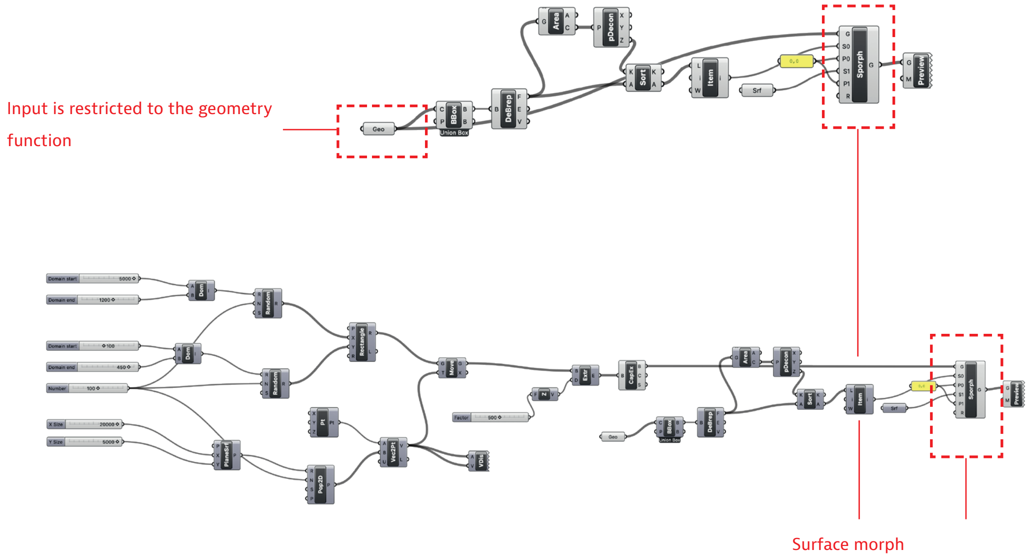

Figure 5.08 Surface morph scripts.

Morphing

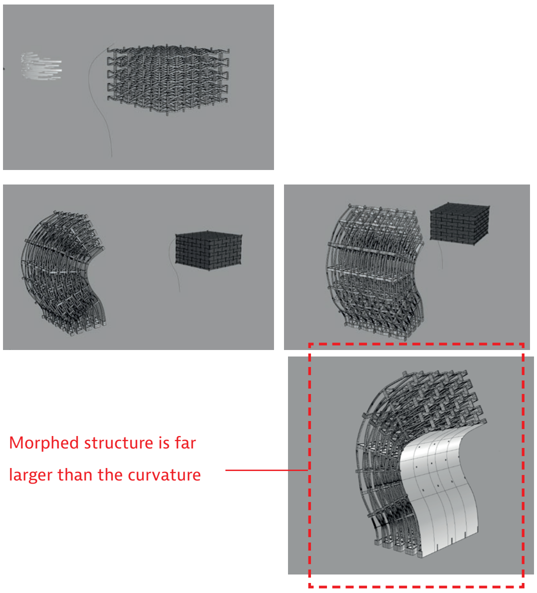

Figure 5.09 Hexagonal Honeycomb surface mapping.

Discoveries

Structures are only mapped to anticlastic curvature, which restricts the form to single axis bending. Units are unevenly skewed.

Chiral **[5.5] Exploration 2: Surface Morph**

Dendro

Design Variable: Curvature

Structures should be mapped to synclastic, multi directional curvature.

Unit Assignment and Curvature Extraction

Meta-Chiral Compression Twist single body unit.

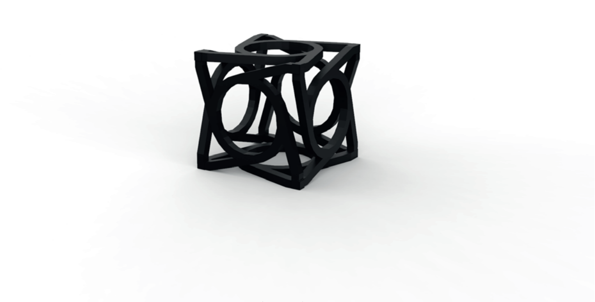

Figure 5.10 Meta-Chiral Compression Twist.

Script Development

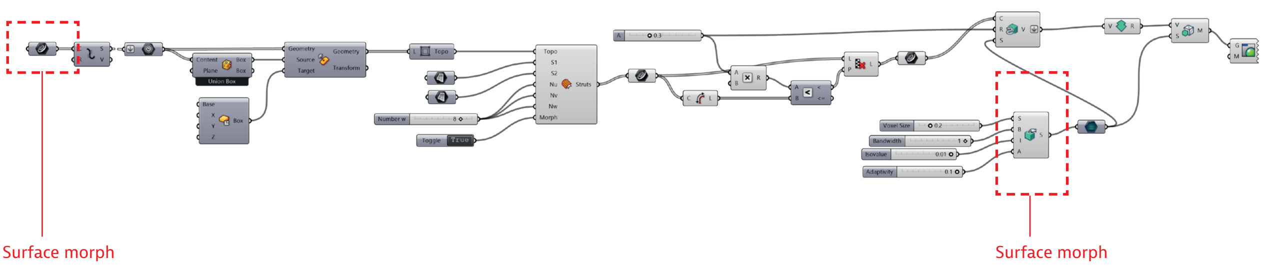

Figure 5.11 Dendro Script.

Morphing

Anti-clastic

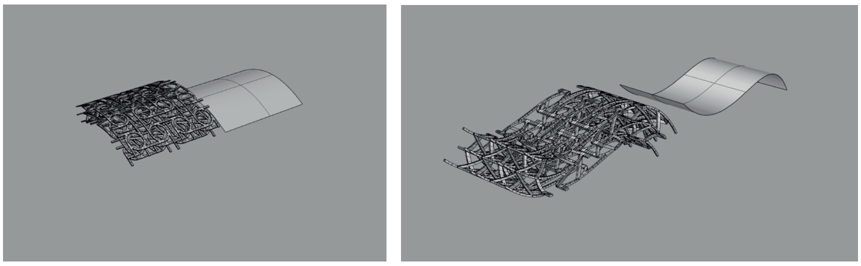

Figure 5.12 Anti-clastic structure morphing.

Synclastic

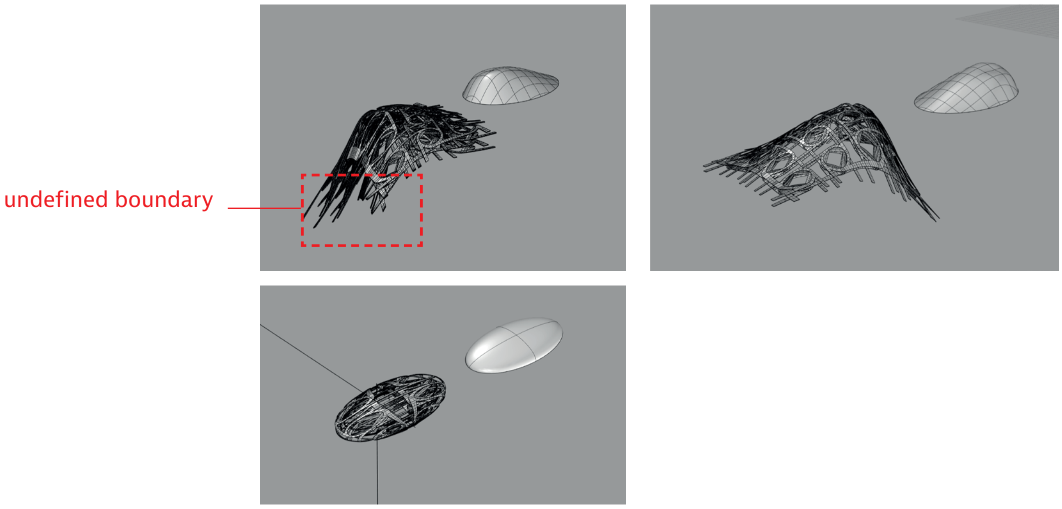

Figure 5.13 Synclastic structure morphing.

Discoveries

Lack of boundary control which is noticeably worse when units are mapped to synclastic curvature, which is necessary to establish in order to map structures to complex anatomical curvature.

Chiral

[5.6] Exploration 3: Synclastic Surface Morph

Pufferfish

Design Variable: Curvature

Unit Assignment and Curvature Extraction

Figure 5.14 Meta-Anti-Tetra-Chiral.

Script Development

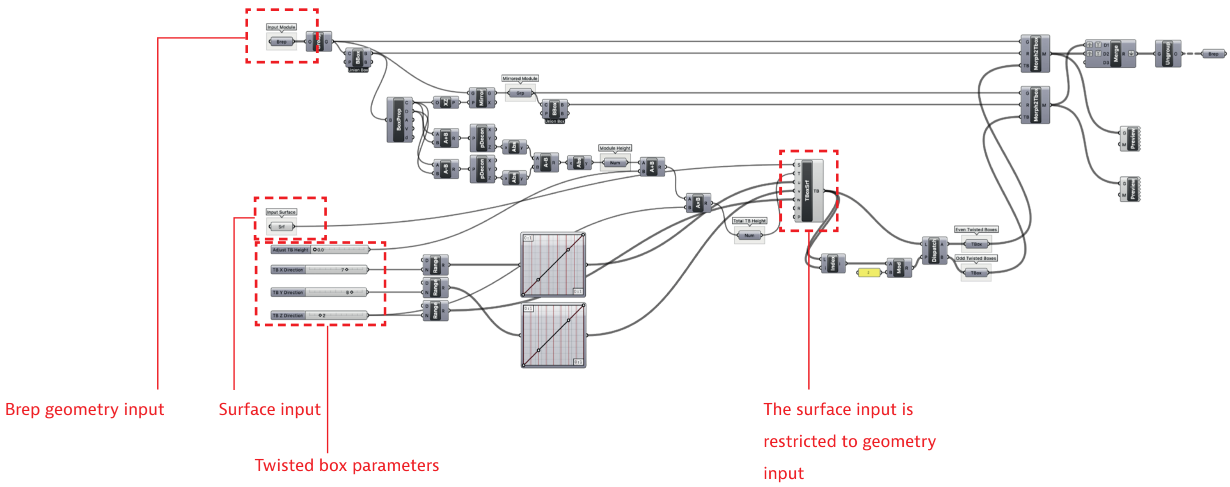

Figure 5.15 Pufferfish Script.

Morphing

Twisted box parameters with lack of intentional settings create unproportional, skewed lattices. Trimmed Surfaces lack the ability to have defined boundaries and therefore the form of the mapped structures is very different to that of the inputs.

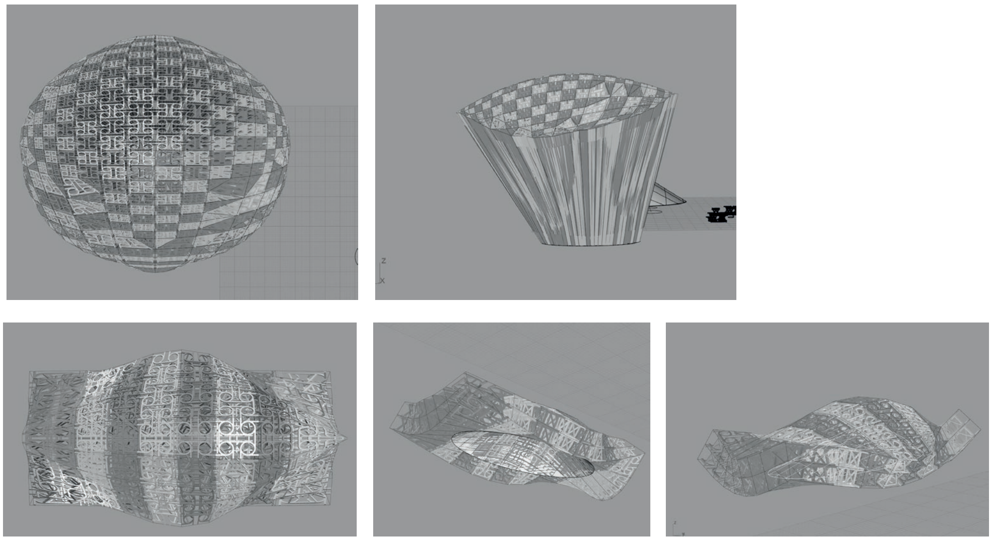

Figure 5.16 Structure morphing.

Discoveries

Surface inputs should be untrimmed surfaces in order to keep defined and predictable boundaries.

[5.7] Exploration 4: Curvature Mapping

Spatial Array

The nature of the surface input, trimmed or untrimmed largely defines the overall form of the morphed geometry. Considering the nature of the mapping of a surface and how the units will fit into that surface will dictate its boundary definition.

Unit Assignment and Curvature Extraction

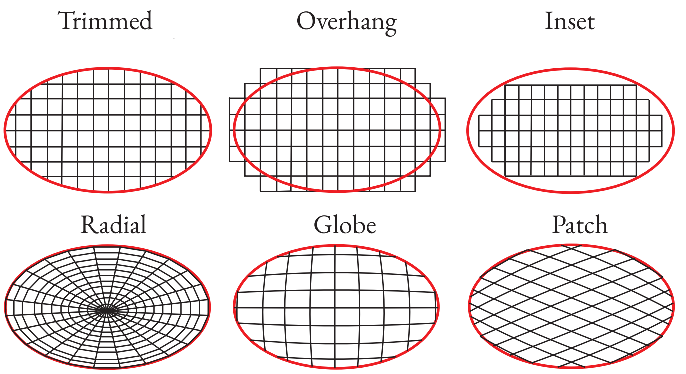

Figure 5.17 Surface mapping.

Script Development

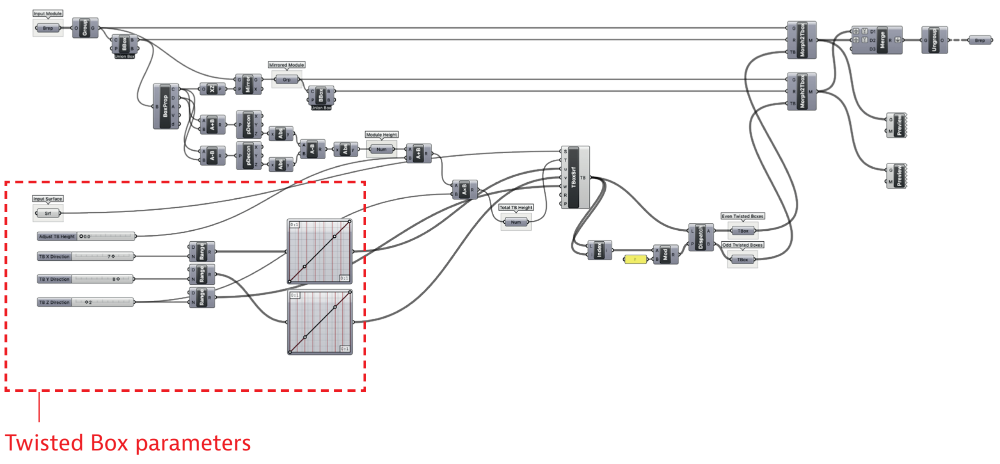

Figure 5.18 Pufferfish Script.

Untrimmed surfaces

Structure
Mapping

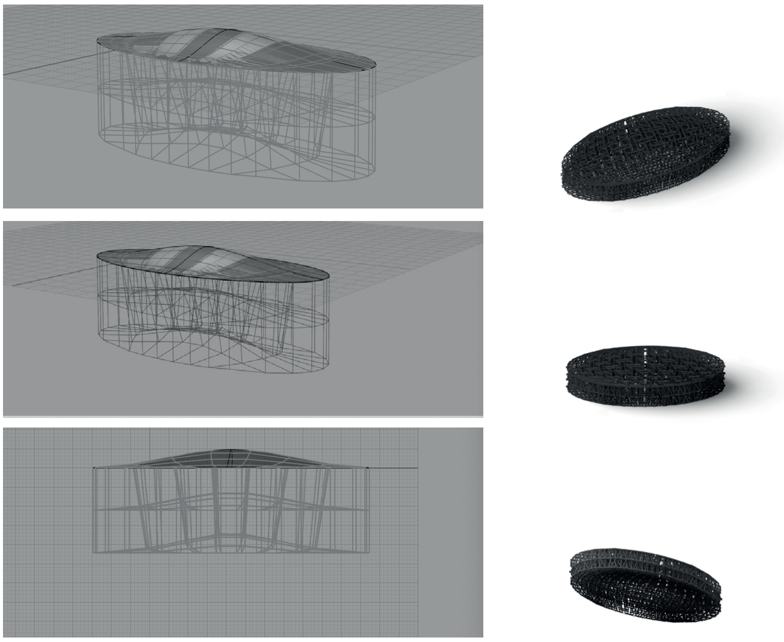

Untrimmed surfaces take standard forms and therefore the ability to assign geometry to bespoke curvature is lost.

Figure 5.19 Synclastic curvature.

Morphing

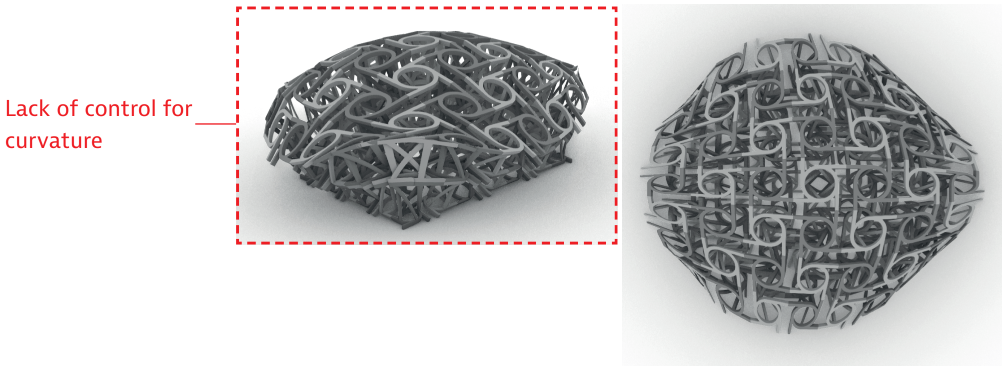

Figure 5.20 Structure morphing.

Discoveries

Untrimmed surfaces produce far better lattice results, however, they limit the range of curvature units can be mapped to, making the structures difficult to map to complex anatomical curvature.

[5.8] Exploration 5: Auxetic Curvature

Pufferfish

Design Variable: Curvature

Unit Assignment and Curvature Extraction

Mesh as the surface input, limits the ability to control the parameters of the twisted box, however, surfaces of an untrimmed or trimmed nature can be mapped to with far greater success.

Script Development

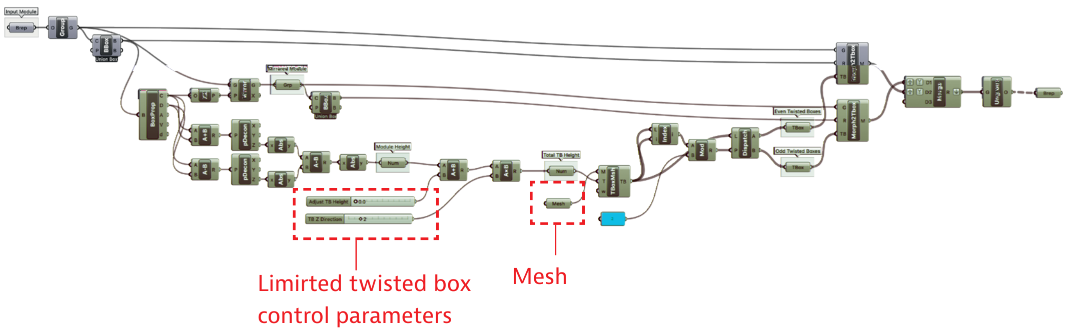

Figure 5.21 Pufferfish Script.

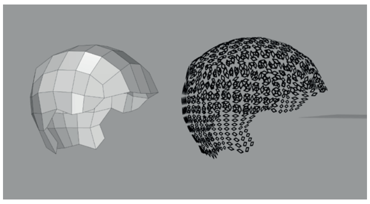

Figure 5.22 Auxetic Curvature.

Final Script

For instances involving the mapping of Chiral structures, which are symmetry based, having the ability to control the nature of the boundary is critical to ensuirng unit relationships are true to theory.

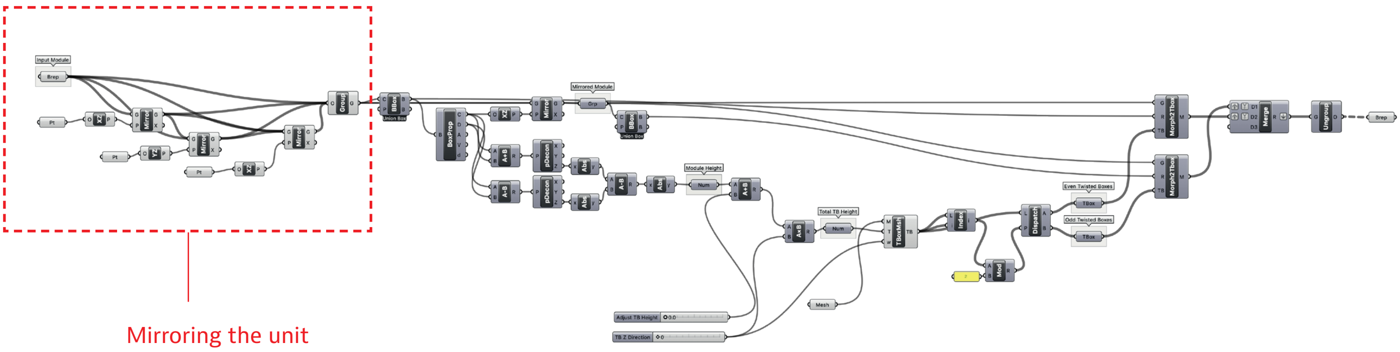

Figure 5.23 Final developed script.

Discoveries

The additional part added to the start of the script enables the control of over the units and their relationship or connection with another unit.

Replacing the mesh input with the surface input eliminates issues at the boundaries of the structures, and the additional control or unit relationships means this is a better option.

6 DESIGN STUDIES

6.1	Overview and Identification	228
6.2	ACC Analysis	229
6.3	Overview	234
6.4	Head Injuries	236
6.5	Knee Injuries	255
6.6	Spinal Injuries	268

The following design studies explore human sports protection in identified sporting scenarios most in need of a design intervention based upon high injury rates retrieved from ACC, NZ.

Figure 6.01 High intensity sports.

[6.1] Preliminaries

Digital Exploration Criteria

The digital experimentation should seek to fulfil the following criteria.

Designs should

Have curvature determined by anatomical site

Be made up of unit geometry, true to Auxetic theory

Have geometric patterning and boundaries true to theory, arranged by quads

In terms of biaxial Auxetic structures, they are a critical part of fulfilling the design criteria. When considering the high impact applications, energy negotiation is critical, where high indentation resistance and energy absorption are key aspects in enabling the highly desired material behaviours. Integral to these mechanical characteristics is the deformation mech-anism which describes the geometries behaviour when exposed to the strain. Biaxial struc-tures in nature, have deformations mechanisms which exhibit Auxetic behaviour or expan-sion in two directions. This is critically important for sports related contexts where a force could strike from any number of directions, and therefore, in scenarios where biaxial Auxe-tic structures are applied and a strain impacts, the material has the capacity to react in the programmed manner in any direction.

[6.2] ACC Analysis

[6.2.1] Head Injuries

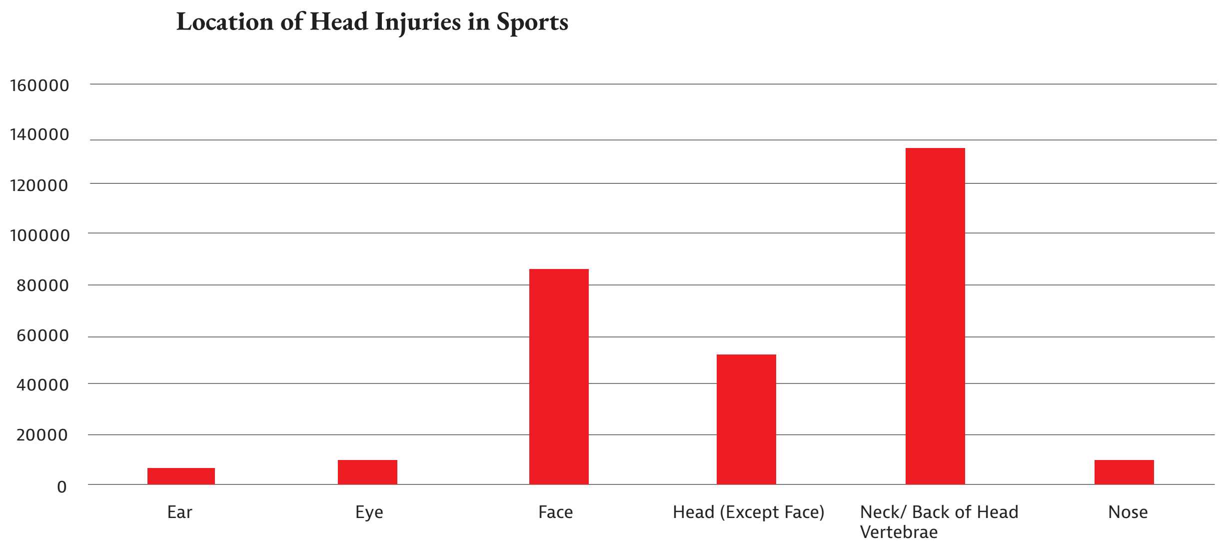

Figure 6.02 Head Injuries, (Author, 2020).

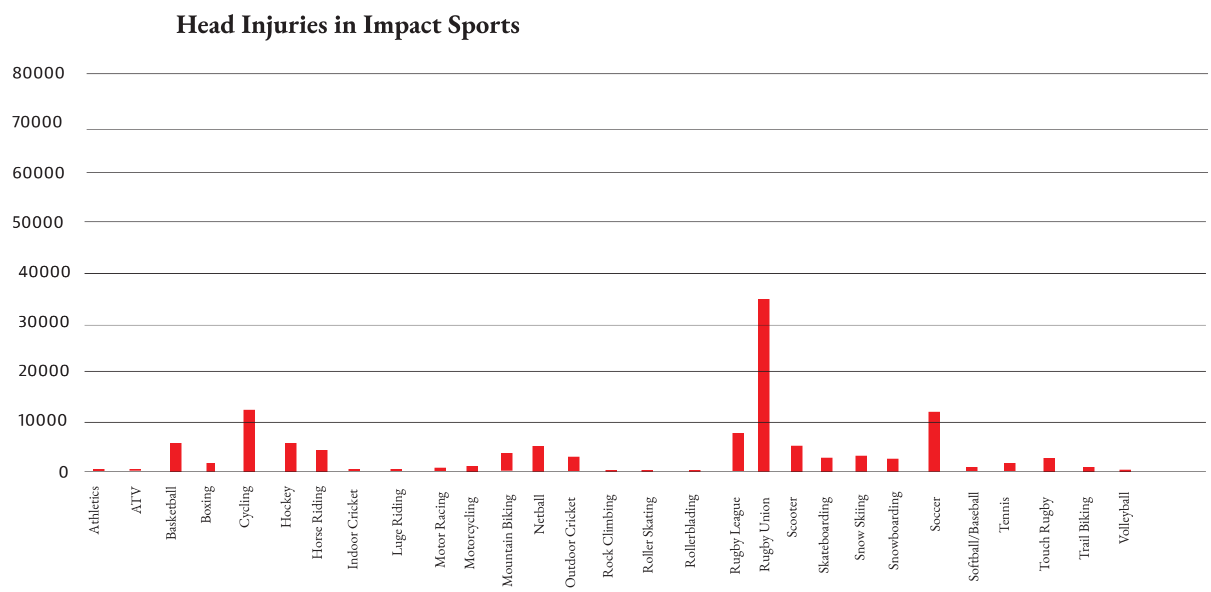

Figure 6.03 Head Injuries.

Causes of Head Injuries in Impact Sports

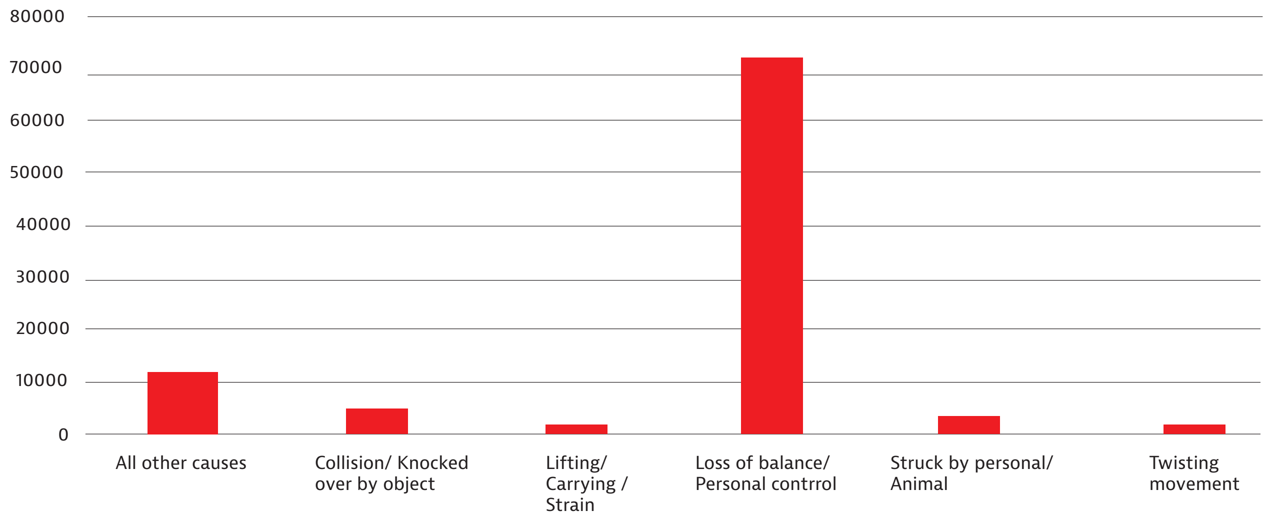

Figure 6.04 Head Injuries, (Author, 2020).

Head Injuries in Rugby League and Union

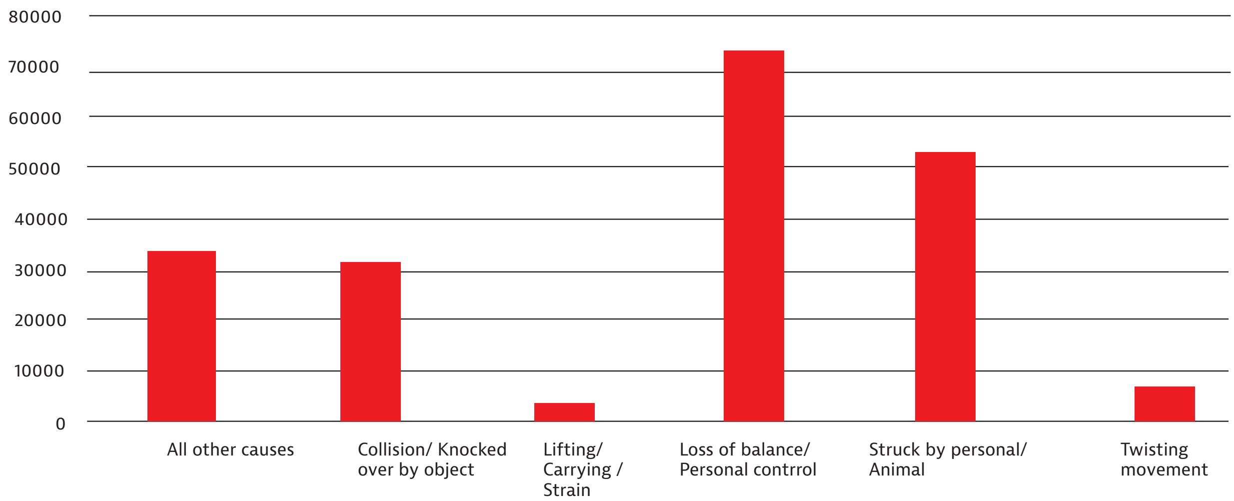

Figure 6.05 Head Injuries, (Author, 2020).

Causes of Head Injuries in Cycling

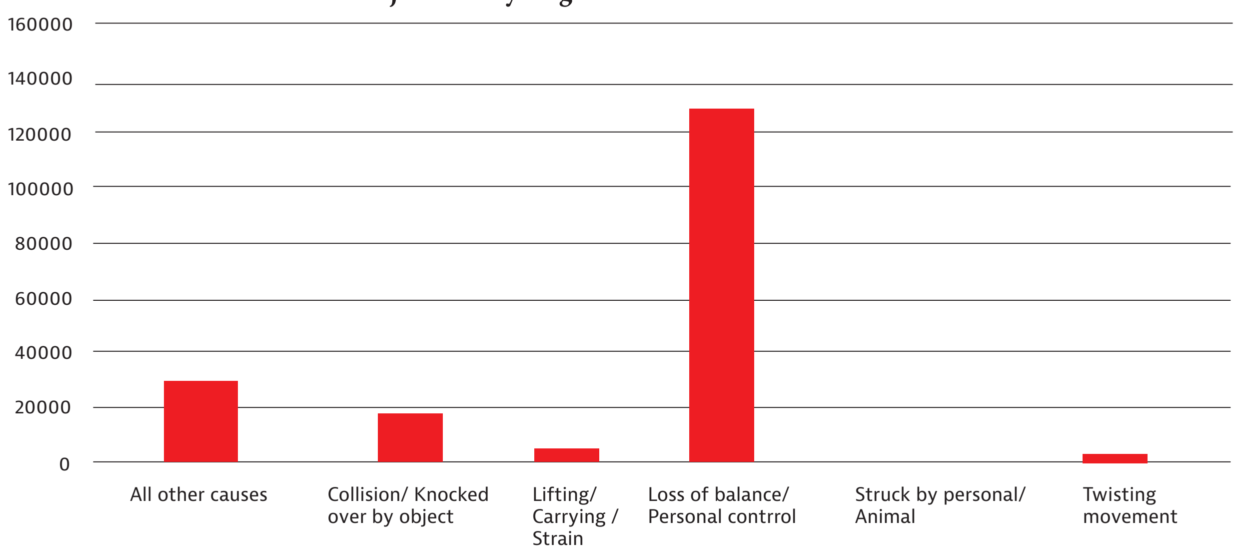

Figure 6.06 Head Injuries.

[6.2.2] Knee Injuries

Causes of Knee Injuries in Impact Sports

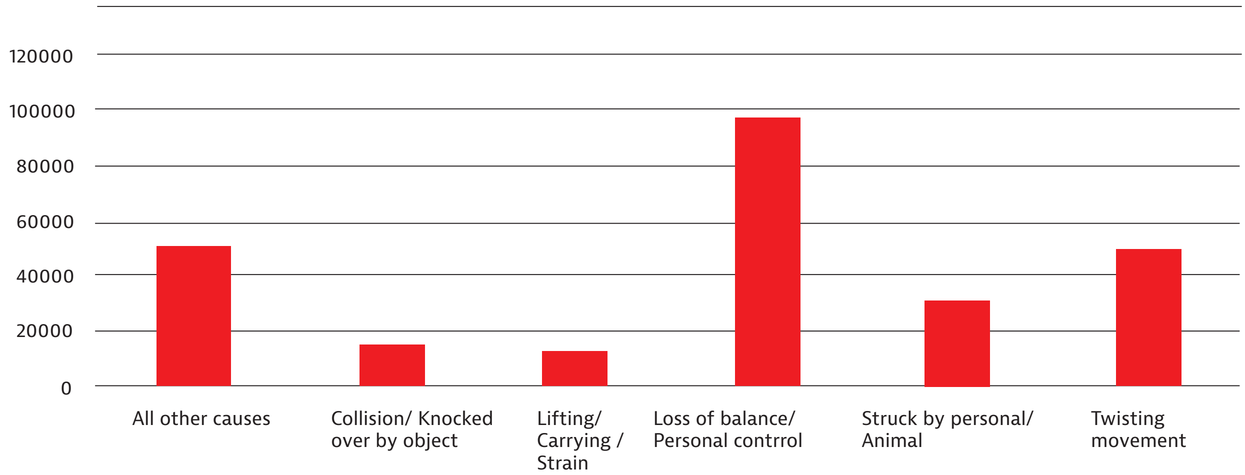

Figure 6.07 Knee Injuries.

Causes of Knee Injuries in Soccer

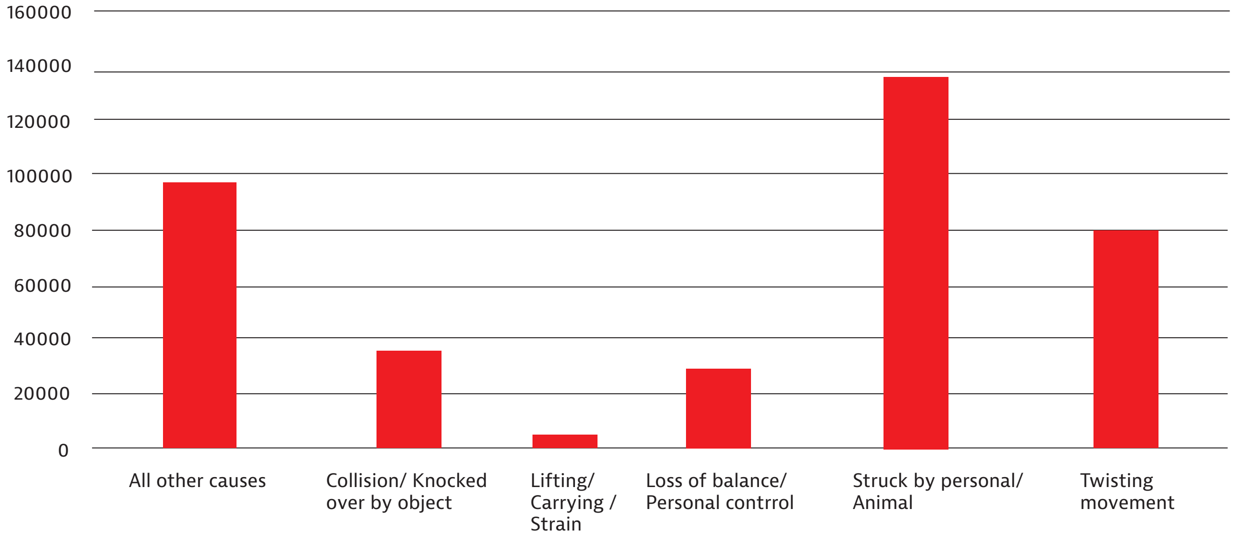

Figure 6.08 Knee Injuries.

[6.2.3] Back/ Spine Injuries

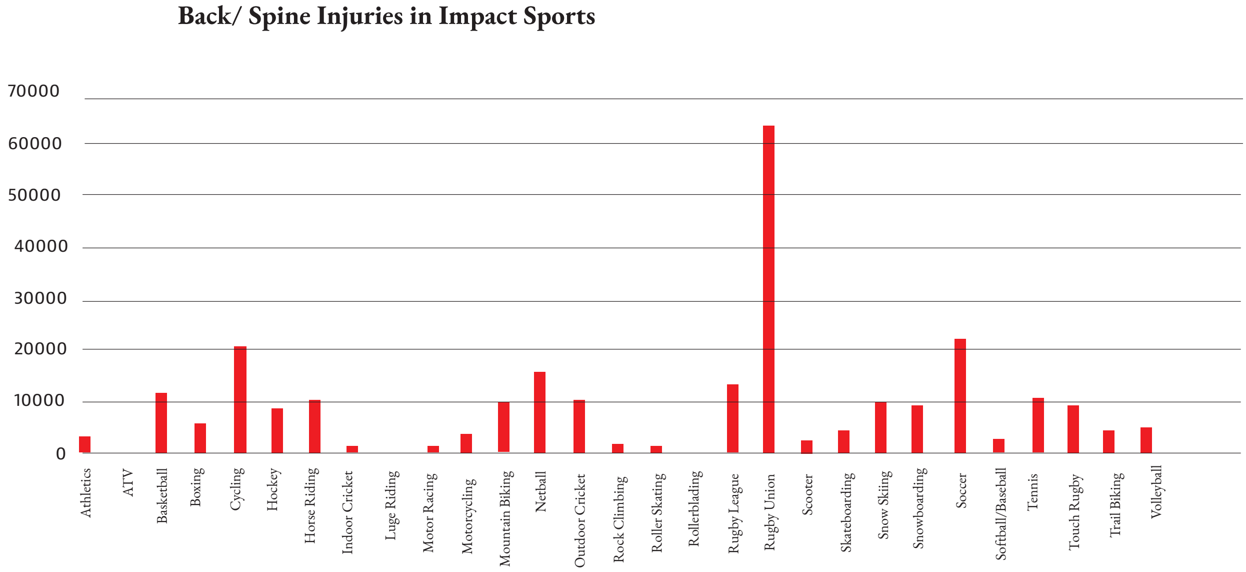

Figure 6.09 Back/ Spine Injuries.

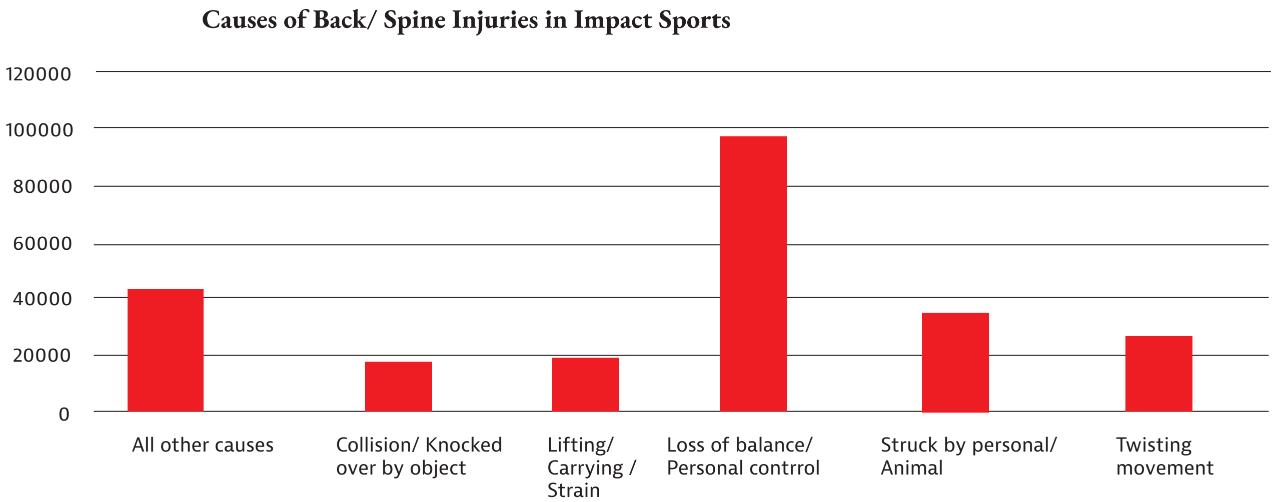

Figure 6.10 Back/ Spine Injuries.

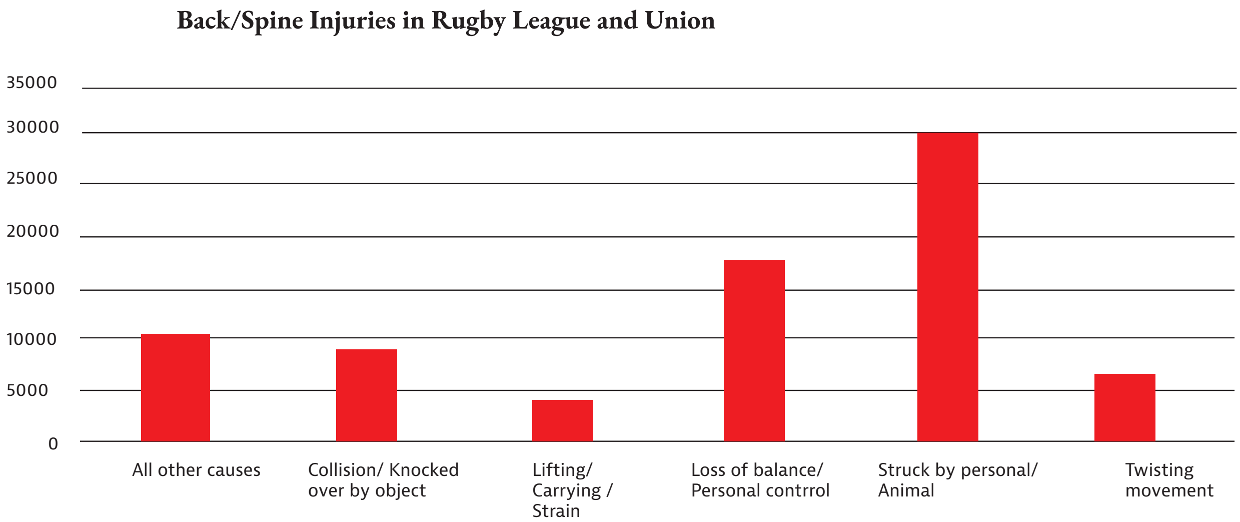

Figure 6.11 Back/ Spine Injuries.

[6.3] Overview

Soccer

Directional Uncertainty + Rotational Stress

ACL Injuries

Auxetic Meta-Chiral

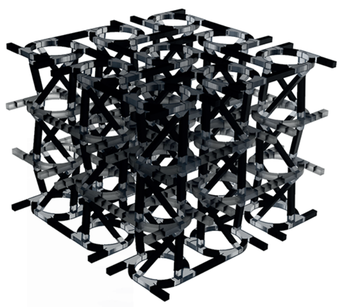

Rotational Deformation Mechanism

Rugby

**Shear Forces +
Hyper Extension**

Back Injuries

Auxetic Star4

**Large Expansion +
High Energy Absorption**

Cycling

**High Impact +
Rotational Stress**

Concussion

Auxetic Compression Twist

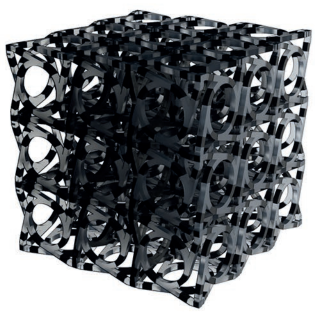

**Rotational Deformation
Mechanism**

[6.4] Head Injuries in Impact Sports

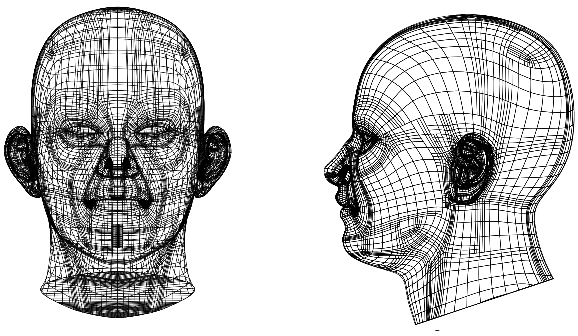

Figure 6.13 The Human Head.

[6.4.1] The Head and Force

Brain injuries induced by biomechanical forces lead to either rapid onset of short lived impairment or a more long term functional disturbance with cognitive effects rather than structural damage (Malcolm, 2019). The most common diagnosis; concussion or traumatic brain injury.

Concussion is defined as a traumatic brain injury, as a result of biomechanical forces. Most often they are caused by one, a direct blow to the body, two, lead to short lived neurological impairment which resolves soon after the event or thirdly involves functional disturbance rather than structural injury.

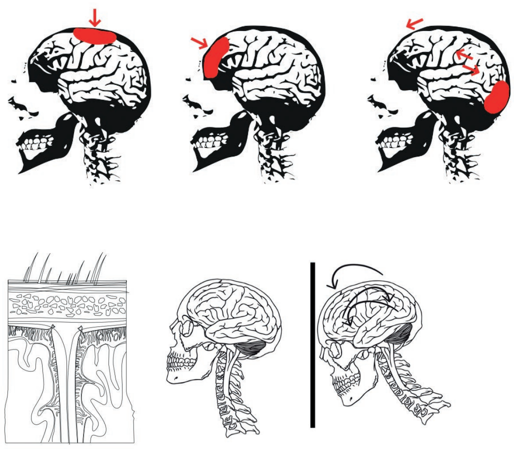

Figure 6.14 Mechanics of the Movement.

[6.4.2] Scenario

ACC data shows that head injuries are one of the most common injuries in impact sports. Head injuries include injury to the ear, eye, face, head, neck or nose.

Head injuries in Cycling

Figure 6.15 Mountain Biking.

[6.4.3] Existing Solution Analysis

Standard hard helmets are comprised of a hard shell and inner foam. The shell is designed to dissipate forces over a larger surface area. The inner foam reduces the peak impact by extending the length of deceleration, and severity of the abrupt impact, whilst also deforming to absorb as much energy as possible.

Hard Helmets are known to protect against traumatic brain injuries, a result of translational movements. However, they are less effective at protecting against rotational movements which cause concussions. Whilst decreasing the level of impact force, they do little to address rotational forces leading to concussion.

Figure 6.16 Existing Helmets: Snow and Cycling.

Currently head protection innovation focuses on new materials and foam, as well as lattices. The social movement of 'The Concussion Crisis' has lead researchers to investigating further ways to limit rotational forces, with the possibility of this including elements which slide against one another upon impact.

[6.4.5] Meta-Chiral Compression Twist

The chiral compression twist has the greatest range of rotational articulation, making it the most suitable to combating rotational forces which cause the most damage in head impacts.

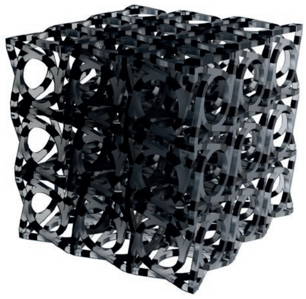

Figure 6.17 Multi-material Auxetic.

Figure 6.18 Meta-Chiral Compression Twist single body.

[6.4.4] Auxetic Intervention: Design 1

The Head

Figure 6.19 Curvature of the Head.

Head Contours

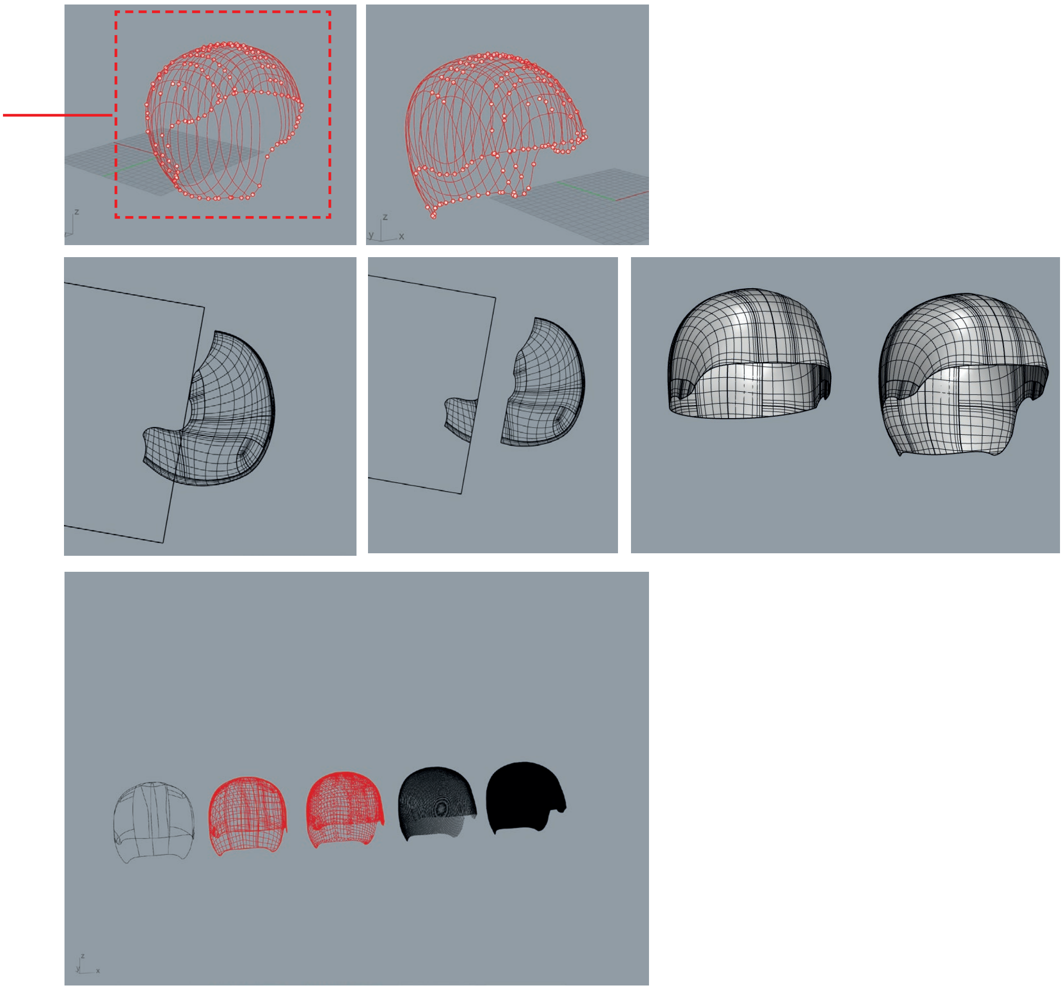

Figure 6.20 Head form finding.

Protection Form

Figure 6.21 Curvature of the Head.

Head Quad Meshed

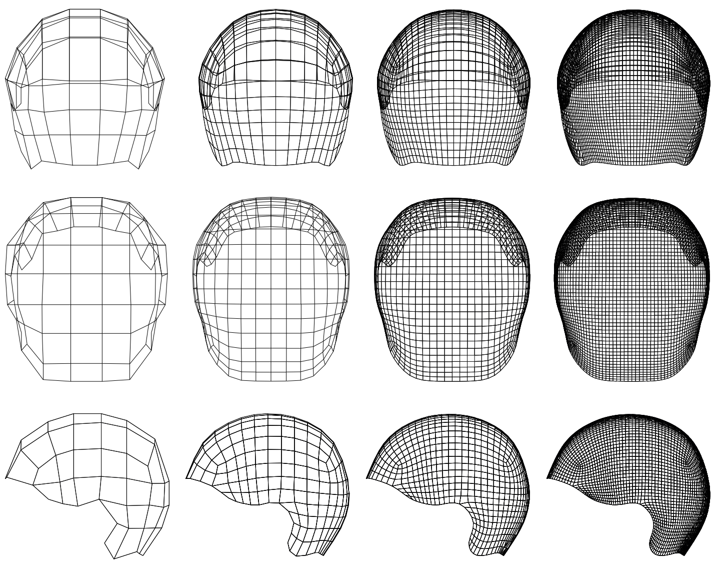

Figure 6.22 Quad Mesh Resolutions.

Mapped Auxetic

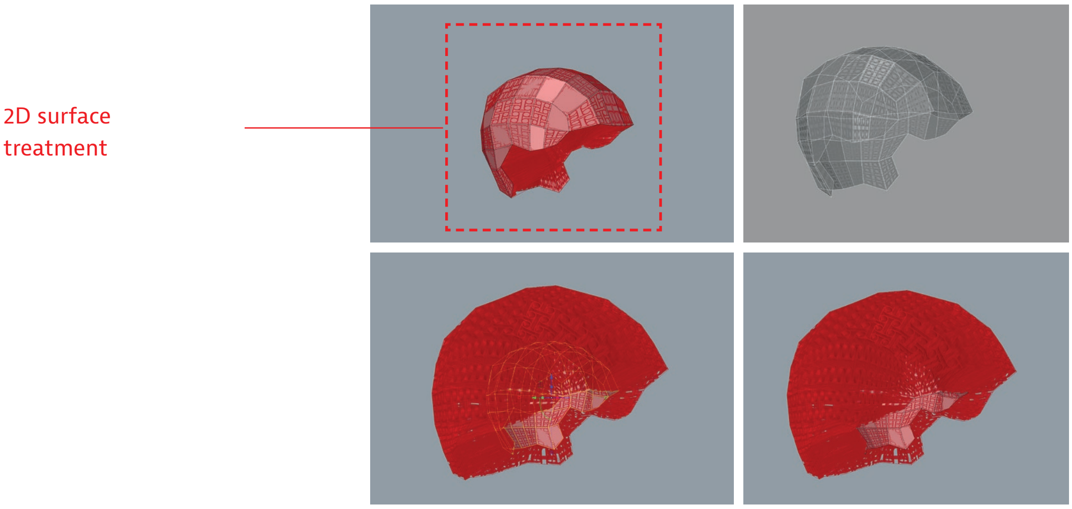

Figure 6.23 Auxetic Dimensionality.

Figure 6.24 Low Resolution Auxetic Helmet.

Dimensional Open Cell Foam

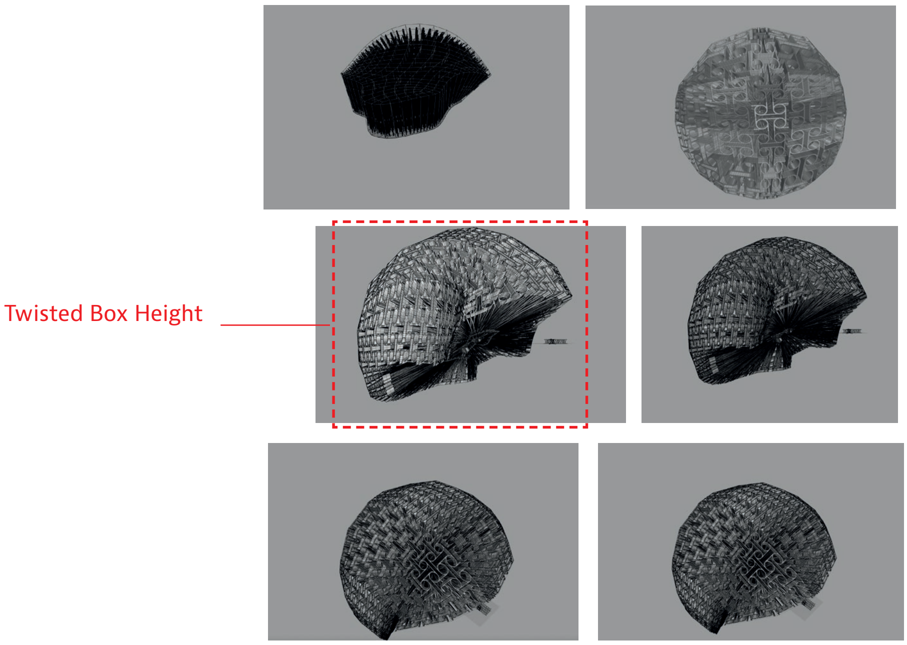

Figure 6.25 Auxetic Dimensionality.

Figure 6.26 Mid Level Resolution Auxetic Helmet.

Refined Variation
Exploration

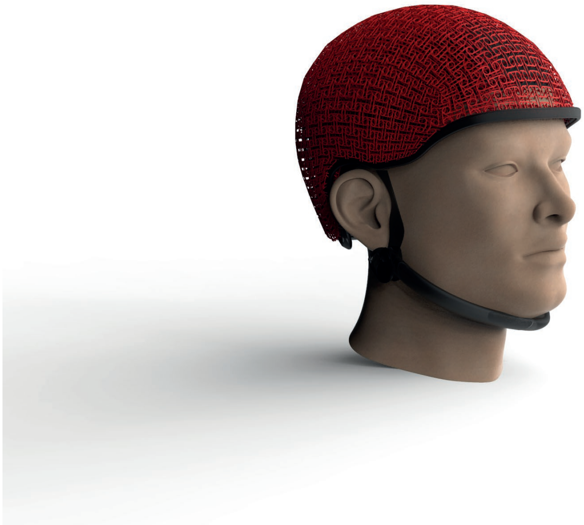

Figure 6.27 Mid Level Resolution Auxetic Helmet.

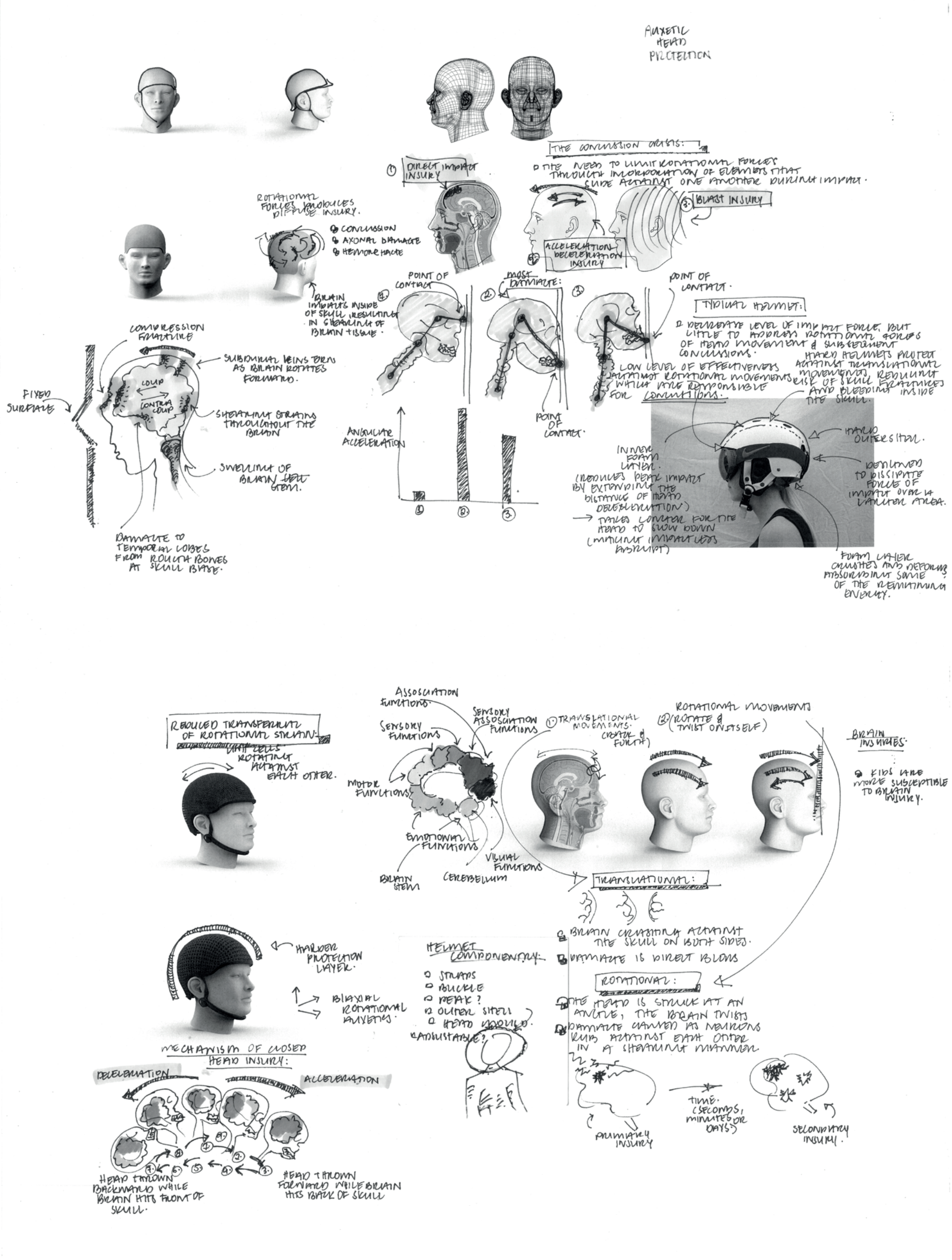

Figure 6.28 Helmet Analysis.

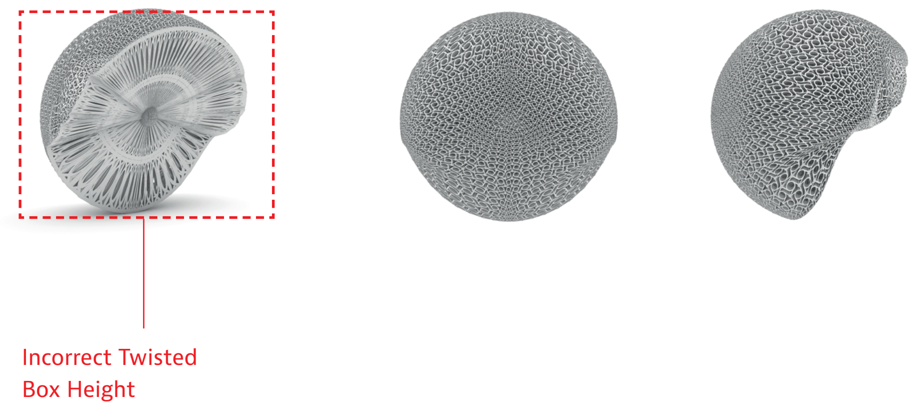

Figure 6.29 Z direction thickness.

Cycling Auxetic Head Protection

Figure 6.30 Meta-chiral Compression Twist Auxetic Helmet.

[6.4.6] Auxetic Intervention: Design 2

Skiing

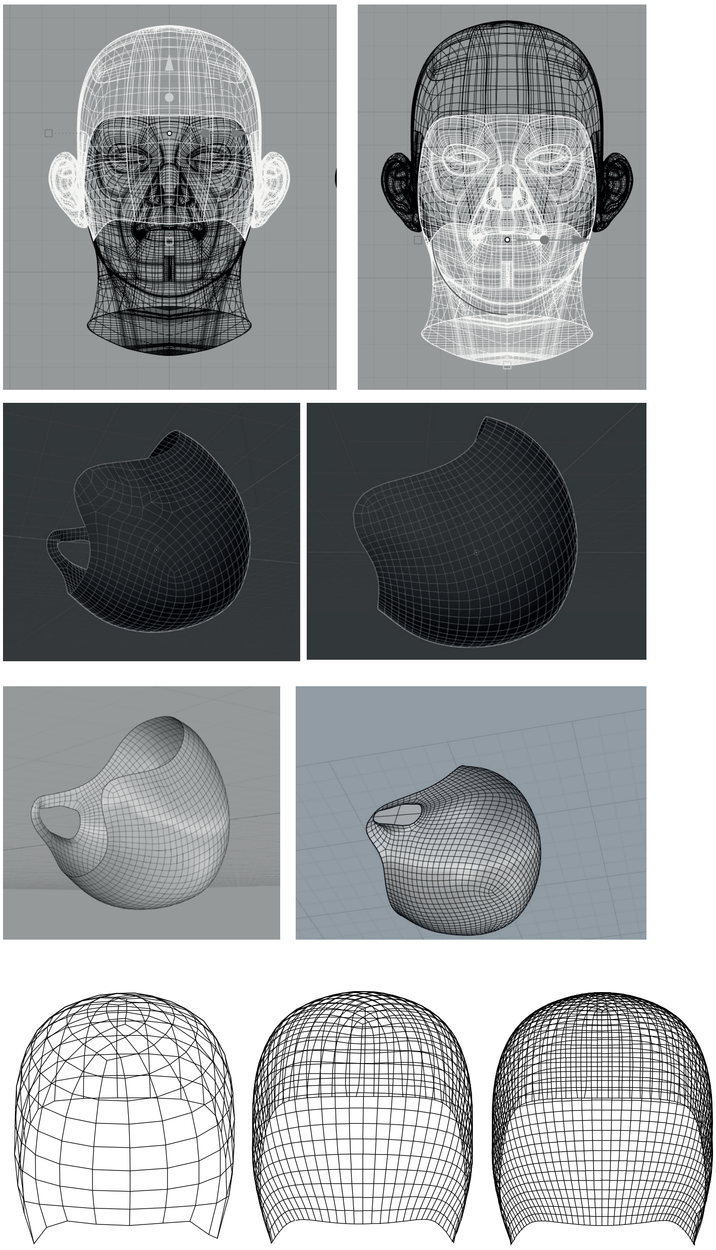

Figure 6.31 Helmet with ear protection.

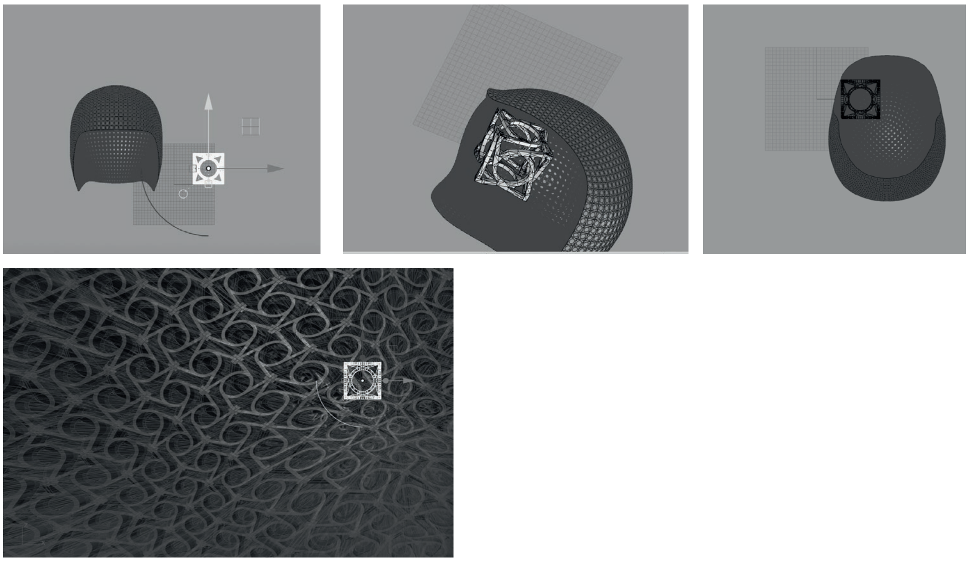

Figure 6.32 Auxetic boundaries.

A major restraint in the development of helemts was teh capacity of the computer, and it revealed flaws in the efficiency of the scripts generating the structures.

Refined Variation Exploration

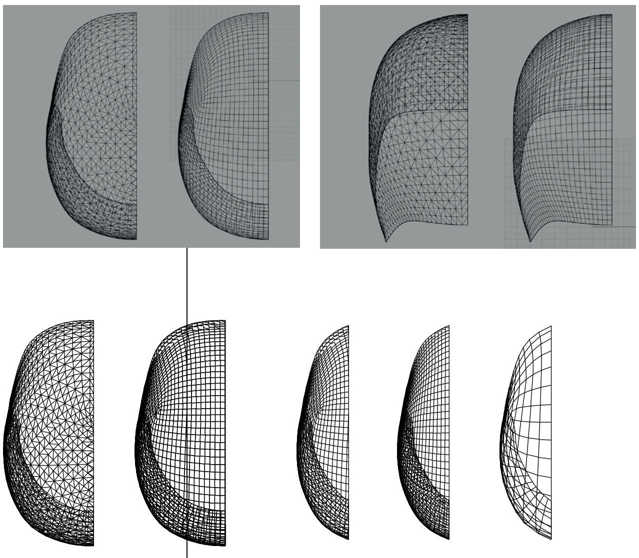

Figure 6.33 Helmet section.

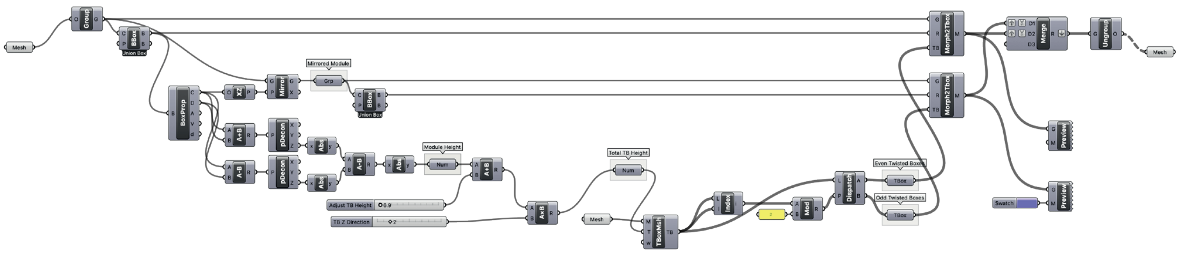

Figure 6.34 Helmet script.

Mesh to mesh

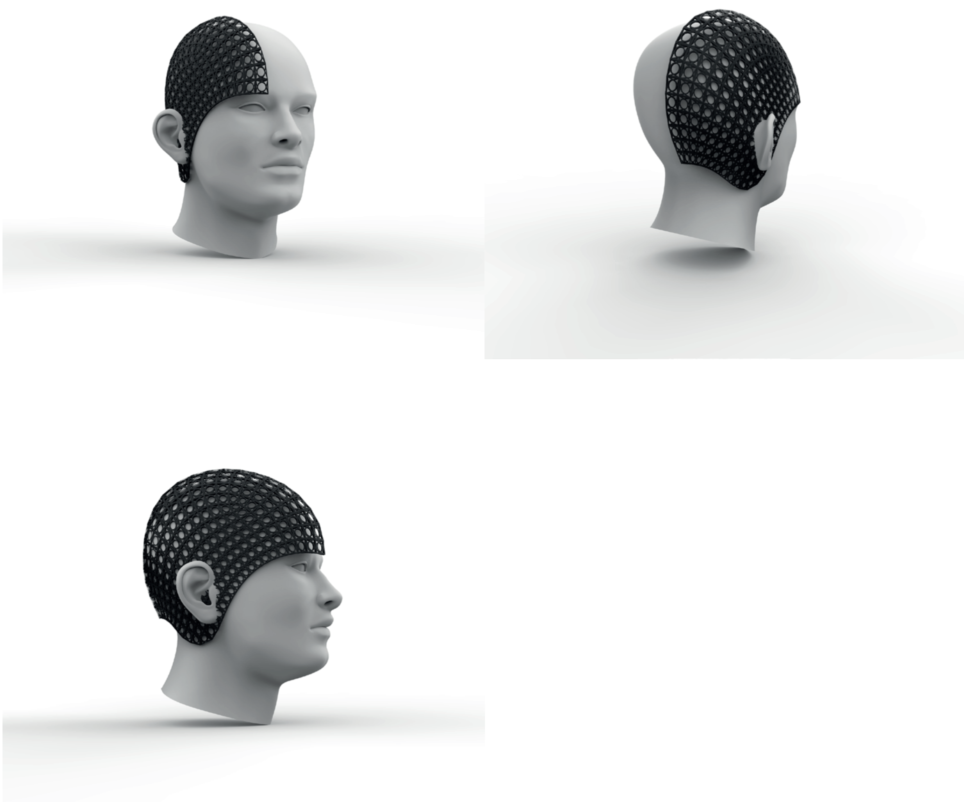

Figure 6.35 Helmet section.

When considerin Auxetic componentry, there are nbumerous integral components of a helmet. Other design considerations developed include, straps and a protective membrane.

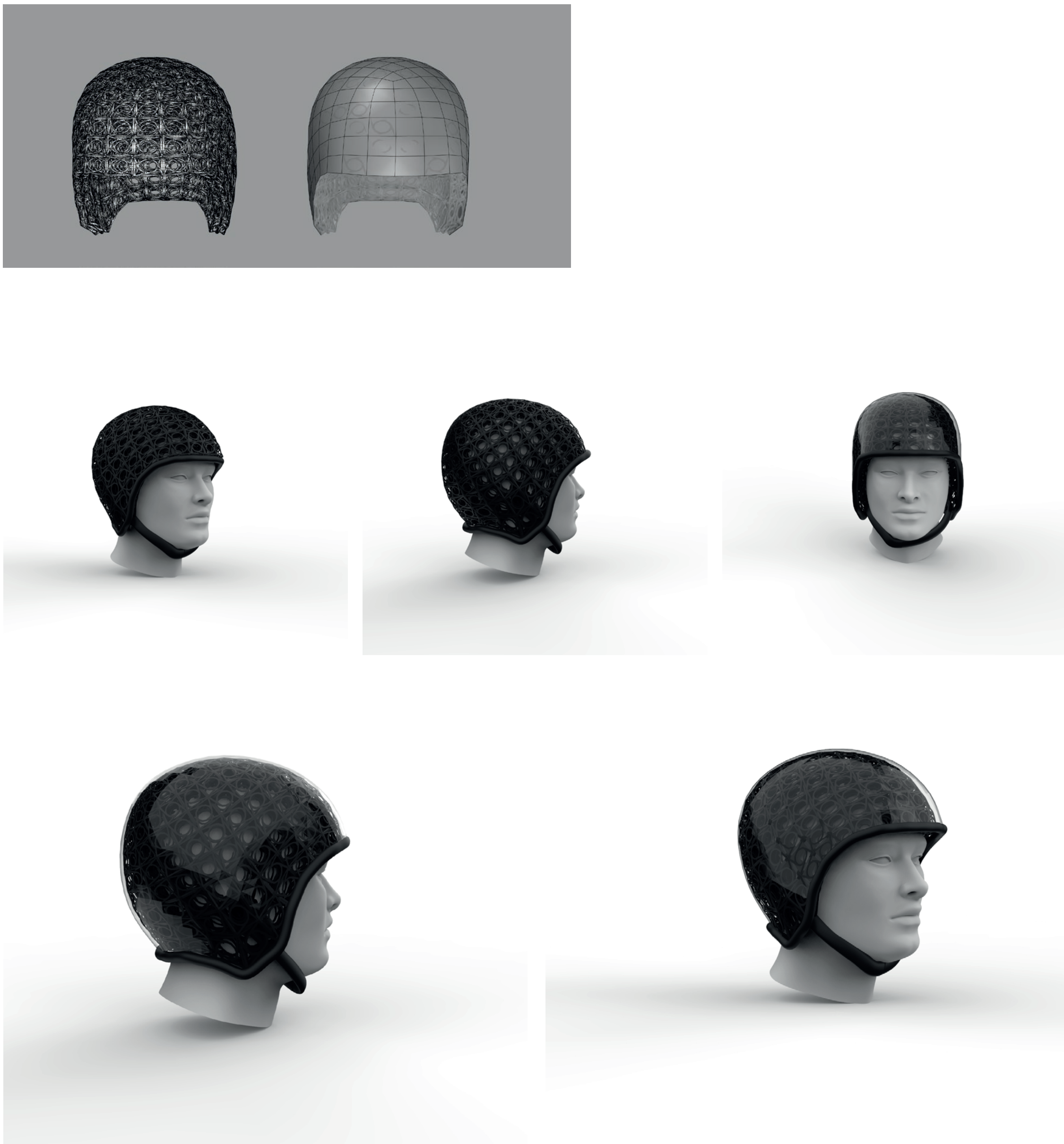

Figure 6.36 *Auxetic Componentry.*

Final Script Analysis

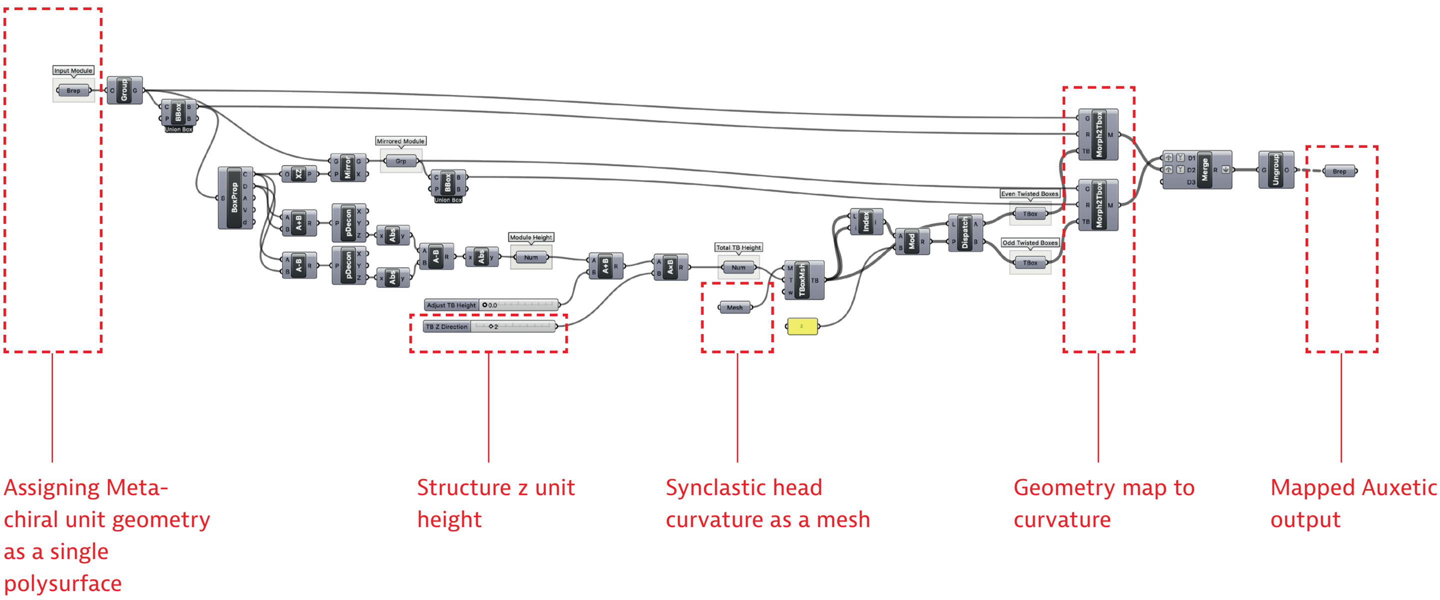

Figure 6.37 Helmet final script.

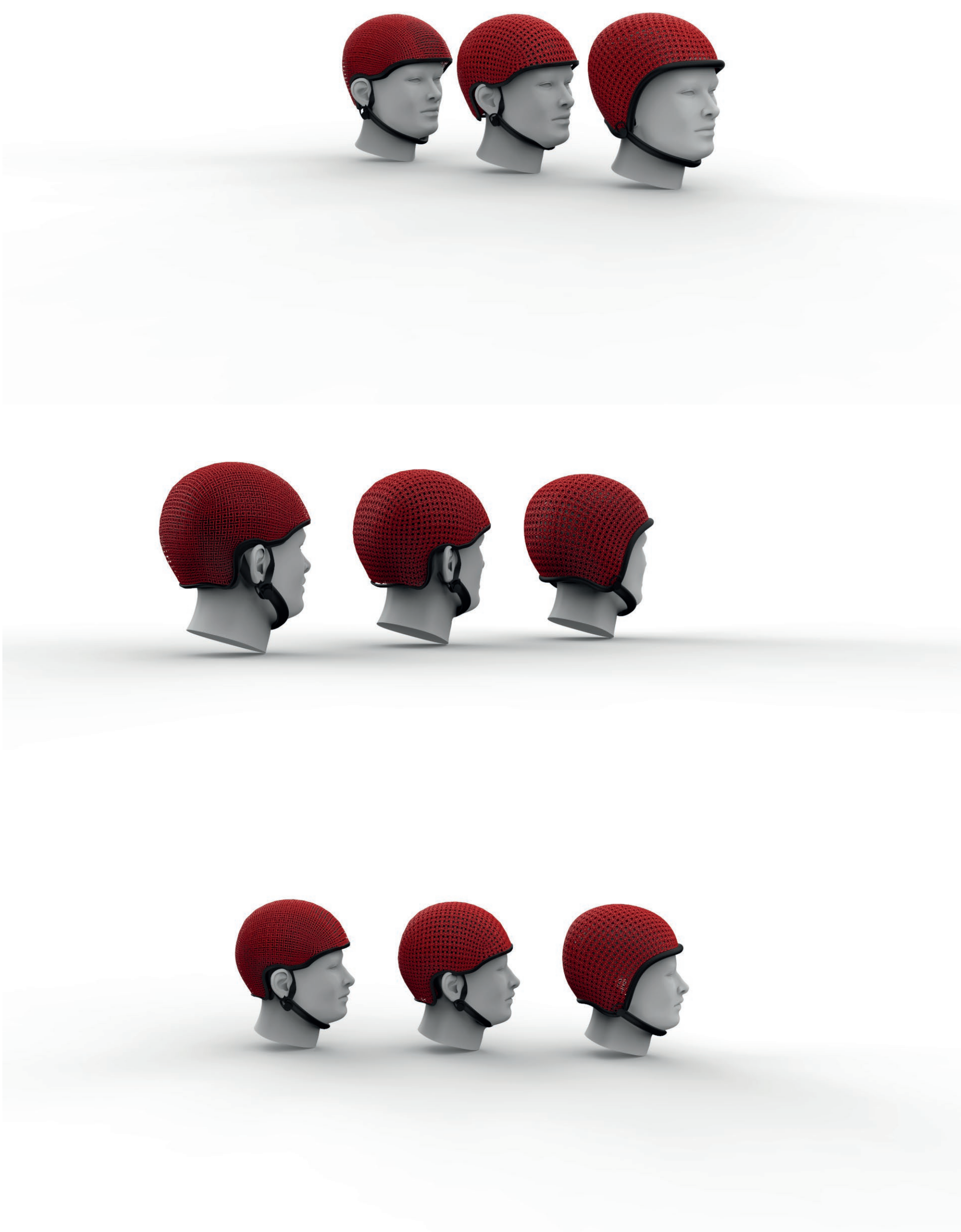

Figure 6.38 Auxetic Helmet.

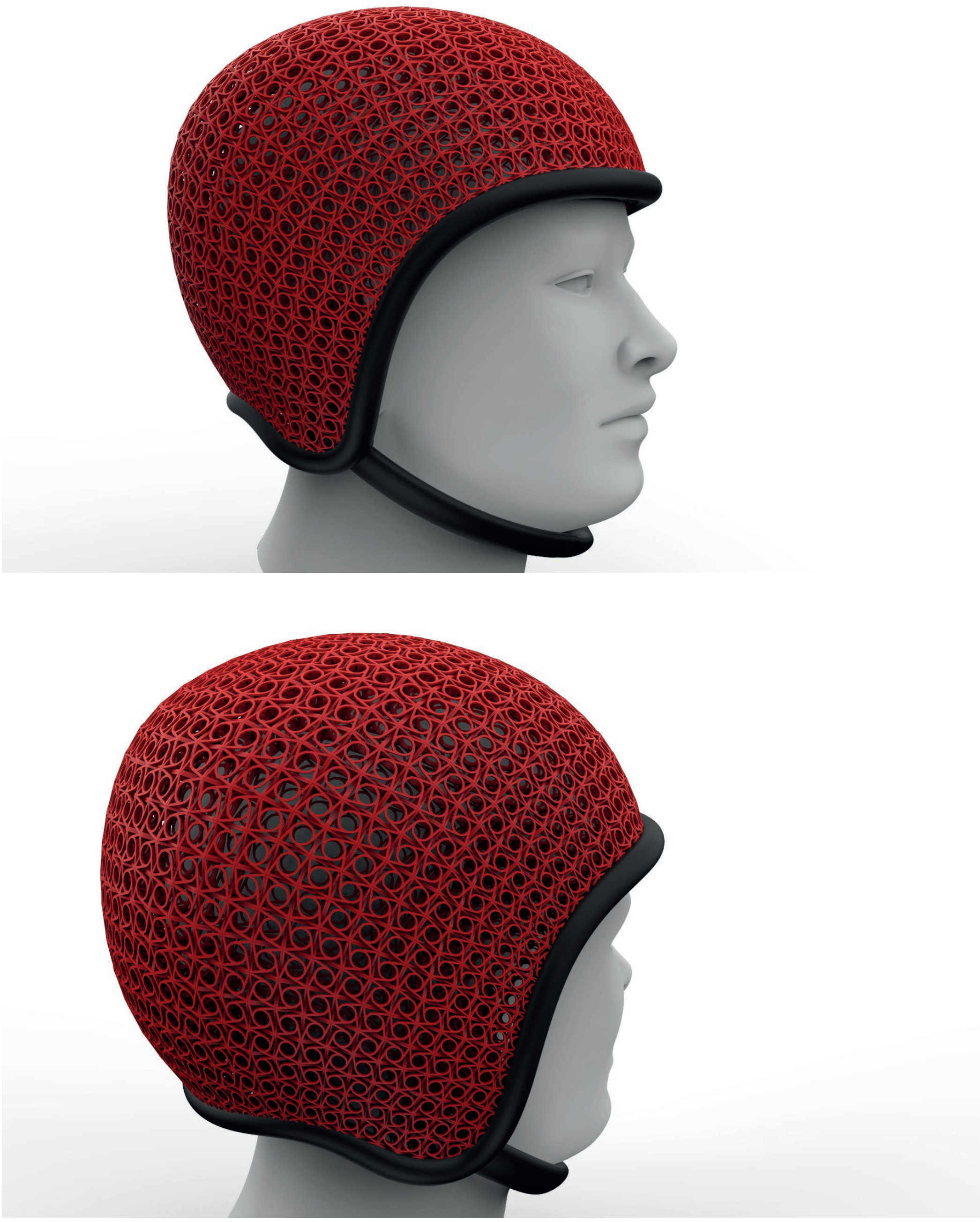

Figure 6.39 Auxetic Helmet.

Auxetic Head Protection Reflection

The helmet structures developed are refined lattices mapped neatly to the curvature, they are ergonomic and customisable. In the future, now the Auxetic open cell foam is developed, further considerations for Auxetic componentry and additional parts to secure the geometry into the head protection is necessary.

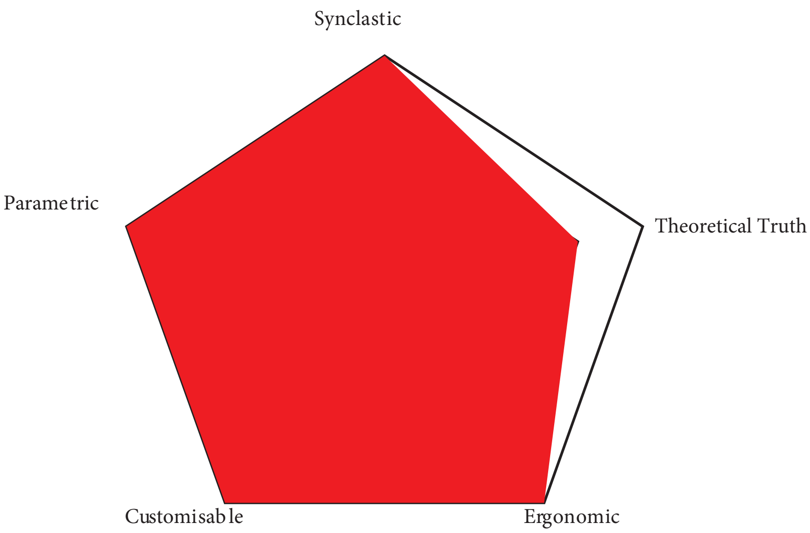

Figure 6.40. Digital Exploration Radar Plot.

[6.5] Knee Injuries in Impact Sports

Figure 6.41 Soccer.

[6.5.1] The Knees and Force

Injuries and Anatomy, including soft tissue knee injuries, the knee joint is where the tibia and femur meet at the patella. The meniscus or cartilage provides both impact support and lubricant to the joint. The ligaments control motion and prevent against unnatural movement, sudden violent movement can damage this area.

Knee includes the knees and lower legs

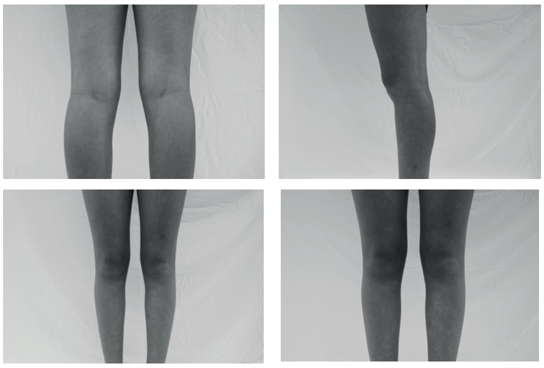

Figure 6.42 Knee Analysis.

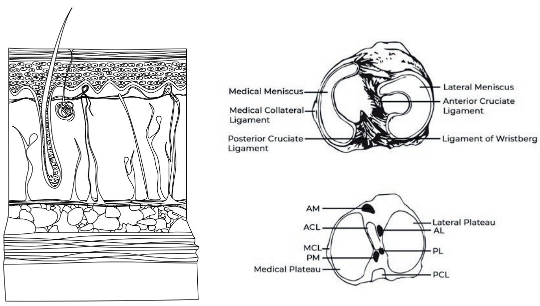

Figure 6.43 Knee Cross Section.

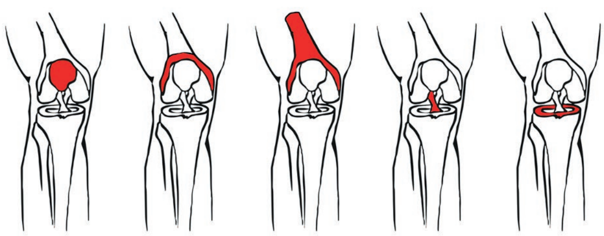

Figure 6.44 Mechanics of the Movement.

[6.5.2] Scenarios

Knee Protection for Soccer

Figure 6.45 Soccer.

Strain rate and energy absorption are key behavioural properties of Auxetic Structures and their ideal application in sporting equipment.

Ligament injuries (ACL/PCL/MCL/LCL)

Often ACL injuries occur when a person suddenly twists and they don't have the necessary strength to counteract this motion, as a result their knee may slip out and the ACL tears. In other circumstances an impact to the inside of the knee compounds stress on the outside of the knee in an overwhelming magnitude and the LCL tears as a result. The meniscus is also commonly torn from violent and sudden movement.

[6.5.3] Existing Solution Analysis

Figure 6.46 Existing Knee Protection.

[6.5.4] Auxetic Intervention: Design 3

Figure 6.47 Knee.

3D Anti-Tetra-Chiral

Utilising the Chiral rotation induced unique sequential cell-opening mechanisms. Frenzel et al. proposed a micro structured 3D elastic chiral mechanical metamaterials which can realize twist deformation upon compression, the proposed tension/compression induced twist deformation (Wu et al., 2018).

By utilising the strain induced twist, Auxetics applied to knee protection can limit the rotational strain that is then transferred to the athletes knee and reducing injury overall.

Knee and ankle injuries are most often a result of an abrupt sudden movement, therefore the Meta-Chiral unit was chosen to combat the rotational strains and limit the amount of rotational energy transferred onto the body.

Figure 6.48 3D Anti-Tetra-Chiral.

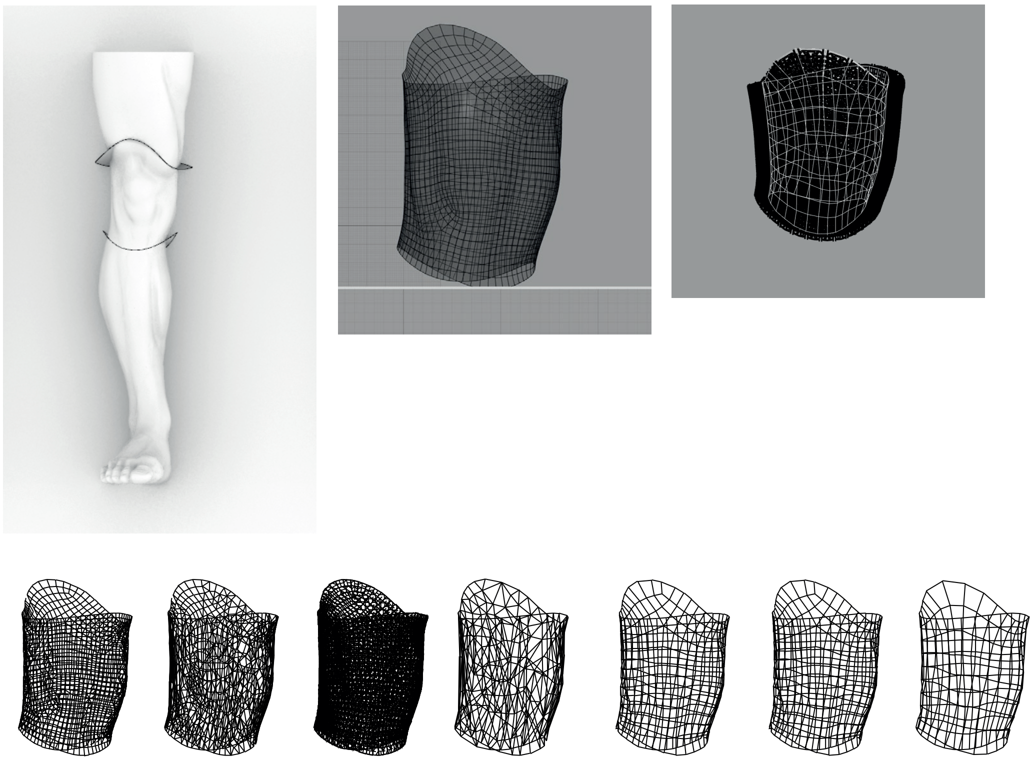

Figure 6.49 Knee Protection.

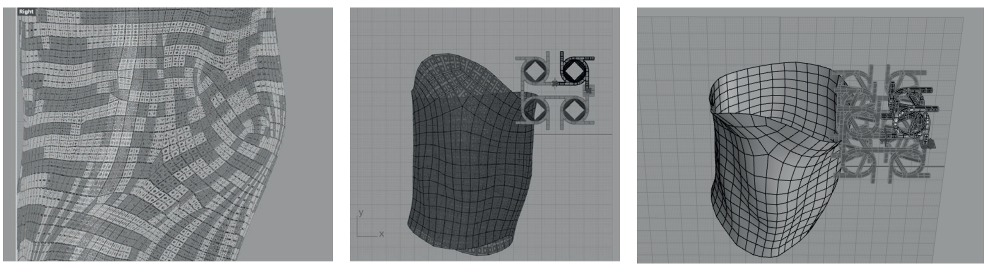

Figure 6.50 Auxetic Knee Protection.

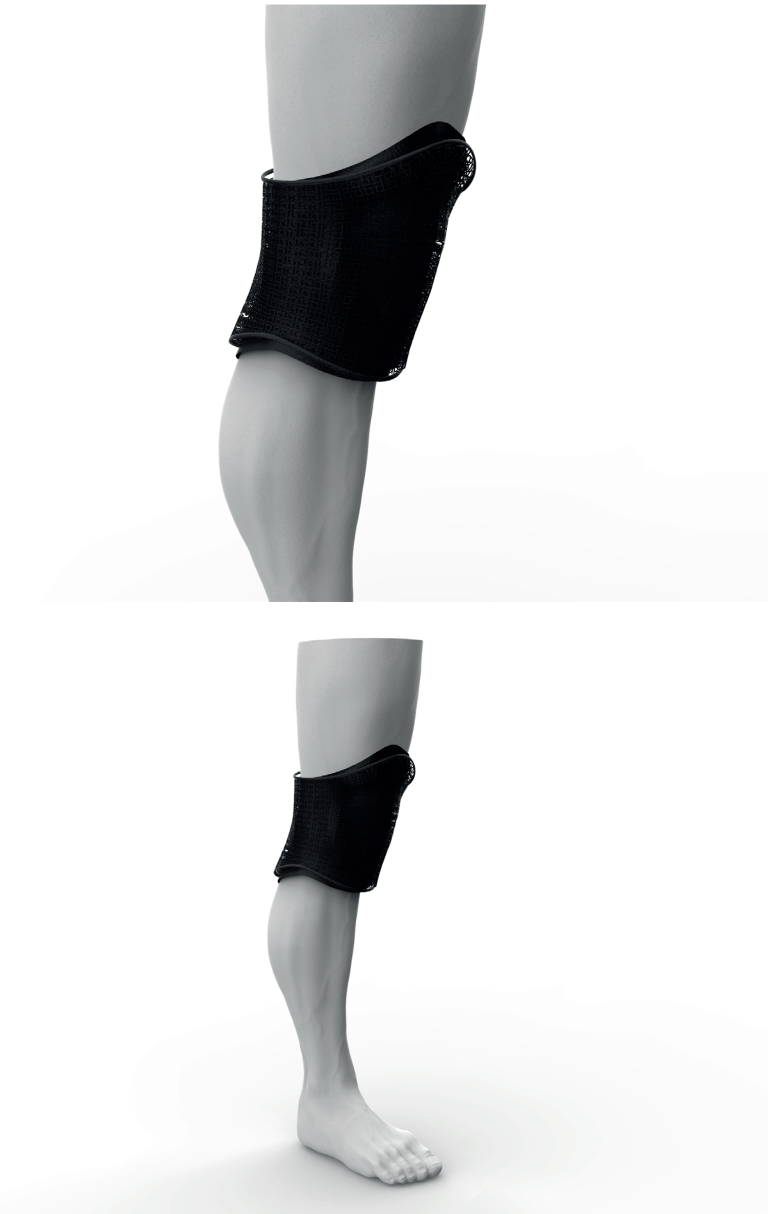

Figure 6.51 Auxetic Knee Protection.

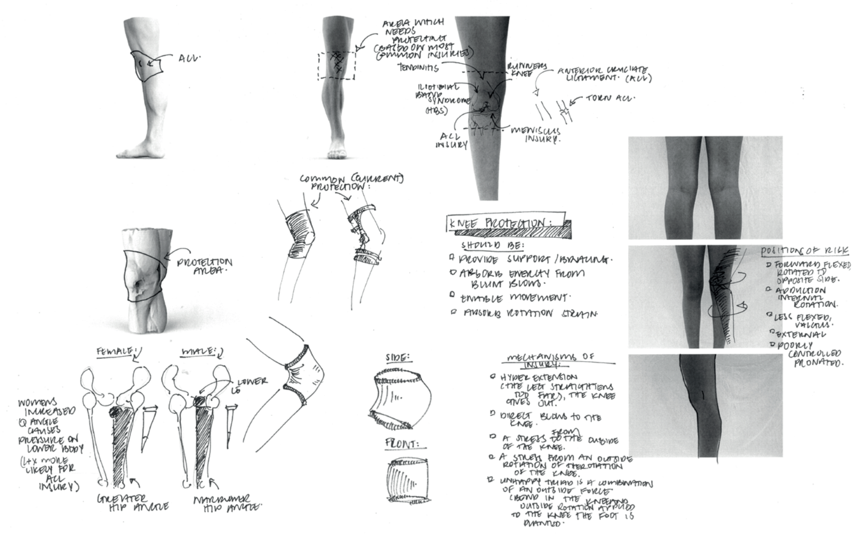

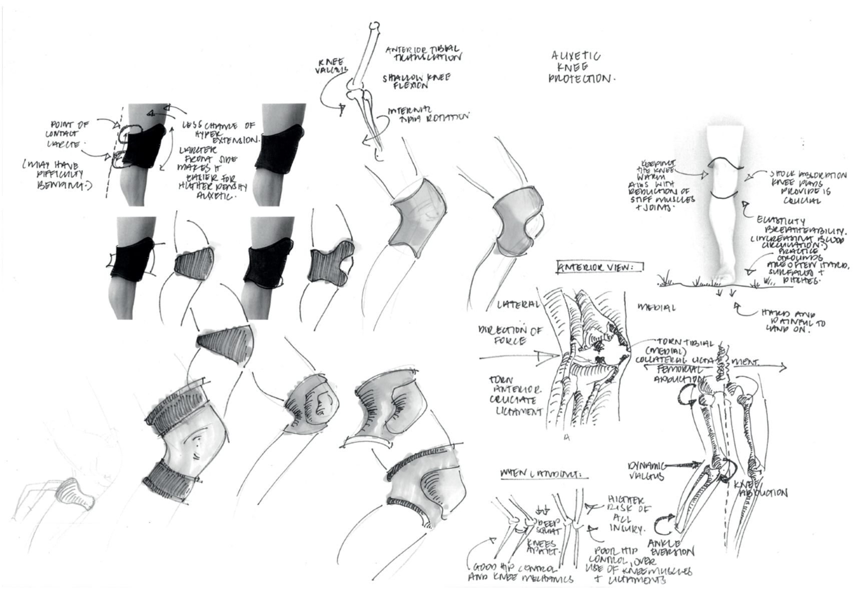

Figure 6.52 Knee Analysis.

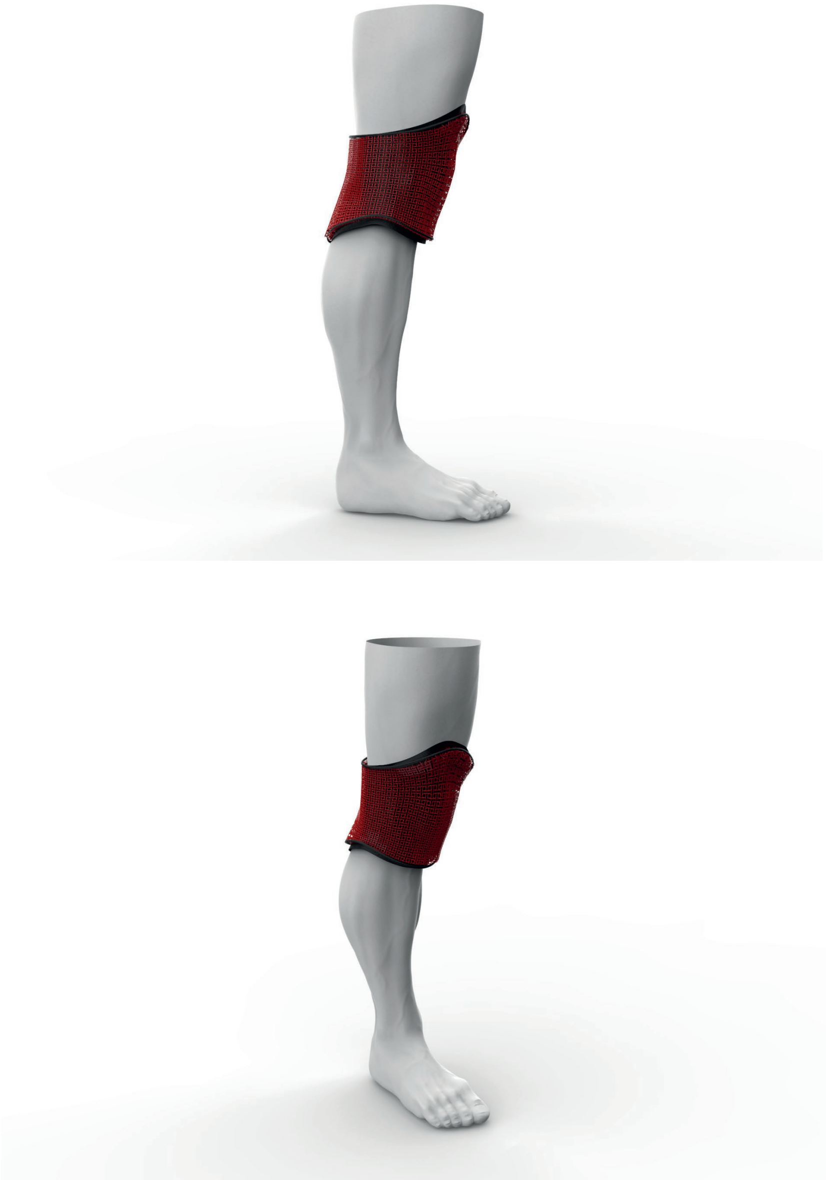

Figure 6.53 Auxetic Knee Protection.

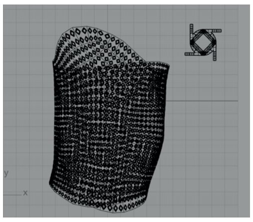

Figure 6.54 Auxetic Knee Protection development.

Mirrored

Mirrored to map Chiral structures to curvature, with correct boundaries.

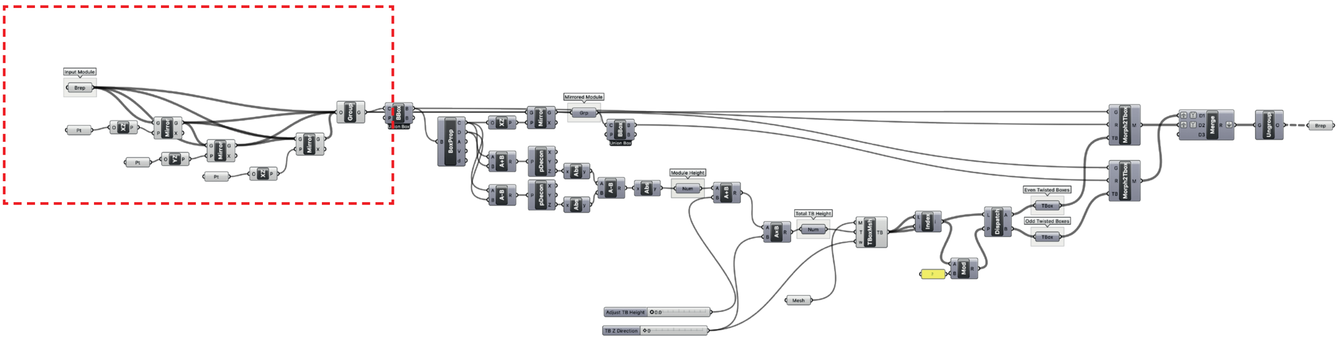

Figure 6.55 Knee Protection script.

Exporting to mesh, to reduce computing time.

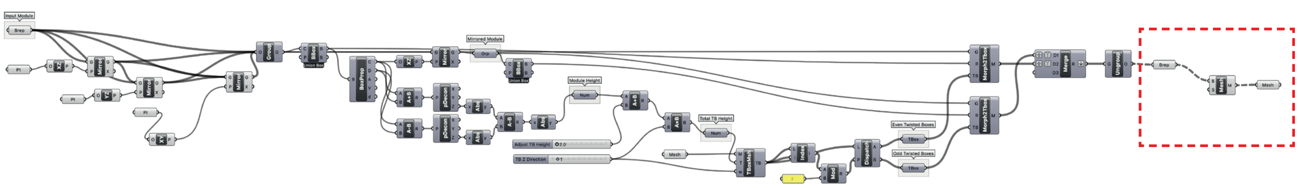

Figure 6.56 Knee Protection script development.

Figure 6.57 Knee injury prevention, (Author, 2020).

Figure 6.58 Auxetic Knee Protection.

Auxetic Knee Protection Reflections

The knee protection follows a similar form to that of already existing knee protection, however, the Auxetic nature aims to give it enhanced qualities to manage rotational strian and avoid transferral of energies to the knee likely to cause injury. The chiral lattice is tightly fitted to the knee area, giving better protection from the athlete whilst not impacting their ability to move freely due to the elastic nature of the lattice.

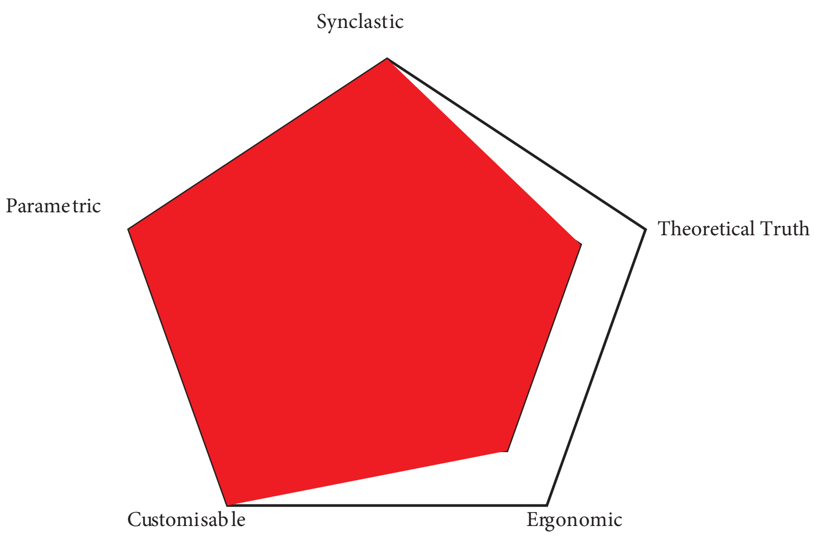

Figure 6.59 Digital Exploration Radar Plot.

[6.6] Spinal Injuries in Impact Sports

ACC dtata showed a particulary high incidence rate for injuries in Rugby.

Figure 6.60 SpinalAnalysis.

[6.6.1] The Spine and Force

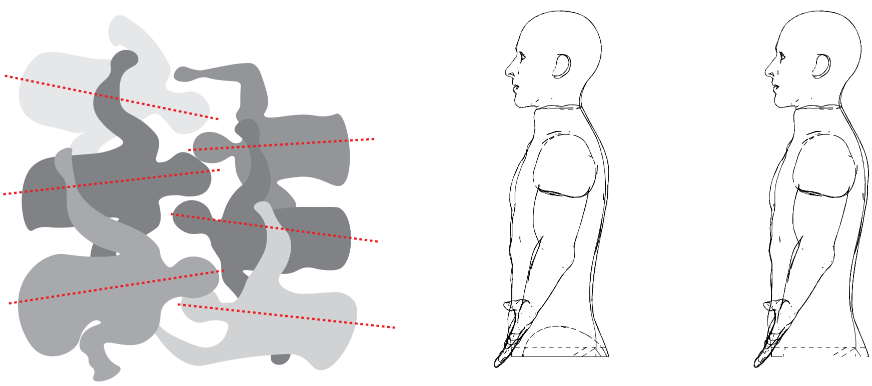

Figure 6.6.1 Spinal Injuries in Rugby.

[6.6.2] Scenarios

Spinal Injuries in Rugby

The scrum in rugby poses one of the greatest risks of spinal injury, this can be a result of continuous trauma over a period of time, or an isolated high impact incident. Players are particularly at risk if the scrum collapses, due to the sheer force applied by each side.

Junior players are especially at risk, in part due to the height and weight disparity between players of similar ages, combined with lack of skills and experience in the sport, further increasing the chances of more frequent scrum collapses (Spinal Injuries in Rugby, 2014).

Figure 6.62 Spinal Injuries in Rugby.

[6.6.3] Existing Solution Analysis

Rigid spinal protection for snow sports, and wearable, soft body armour were among few spinal protection devices which enabled sporting movement whilst being worn.

Figure 6.63 Back Protection.

[6.6.4] Auxetic Intervention: Design 4

Figure 6.64 The Spine.

The STAR 4 is known to be most Auxetic, therefore it translates to exhibit the greatest Auxetic effect, this large expansion makes it the ideal candidate for increasing surface area protection across the back, the largest area of protection application on the body.

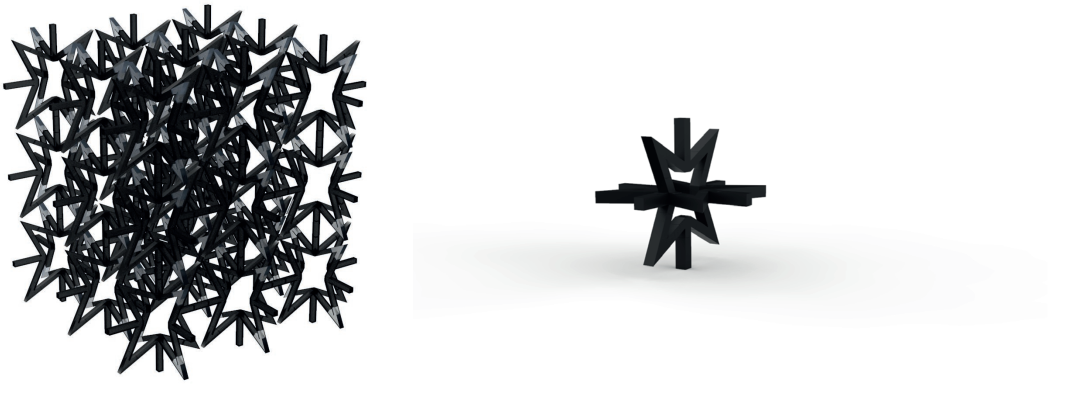

Figure 6.65. Star4.

[6.6.5] Auxetic Intervention: Design 5

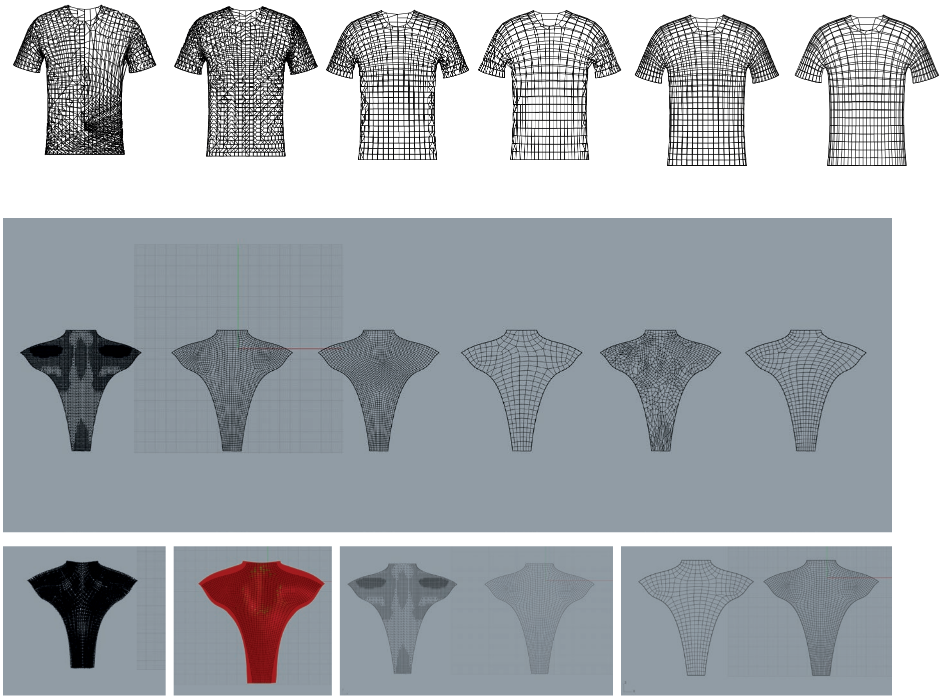

Figure 6.66 Spinal curvature.

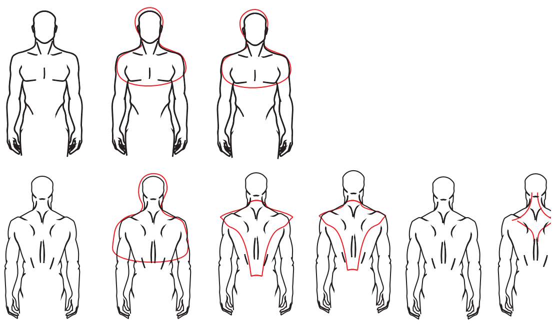

Figure 6.67 Spinal ergonomics.

Figure 6.68 Auxetic Spinal Protection.

Mirrored

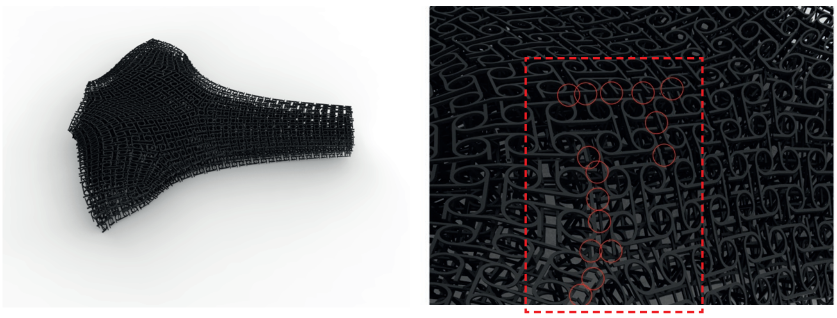

Figure 6.69 Auxetic Spinal Protection development.

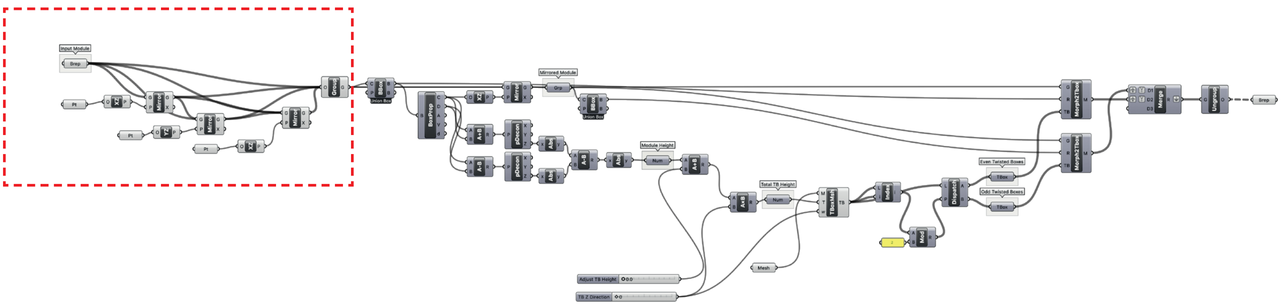

Figure 6.70 Auxetic Spinal Protection script.

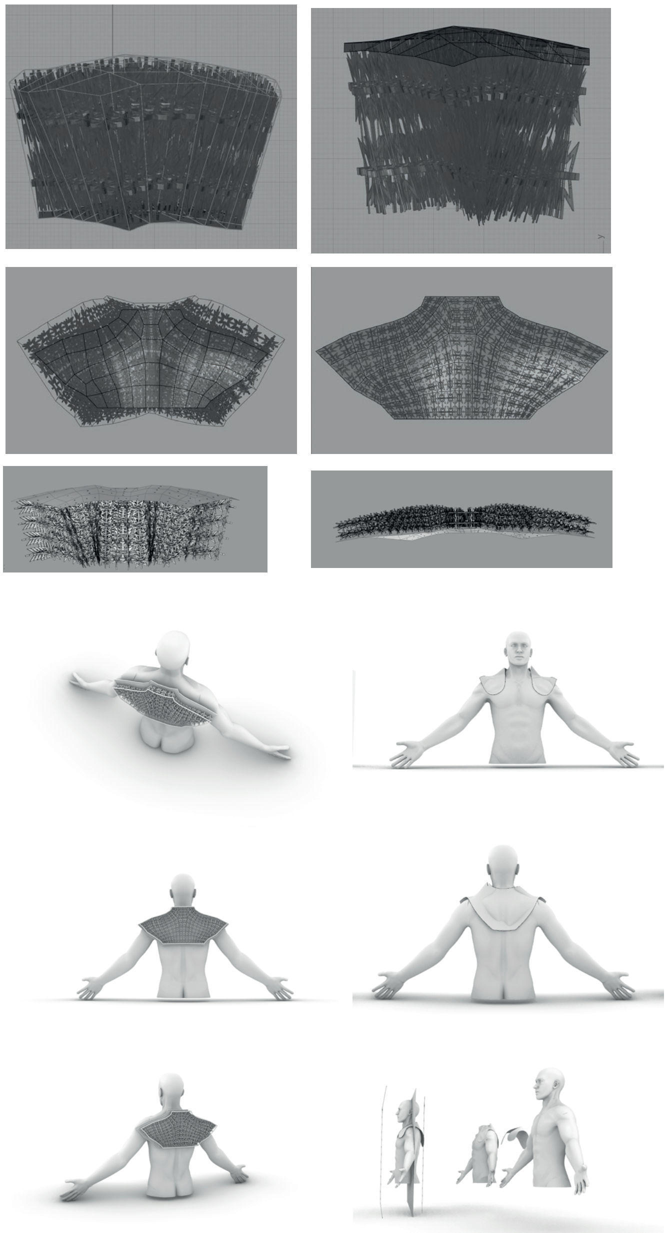

Figure 6.71 Auxetic Spinal Protection.

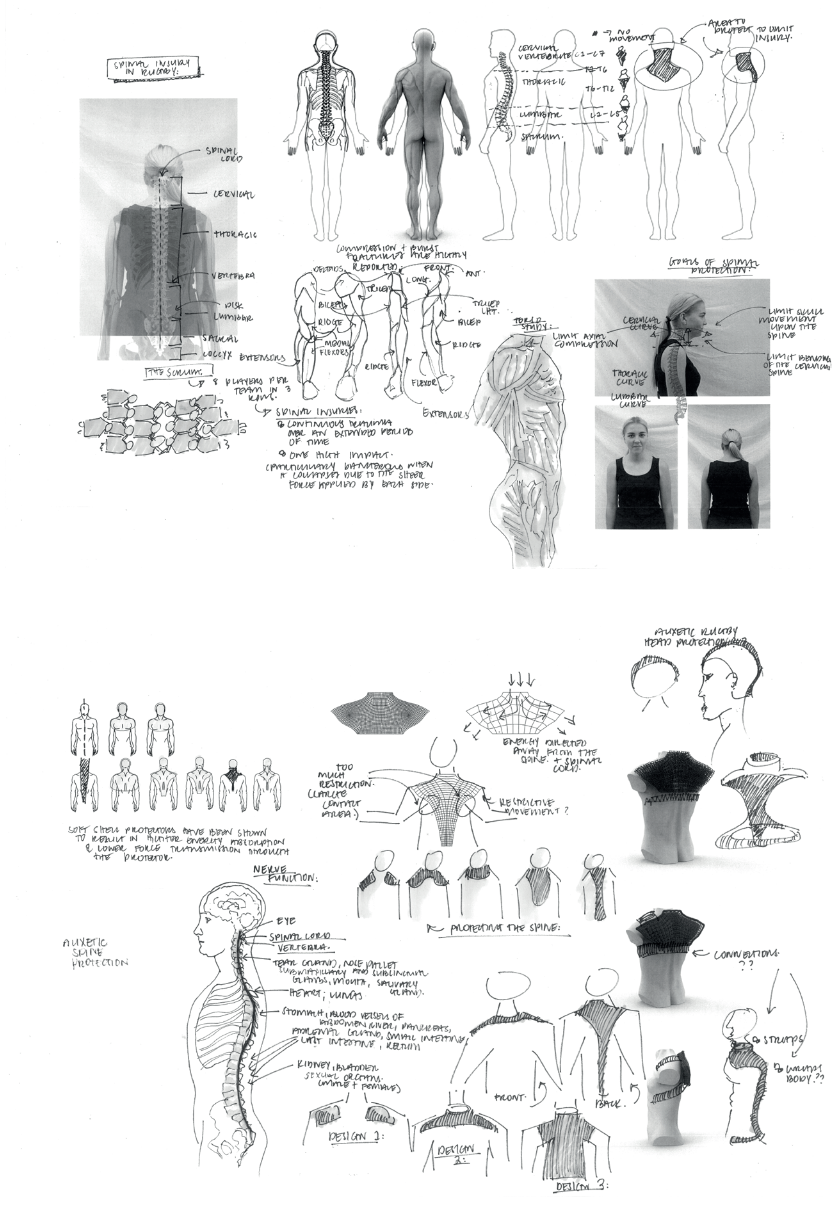

Figure 6.72 Spinal Analysis.

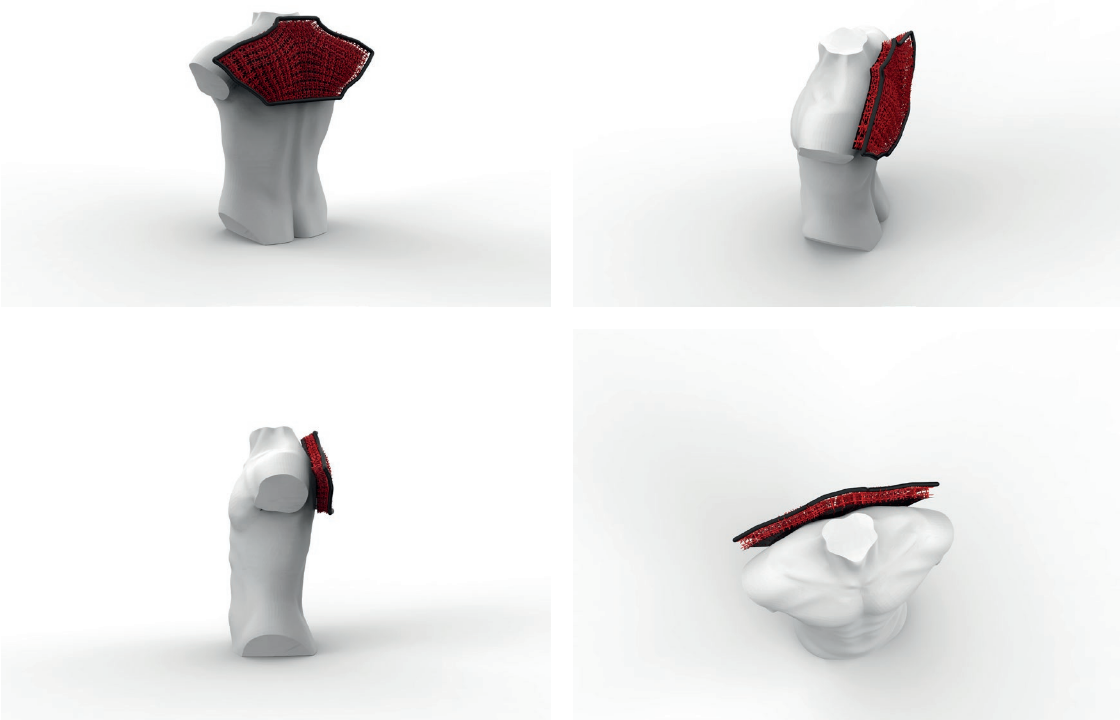

Figure 6.73 Auxetic Spinal Protection.

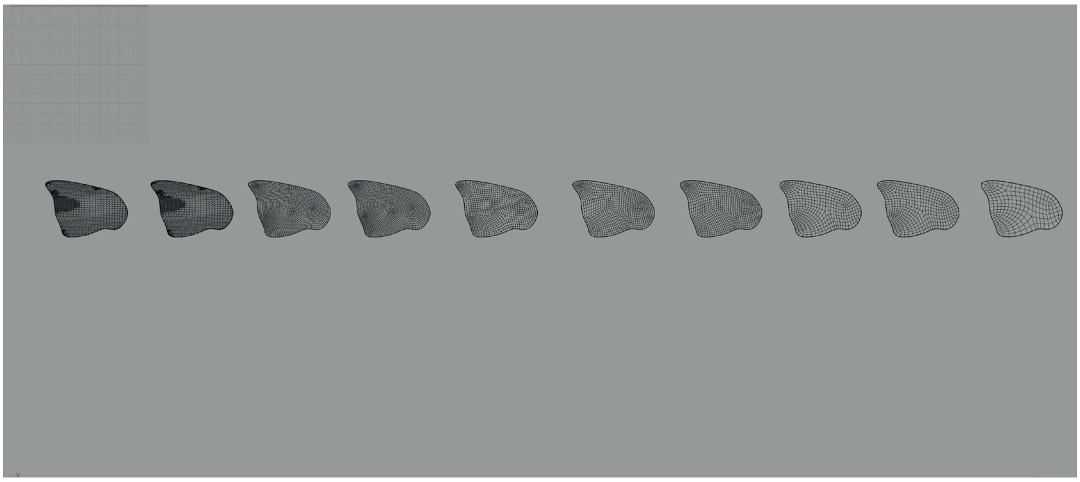

Figure 6.74 Auxetic Shoulder Protection.

Figure 6.75 Auxetic Shoulder Protection.

Figure 6.76 Auxetic Shoulder Protection.

Spinal Protection Reflections

Upon development of the spinal protection and implementation of the Star4 geomtery it became clear it was the most difficult unit to control when assigned to anatomical curvature. It was also the least likely geometry to succeed during the part one mechanical testing phase. Spinal protection with Star4 units were often bulky in mass and difficult to control with many irregularities within the lattice.

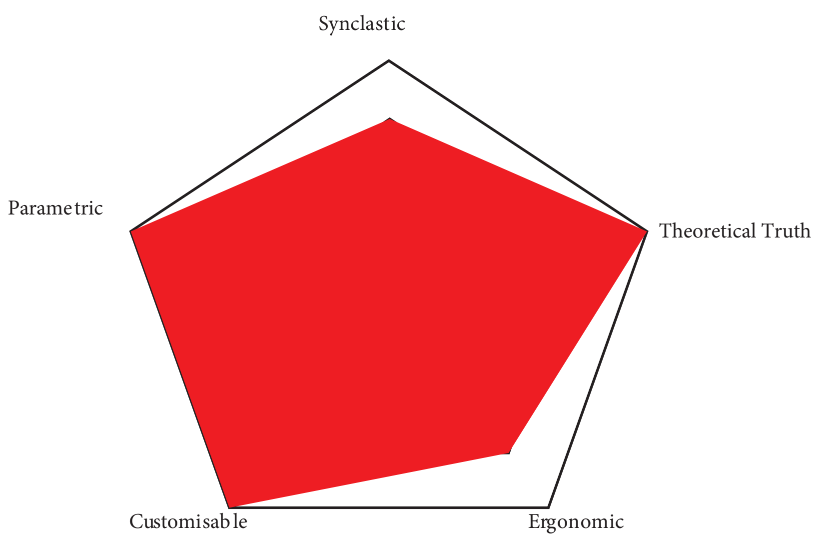

Figure 6.78 Digital Exploration Radar Plot.

Auxetic Design Studies Evaluative Matrix

Topology	**Ergonomic** Anatomical Curvature	**Synclastic** Multi Dimensional Curvature	**Auxetic Theory Based** Unresolved — Auxetic Configuration (0 1 2 3)	**Parametric Auxetic** CAD Manual Assembly — Generative Design (0 1 2 3)
Head				
Design 1	✓	✓	2	3
Design 2	✓	✓	2	3
Knee				
Design 3	✓	✓	2	3
Spine				
Design 4	✓	✓	3	2
Design 5	✓	X	3	2

Design Studies Reflection

Successfully demonstrated a good correlation between modelled intention and fabricated outcomes. This indicates the successful integration and contribution of parametric modelling in auxetic structures. It also shows that there is a viable strategy for the translation of theory and fabrication to the realisation of performative geometries.

Subsequent work has focused on the open modelling challenge of real time structural conformability and the following approach taken is to modify theory into performative structures.

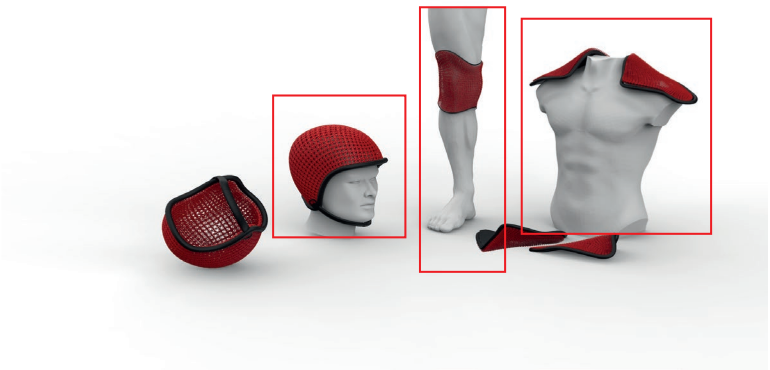

Figure 6.79 Digital design exploration, (Author, 2020).

7 APPLICATION

7.1	Context Identification	284
7.2	Anatomical Customisation	286
7.3	Digital	287
7.4	Physical	291

The application involves the connection of the entire research workflow, from identifying a feasible scenario in need of an Auxetic intervention, to scanning anatomy and extracting the curvature of the body area, determining the most suitable Auxetic geometry and applying the structure to the curvature, assigning the proven successful materials combinations and manufacturing the product, or in this circumstance a section of the design.

Figure 7.01 Auxetic Ski helmet.

7.1] Context Identification

The final phase of the research involves the integration of the research, that is the resolved workflow and discovered conclusions are tied together to produce a final scenario where the entirety of the value in the research is exhibited. The workflow is resolved to optimise the capabilities of the parametric software, the materials assigned to ensure greatest success and the geometries assigned to scenarios where the programmed characteristics are best utilised, to ultimately demonstrate the most refined example of the research process and design mastery.

High Impact Sport

Figure 7.02 Skiing.

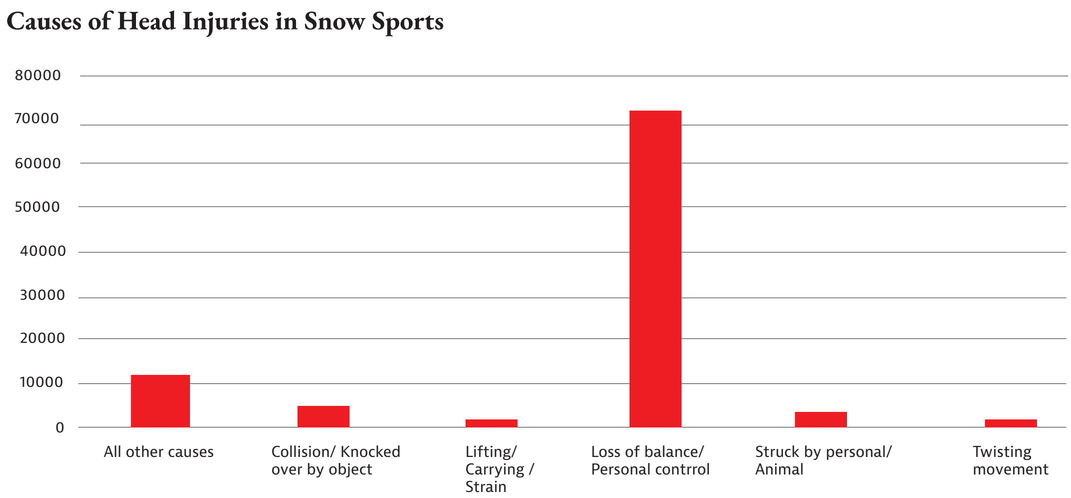

Figure 7.03 Head injuries.

Tailored Auxetic

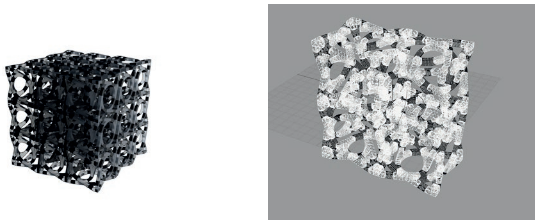

Figure 7.04 Meta-Chiral Compression Twist Auxetic.

7.2] Anatomical Customisation

Figure 7.05 3D Scanning of the body.

Figure 7.06 Scan Outputs.

7.3] Digital

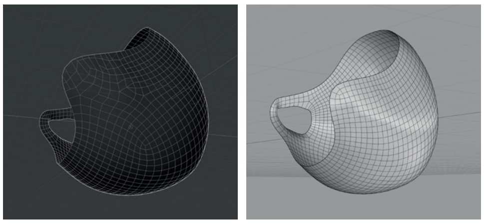

Figure 7.07 Anatomy mapping.

Quad Count

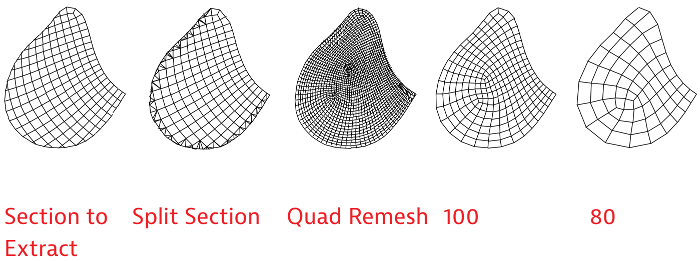

Figure 7.08 Sinclastic curvature mapping.

Parameters

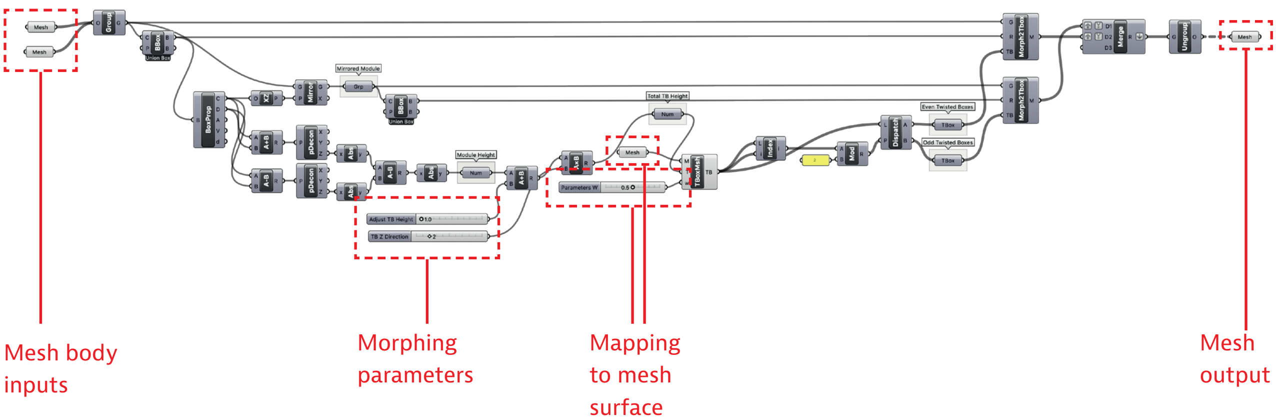

Figure 7.09 Application script.

Initial Preview

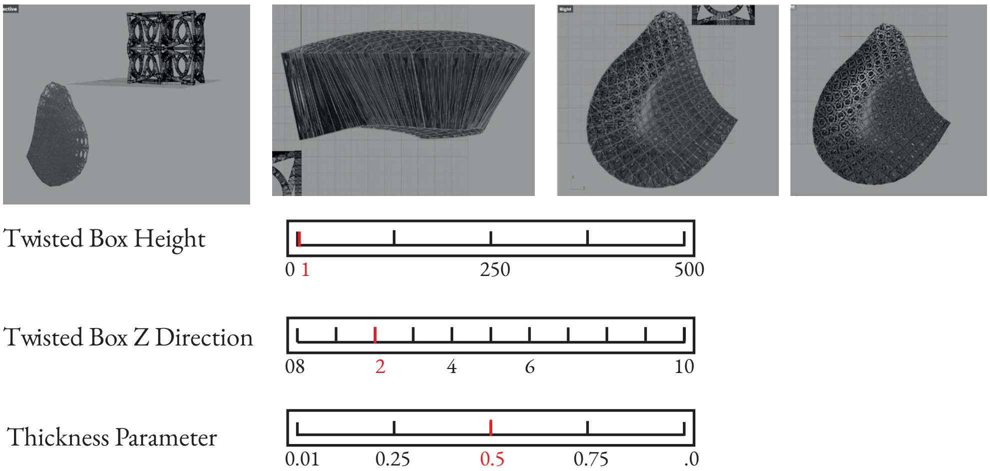

Figure 7.10 Auxetic helmet parameters.

Distorted Dimensional Twist

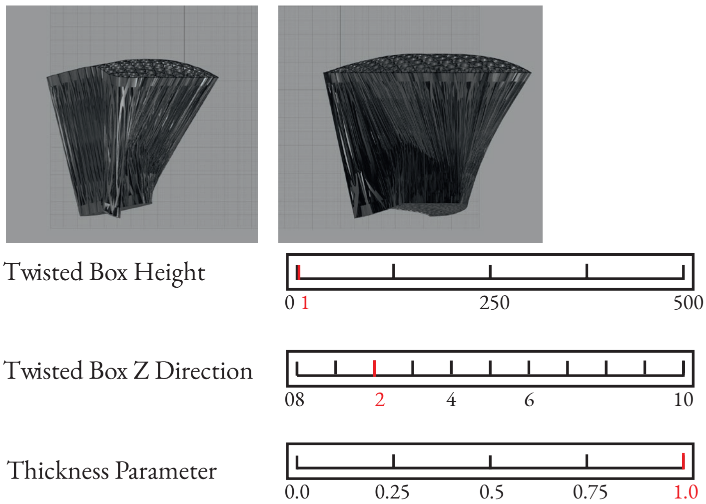

Figure 7.11 Auxetic helmet parameters.

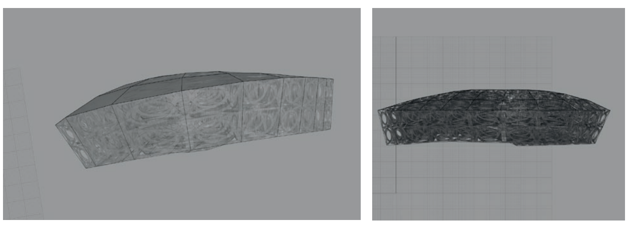

Figure 7.12 Helmet section development.

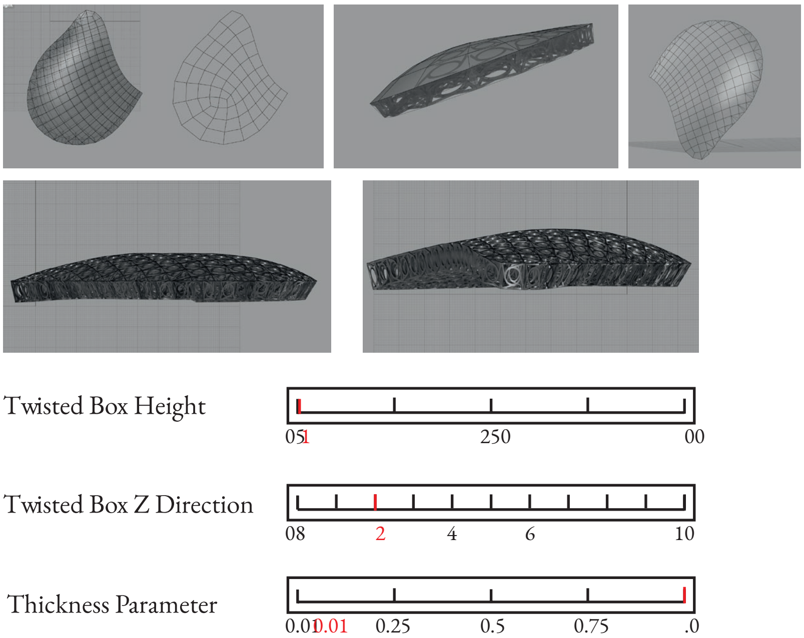

Figure 7.13 Auxetic helmet parameters.

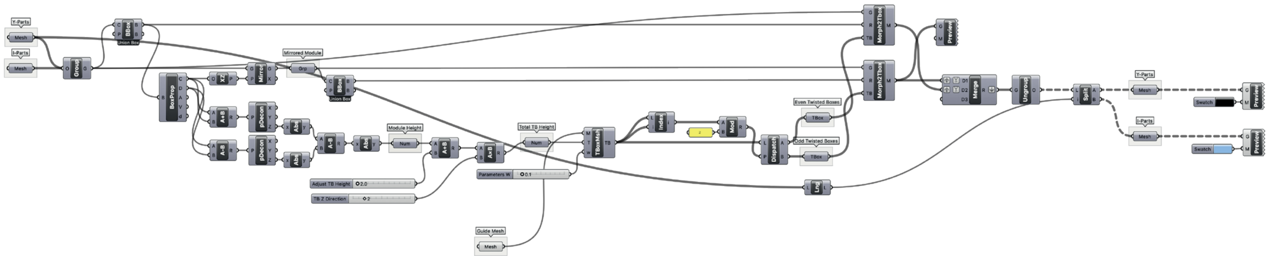

Figure 7.14 Final application script.

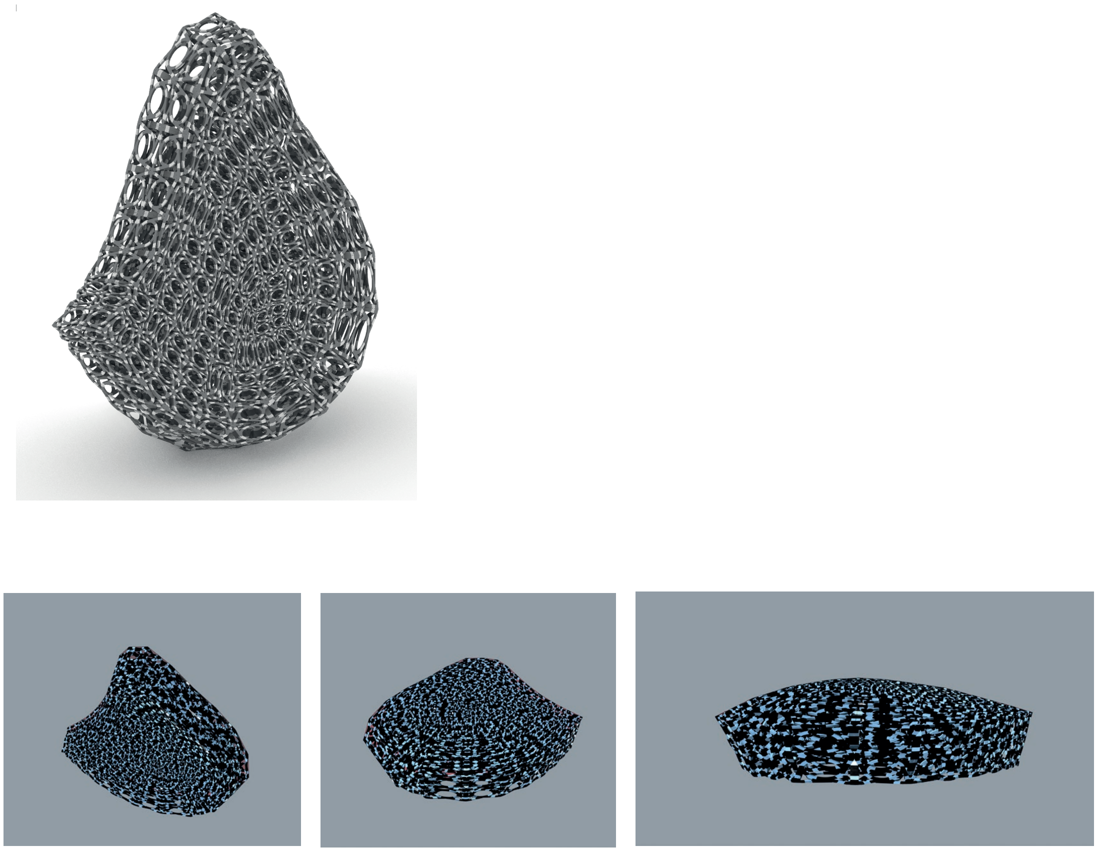

Figure 7.15 Helmet section parametric CAD model.

7.4] Physical

GrabCAD file preparation

J750 print bed

Straight off print bed, incased in support material

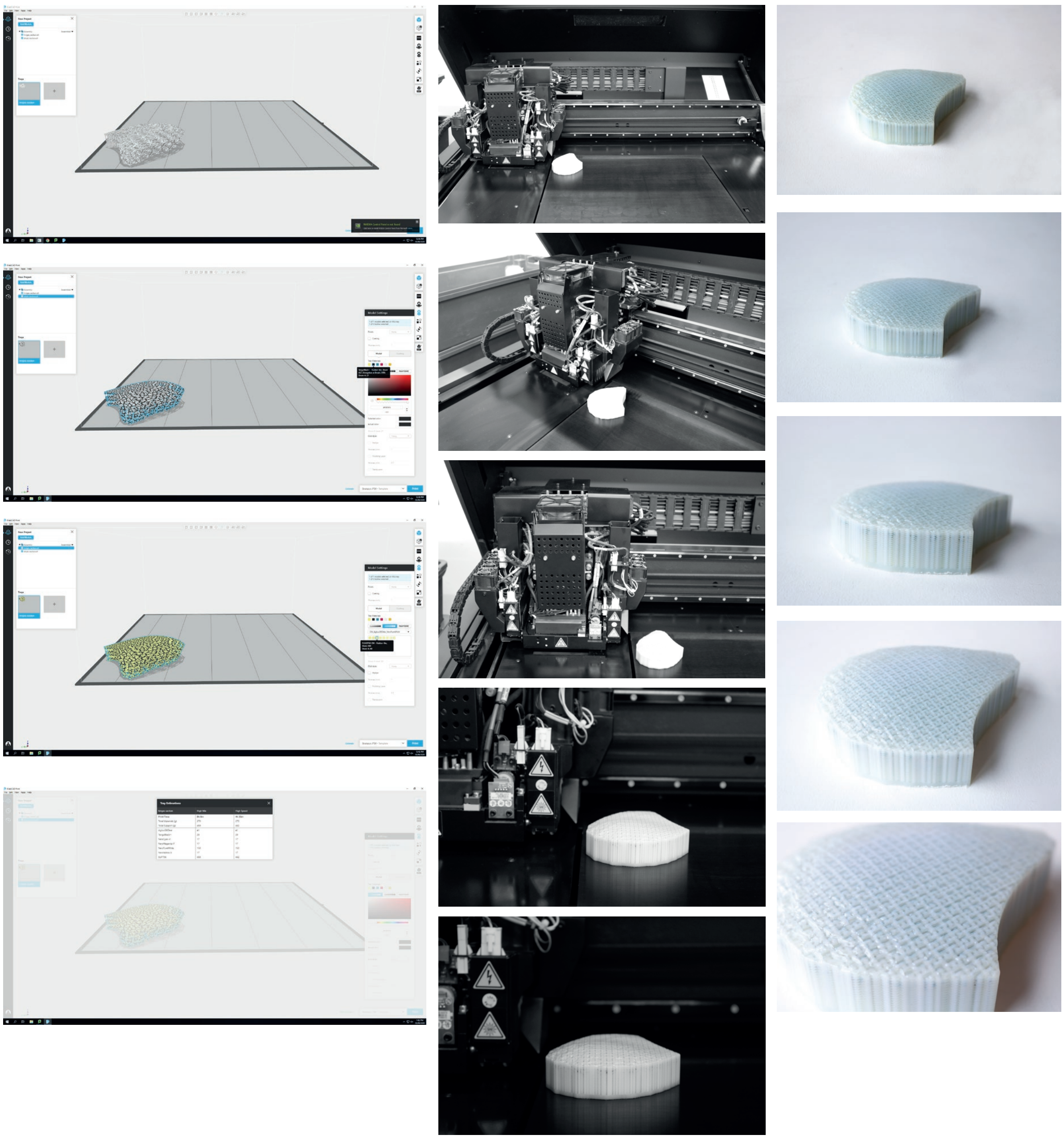

Figure 7.16 Auxetic helmet section fabrication material.

Post Processing

Manual removal of support material

Support material removal through chemical solvent bath

Figure 17 Helmet Auxetic section.

Figure 7.18 Auxetic multi-material manufactured Chiral structure.

7.5] The Digital and Physical Connection

Figure 7.19 Auxetic head protection.

Helmet Section 4D Auxetics, Printed and Parametric

Figure 7.20 Auxetic head protection.

Figure 7.21 Auxetic head protection.

7.6] Final Design Outputs

Design Customisation

Final Auxetic head protection concepts, utilising Auxetic Chiral deformation mechanism to manage damaging rotational strains endured through high impact sports.

The Auxetic structure used performed best in the mechanical testing, produced the best manufacturing results and mapped most accurately to sinclastic curvature for wearable protection.

Figure 7.22 Auxetic head protection.

Application Reflection

The section was fabricated with Shore 70 hinges, this was harder than the optimal elasticity of the hinge identified in the experimentation, however, when the model became scaled, the flexibility appeared to not scale to have the same material properties, most likely because such small quantities of material will be less robust than larger bodies of the same material. When placed in the chemical solvent bath to loosen the support material, it was observed to expand and cause structural damage whilst only actually removing a little more support than what was possible by hand. Although the geometry is open cell removal of support material is still an ongoing problem.

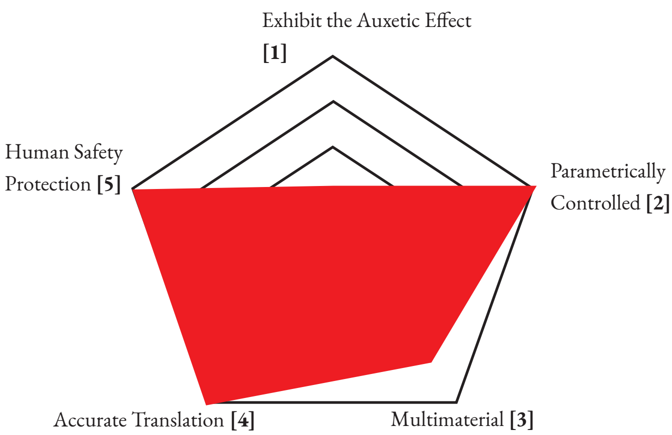

Figure 7.23 Research Radar Plot.

7.7] Expert Opinion

Speaking with Justin Hughes, from Pacific Helmets gave invaluable insight throughout the research into the types of considerations and practicalities associated with introducing new technology into industry.

Through his role in helmet design development, Justin described the inflexibility of retrospective part modification after tooling involved with Injection Moulding.

Here, he mentioned the increasing advantage of AM to customise helmets to fit individuals, or rather a range of individual skull shapes and sizes which only needed small alterations to effectively fit the user would enable them to minimise analogue fitting methods.

Also discussed was the advantage of using an open cell shock abortion system in helmets to reduce the weight, but also importantly enabling airflow, as heat stroke is a real concern amongst firefighters.

He offered Pacific Helmets capacity to do in-house deceleration and impact force testing, a key step in future research, to understand materials and the designs responses to high impact strains, ultimately, he was encouraged by the research and its future in helmet protection.

8 DISCUSSION & CONCLUSION

8.1 Discussion 301

8.2 Conclusion 309

[8.1] Discussion

Through the nature of the research, both the process and the outputs were extremely exploratory. The research was as much about developing and refining a workflow, through creating an infrastructure in which to comprehend and breakdown Auxetic theory, interpret it in terms of the design process, translate the parameters and form digital models to be AM with a range of material variables to test for the combinations which most closely enable the geometries to exhibit the desired Auxetic effect. This process became more refined as the various steps were made more efficient and errors were eliminated to make a streamline translation and iterative process of physical and digital realisation of Auxetic Structures.

The primary research was broken down into these two parts, both required the translation of Auxetic Structure theory into different design parameters for physical and digital realisation. The negotiation of these design parameters and the relationship of their intersection ultimately shaped the transition from theory to digital to physical and back, both enabling the developement of the research and demonstrating the paramount role design plays and will continue to play in the realisation of Auxetic Structures.

So too did design enable the development of the Auxetic application. Through injury analysis, instance identification, anatomical exploration and later curvature mapping the geometries were implemented and shaped to aim to meet the needs and protect future athletes. And although the outputs remain speculative in nature, this research sought to continue to pave the way in the development of synthetic materials for personal sporting protection through the design workflow which will continue to evolve in future work done in this field.

Part one of the primary research began with identifying relevant precedents and an extensive literature review to define a clear starting point, it was found there were very limited examples of Auxetic Structures manufactured with multi-material properties and even fewer were 3D structures. The fabrication of multi-material printed structures revealed deficiencies in the strength of the materials, hopefully this will improve as the quality of AM materials continues to develop. Regardless, what emerged as the greatest opportunity for situating the research was the power of digital design in regard to modelling Auxetic Structures and simulating their mapping to complex, customised curvature through cutting edge and experimental parametric software. These generative designs demonstrated the computers capability to assign microscale geometries to anatomical curvature and forced the exploration of the relationship between defined, mathematical unit models set by the designer with the computers ability to utilise parametric software to generate highly complex geometrical materials, which in the past, have been too difficult to achieve. The established workflow developed this relationship to exploit both the capabilities of the computer, and the machine whilst celebrating the creativity, and harnessing the skills of the designer.

The Research Question

The problem-solving research question asked at the beginning of the research; How can we optimise multi-material 4D printing to dictate dynamic performance in Biaxial Auxetic Structures, for enhanced human protection in safety applications? ultimately guided the analytical path of the research. Initially, it was predicted parametric design will be paramount to the ability to manufacture structures, in part because of the customisable nature of the geometries, but also its ability to enable variations of material assignment.

The aims and objectives met through the design process sought to fulfil the outlined criteria. The research was successful in meeting the criteria, it produced models which exhibited the Auxetic effect with biaxial deformation mechanisms, the geometries were parametrically controlled, manufactured with a range of material elasticities and digitally portrayed as enhanced, impact, protection through speculative outputs. Ultimately, the research addressed the criteria through the outputs and outcomes guided by a systematic design process.

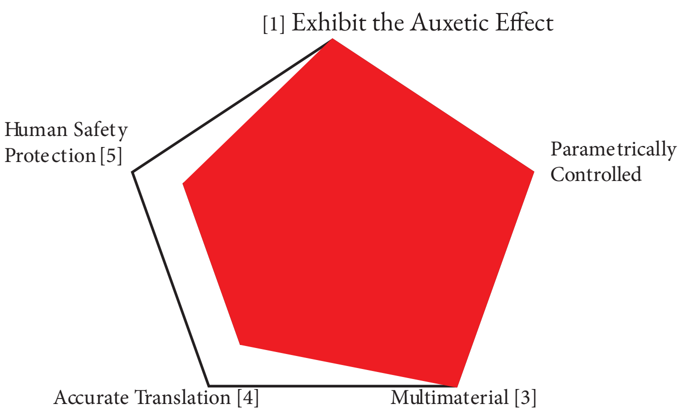

Figure 8.01 Radar Plot.

Application

The contextualised outputs were achieved through two key enquiries. The first included the analysis of sports injury data from ACC which enabled the identification of high impact instances causing significantly more injuries when compared to other sports, these were then used as case study scenarios from which to base the outputs off. Whilst the expert opinion from Pacific Helmets formed part of the evaluation of these designs, with a market application focus.

The final outputs vary in media, the application chapter sought to accurately combine the knowledge gained, with the skills learnt through experimentation and exploration and although the application case study revealed the limitations most clearly, it brought Auxetic Structures into an interpretable realm for potential users.

It can be hoped that this research excites designers and athletes with the opportunities Auxetics possess, triggered through the contextualised renders which are everyday scenario based. It also encourages the development of Auxetic Structures by engineers and scientists, with the hopes of implementation for the better good and safety of athletes in the not so distant future.

However, the final outputs of this research are not resolved replacements to currently existing sports protection, rather they consider the possibilities of Auxetic Structures as enhancement componentry for currently existing protection to further protect athletes across a range of sporting scenarios.

Synthesising Disciplinary Trends

This is one of the very first instances where Auxetic Structures have been multi-material manufactured and through this research many parameters have been achieved and refined. Through understanding materials and fabrication techniques, developed understanding of material qualities, limitations have been more closely understood, setting the path for future research into the fabrication of Auxetic geometries as performative prototypes for strain testing. But this research also expands the capabilities for realisation of Auxetic Structures through the integration of parametric software to generate complex lattices. It removes the need for manual configuration and offers opportunities for assigning detailed unit geometries to large synclastic forms.

The mechanical exploration grew from the precedent of Miller & Wilson, (2016) further exploring the benefits of multi-material Auxetics and expanding the experimentation to a 3D realm. The digital explorations used the work of (Konaković- Luković et al., 2018) as a starting point for further developing wearable Auxetics. Precedents such as (Franz, 2018), although design for head protection were very speculative in nature and lacked the material leverage to mould to the head in an ergonomic manner. Although this research didn't have the time to manufacture full scale protection, it demonstrates the capabilities to model complex synclastic geometry and manufacture Auxetic units cells which in further research can be manufactured as lattices for mechanical testing.

Ultimately, it sought to connect the different domains exploring Auxetic Structures, that is digital design, material science, engineering and manufacturing and draw connections, forming relationships between the different roles within the process of realising Auxetics in the future, streamlining their development.

Limitations

Limitations can be categorised as technical, which are technology based or research centred which are circumstantial to this research.

Throughout this research, several limitations became apparent. Such limitations are described below with their consequences recognised.

Technical Limitations
Many limitations in regard to the J750 became apparent, in particular scale. Models were often printed at a reasonably small scale for economic reasons. However, as the research progressed, it was apparent printing small scale for future micoscale application, was necessary to get an accurate reflection of the issues associcated with the structures at the closest to true scale. Models printed as smaller units consistently lacked structural integrity, even those printed with high end Shore hardness's struggled to remain in tack, hold their form and perform in an Auxetic manner.

There is space between the theoretical capabilities of manufacturing materials and the observed strength and capability of the materials in a tangible application. When scaled to small geometries the material qualities and freedom of elasticities through the Shore hardness's were lost. This research has proven the need for further development of multi-material resins in order to ensure their capability of withstanding anticipated mechanical strains in applications.

As the complexity of the structures increased and the scale was decreased, highly complex geometries were being mapped to curvature, and so the amount of computing power required also increased.

When structures were modelled parametrically in part one of the primary research, the hinge bodies were separate to those of the struts. This was to enable multi-material fabrication and the ability to assign different materials to particular bodies. However, in section two, when the research was digitally focused, to develop complex geometrical configurations, the need for separate hinge and strut bodies was removed as structures were experimental in nature exploring mapping and morphing. To increase processing speed the units were made into one joined body. The disadvantage of this was, when fabrication comes around, structures will lack the ability to have different materials assigned to the parts. In future, more development of the system will be required to make mapping efficient and capable of processing numerous unit parts within the unit and lattice.

Current Grasshopper uses single threaded processing, its disadvantages became apparent as the complexities of the structures increased, making the iterative process slow. In the future developing a parallel computing system which promoted multithread processing, would enable the system to fully utilise its capacity.

Research Limitations
Unfortunately, for this research Covid19 also slowed the ability to have materials manufactured on the J750, through lack of accessibility to the campus. Initially it was hoped application strain testing would take place, however, due to reduced campus access and remote work, these tests take couldn't place at Pacific Helmets.

Additionally, although remote computing took place, it slowed the digital workflow considerably and disrupted the streamline transition between stages in the design process, as well as causing significant restrictions to computer processing power.

Critique of the Methodology

The nature of such a new field means there is an incredible amount of unexplored terrain, making it easy to stray from the foundation enquiry. However, ensuring the workflow involved ideation, translation development and evaluation, specific to multi-material manufacturing and parametric experimentation, guaranteed there was an analytical system established and adhered to, ultimately ensuring the research followed a systematic process.

The methodologies used included, Research for Design, Research through Design, as well as, Scientific Research. As anticipated, it was necessary to develop a methodology specific to this investigation, based on the foundation's workflows. The workflow developed here was a hybrid methodology, it combined the design steps from several previous studies to develop a system which best utilised the technology and skills available to this research. The methodology was key to ensuring a systematic enquiry, which had a consistent focus on the research question, as well as purpose to fulfil the design criteria.

Perspectives on the Future

It is still sometime before Auxetic Structures are widely implemented into popular protection Applications. This research is a necessary step in bringing Auxetics closer to market production for enhanced safety in high impact sports.

This research has established a successful workflow for translating and applying Auxetics and although performative manufacturing took place, it requires the development of Polyjet materials with greater toughness, in order to manufacture strain capable protection.

Although, this research clearly does delimit the ability to manufacture multi-material Auxetic Structures on a single print tray, they were often found to be fragile or lack longevity. In the future as materials for AM become more suitable, the methodological workflow executed here can be full utilised as an effective tool in the application of Auxetic Structures. When this does occur, the relationship the Auxetic material has with other components within the protection can be fully explored. It is speculated here that Auxetic Structures could be an enhancing addition of componentry to already existing designs, however, the role they would play needs to be explored more widely.

A range of techniques were used to map geometries to synclastic curvature, although the unit geometries were monitored so as to retain depth and connection, some warping during the morphing process did take place. Perhaps running the Grasshopper outputs through Finite Element Analysis would enable observations in regard to the effects of the morphing taking place, to allow a better understanding of any Auxetic implications. Additionally, varying the state in which the structures are printed in, may enhance or better control this deformation and reduce unwanted skewing of geometry to retain the Auxetic effect.

Design Recommendations

This research does not engage with every aspect of the design process. For example, parametric design is well explored, however, strain testing is yet to be experimented with. What makes this research valuable is the discovery of a workflow which enables the connection of the various methods and design actions in the process, to demonstrate the steps required to realise structures from theory to

[8.2] Conclusion

It is hoped that this work will stimulate continued research in material science, engineering and design to further develop Auxetic structures and analyse the questions and recommendations left here in greater detail. In the future the development of the workflow established here will continue to strengthen the virtuous feedback loop between theory and reality as experimental and computational design of Auxetic Structures develop.

However, the fabricated outputs here are proof of concept prototypes which aid in illustrating the process of establishing a digital parametric workflow, the realisation of multi-material printed structures demonstrating physical Auxetic movement and through design, illustrating potential applications in a range of domains.

ACC. (2019). *Injury-free sport and recreation*. ACC. https://www.acc.co.nz/preventing-injury/sport-recreation/

Ago. (2019). *Physics—Classical Mechanics—Volumetric Stress and Strain*. Steemit. https://steemit.com/physics/@drifter1/physics-classical-mechanics-volumetric-stress-and-strain

Allen, T., Duncan, O., Foster, L., Senior, T., Zampieri, D., Edeh, V., & Alderson, A. (2017). Auxetic Foam for Snow-Sport Safety Devices. In I. S. Scher, R. M. Greenwald, & N. Petrone (Eds.), *Snow Sports Trauma and Safety* (pp. 145–159). Springer International Publishing.

Barner, B. E. S. (2015). Mechanical Properties of Additive Manufactured Honeycomb Structures. *2015*, 110.

Benyus, J. M. (1997). *Biomimicry: Innovation inspired by nature* (1st ed..). Morrow.

Bezazi, A., & Scarpa, F. (2007). Mechanical behaviour of conventional and negative Poisson's ratio thermoplastic polyurethane foams under compressive cyclic loading. *International Journal of Fatigue*, *5*(29), 922–930. https://doi.org/10.1016/j.ijfatigue.2006.07.015

Bhate, D. (2016). *The Additive Manufacturing Cellular Solids Research Landscape – PADT, Inc. – The Blog*. http://www.padtinc.com/blog/additive-manufacturing-cellular-structures-research/

Bickel, B., Bächer, M., Otaduy, M., Lee, H., Pfister, H., Gross, M., & Matusik, W. (2010). Design and fabrication of materials with desired deformation behavior. *ACM Transactions on Graphics*, *29*, 1. https://doi.org/10.1145/1833351.1778800

Bückmann, T., Stenger, N., Kadic, M., Kaschke, J., Frölich, A., Kennerknecht, T., Eberl, C., Thiel, M., & Wegener, M. (2012). Tailored 3D Mechanical Metamaterials Made by Dip-in Direct-Laser-Writing Optical Lithography. *Advanced Materials*, *24*(20), 2710–2714. https://doi.org/10.1002/adma.201200584

Carlos, J. (2012). *Comparative study of auxetic geometries by means of computer-aided design and engineering*.

Carneiro, V. H., Puga, H., & Meireles, J. (2016). Analysis of the geometrical dependence of auxetic behavior in reentrant structures by finite elements. *Acta Mechanica Sinica*, *32*(2), 295–300. https://doi.org/10.1007/s10409-015-0534-2

Chen, D., & Zheng, X. (2018). Multi-material Additive Manufacturing of Metamaterials with Giant, Tailorable Negative Poisson ' s Ratios. *Scientific Reports*, *8*(1), 1–8. https://doi.org/10.1038/s41598-018-26980-7

Chen, Y., & Fu, M.-H. (2017). A novel three-dimensional auxetic lattice meta-material with enhanced stiffness. *Smart Materials and Structures*, *26*(10), 105029. https://doi.org/10.1088/1361-665X/aa819e

Cho, H., Seo, D., & Kim, D.-N. (2019). Mechanics of Auxetic Materials. In S. Schmauder, C.-S. Chen, K. K. Chawla, N. Chawla, W. Chen, & Y. Kagawa (Eds.), *Handbook of Mechanics of Materials* (pp. 733–757). Springer Singapore. https://doi.org/10.1007/978-981-10-6884-3_25

Creswell, J. D., & Creswell, J. W. (2018). *Research Design: Qualitative, Quantitative, and Mixed Methods Approaches* (Fifth Edition). Sage.

Cross, N. (2001). Designerly Ways of Knowing: Design Discipline versus Design Science. *Design Issues*, *17*(3), 49–55. JSTOR.

Cross, T. M., Hoffer, K. W., Jones, D. P., Kirschner, P. B., Langvin, E., & Meschter, J. C. (2016). *Auxetic structures and footwear with soles having auxetic structures* (United States Patent No. US9402439B2). https://patents.google.com/patent/US9402439B2/en

Cucakovic, A., Jovic, B., & Komnenov, M. (2016). Biomimetic Geometry Approach to Generative Design. *Periodica Polytechnica. Architecture; Budapest*, *47*(2), 70–74. http://dx.doi.org.helicon.vuw.ac.nz/10.3311/PPar.10082

Duncan, O., Foster, L., Senior, T., Alderson, A., & Allen, T. (2016). Quasi-static characterisation and impact testing of auxetic foam for sports safety applications. *Smart Materials and Structures*, *25*(5), 054014. https://doi.org/10.1088/0964-1726/25/5/054014

Duncan, O., Shepherd, T., Moroney, C., Foster, L., Venkatraman, P. D., Winwood, K., Allen, T., & Alderson, A. (2018). Review of Auxetic Materials for Sports Applications: Expanding Options in Comfort and Protection. *Applied Sciences*, *8*(6), 941. https://doi.org/10.3390/app8060941

Ebrahimi, H., Mousanezhad, D., Nayeb-Hashemi, H., Norato, J., & Vaziri, A. (2018). 3D cellular metamaterials with planar anti-chiral topology. *Materials & Design*, *145*, 226–231. https://doi.org/10.1016/j.matdes.2018.02.052

Eilouti, B. (2019). *Precedent-Based Design as a Case-Driven Problem-Solving Technique in Engineering Design*.

Frankel, L., & Racine, M. (2010). The Complex Field of Research: For Design, through Design, and about Design. *The International Conference of the Design Research Society*, 12.

Frenzel, T., Kadic, M., & Wegener, M. (2017). Three-dimensional mechanical metamaterials with a twist. *Science*, *358*(6366), 1072–1074. https://doi.org/10.1126/science.aao4640

Grima, J. N., Gatt, R., Bray, T. G. C., Alderson, A., & Evans, K. E. (2005). Empirical modelling using dummy atoms (EMUDA): An alternative approach for studying "auxetic" structures. *Molecular Simulation*, *31*(13), 915–924. https://doi.org/10.1080/08927020500401121

Hale, L., Linley, E., & Kalaskar, D. (2020). A digital workflow for design and fabrication of bespoke orthoses using 3D scanning and 3D printing, a patient-based case study. *Scientific Reports*, *10*. https://doi.org/10.1038/s41598-020-63937-1

Hannington, B., & Martin, B. (2012). *Universal Methods of Design* (1st edition). Rockport Publishers.

Hu, H., Zhang, M., & Liu, Y. (2015). *Auxetic Textiles*. 19–56.

Janssen, P., Chen, K., & Basol, C. (2011). Iterative virtual prototyping: Performance based design exploration. *Proceedings of the ECAADe Conference*, 253–260.

Javadi, A., Faramarzi, A., & Farmani, R. (2011). Design and optimization of microstructure of auxetic materials. *Engineering Computations*, *29*, 260–276. https://doi.org/10.1108/02644401211212398

Kim, J., Shin, D., Yoo, D.-S., & Kim, K. (2017). Regularly configured structures with polygonal prisms for three-dimensional auxetic behaviour. *Proceedings. Mathematical, Physical, and Engineering Sciences*, *473*(2202). https://doi.org/10.1098/rspa.2016.0926

Kolken, & Zadpoor. (2017). Auxetic mechanical metamaterials. *RSC Advances*, *7*(9), 5111–5129. https://doi.org/10.1039/C6RA27333E

Konaković, M., Crane, K., Deng, B., Bouaziz, S., Piker, D., & Pauly, M. (2016). Beyond developable: Computational design and fabrication with auxetic materials. *ACM Transactions on Graphics*, *35*(4), 1–11. https://doi.org/10.1145/2897824.2925944

Konaković-Luković, PanettaJulian, CraneKeenan, & PaulyMark. (2018). Rapid deployment of curved surfaces via programmable auxetics. *ACM Transactions on Graphics (TOG)*. https://dl.acm.org/doi/abs/10.1145/3197517.3201373

Lakes, R. (1987). Foam Structures with a Negative Poisson's Ratio. *Science (New York, N.Y.)*, *235*(4792), 1038–1040. https://doi.org/10.1126/science.235.4792.1038

Laurel, B. (Ed.). (2003). *Design research: Methods and perspectives*. MIT Press.

Li, T., Chen, Y., Hu, X., Li, Y., & Wang, L. (2018). Exploiting negative Poisson's ratio to design 3D-printed composites with enhanced mechanical properties. *Materials & Design*, *142*, 247–258. https://doi.org/10.1016/j.matdes.2018.01.034

Li, T., Hu, X., Chen, Y., & Wang, L. (2017). Harnessing out-of-plane deformation to design 3D architected lattice metamaterials with tunable Poisson's ratio. *Scientific Reports*, *7*(1), 1–10. https://doi.org/10.1038/s41598-017-09218-w

Lim, T.-C. (2015). Micromechanical Models for Auxetic Materials. In T.-C. Lim (Ed.), *Auxetic Materials and Structures* (pp. 45–105). Springer. https://doi.org/10.1007/978-981-287-275-3_2

Lu, Z.-X., Li, X., Yang, Z.-Y., & Xie, F. (2016). Novel structure with negative Poisson's ratio and enhanced Young's modulus. *Composite Structures*, *138*, 243–252. https://doi.org/10.1016/j.compstruct.2015.11.036

Malcolm, D. (2019). *The Concussion Crisis in Sport*. Routledge.

McNulty, T., Bhate, D., Zhang, A., Kiser, M. A., Ferry, L., Suderf, A., Bhattacharya, S., & Boradkar, P. (n.d.). *A Framework for the Design of Biomimetic Cellular Materials for Additive Manufacturing*. 13.

Miller, T., & Wilson, M. (2015). Additive Manufactorung Facility. *Victoria University of Wellington, New Zealand*.

Milton, A., & Rodgers, P. (2013). *Research Methods for Product Designers*. Laurene King.

Mir, M., Ali, M. N., Sami, J., & Ansari, U. (2014). *Review of Mechanics and Applications of Auxetic Structures*

[Review Article]. Advances in Materials Science and Engineering. https://doi.org/10.1155/2014/753496

Mirante, L. (2015). *Auxetic Structures*. https://issuu.com/lorenzomirante/docs/2015_12_mirante_b

Naboni, R. (2015). *Metamaterial computation and fabrication of auxetic patterns for architecture*. https://www.academia.edu/24743042/Metamaterial_computation_and_fabrication_of_auxetic_patterns_for_architecture

Oxman, R., & Gu, N. (2015). *Theories and Models of Parametric Design Thinking*.

Rodríguez Ramírez, E. (2017). A Postgraduate Thesis Model for Research through Design Based on Design Criteria. *The International Journal of Designed Objects*, *11*(4), 11–27. https://doi.org/10.18848/2325-1379/CGP/v11i04/11-27

Saxena, K. K., Das, R., & Calius, E. P. (2016). Three Decades of Auxetics Research − Materials with Negative Poisson's Ratio: A Review. *Advanced Engineering Materials*, *18*(11), 1847–1870. https://doi.org/10.1002/adem.201600053

Shepherd, T., Driscoll, H., Winwood, K., Venkatraman, P., & Allen, T. (2017). *Review of modelling and additive manufacturing of auxetic materials for application in sport*. 7.

Slann, A., White, W., Scarpa, F., Boba, K., & Farrow, I. (2015). Cellular plates with auxetic rectangular perforations. *Physica Status Solidi (b)*, *252*(7), 1533–1539. https://doi.org/10.1002/pssb.201451740

Stratasys. (2020). *Polyjet Materials*. Stratasys.

Tong, X. C. (2018). Mechanical Metamaterials and Metadevices. In X. C. Tong (Ed.), *Functional Metamaterials and Metadevices* (pp. 219–242). Springer International Publishing. https://doi.org/10.1007/978-3-319-66044-8_11

Wang, K., Chang, Y.-H., Chen, Y., Zhang, C., & Wang, B. (2015). Designable dual-material auxetic metamaterials using three-dimensional printing. *Materials and Design*, *67*, 159–164. https://doi.org/10.1016/j.matdes.2014.11.033

Wu, W., Hu, W., Qian, G., Liao, H., Xu, X., & Berto, F. (2019). Mechanical design and multifunctional applications of chiral mechanical metamaterials: A review. *Materials & Design*, *180*, 107950. https://doi.org/10.1016/j.matdes.2019.107950

Wu, W., Qi, D., Liao, H., Qian, G., Geng, L., Niu, Y., & Liang, J. (2018). Deformation mechanism of innovative 3D chiral metamaterials. *Scientific Reports*, *8*(1), 1–10. https://doi.org/10.1038/s41598-018-30737-7

Yang, L., Harrysson, O., West, H., & Cormier, D. (2015). Mechanical properties of 3D re-entrant honeycomb auxetic structures realized via additive manufacturing. *International Journal of Solids and Structures*, *69–70*, 475–490. https://doi.org/10.1016/j.ijsolstr.2015.05.005

Yin, R. K. (2017). *Case study research and applications: Design and methods*. Sage publications.

Zadpoor, A. A. (2016). Mechanical meta-materials.

Materials Horizons, *3*(5), 371–381.

https://doi.org/10.1039/C6MH00065G